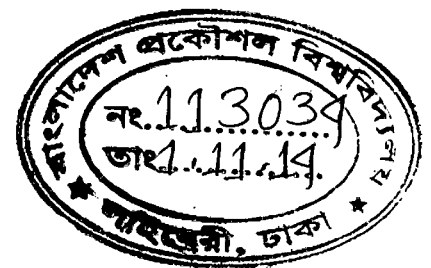
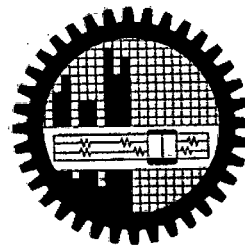


**“AN EXPERIMENTAL STUDY OF BANK PROTECTION WORK AND
LAUNCHING BEHAVIOUR FOR OBLIQUE FLOW ON A STRAIGHT
RIVER BANK”**

POLY DAS
Roll No- 0409162016 (P)



**DEPARTMENT OF WATER RESOURCES ENGINEERING
BNGLADESH UNIVERSITY OF ENGINEERING AND TECHNOLOGY
DHAKA-1000, BANGLADESH**

July 2014

**“AN EXPERIMENTAL STUDY OF BANK PROTECTION WORK AND
LAUNCHING BEHAVIOUR FOR OBLIQUE FLOW ON A STRAIGHT
RIVER BANK”**

by

**Poly Das
Roll No- 0409162016 (P)**

**Department of Water Resources Engineering
BANGLADESH UNIVERSITY OF ENGINEERING AND TECHNOLOGY
DHAKA-1000, BANGLADESH**

July 2014

**“AN EXPERIMENTAL STUDY OF BANK PROTECTION WORK AND
LAUNCHING BEHAVIOUR FOR OBLIQUE FLOW ON A STRAIGHT
RIVER BANK”**

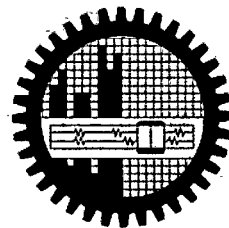
by

Poly Das

Roll No- 0409162016 (P)

In partial fulfillment of the requirement for degree
of

MASTER OF ENGINEERING IN WATER RESOURCES ENGINEERING



**Department of Water Resources Engineering
BANGLADESH UNIVERSITY OF ENGINEERING AND TECHNOLOGY
DHAKA-1000, BANGLADESH**

July 2014

CANDIDATE'S DECLARATION

It is hereby declared that this project work or any part of it has not been submitted elsewhere for the award of any other degree or diploma.

Signature of the candidate

P. Das

Poly Das

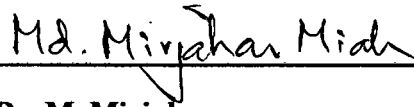
CERTIFICATE OF APPROVAL

We here by recommended that the Master of Engineering Project work entitled "An experimental study of bank protection work and launching behaviour for oblique flow on a straight river bank" submitted by Poly Das, Roll no- 0409162016 (P), Session- April, 2009 has been accepted as satisfactory partial fulfillment of the requirement for the degree of Master of Engineering in Water Resources Engineering on July 01, 2014.



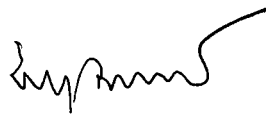
Dr. Umme Kulsum Navera
Professor,
Department of Water Resources Engineering
BUET, Dhaka.

Chairman
(Supervisor)



Dr. M. Mirjahan
Professor,
Department of Water Resources Engineering
BUET, Dhaka.

Member



Dr. Md. Sabbir Mostafa Khan
Professor and Head,
Department of Water Resources Engineering
BUET, Dhaka.

Member

Table of Contents

	Page No
Table of Contents	i
List of Figures	iv
List of Tables	vii
List of Notations	viii
List of Abbreviations	x
Acknowledgement	xi
Abstract	xii
Chapter 1: Introduction	
1.1 General	1
1.2 River System of Bangladesh and Nature of Rivers	1
1.3 Background of the Study	6
1.3.1 Bank Erosion Pattern and Magnitude in Rivers of Bangladesh	7
1.3.2 Erosion in Different Rivers of the World	8
1.3.3 River Bank Erosion-A Natural Threat	10
1.3.4 Selection of the Study	11
1.4 Research Objective	14
1.5 Possible Outcome of the Research	14
1.6 Organization of the Report	14
Chapter 2: Literature Review	
2.1 General	16
2.2 Hydro-morphological Characteristics of River System in Bangladesh	17
2.3 Previous Studies on Braided River and Protection Work	18
2.4 Summary	25
Chapter 3: Theory and Methodology	
3.1 General	26
3.2 Classification and Causes for Formation of Different Channel Patterns	26
3.3 Aggradation/Deposition and Degradation/Erosion of Channel	29
3.4 Causes of Bank Erosion	30
3.5 Processes of stream Bank Erosion	32

	Page No
3.6 Channel Migration and Expansion	34
3.7 Process for Understanding River Behaviour	34
3.8 Outline of the Methodology for Physical Modelling	35
3.9 Summary	41
Chapter 4: Physical Model Setup	
4.1 General	43
4.2 Preliminary Calculated Parameters for Physical Model	43
4.3 Physical Model Setup	46
4.4 Different Components of Physical Model	47
4.5 Equipments Used for the Physical Model	52
4.6 Process of Experimental Setup	54
4.7 Design of Protective Work	56
4.8 Measurement for Each Experimental Setup	61
4.9 Summary	64
Chapter 5: Results and Discussions	
5.1 General	65
5.2 Experimental Details Before and After Physical Model Run	65
5.2.1 Straight Channel without Oblique Flow and Protected Bank	65
5.2.2 Straight Channel, Unprotected Bank with Different Oblique Flow Angle	67
5.2.3 Straight Channel, Protected Bank, 20° Oblique Flow Angle with Different Discharge Ratio	72
5.2.4 Straight Channel, Protected Bank, 40° Oblique Flow Angle with Different Discharge Ratio	76
5.2.5 Straight Channel, Protected Bank, 60° Oblique Flow Angle with Different Discharge Ratio	80
5.2.6 Straight Channel, Protected Bank by Stone Boulder and Main Channel Close	85
5.2.7 Straight Channel, Protected Bank by Geo-bag Type-1, 60° Oblique Flow Angle with Different Discharge Ratio	87
5.2.8 Straight Channel, Protected Bank by Geo-bag Type-1 and Main Channel Close	88
5.2.9 Straight Channel, Protected Bank by Geo-bag Type-2, 60° Oblique Flow Angle with Different Discharge Ratio	91
5.3 Comparison of Channel Cross Sections for Maximum Scour	100
5.3.1 Comparison of Channel Cross Section for Group-1	101

	Page No
5.3.2 Comparison of Channel Cross Section for Group-2	104
5.3.3 Comparison of Channel Cross Section for Group-3	107
5.3.4 Comparison of Channel Cross Section for Group-4	108
5.3.5 Comparison of Channel Cross Section for Group-5	110
5.3.6 Comparison of Channel Cross Section for Group-6	112
5.3.7 Comparison of Channel Cross Section for Group-7	115
5.3.8 Comparison of Channel Cross Section for Group-8	117
5.3.9 Comparison of Channel Cross Section for Group-9	119
5.3.10 Comparison of Channel Cross Section for Group-10	121
5.4 Comparison of Estimated and Measured Scour Depth	124
5.5 Assessment of Flow Behaviour for Oblique Flow	125
5.6 Launching Behaviour of Protection Work due to Oblique Flow	127
5.7 Some observations on Development and Execution of Physical Model	131
5.8 Effect of Discharge Ratio on Scour	133
5.9 Effect of Oblique Flow Angle on Scour	134
5.10 Bare Space in Launching Slope	135
5.11 Summary	136
Chapter 6: Conclusions and Recommendations	
6.1 General	137
6.2 Conclusions of the Study	137
6.3 Recommendations of the Study	138
References	139
Appendices	
Appendix-A: Pictures for Physical Model Setup and Model Run	146
Appendix-B: Dynamic Equilibrium State of Physical Model	156
Appendix-C: Flow Line Diagram Drawn by Float Position	165
Appendix-D: Calibration of Weir for Discharge	175

List of Figures

Figure No		Page No
Figure 1.1:	Basin of River System in Bangladesh	2
Figure 1.2:	River System of Bangladesh	4
Figure 1.3:	Major Areas in Bangladesh which is Under Attack of Riverbank Erosion	6
Figure 1.4:	Presence of Oblique Flow in Bangladesh	12
Figure 3.1:	Channel Patterns	27
Figure 3.2:	Various Features of Channels	28
Figure 3.3:	Undercutting of the Bank Toe-A Sign of Bank Scour	33
Figure 3.4:	Slumping- A common Type of Mass Failure	33
Figure 3.5:	General Consideration for Protection Work	39
Figure 4.1:	General Layout of the Experimental Setup	43
Figure 4.2:	Average Section of Main Channel	44
Figure 4.3:	Average Section of Chute Channel	44
Figure 4.4:	Physical Model Layout at RRI, Faridpur	47
Figure 4.5:	Line Diagram of Physical Model Layout	49
Figure 4.6:	Introduction of Physical Model Components	50
Figure 4.7:	Photo of 2-D Velocity Meter	53
Figure 4.8:	Photo of ADV Meter	54
Figure 4.9:	Definition Sketch of Design of Bank Protection Work	58
Figure 4.10:	Thickness and Length of L.A	59
Figure 5.1:	Bed and Bank Details for T-0	66
Figure 5.2:	Bed and Bank Details for T-1	68
Figure 5.3:	Bed and Bank Details for T-2	70
Figure 5.4:	Bed and Bank Details for T-3	71
Figure 5.5:	Bed and Bank Details for T-4	73
Figure 5.6:	Launching Behaviour of Stone Boulder for T-4	74
Figure 5.7:	Bed and Bank Details for T-5	75
Figure 5.8:	Launching Behaviour of Stone Boulder for T-5	76
Figure 5.9:	Bed and Bank Details for T-6	77
Figure 5.10:	Bed and Bank Details for T-7	78
Figure 5.11:	Bed and Bank Details for T-8	79
Figure 5.12:	Bed and Bank Details for T-9	81
Figure 5.13:	Launching Behaviour of Stone Boulder for T-9	82
Figure 5.14:	Bed and Bank Details for T-10	83
Figure 5.15:	Bed and Bank Details for T-11	84

Figure No		Page No
Figure 5.16:	Bed and Bank Details for T-12	86
Figure 5.17:	Launching Behaviour of Stone Boulder for T-12	87
Figure 5.18:	Bed and Bank Details for T-13	89
Figure 5.19:	Bed and Bank Details for T-14	90
Figure 5.20:	Launching Behaviour of Geo-bag Type-1 for T-14	91
Figure 5.21:	Bed and Bank Details for T-15	92
Figure 5.22:	Launching Behaviour of Geo-bag Type-1 for T-15	93
Figure 5.23:	Bed and Bank Details for T-16	94
Figure 5.24:	Launching Behaviour of Geo-bag Type-1 for T-16	95
Figure 5.25:	Bed and Bank Details for T-17	95
Figure 5.26:	Launching Behaviour of Geo-bag Type-1 for T-17	96
Figure 5.27:	Bed and Bank Details for T-18	97
Figure 5.28:	Launching Behaviour of Geo-bag Type-2 for T-18	98
Figure 5.29:	Bed and Bank Details for T-19	98
Figure 5.30:	Bed and Bank Details for T-20	99
Figure 5.31:	Launching Behaviour of Geo-bag Type-2 for T-20	100
Figure 5.32:	Scour for Group-1 at Cross Section 4	102
Figure 5.33:	Scour for Group -1 at Cross Section 5	102
Figure 5.34:	Scour for Group-1 at Cross Section 6	102
Figure 5.35:	Scour for Group-1 at Cross Section 7	103
Figure 5.36:	Scour for Group-1 at Cross Section 8	103
Figure 5.37:	Scour for Group-1 at Cross Section 9	103
Figure 5.38:	Scour for Group-2 at Cross Section 6	104
Figure 5.39:	Scour for Group-2 at Cross Section 7	105
Figure 5.40:	Scour for Group-2 at Cross Section 8	105
Figure 5.41:	Scour for Group-2 at Cross Section 9	105
Figure 5.42:	Scour for Group-2 at Cross Section 10	106
Figure 5.43:	Scour for Group-2 at Cross Section 11	106
Figure 5.44:	Scour for Group-2 at Cross Section 12	106
Figure 5.45:	Scour for Group-3 at Cross Section 8	107
Figure 5.46:	Scour for Group-3 at Cross Section 9	107
Figure 5.47:	Scour for Group-3 at Cross Section 10	108
Figure 5.48:	Scour for Group-4 at Cross Section 8	109
Figure 5.49:	Scour for Group-4 at Cross Section 9	109
Figure 5.50:	Scour for Group-4 at Cross Section 10	109
Figure 5.51:	Scour for Group-4 at Cross Section 11	110
Figure 5.52:	Scour for Group-5 at Cross Section 10	111

Figure No	Page No
Figure 5.53: Scour for Group-5 at Cross Section 11	111
Figure 5.54: Scour for Group-5 at Cross Section 12	111
Figure 5.55: Scour for Group-6 at Cross Section 6	112
Figure 5.56: Scour for Group-6 at Cross Section 7	112
Figure 5.57: Scour for Group-6 at Cross Section 8	113
Figure 5.58: Scour for Group-6 at Cross Section 9	113
Figure 5.59: Scour for Group-6 at Cross Section 10	113
Figure 5.60: Scour for Group-6 at Cross Section 11	114
Figure 5.61: Scour for Group-6 at Cross Section 12	114
Figure 5.62: Scour for Group-7 at Cross Section 9	116
Figure 5.63: Scour for Group-7 at Cross Section 10	116
Figure 5.64: Scour for Group-7 at Cross Section 11	116
Figure 5.65: Scour for Group-8 at Cross Section 8	117
Figure 5.66: Scour for Group-8 at Cross Section 9	117
Figure 5.67: Scour for Group-8 at Cross Section 10	118
Figure 5.68: Scour for Group-8 at Cross Section 11	118
Figure 5.69: Scour for Group-8 at Cross Section 12	118
Figure 5.70: Scour for Group-9 at Cross Section 6	119
Figure 5.71: Scour for Group-9 at Cross Section 7	119
Figure 5.72: Scour for Group-9 at Cross Section 8	120
Figure 5.73: Scour for Group-9 at Cross Section 9	120
Figure 5.74: Scour for Group-9 at Cross Section 10	120
Figure 5.75: Scour for Group-9 at Cross Section 11	121
Figure 5.76: Scour for Group-9 at Cross Section 12	121
Figure 5.77: Scour for Group-10 at Cross Section 7	122
Figure 5.78: Scour for Group-10 at Cross Section 8	122
Figure 5.79: Scour for Group-10 at Cross Section 9	122
Figure 5.80: Scour for Group-10 at Cross Section 10	123
Figure 5.81: Scour for Group-10 at Cross Section 11	123
Figure 5.82: Scour for Group-10 at Cross Section 12	123
Figure 5.83: Sketch for Measurement of Launching Behaviour of Protection Work	127
Figure 5.84: Relation of Scour Depth with Discharge Ratio for Oblique Flow	134
Figure 5.85: Relation of Scour Depth with Oblique Flow Angle	135

List of Tables

Table No		Page no.
Table 1.1:	Sediment Carried by Rivers in the World to Express Erosion	9
Table 1.2:	Mean Erosion Rates in Different Countries	9
Table 4.1:	Preliminary Calculation of Parameters	45
Table 4.2:	Schedule for Experimental Setup and Description of Physical Model Conditions	63
Table 5.1:	Group Description for Comparison of Maximum Scour Sections (Based on fixed angle)	101
Table 5.2:	Group Description for Comparison of Maximum Scour Sections (Based on fixed discharge ratio)	115
Table 5.3:	Comparison between Estimated and Measured Scour	124
Table 5.4:	Assessment of Flow Behaviour for Oblique Flow	126
Table 5.5:	Analysis of Launching Behaviour for Different Protective Materials and Oblique Flow	127
Table 5.6:	Calculation of Bare Spaces in Launching Slope	136

List of Notations

L_m	Horizontal scale of model	-
L_p	Horizontal scale of prototype	-
L_r	Horizontal scale	-
L	Length	m
T	Top width	m
W	Bottom width	m
Y_m	Vertical scale of model	-
Y_p	Vertical scale of prototype	-
Y_r	Vertical scale	-
F_m	Froude no in model	-
F_p	Froude no in prototype	-
D_{50}	Mean diameter of particle	mm
V_m	Velocity in model	m/s
V_p	Velocity in prototype	m/s
v	Average velocity	m/s
Q_m	Discharge in model	m ³ /s
Q_p	Discharge in prototype	m ³ /s
T_p	Time in prototype	hr
T_m	Time in model	hr
S_p	Slope in prototype	-
S_m	Slope in model	-
S_f	Water surface slope	-
R	Scour depth	m
f	Silt Factor	-
Q	Design Discharge	m ³ /s
D	Depth of anticipated Scour	m
ρ_s	Particle density	kg/m ³
ρ_w	Water density	kg/m ³
R_D	Relative density	-
Δ	Relative density of submerged material	-
ν_s	Kinematic viscosity	m ² /s
K_D	Dynamic viscosity	kgs/m ²
f_m	Fineness modulus	-
g	Gravitational acceleration	m/s ²
D_{90}	Average dia of bed material	mm
ks	Effective bed roughness of a flat bed (m) for sand and gravel material	m
D^*	Dimensionless particle diameter	-
h	Water depth	m

A	Cross-sectional area	m ²
P	Wetted perimeter	m
R	Hydraulic radius	m
D	Hydraulic depth	m
U*	Shear velocity	m/s
θ	Shields parameter	-
Fr	Froude number	-
θ_{cr}	Critical Shields parameter	-
U* _{cr}	Critical shear velocity	m/s
Re	Reynolds number	-
R*e	Particle Reynolds number	-
C	Chezy roughness co-efficient	-
V _{cr}	Critical velocity by shields	-
V _{cr}	Critical velocity by Van Rign	-
w	Fall velocity	m/s
V _i	Velocity for incipient motion	m/s
Y	Depth at 1/3 bank height	m
K ₁	Side slope correction	-
C _s	Shape co-efficient	-
C _v	Co-efficient for vertical velocity distribution	-

List of Abbreviations

ADV	Acoustic Doplar Velocitymetry
BUET	Bangladesh University of Engineering and Technology
BWDB	Bangladesh Water Development Board
RRI	River Research Institute
RL	Reduced Level

Acknowledgements

I would like to thank God for being enough merciful to bestow strength and patience upon me and also the very necessary helping and capable hands from some wonderful persons who have given their heart whelming full support in making this compilation an interesting magnificent and rewarding experience to me. The research project is the contribution of many individuals in different ways.

First and foremost I would like to express my sincerest gratitude to my supervisor, Dr. Umme Kulsum Navera (Professor, Department of Water Resources Engineering, BUET) for her continuous support and guidance with patience, motivation, enthusiasm and immense knowledge. One simply could not wish for a better or friendlier supervisor.

I would like to thank the authority of Institute of Water Modelling (IWM) for funding the experimental part of the research at RRI, Faridpur. I also like to express my deepest thanks to the authority of River Research Institute (RRI), Faridpur for giving full support in using facilities of the organization to carry out the experimental part of the research work.

I am highly indebted for the valuable and constructive suggestions and technical solution during planning and development of this work given by Md. Motaher Hossain, Superintending Engineer, Design Circle-6, Bangladesh Water Development Board and Md. Abu Ala Moududi, Principal Scientific Officer, River Research Institute, Faridpur. Their crucial role was an enormous benefit for me.

I take immense pleasure in thanking Md. Saif Uddin, Sub-Divisional Engineer, Design Circle-2, BWDB, Md. Motiur Rahman Jewel, Director, Survey & Data Consultants, Md. Amin, Assistant Engineer, Dhaka Division-1, BWDB and Mr. Sudip Sarkar, Student, M Sc., BUET for their generous co-operation to run the work smoothly.

Last but not the least; I would like to thank all my family members, friends and colleagues for giving me mental support so that I could complete my work.

Abstract

Bangladesh is an alluvial delta of the Ganges, the Brahmaputra and the Meghna River. Hydro-dynamically rivers are very active in nature in this country. Bank erosion, deposition, char development, flood etc is common scenario for rivers in Bangladesh. Among these, river erosion is a common threat in Bangladesh. The rivers are generally meandering and braided in nature. Normally erosion occurs in outflanking bank of meandering channels. There is no systematic pattern of erosion in the braided river system. Erosion pattern in a braided river have a unique nature due to presence of frequent bars and islands within the channel which creates oblique flow in the channel. Oblique flow changes and accelerates the erosion process in a braided river than meandering river.

There are a number of variables in the braided river system and is very important to understand its behaviour to prevent erosion. Different studies on braided river are mostly qualitative. But there is a significant lack of quantitative studies in braided rivers. This study has been done to understand the fluvial process of braided river.

To understand the behaviour of different processes in the river system physical model and numerical models are used. Physical modelling is a better way for perception of the nature of rivers due to flow current interactions. Different behaviour of river can be incorporated in physical models. The present study has been conducted by physical modelling to understand the behaviour of a part of braided river when it is under attack of oblique flow.

The physical model for this study has been developed in River Research Institute (RRI), Faridpur which is funded by Institute of Water Modelling (IWM). The physical model is developed in a scale ratio of 1:50 for a straight bank with variable oblique channel angle and discharge ratio which falls under twenty one setup. Each setup has been developed to understand the effect of oblique flow on main channel. Naturally river bank can be straight or bend. Straight bank has been considered in the study. Effect on unprotected bank, bank protection work and launching behaviour of protection material due to oblique flow has been identified. Stone boulder and geo-bags has been used as river bank protection material.

Bank shifting tendency and bed scour in unprotected bank has been observed and measured. Revetment work by stone boulder and geo-bags has been done with the analyzed results of unprotected conditions. Launching behaviour of both the materials has been analyzed in this study. Some factor for design of bank protection work has been reassessed according to the results obtained from the model. Relation of oblique flow angle and discharge ratio with respect to main channel on scour has also been established. Some recommendations for further research have been provided.

Chapter 1

INTRODUCTION

1.1 General

Bangladesh is a land of rivers within an area of about 1,47,570 square kilometer and the country is criss-crossed by about 405 rivers with a total length of about 24,140 kilometer (BWDB, 2012). The natural setting of Bangladesh is between the Himalayas and the Bay of Bengal together with the prevalence of tropical monsoon climate (Sarker et al., 2003). The country is the delta of the Ganges-Brahmaputra-Meghna river system and representing the lowermost fertile alluvial system. These three rivers combine with numerous tributaries within the country via frequent changes in courses which is draining to the Bay of Bengal (BWDB, 2010).

The catchment area of the three major rivers is about 1.72 million square km of which only 7.5 percent lies within the border of Bangladesh that generates 1200 km³ of run-off annually, only 10 percent of which is generated within Bangladesh. In addition to vast quantities of water, these rivers carry about 1.1 billion tons of sediment every year (Sarker et al, 2003) and are responsible for the prevalence of flooding and riverbank erosion in Bangladesh (Uddin et al, 2012).

River bank erosion is common problem in Bangladesh. Devastating flood with different flow characteristics and excessive rainfall are accelerating the erosion process which results immense damage to agriculture and infrastructures every year (Hossain et al., 2010).

1.2 River System of Bangladesh and Nature of Rivers

The river system of Bangladesh can be divided into four major networks: (a) Brahmaputra-Jamuna river system, (b) Ganges-Padma river system, (c) Surma-Meghna river system, and (d) Chittagong region river system. The combined annual discharge passing through the system into the Bay of Bengal reaches up to 1,174

billion cumec. Most of the rivers are characterized by fine sandy bottoms, flat slopes, substantial meandering, banks susceptible to erosion, and channel shifting (Uddin et al., 2012).

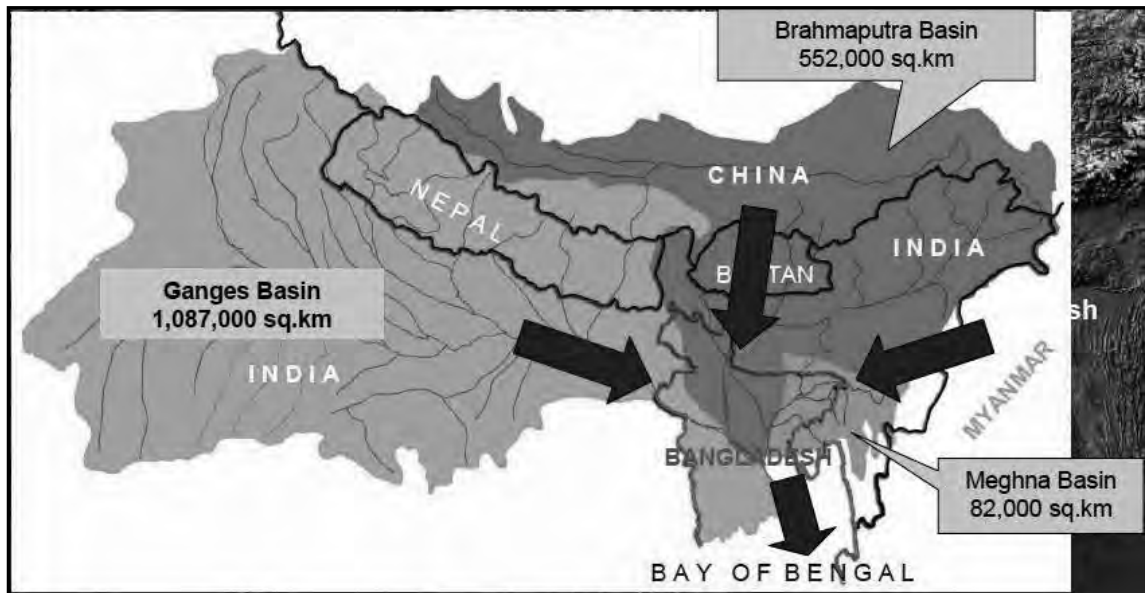


Figure 1.1: Basin of River System in Bangladesh (Source: Ahmad, 2008)

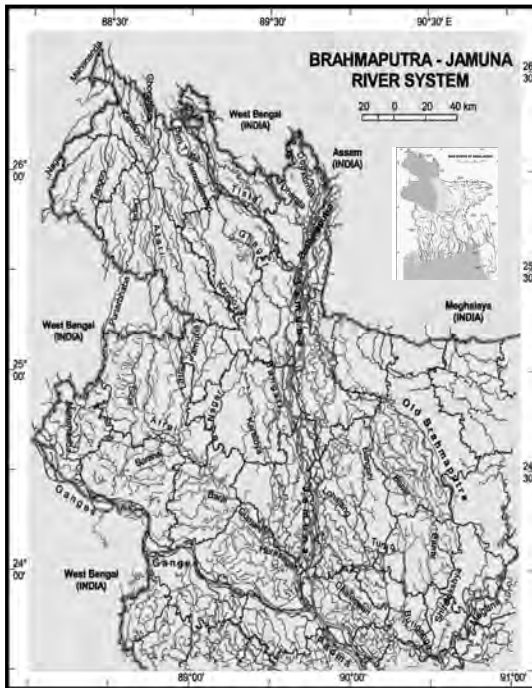
(a) The Brahmaputra-Jamuna River system (Figure 1.2) is about 280 km long and extends from northern Bangladesh to its confluence with the Ganges. The Brahmaputra has a length of 2,850 km and a catchment area of about 552,000 square km before entering into Bangladesh. The river originates in Tibet as the Yarlung Zangbo Jiang and passes through Arunachal Pradesh of India as Brahmaputra. The river receives water from five major tributaries along this route, of which Dihang and Luit are prominent. At the point where Brahmaputra meets the Teesta in Bangladesh, it is called the Jamuna. The Brahmaputra-Jamuna throughout its broad valley section in Assam and in Bangladesh is famous for its braided nature, shifting sub channels, and for the formation of chars (island/sandbars) within the channel. The recorded highest peak flow of Brahmaputra-Jamuna is 98,000 cumec (cubic meter per second) in 1988 and the maximum velocity ranges from 3-4 m/sec with a depth of 21-22m. The average discharge of the river is about 20,000 cumec with average annual silt load of 1,370 tons/sq. km.

(b) Ganges-Padma river system is one of the three major river systems of Bangladesh. Continual shifting of courses or migrating laterally and occupying new sites are the main behaviour of the rivers in the basin system. Even the minor channels of the delta show the same tendency. The main channel of the Ganges-Padma has long been maintaining a south- easterly direction. The Ganges delta shows a mixed drainage pattern. The stem-stream of the delta, the Ganges-Padma, is a braided channel with a meandering course. Most of the other major distributaries also follow a sinuous course. A number of major streams, however, follow straight courses. The coastal drainage system of the Ganges delta includes the Sundarbans tidal channels and creeks as well as the estuarine channels of the eastern coast of the delta up to the Meghna mouth.

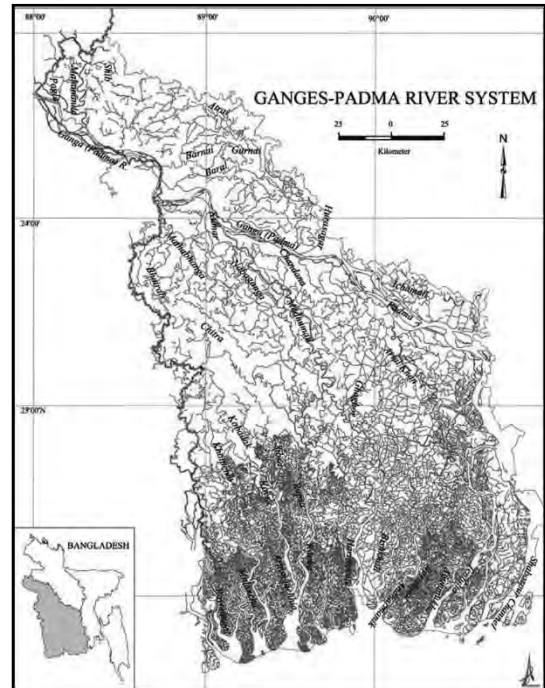
The Ganges and the Padma are the main channels of this river system. The Jalangi, Bhairab, Mathabhanga, Kobadak, Bhadra, Ichamati, Kumar, Nabaganga, Barisal river, Kalijira river, Gabkhan Khal, Rajapur Don, Bukhianagar Don, Bakerganj and Punjab rivers, Burishwar, etc are some of the numerous rivers and streams of the Ganges delta under the Ganges-Padma river system.

The Ganges has a total length of about 2,600 km and a catchment area of approximately 907,000 square km. The total drainage area of the Ganges river system is about 1,087,000 square km, of which about 46,300 sq km lies within Bangladesh. The recorded highest flow of the Ganges was 76,000 cumec in 1981, and the maximum velocity ranging from 4-5 m/sec, with depth varying from 20m to 21m. The average discharge of the river is about 11,500 cumec with an annual silt load of 492 ton/sq km.

(c) Surma-Meghna river system has a catchment area of about 82,000 square km. Main river of this river system is Surma which flows west and then southwest to Sylhet town. Then it flows northwest and west to Sunamganj town and maintains a course southwest and Markuli to meet Kushiya. Surma receives tributaries from Khasi and Jaintiahills of Shilong plateau. Surma bifurcates south of Mohanganj after it receives Kangsa and further south the Mogra.



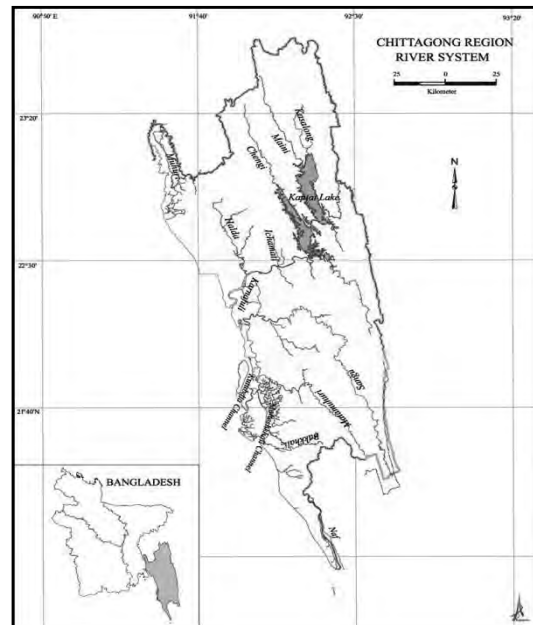
(a)



(b)



(c)



(d)

Figure 1.2: River System of Bangladesh: (a) Brahmaputra-Jamuna River system, (b) Ganges-Padma River system, (c) Surma-Meghna river system and (d) Chittagong Region river system. (Source:Banglapedia, 2006)

It joins Kalni near Bhairab Bazar of Kishoreganj district and the name Meghna which is given to the course from this confluence to the Bay of Bengal. On the other hand most of the Surma system falls in the haor basin.

Meghna receives old brahmaputra on its right-bank at Bhairab Bazar and on the way to the Bay it carries the water of Padma from Chandpur. Meghna has two distinct parts upper Meghna and lower Meghna. The net discharge through this river varies from 10,000 cumec in the dry season to 160,000 cumec in the wet season. The width of the river there is three quarters of a kilometer.

Several small channels branch out from Meghna, meander through the low land bordering the marginal. Offshoots of the Meghna are Pagli, Katalia, Dhanagoda, Matlab and Udhamdi. Meghna and these offshoots receive the waters of a number of streams from Tripura hills including Gumti, Howrah, Kagni, SenaiBuri, Hari, Mangal, Kakri, Pagli, Kurulia, Balujuri, Sonaichhari, Handachhora, Jangalia and Durduria. All of these are liable to flash floods, but Gumti, Kakri and Howrah are the major ones.

(d) The Chittagong Region system the rivers of Chittagong and Chittagong hill tracks are not connected to the other river systems of the country. The main river of this region is Karnafuli. It flows through the region of Chittagong and the Chittagong hills. It cuts across the hills and runs rapidly downhill to the west and southwest and finally to the Bay of Bengal. Other important rivers of the region are the Feni, Muhuri, Sangu, Matamuhuri, Bakkhali, and Naaf having meandering nature.

The four mighty river systems flowing through Bangladesh drain an area of 1.5 million sq km. During the wet season the rivers of Bangladesh flow to their maximum level, at about 140,000 cusec, and during the dry period, the flow diminishes to 7,000 cusec.

1.3 Background of the Study

Riverbank erosion is one of the major natural disasters in Bangladesh which causes untold miseries every year to thousands of people living along the banks of the rivers of Bangladesh.

The major rivers of Bangladesh consume several thousand hectares of floodplain annually, leaving thousands of people landless and homeless. The major rivers such as the Jamuna, the Ganges, the Padma and lower Meghna swallow large areas of cities, towns, agricultural lands and villages and destroy valuable infrastructures every year. Major areas that are under threat of bank erosion have been presented by Figure 1.3.

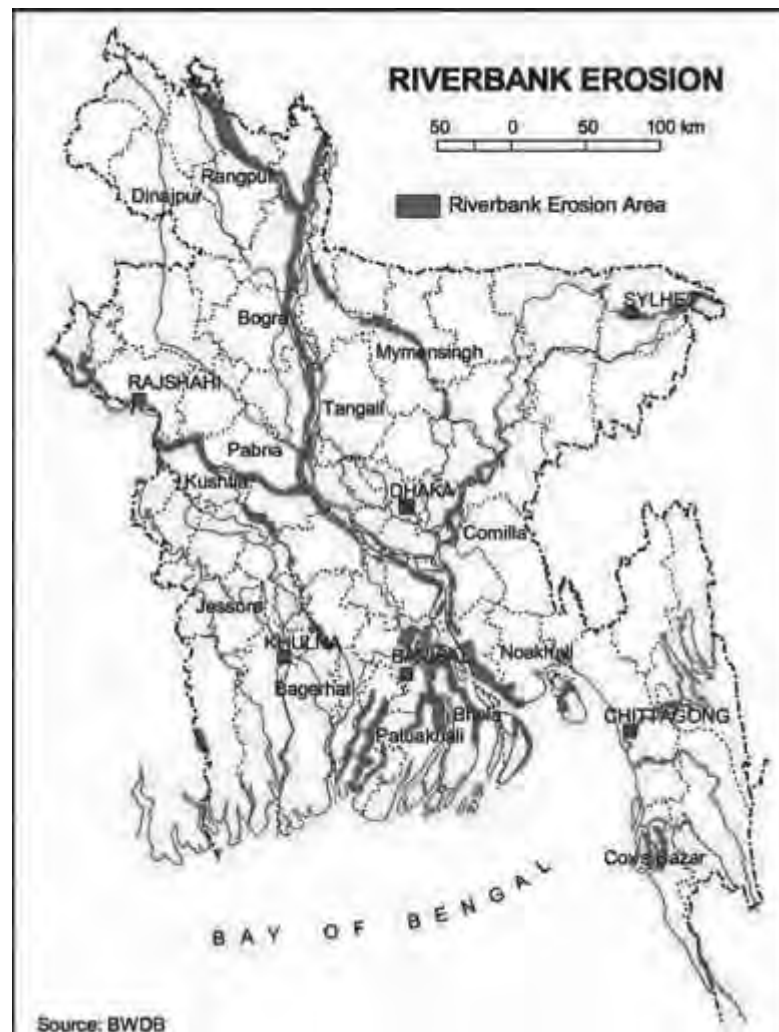


Figure 1.3: Major Areas in Bangladesh which is Under Attack of Riverbank Erosion

1.3.1 Bank Erosion Pattern and Magnitude in Rivers of Bangladesh

Bangladesh is one of the most disaster prone countries around the world with severe cyclone, destructive floods and associated riverbank erosion, drought etc. The funnel shaped coast and lowering topography makes the country vulnerable to different disasters. Bangladesh experienced huge rainfall during monsoon for being a country of temperate region. In addition, abundant water run after the upper catchment areas increase the intensity and vulnerability of floods and associated riverbank erosion.

The combined annual average sediment load entering Bangladesh and conveyed to the Bay of Bengal via the main rivers. A part of this sediment load is deposited on the floodplain during the flood season, gradually changing its topography and drainage conditions. Most of the sediment is deposited in the coastal areas, giving rise to land accretion and a gradually changing coastline. The large seasonal variation in river flow results in a fluctuating sediment transport capacity and causes river-bank erosion, migration of river-banks and meandering river channels.

The Brahmaputra–Jamuna river faces frequent and rapid bank line erosion at a rate of 160 meter per year (m/y) between 1973 and 1992. In addition, the river has migrated westwards at an average movement rate of 50 m/y during the period of 1830– 1992 while an average width was 6.2 km and 10.6 km in 1830 and 1992 respectively indicating the severity of erosion hazard along the river. The widening rate of the channel has increased from the year 1914. The channel has widened at an average rate of 27 m/y before 1914 while an average rate of 65 m/y was followed afterward as the average width of the river has increased about 130 m/y since 1973 (The World Bank, 1995).

Major rivers like the Jamuna, the Ganges and the Padma eroded around 1590 square km flood plains making 1.6 million people homeless since 1973 (CEGIS, 2009). In 2013, 1,330 ha and 510 ha of land were eroded along Ganges and Padma river respectively (CEGIS, 2013). It has been found that the Jamuna River is widening and both banks are migrating outwards at a high rate for the last few decades. During the period, net erosion along the 240 km long Jamuna River is about 80,690 ha. The rate

of erosion varies over time in association with climatic variables mainly precipitation in the form of rainfall and with locational factors (Uddin et al, 2012).

The upper Meghna is more or less stable, while the lower Meghna experienced extensive and extreme erosion during 1984-93, particularly on the right bank. Sustained annual erosion rates of 100 meters or more over a 10-year period are notable, and occurred on both the lower Meghna and Padma, where satellite image analysis in the inventory reports reveals major changes in the river courses in this period and 410 ha of land is vulnerable to erosion. Landsat image analysis also gives an estimate that average about 8,700 ha of mainland are lost each year to erosion by main rivers (CEGIS, 2009).

1.3.2 Erosion in Different Rivers of the World

The sediment yield is made of suspended load and bed-load. Sediment yield gives a valuable idea about rates of erosion and soil loss from the drainage basin. It is rather difficult to measure the bed-load except when the depth is small and material is coarse. Hence most of available data on erosion rates only include suspended load, which is normally expressed in tons/km²/year or tons/year.

High values of suspended sediment yield can be attributed to various factors such as underlying geology, topography, climatic conditions, high erodibility of soils and land use. Steep slopes and high intensity of rainfall can also cause high values of sediment yield. Holeman (1968) has given valuable information on the sediment yield of major rivers of the world. Table 1.1 and 1.2 gives such data for some rivers in the world, which discharge more than 10⁴ tons of sediment each year into the sea (Garde R.J., 2006).

Table 1.1 and 1.2 indicates that the highest sediment load is fed to the oceans every year by Asia and the next in line is South America and North and Central America.

Table 1.1: Sediment Carried by Rivers in the World to Express Erosion

River	Location	Total drainage area, 10 ³ km ²	Average annual Sediment load		Average water discharge, 10 ³ m ³ /s
			10 ³ tons	tons/km ²	
Yellow	China	666	2080 000	2945	1.5
Ganga	India	945	1600 000	1563	11.8
Brahmaputra	Bangladesh	658	800 000	1445	12.2
Yangtze	China	1920	550 000	547	21.8
Indus	Pakistan	957	480 000	508	5.6
Ching (tributary of Yellow)	China	56	450 000	8008	0.057
Amazon	Brazil	5709	400 000	67	181.4
Mississippi	U.S.A.	3185	344 000	109	17.9
Irrawaddy	Myanmar	425	330 000	914	15.6
Missouri	U.S.A.	1354	240 000	176	2
Lo (tributary of yellow)	China	26	210 000	7890	—
Kosi	India	61	190 000	3117	1.8
Mekong	Thailand	786	187 000	484	11.1
Colorado	U.S.A.	630	149 000	422	0.16
Red	Vietnam	118	143 000	1207	3.9
Nile	Egypt	2944	122 000	39	2.8

(Source: Garde R.J., 2006).

Table 1.2: Mean Erosion Rates in Different Continents

Continent	Area, 10 ⁶ km ²	Erosion rate, tons/km ² /year
Africa	29.81	35 - 72
Asia	44.89	208 - 229
Australia	7.86	43
North and Central America	20.44	84 - 113
South America	17.9	100 - 148
Europe	9.7	50 - 75

(Source: Garde R.J., 2006)

1.3.3 River Bank Erosion-A Natural Threat

Riverbank erosion is one of the major natural threats in Bangladesh. Every year, millions of people are affected by erosion that destroys standing crops, farmland and homestead land. It is estimated that about 5% of the total floodplain of Bangladesh is directly affected by erosion. Some researchers have reported that bank erosion is taking place in about 94 out of 489 upazilas of the country. A few other researchers have identified 56 upazilas with incidence of erosion. At present, bank erosion and flood hazards in nearly 119 upazilas have become almost a regular feature (BWDB, 2011). Of these, 35 are severely affected.

The effects of bankline erosion and widening of the river channel have been great. Analysis of population data, combined with the satellite image analysis indicates that during the period 1981-92/93, an average of almost 64,000 people were displaced by bank erosion every year or 728,000 people over the whole period. More than half the displacement is along the Brahmaputra-Jamuna. This ignores changes in the chars within the changing banklines. Char erosion and accretion results in more people being displaced, and in the Brahmaputra-Jamuna it is found that 90 percent of the bank area had changed between char and water at least once during 1973-92. Therefore, a majority of char inhabitants are likely to have moved during this period. Due to this bank erosion is marked as a significant and growing economic hazard (The World Bank, 1995).

During the last 200 years or so, the channels have been swinging between the main valley walls. During the monsoon, extensive overbank spills, bank erosion and bank line shifts are typical. The gradual migration or shifting of channels of the major rivers in Bangladesh amount to anywhere between 60m to 1,600m annually. In a typical year, about 2,400 km of the bank line and 6000 hector land experiences major erosion (Rahman, 2010). The unpredictable shifting behaviour of the rivers and their encroachments not only affect the rural floodplain population but also urban growth centers and infrastructures.

Rivers erode landmasses and carry the water sediment to the ocean. A well-controlled system of physical and hydraulic features is maintained in water and sediment transport processes. The inter relationship between the attributes and their details in this organized system are highly complex and it is hard to visualize many of them simultaneously (Rahman et al, 2012). However these interrelationships from the typical characteristics of rivers and some knowledge of the basic types of rivers are necessary before complex relationships can be understood. So understanding the river behavior for erosion is a major work to prevent the losses.

1.3.4 Selection of the Study

The rate of erosion along the major rivers varies over time and space. It has been observed that the rate of erosion along a river varies with the magnitude of flood flow, characteristics of bank material and phases of planform developments as development of chars which changes the flow characteristics etc.

Riverbank erosion generally occurs at the outer banks of flanking meandering channels but for braided river, bank and bed scour is mostly associated with channel confluence and bends (Halcrow, 2002). Oblique flow plays a vital role for erosion due to presence of frequent bars and islands. Not only that rate, of erosion largely depended on the characteristics of bank and bed material. The bank materials of the rivers in Bangladesh have been broadly categorized into two groups-highly erodible and less erodible. With an oblique flow attacking the bank, the rate of erosion is 1 to 20m/yr if the bank is composed of less erodible materials. On the other hand, the rate of erosion would be several hundred meters per year in the case of highly erodible bank material (BWDB, 2013).

The braided rivers have unique behavior due to the presence of oblique flow. Braided rivers consist of numerous alluvial channels that divide and rejoin around bars and islands, forming an intertwining structure that resemble a braid. The dynamic nature of a braided river causes these channels to shift and migrate across the river's braidplain. It is this dynamic nature that makes braided rivers both interesting and

difficult to study, especially in a quantitative way. There are several ways in which such large, complex systems could be quantitatively approached.

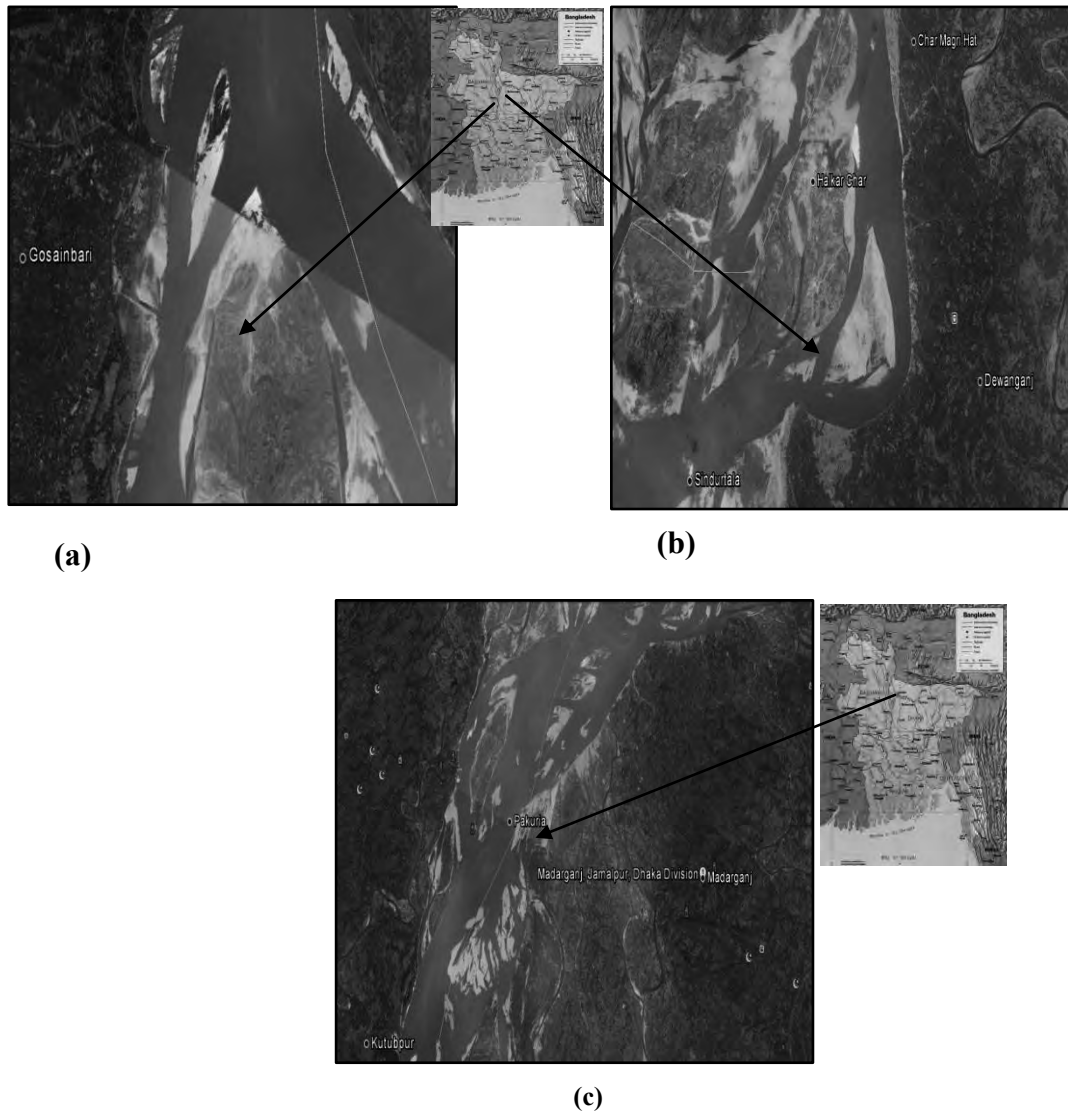


Figure 1.4: Presence of Oblique Flow in Bangladesh: (a) Oblique Flow at Gosainbari, (b) Oblique Flow at Dewanganj, (c) Oblique Flow at Madarganj
(Source: Google earth on 18/07/2013)

The Brahmaputra-Jamuna in Bangladesh is a classic example of a braided river and is highly susceptible to channel migration and avulsion. These oscillations cause massive riverbank erosion. Many braided rivers in Bangladesh are affected by significant bank erosion but the effect becomes most severe when oblique flow

develop in a channel i.e erosion pattern changes when secondary flow contributes to a straight flow.

Erosion pattern of Jamuna River is mostly affected due to oblique flow among all braided rivers in Bangladesh. Sirajgonj Hard Point is one of the most important examples of effect for oblique flow (Rahman et. al, 2012). Moreover, there is oblique flow in many parts of rivers in Bangladesh. Figure 1.4 represents some example of the process in Bangladesh.

Many bank protection works for major and minor river has been carried out by BWDB e.g. Jamuna-Meghna River Erosion Mitigation project, Sirajgong Hard point protection (Jamuna river), revetment work at Chandpur (Meghna river), Godagari (Ganges river), Titporal (Jamuna river) etc to prevent river bank erosion. Stone block, geo-bag and boulders have been used as bank protective material. Pre and post intervention of river training works showed that after completion of protection works some problem occurred such as i) velocity reduction which results in closing of main channel, ii) diversion of flow, iii) erosion in near char area, iv) sever bank erosion near adjacent area of protective work due to direct hit of flow (Rahman, 2012) etc. Studies on feasibility study and morphological changes have been carried out for those projects. The problems could be overcome if flow characteristics can be analyzed before implementation and detail physical model study is the only way for better understanding the flow behaviour of rivers (DHV Consultants, 2000).

So, there is a huge opportunity of research work on oblique flow and bank protection work to observe its effect on hydrologic and hydraulic parameters of a river. This type of research is also helpful for understanding the behavior of erosion pattern to make a protective work and materials workable and sustainable under the effect of oblique flow.

The study has been done to observe a part of a braided river i.e. the effect of oblique flow on a straight river bank and as well as on protection work. This research has been

done as an independent work to define behavior of a straight river bank for oblique flow.

1.4 Research Objective

The research has been carried out in order to observe the detail behaviour of a braided river due to oblique flow through physical modeling.

The specific objectives of the study are:

1. To observe the fluvial process (specially erosion on straight bank and bed) under oblique flow condition and with char (island) movement.
2. To analyze the effect of oblique flow on different bank protection works.
3. To analyze the behaviour of launching apron for different protection material.

1.5 Possible Outcome of the Research

The study has been done as a unique work to understand the effects of oblique flow. This work would be helpful as a knowledge bank for:

1. Better understanding the effect of oblique flow on bank protection work.
2. Assessment of factors for launching apron equation due to oblique flow on a straight bank.

1.6 Organization of the Report

This paper consists of six (6) chapters to present the work clearly. The contents of the chapters are as follows:

Chapter one includes general discussion on river system of Bangladesh and nature of rivers. Channel shifting tendency due to bank erosion in Bangladesh and around the world has been presented. This chapter gives emphasis on better understanding of the erosion pattern by means of Physical Modelling works. It also contains the research objectives.

A short presentation of available studies on modelling works on oblique flow and bank protection work has been included in chapter two as literature review. Hydro morphological behaviour of rivers in Bangladesh has also been discussed in the chapter.

Chapter three contains the basic theory on river characteristics and bank erosion. The theory for set up of a physical model has also been included here. The step by step methodology that has been adopted to complete the physical modelling work has been presented in this chapter.

A detail description of development of physical model with its initial parameters, model layout fixation procedure and planning for execution of the modelling work has been discussed in chapter four.

Chapter five contains experimental results from the physical model that are associated with bank erosion and protection work. A short description on the test conditions, observations and channel behaviour on each experimental setups has been discussed in this chapter.

The study ends in chapter six by conclusion of the study and recommendation for future study. This chapter also contains an overall summary on behaviour of river due to oblique flow based on experimental setups.

Chapter 2

LITERATURE REVIEW

2.1 General

The large rivers Jamuna, Brahmaputra, Meghna are braided in Bangladesh (Wheelock, 2002). Braided rivers means rivers “having a number of alluvial channels with bars and islands between confluences & bifurcations again” (Lane, 1957). Braided form developed before any depositional changes (Richardson and Thorne, 2001). Most rivers take the braided form when the width becomes 60 times the depth (Shawn Wheelock, 2005). Individual channels and bars in such rivers can evolve, migrate, and switch position within days or hours of competent flow, so that the overall pattern is bewilderingly variable and complex (Ferguson et al, 1992).

The arrangement of secondary channels is dynamic through time, changing as the river modifies its channel through the transportation and deposition of sediment. During the last decade, the trend in braided river research has shifted from describing and analyzing static characteristics to studying characteristic aspects of the dynamic behavior. This shift has not only been the result of advanced technology in measuring equipment and computational power required to study dynamic properties.

Increment of flood frequencies at braided rivers in Bangladesh has caused substantial changes in the river plan form, which imposed dramatic damages to the inhabitants and to the infrastructure of the corresponding regions. These catastrophes demonstrate the urgent need for a thorough understanding of braided river dynamics and for the ability to forecast the evolution of the plan form changes in the short and medium-term future (Hossain et al., 2010).

The braided stream characterized by a network of interlacing channels with numerous sandbars enclosed in between them. The sandbars, known in the Bengali as chars do not, however, occupy a permanent position. The river deposits them in one year very often to destroy and redeposit them in the next rainy season and it is difficult to

predict the behavior for a braided river. For example the process of deposition erosion and re-deposition has been going on continuously making it difficult to precisely demarcate the boundary between the district of Pabna on one side and the district of Mymensingh, Tangail and Dhaka on the other. Breaking of a char or the emergence of a new one is also a cause of much violence and litigation (Best, 1997).

Riverbank erosion is a major problem associated with the large rivers in Bangladesh, such as the on average 12 km wide Brahmaputra/Jamuna and has severe consequences to the livelihoods of those living on floodplains. While normal floods are considered beneficial for agriculture and fisheries, erosion and continuous river widening causes the loss of important infrastructure as well as highly productive agricultural lands and threatens settlements. Erosion continues to impact on those living on the increasingly denser populated floodplains, and is likely to be exacerbated by climate change. Uncontrolled and increased riverbank erosion increases the risk of flood damage apart from the loss of vital infrastructure. Further investments are deferred and the full agricultural potential of the fertile floodplain land cannot be realized (Best, 1997).

2.2 Hydro-Morphological Characteristics of River System in Bangladesh

Natural rivers are dynamic and physically and biologically complex (Tockner & Stanford, 2002). They are characterized by a set of fluvial styles including straight, braided, wandering and meandering channels (Richards et al., 2002). Conditions which promote braided channel formation include (i) an abundant supply of sediment, (ii) rapid and frequent variations in water discharge and (iii) erodible banks of non-cohesive material (Church & Jones, 1992).

The major rivers in Bangladesh are characterized by wide meandering braided at places and are of very flat gradient. The principal geometric feature of much of Bangladesh is the deltaic deposits of alluvium brought down by the rivers from the large catchment lying outside the border of Bangladesh (EU, 1993).

The Brahmaputra and Jamuna river is wandering braided and anabranching with a discharge of $3,000\text{m}^3/\text{s}$ to $1,00,000\text{m}^3/\text{s}$ and grain size of bed material varies from

0.165 mm to 0.22mm with a slope of 0.00007. On the other hand the Padma river is meandering and braiding combination with a discharge of 5,000m³/s to 1,20,000m³/s and channel slope is 0.00009 with 0.009mm to 0.14mm grain size of bed material. The Meghna river is meandering, locally anabranching having a varying discharge of 10,000m³/s to 1,60,000 m³/s with a channel slope of 0.00002 and grain size of bed material is 0.14mm . The Brahmaputra, the Padma and the Meghna are 11km, 3-15km and 1-13 km wide respectively (BWDB, 2010).

Among the three rivers Brahmaputra carries highest sediment and it has been estimated as 387 to 815 million tons annually which increases up to 10 million metric ton/day in flood. Padma river carries combined flow of Ganges and Brahmaputra and annual estimated suspended sediment varies from 563 to 894 million tons. The upper Meghna river transports about 13 million tons of suspended sediment annually.

Studies stated that the bank erosion rates of the three main rivers are very similar but for Padma the bank erosion is restricted to the boundary of active corridor that consists of alluvial and deltaic silt deposits, whereas the floodplain outside of it is more resistant to erosion. Flow attacks any bank of Brahmaputra/Jamuna and new courses outside the active floodplain are created frequently (BWDB, 2010). Braided rivers as Brahmaputra/Jamuna consist of multiple channels with bars and islands and often with poorly defined banks of non-cohesive sedimentary materials which is much vulnerable to erosion (Tockner, 2003).

2.3 Previous Studies on Braided River and Protection Work

Braided river is highly susceptible to channel migration and avulsion. Those rivers prevail in mountainous and glacial regions and are highly dynamic systems characterized by intensive erosion, sediment transport and deposition, and frequent channel shifting. When rivers enter the developing stage they become sluggish and braid. Some rivers cause erosion in large scale and high frequency due to their unstable character. These rivers assume a braided pattern consisting of several channels separated by small islands in their courses. River bank Erosion in braided river is an endemic and recurrent natural common threat in Bangladesh.

The abrupt meeting of two channels each having independent flow and sediment discharge regimes creates unique erosional and depositional environments with consequent changes in channel morphology (Miller, 1958; Best, 1986). The studies on braided river can be divided into three parts as (a) Physical modeling, (b) Mathematical modelling and (c) Neumerical modelling.

(a) Physical modelling:

Work on tributary effects on main stem morphology done by Mosley (1976) and Best (1988) focused primarily on changes in hydraulic geometry (i.e., width, depth and form ratio) due to changes in flow discharge between tributaries and main stems. Changes in hydraulic geometry due to secondary flow were evaluated in terms of the ratio between discharge or its surrogate drainage area by Miller (1958) among the minor tributary (Q_2), major tributary (Q_1), and the main stem downstream of the meeting channel (Q_0) (Roy and Woldenberg, 1986).

Leopold et. al. (1964) found that consistent morphological changes in the anticipated directions occurred when the symmetry ratio (Q_2/Q_1) approached approximately 0.6 to 0.7, indicating a threshold relationship between tributary and main stem river sizes. Although different types of changes in channel and valley morphology due to large influxes of sediment from tributaries has been studied by Small, 1973; Church, 1983; Benda, 1990; Wohl and Pearthree, 1991; Pizzuto, 1992; Grant and Swanson, 1995; Hogan et al., 1998; Benda et al.,(2003a, 2003b).

Study of the morphology of the braided rivers and processes governing their behavior is important in geomorphology, geology, hydrology, and environmental studies (Victor et. al, 1999). Model study Salt river channelization project done by Yung et al. (1985) determine the adequacy of a channelization scheme on for Salt River near Sky Harbor International Airport. Distorted movable-bed model is utilized to study erosion and deposition patterns, velocity pattern, incipient motion of bed particles and bank stability in the proposed scheme. The purpose of the study was to investigate the

behavior of the channel reach under 10 yr, 50 yr, and 100 yr floods and to determine the expected depths of scour and deposition and the degree of damages caused by such floods; and suggest recommended design improvements for the channelization project.

A joint study was undertaken by the University of Nottingham and Flood Action Plan 24 (FAP-24), the River Survey Project of Bangladesh, to investigate patterns of secondary flow around a braid bar on the Brahmaputra River in Bangladesh. Secondary currents defined as velocities in the plane perpendicular to the axis of primary flow (Prandlt 1952). Measurements of primary and secondary flow taken at study section a strongly curved anabranch channel apex, indicate that flow structures in bends of braided rivers share common features with patterns observed in meander bends of single thread rivers. This finding suggests that at least some elements of the current understanding of process-form interaction in meandering rivers may be transferable to braided rivers. The results at another part of the study area shows the flow bifurcation and helical flow associated with each thalweg affects the distributions of primary and secondary flow, which in turn drive the morphological change of the bifurcation through their influence on the distribution of near boundary velocity, sediment concentration, and pattern of sediment, scour and deposition (Richardson et al., 1998).

(b) Mathematical modelling

A conventional one-dimensional mathematical model for unsteady sediment-laden flow had been developed by Zhang et al. in 2004 on the Lower Yellow River. It is found that sediment transport is of significance with regard to the flooding behavior of hyper concentrated flows.

Swanson (1995) found that abrupt introduction of sediment and organic materials at tributaries trigger numerous types of changes in morphology in the vicinity of combined channel. Channel gradient-induced longitudinal variations in sediment transport rate reduce substrate size and increase floodplain width upstream of combined channel, offset by other tendencies on the downstream side of channel

including coarser substrates, increased channel width, increased pool depth, and increased occurrence of bars (BWDB and IWM, 2006).

(c) Neumerical modelling

Between Peale's (1879) and that of Leopold and Wolman (1957), most of the work done on braided rivers was largely qualitative in nature. Although, several studies such as Melton (1936) began developing the empirical relationships that have become the staple of modern fluvial geomorphology. In 1952, Rubey brought the prospect that the braided condition may represent an equilibrium state to the forefront of geomorphic inquiry (Wheelock, 2002).

In 2001, a 2 dimensional numerical analysis of river channel processes with bank erosion had been done by Duan and detail bank failure mechanism has been discussed in the analysis.

The scope of research which had been done by Nykanen D. Sapozhnikov V. and Georgiou E. at 1998 is to investigate further the presence of spatial scaling relationships in natural braided river patterns using SAR imagery and to explore how this scaling might be affected by flow rate, braiding index, and large-scale topographic controls such as mountains.

A two-dimensional composite numerical model is developed by Wang et al., (2008) that consists of a depth-averaged 2D flow and sediment transport sub model and a bank-erosion sub model. The model incorporates a new technique for updating bank geometry during either degradational or aggradational bed evolution, allowing the two sub models to be closely combined. Using the model, the fluvial processes in the braided reach of the Lower Yellow River between Huayuankou and Laitongzhai are simulated including the water-surface elevation, variation of water-surface width, and variations of cross-sectional profiles.

Murray and Paola (1994) developed a cellular automaton model of a braided river using a simple, deterministic approach of water flow over a cohesionless bed. Their model reproduced the main spatial and temporal features of natural braided rivers. Their results suggested that the main factors essential for braiding were bed load sediment transport and laterally unconstrained free-surface flow.

Sapozhnikov and Foufoula-Georgiou (1996, 1997) have shown that an effective and fruitful way to study interactions of small-scale and large scale dynamics of complex natural systems is via statistical scaling analyses, i.e., analyses aimed at determining how morphological or dynamical properties of the system at one scale relate to those at another scale. Such scaling relationships are commonly found in natural systems, including single channels and river networks. This study has been done by some researchers as Tarboton et al., 1988; La Barbera and Rosso, 1989; Nikora, 1991; Sapozhnikov and Nikora, 1993; Peckham, 1995; Beauvais and Montgomery, 1996. But those works have not yet been fully developed or understood in braided rivers.

Braided river systems manifest themselves over a large range of scales (e.g., from the smallest channels of a few meters to the whole braidplain width of tens of kilometers). The issue of scale is an essential element when applying the knowledge gained from a small part of a braided river to a larger part of it, from one braided river to another of different size, or from a laboratory model to a real braided river.

Again Sapozhnikov and Foufoula-Georgiou (1996) found through analysis of the spatial structure of traced, digitized aerial photographs, that spatial scaling exists in the morphology of natural braided rivers. Spatial scaling implies that morphological properties (e.g., area covered by water) of the system at one scale relate to those at another scale via a transformation which involves only the ratio of the two scales. Through the production of a laboratory braided river in a small experimental facility (0.75 m, 35 m) at the St. Anthony Falls Laboratory, Copyright 1998 by the American Geophysical Union.

Sapozhnikov and Foufoula-Georgiou (1997) also found the presence of scaling in the temporal evolution of braided rivers, called dynamic scaling. Dynamic scaling implies that space and time can be appropriately rescaled such that the evolution of the spatial structure of a small part of a braided river is statistically indistinguishable from that of another larger part or of the whole river. Such relationships could be used, for example, to statistically predict large less frequently occurring changes in the river from smaller more frequent changes or could be used to make inferences about the underlying physical mechanisms controlling the evolution of braided rivers.

It is imperative that the above findings of dynamic scaling are further investigated and that the presence of spatial scaling is further verified using a wide range of natural braided rivers. Braided rivers often exist in scarcely inhabited, high-latitude, glaciated areas and are also constantly evolving, which makes it difficult to perform any sort of ground-based measurements. Also, obtaining aerial photographs at an adequate temporal resolution is difficult and often prohibiting for a single investigator. On the other hand, remote sensing is an attractive means of continually monitoring these complex systems from space. The technology of synthetic aperture radar (SAR) imagery has opened a door of opportunity in the area of quantitative studies of braided rivers, but only a very few studies have existed to date (e.g., Smith et al., 1995, 1996).

Simulation of Missouri river bed degradation has been observed by Forrest et al. (1986). The purpose of study was to simulate the long-term bed evolution in Missouri river having non-uniform bed sediment.

George A. Griffiths (1993) found that bed load transport capacity in braided gravel-bed rivers varies with downstream changes in hydraulic geometry by numerical modelling.

Numerical model has been developed by Millar et al., (1993) to find the effect of bank stability on geometry of gravel rivers. They found some relations that calculate the mean bed, bank shear stress and bank stability. The outcome of the study was mainly done for understanding channel geometry.

Numerical modeling approaches for assessing river channel width adjustments and complements the review of fluvial hydraulics had been carried out by the ASCE Task Committee on Hydraulics in 1998. The study revealed the field-based approach for assessing channel width adjustments.

The analysis results of parameter sensitivity tests indicate that bank erodibility coefficient and critical shear stress for bank material are sensitive to the simulated bank erosion process.

Most research on braided rivers to date has concentrated on understanding the small scale processes such as flow and sediment flux around an individual channel bar (Ashmore et. al, 1983 and 1992; Best, 1986, 1988; Bristow et. al, 1993; Mosley, 1976, 1977 and Robert, 1993). These detailed studies of processes in a small area are valuable but do not necessarily lead to improved understanding of the mechanics of the entire system. Physically based studies and mechanistic modeling of braided rivers aimed at understanding the entire system would be too computationally intensive. A full solution of the governing equations for flow around a single confluence is intensive, and a braided river reach involves many such converging and diverging flow regimes around its numerous bars and islands. Also, there is relatively little quantitative information on how changes in one part of the system propagate to other parts and on which components of the small-scale flow and sediment dynamics contribute to the overall behavior of the system.

Recently, some alternative approaches to studying the morphology and dynamics of braided rivers have been proposed. These type of studies aim to determine which physical processes are critical and how they affect the dynamics of the system as a whole and then concentrate on detailed studies of these processes.

2.4 Summary

The existing models and frameworks are mostly qualitative. Despite of changing nature, braided rivers have not been studied as extensively as single-channel rivers and river networks. In particular, there is a significant lack of quantitative studies in braided rivers.

No systemic pattern has yet been observed of the erosion hazards because of the involvement of a large number of variables in the process. The intensity of bank erosion varies widely from river to river as it depends on such characteristics as bank material, water level variations, near bank flow velocities, plan form of the river and the supply of water and sediment into the river. For example, loosely packed, recently deposited bank materials, consisting of silt and fine sand, and are highly susceptible to erosion. Rapid recession of floods accelerates the rates of bank erosion in such materials.

So, this study has been done to observe the fluvial process of braided river due to oblique flow by Physical Modelling. A part of braided river that means oblique flow with a straight river bank has been considered in the study. Details of model work have been presented in chapter 4.

Chapter 3

THEORY AND METHODOLOGY

3.1 General

This chapter consists of a short description of common river types, erosion pattern, reasons for erosion, theory for bank protection work with scaling of different parameters between model to prototype for the study and experimental methodology.

3.2 Classification and Causes for Formation of Different Channel Patterns

Classification of channel patterns proposed by Leopold (1957) is popularly accepted all over the world. Leopold divided alluvial channels into three patterns that are straight, meandering and braided mainly based on the planform of a river. According to the composition of incoming sediment from the river basin, Schumm (1981) divided alluvial rivers into three major patterns that are bed load type, wash load type and mixed type. He further divided alluvial rivers into fourteen sub-patterns according to valley slope, stream power and amount of incoming sediment (Reza, 2011). It is familiar to most morphologists and here it is not discussed in details.

Classification proposed by Russian scientist Rosinski (1958) is rather popular in China in fifties and sixties. According to Rosinski's concept, depending on relative erodibility of river bed and bank, river can be divided into three categories: Straight, braided and meandering. The corresponding fluvial are periodically widening, migrations of meanders and wandering. Figure 3.1 and 3.2 shows the illustrations of the basic type of rivers:

(a) Straight Channel

A straight channel is one that does not follow a sinuous course. Straight channels are rare in nature according to Leopold and Wolman (1957). The river bank is not easy to be eroded and bars move relatively fast, alternative bars move relatively downstream wards. Before obvious bank erosion happens and bend is formed, the attacking point

by the flow and the corresponding erosion location has changed. Therefore no regular bends are formed and the river keeps its straight outline. Such situation happens when high flood plain consisting of cohesive soil and covered by plants, which is hardly erodible and sand bed exists. Under such condition a straight river is formed (Reza, 2011).

A stream may have moderately straight banks but the thalweg or path of greatest depths along the Channel is usually sinuous. Straight channels with prismatic cross-section are not typical in nature. It is only feasible for artificial channel. To differentiate between straight and meandering channels and sinuosity of a river, the relation between thalweg and length to down valley distance is most frequently used. Sinuosity varies from 1 to 3. Sinuosity of 1.5 is taken as the division between meandering and straight channels by Leopold et al. (1964). A series of shallow crossings and deep pools is formed along the channels in a straight channel with a sinuous thalweg developed between alternate bars (Figure 3.1 and 3.2).

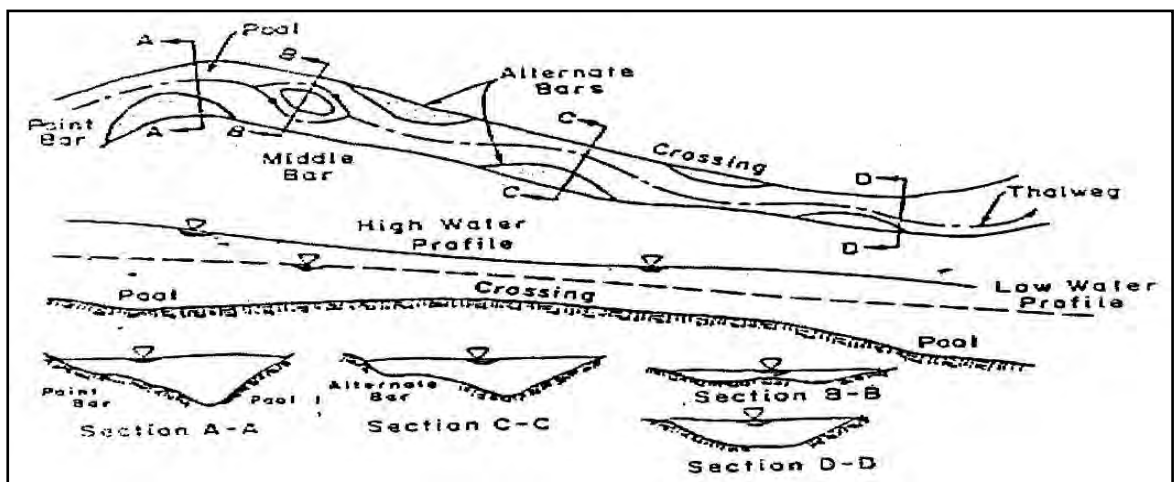


Figure 3.1: Channel Patterns

(Source: Schumm, 1977)

(b) Meandering Channel

A meandering channel is one that consists of alternating bends, creating an S-shape to the top-view of the river. In particular Lanne (1957) showed that a meandering channel is one where channel alignment consists mainly of distinct bends, the shape of which have not been established principally by the varying nature of the topography

through which the channel flows. In that case river banks are prone to be eroded and bars move relatively slowly, a meandering river is formed. When river bed consists of gravel or the bed is covered by hardly erodible material, such situation happens (Reza, 2011).

The meandering river contains a sequence of deep pools in the bends and shallow crossings in the short straight reach connecting the bends. The thalweg flows from a pool through a crossing to the next pool forming the typical S-curve of a single meander loop at higher stages. In the severe case, the changing of the flow causes chute channels to develop across the point bar at high stages.

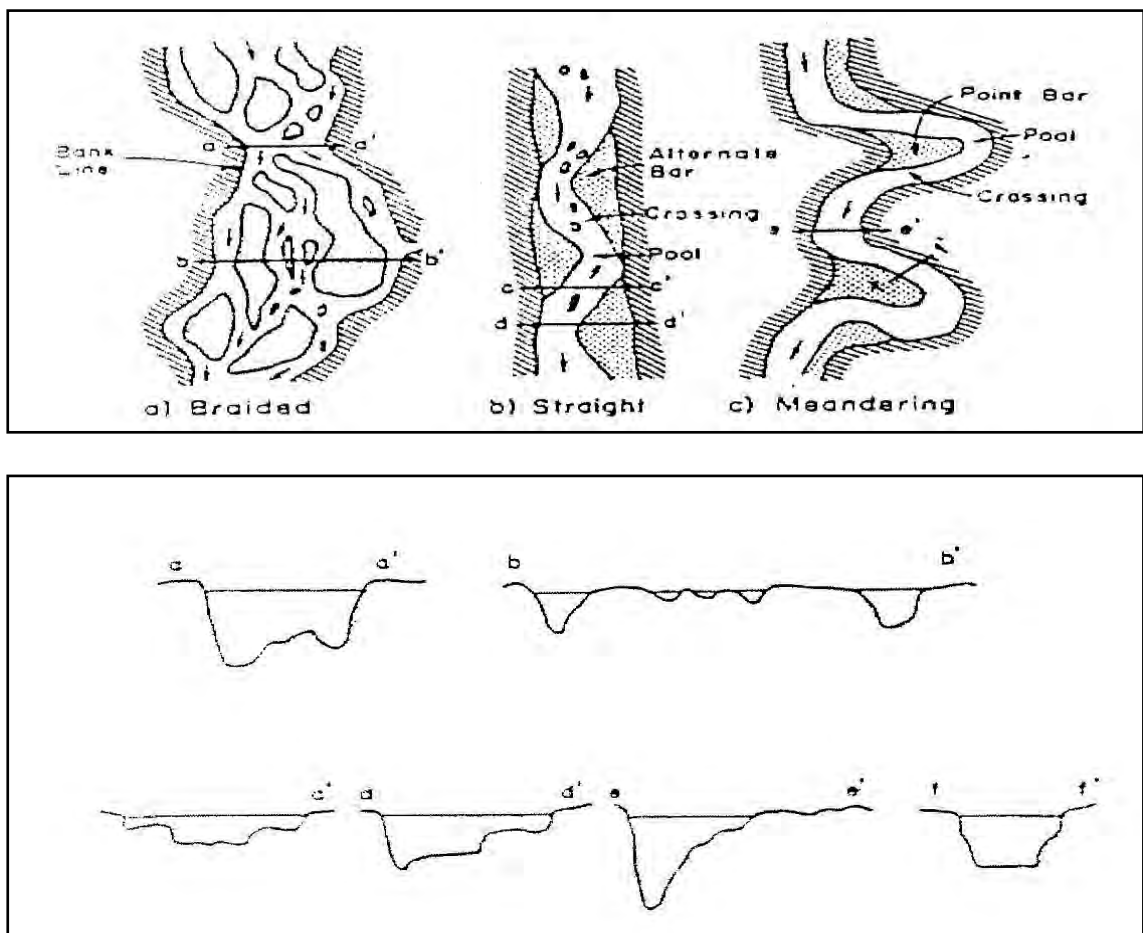


Figure 3.2: Various Features of Channels

(Source: Schumm, 1977)

(c) Braided Channel

A braided river is one with generally wide and poorly delineated unstable banks, and is depicted by a steep, shallow route with multiple channel divisions around alluvial islands (Figure 3.2 a). When river banks and river bed consist of similar material and both of them are easily erodible braided river is formed. Leopold and Wolmen (1957) studied braiding in a laboratory flume. They deduced that braiding is one of many patterns that can maintain quasi-equilibrium among the variables of discharge, sediment load and transporting ability. The two primary reason that may be accountable for the braiding is stated by Lane (1957) as: (1) Overloading, that is the channel may be full with more sediment than it can transport consequently accumulating part of the load, deposition occurs, the bed aggrades and the slope of the channel increases in an effort to maintain a graded condition and (2) steep slopes, which generate high velocity, multiple channels develop resulting the overall channel system to widen with rapidly forming bars and islands. The multiple channels are generally unstable and change position with both time and stage (Reza, 2011).

3.3 Aggradations/Deposition and Degradation/Erosion of Channels

Aggradations (i.e. rising of the river bed by deposition) occur in a river if the amount of sediment coming into a given reach of a stream is greater than the amount of sediment going out of the reach. Part of the sediment load must be deposited and hence, the bed level must rise (Ranga Raju, 1980). In alluvial channels or streams bed aggradations evolves primarily form the passage of flood events. The bed profile consequently reduces the section factor of the channel. Sediment deposition along streams or in reservoirs is a complex and troublesome process. It creates a variety of problems such as, rising of river beds and increasing flood heights, meandering and over flow along the banks, chocking up of navigation and irrigation canals and depletion of the capacity of storage reservoir (Hossain, 1997).

Bed degradation (i.e. lowering of the bed by scouring) occurs when the amount of sediment coming into a given reach of a river is less than the amount of sediment going out of it (Ranga Raju, 1980). The excess sediment required to satisfy the

capacity of the river will come from erosion of the bed and there will be lowering of the bed level, which will result in shifting of thalweg line of the river. If the banks are erodible material can be picked up from the banks and widening of the river will also result. Hence the whole process of aggradations and degradation of rivers have potential effects on various hydraulic and geometric features of rivers such as cross sectional area, section factor, shifting of thalweg line etc (Reza, 2011).

(a) Types of Erosion and Deposition

Erosion and deposition is a result of sediment transport. Erosion can be classified into two kinds- a) lateral erosion and b) vertical erosion.

Flow attacks the toe of a bank and carries away eroded sediment and gradually water depth along the bank becomes larger and larger and finally the bank collapses. By this way the bank line retreats. That type of erosion is lateral erosion. Erosion along the concave bank of a bend is typical lateral erosion.

During large flood water depth on flood plain becomes large enough and flow velocity reaches a high enough value. Such flow erodes flood plain and gradually excavates a branch. That type of erosion is vertical erosion. Natural cutoff at the neck of a river loop is an example of vertical erosion.

Deposition is also two types as channel siltation and flood plain deposition. Siltation in channels or branches can be called as channel siltation and deposition on flood plain is called as flood plain deposition (EU, 1993).

3.4 Causes of Bank Erosion

Rivers and streams are products of their catchments. They are often referred to as dynamic systems which mean they are in a constant state of change. The factors controlling river and stream formation are complex and interrelated. These factors include the amount and rate of supply of water and sediment into stream systems, catchment geology, and the type and extent of vegetation in the catchment. As these

factors change over time, river systems respond by altering their shape, form and/or location.

Stream bank erosion is a natural process that over time has resulted in the formation of the productive floodplains and alluvial terraces. The rate at which erosion is occurring in stable systems is generally much slower and of a smaller scale than that which occurs in unstable systems (Queensland Government, 2006).

Events like flooding can trigger dramatic and sudden changes in rivers and streams. However, land use and stream management can also trigger erosion responses. The responses can be complex, often resulting in accelerated rates of erosion and sometimes affecting stability for decades. Over-clearing of catchment and stream bank vegetation, poorly managed sand and gravel extraction, and stream straightening works are examples of management practices which result in accelerated rates of bank erosion.

Erosion can also be accelerated by factors such as:

- Stream bed lowering or infill.
- Inundation of bank soils followed by rapid drops in flow after flooding.
- Saturation of banks from off-stream sources.
- Redirection and acceleration of flow around infrastructure, obstructions, debris or vegetation within the stream channel.
- Removal or disturbance of protective vegetation from stream banks as a result of trees falling from banks or through poorly managed stock grazing, clearing or fire.
- Bank soil characteristics such as poor drainage or seams of readily erodible material within the bank profile.
- Wave action generated by wind or boat wash.
- Excessive or inappropriate sand and gravel extraction.
- Intense rainfall events (e.g. cyclones).

This research has been done based on bank erosion. Bank Erosion is a function of Erodibility and Erosivity that means Bank Erosion is proportional to multiplication of Erodibility and Erosivity. Where, Erosion is the lateral movement of the bank, Erodibility is resisting force i.e intrinsic property of bank which is a function of soil, vegetation, bank angle etc and Erosivity is the driving force i.e property of hydraulics and function of near bank shear stress (Wheelock, 2002). In this study erosivity is main consideration.

3.5 Processes of Stream Bank Erosion

The various mechanisms of stream bank erosion generally fall into two main groups, bank scour and mass failure. In many cases of bank instability both become evident, often with either scour or mass failure being dominant. Bank scour is the direct removal of bank materials by the physical action of flowing water and is often dominant in smaller streams and the upper reaches of larger streams and rivers. Mass failure, which includes bank collapse and slumping, is where large chunks of bank material become unstable and topple into the stream or river in single events. Mass failure is often dominant in the lower reaches of large streams and often occurs in association with scouring of the lower banks. By looking carefully at the processes operating at a site it may be possible to narrow down the probable causes of instability.

(a) Bank Scour

Bank scour is the direct removal of bank materials by the physical action of flowing water and the sediment that it carries.

As flow speed increases, the erosive power of flowing water also increases and scour may occur. Increases in flow speed can be the result of natural or human induced processes. Undercutting of the bank toe is an obvious sign of scour processes. Effective strategies for combating scour are generally aimed at reducing flow speed through re-vegetation and in some cases through strategic bank or channel works (Queensland Government, 2006).

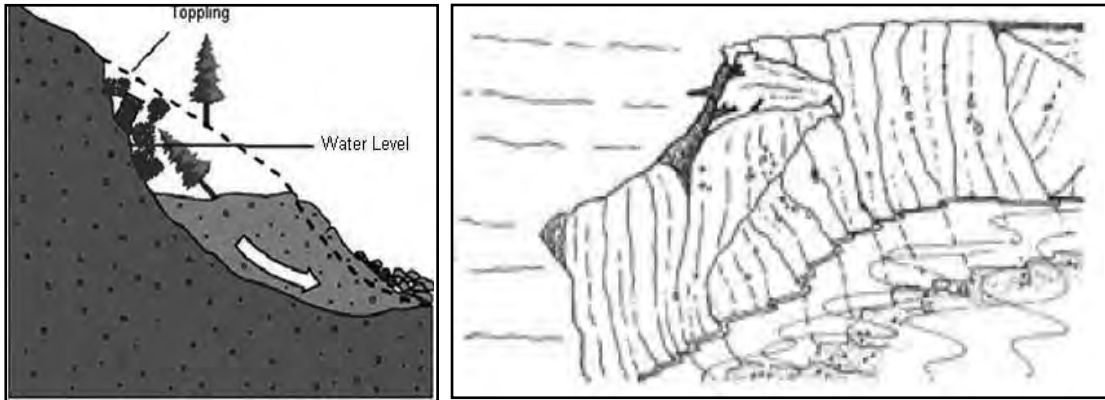


Figure 3.3: Undercutting of the Bank Toe- A Sign of Bank Scour

(Source: Queensland's Government, 2006)

(b) Mass Failure

Mass failure describes the various mechanisms of bank erosion that result in sections of the bank sliding or toppling into the stream. Mass failure is sometimes described as collapse or slumping.

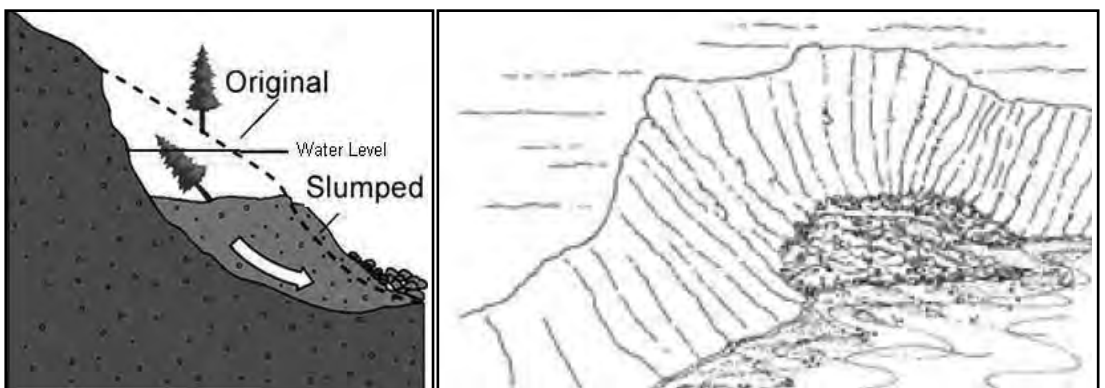


Figure 3.4: Slumping- A Common Type of Mass Failure

(Source: Queensland's Government, 2006)

Bare and near-vertical banks or areas of slumped bank materials are obvious signs of these processes. The causes of these types of failures are often difficult to determine but can include natural or collapse following undermining of the bank toe and slumping as a result of saturation after flooding are common examples of mass failure. Effective strategies for combating slumping or bank collapse are generally aimed at

stabilizing the bank toe and restoring bank vegetation and human factors (Queensland Government, 2006).

3.6 Channel Migration and Expansion

Bank stability depends on the behavior of the river during flood stage and the subsequent fall of the river. In a meandering river, changes and migration pattern are predictable because the river cuts on one bank and deposits on the opposite. Such scouring and bank erosion and deposition are related to the quantum of flow discharge, sediment transport, channel gradient and character of bank materials (EU, 1993).

In a braided stream, this type of cut and fill does not occur. Both banks may experience erosion or deposition simultaneously. Several factors are responsible, but Coleman (1969) identified the following:

- Rate of rise and fall of river level.
- Number and location of major channels during flood stage.
- Angles at which the thalweg approach the banks
- Amount of scour and deposition.
- Formation and movement of large bed forms.
- Cohesion and variability of bank materials.
- Intensity of bank slumping.

3.7 Process for Understanding River Behaviour

It is an urgent need to understand the river behaviour i.e its fluvial process to prevent the erosion. Riverbank erosion can be predicted through different approaches. The commonly exercised methods are: i) physical modeling, ii) numerical modeling and iii) empirical modeling (BWDB, 2013).

Physical modeling is done to

- Get a clear understanding of the processes.
- Identify the parameters controlling the process.
- Simulate the actual scenario in the field.

- Ensure the range of governing parameter controlling the river characteristics.

On the other hand MIKE21C is an advanced model for Mathematical modeling which is a 2-D flow solver that solves incompressible Reynolds-averaged and depth-averaged Navier-Stokes equations. The model is incorporated by k- ϵ turbulence model. Near field morphology, velocity, flow field, sediment transport etc can be obtained from a mathematical modeling. (Sumer B. M., 2013).

Moreover the numerical modeling embodies the numerical techniques used to solve the set of governing equation. The data from prototype is interpreted and placed in the appropriate prototype context. These interpretation processes close the modeling cycle and ultimately provides the scenarios to be compared (U.S.B.R, 2011).

Structural interventions to protect riverbank erosion are very costly. Physical modeling is a suitable method for predicting river behavior and also cost effective.

3.8 Outline of the Methodology for Physical Modelling

The outline of the methodology for the physical modelling has been divided into three parts – i) physical model setup ii) measurement of data for selected setup and observations and iii) analysis. With the view of achieving this research objective, working methodology has been predefined as follows:

(a) Selection of Model Type

First of all model type has to be fixed either it is distorted or undistorted. Selection of model details has been done based on “Hydraulic Modelling by J. J. Sharp”. Literature shows that when all the similarity requirements are fulfilled in a model or if a model is perfectly similar to its prototype then the model is said to be undistorted. A model is said undistorted model when all vertical lengths and horizontal lengths are reduced with a constant scale factor.

The research has been carried out as a basic research so model is considered as undistorted. The similarity of boundary resistance is ensured in a mobile bed model. The name movable-bed implies that in this type of model due attention is to be paid to sediment transport, erosion, deposition and bed-forming processes. The research objective is to focus on river bed so the model bed has been selected as mobile.

(b) Fixation of Model Scale

Model scale has been fixed based on the available facilities in the RRI. This scaling is needed to convert model data into prototype. The model has been developed at a scale ratio of 1:50 (both for horizontal and vertical) to use the existing model facilities of RRI.

Horizontal Scale ratio model to prototype, $\frac{L_m}{L_p} = \frac{1}{50}$

Vertical Scale ratio model to prototype, $\frac{Y_m}{Y_p} = \frac{1}{50}$

(c) Conversion of Gravitational Forces

Froude law models assert that the primary force causing fluid motion is gravity and that all other forces such as fluid friction and surface tension can be neglected.

$$F_m = F_p$$

$$\text{So, } \left[\frac{v}{(gL)^{\frac{1}{2}}} \right] m = \left[\frac{v}{(gL)^{\frac{1}{2}}} \right] p \dots\dots\dots(3.1)$$

As $g =$ gravitational acceleration is constant over the surface of the earth so,

$$\left[\frac{v}{(L)^{\frac{1}{2}}} \right] m = \left[\frac{v}{(L)^{\frac{1}{2}}} \right] p \dots\dots\dots (3.2)$$

Then, $V_p = \frac{v_m}{\left(\frac{L_m}{L_p}\right)^{\frac{1}{2}}} \dots\dots\dots (3.3)$

Scales for discharge can be verified by transforming the Froudian requirements into different forms. Q is proportional to the product of velocity and area so,

$$V \propto \frac{Q}{L^2}$$

Substituting in equation (3.1)

$$\frac{Q_p}{Q_m} = \left(\frac{L_p}{L_m}\right)^{\left(\frac{5}{2}\right)} \dots\dots\dots (3.4)$$

Transformation to take account of time is made using, $V \propto \frac{L}{T}$

$$\text{So, } \frac{T_p}{T_m} = \left(\frac{L_p}{L_m}\right)^{\left(\frac{1}{2}\right)} \dots\dots\dots (3.5)$$

(d) Conversion of Model Bed Slope

The regime theory refers to conditions in a river which is in equilibrium. For a particular discharge these conditions are developed over a period of times as the width, depth and bed slope adjusted through movement of sediment until scour balances deposition and the bed becomes stable. Studies have indicated that width is proportional to (discharge)^{1/2}, the depth is proportional to (discharge)^{1/3} and slope is inversely proportional to (discharge)^{1/6}.

Now when a river is considered to be a model it follows:

$$\frac{x_m}{x_p} = \left(\frac{Q_m}{Q_p}\right)^{\left(\frac{1}{2}\right)} \dots\dots\dots (3.6)$$

$$\text{and } \frac{y_m}{y_p} = \left(\frac{Q_m}{Q_p}\right)^{\left(\frac{1}{3}\right)} \dots\dots\dots (3.7)$$

$$\text{again } \frac{s_m}{s_p} = \frac{y_m x_p}{y_p x_m} = \left(\frac{Q_m}{Q_p}\right)^{-\left(\frac{1}{6}\right)} \dots\dots\dots (3.8)$$

(e) Selection of Bed Material

The bed material for a physical model is selected by two criteria. The first criterion provides information on the magnitudes of the required model velocities than on the nature of the bed. The second criterion states that the model bed must be denser than water.

D₅₀ = 0.168mm has been selected for the model. Scaling of bed material is not possible in the existing model facilities of RRI.

(f) Selection of Protection Work Type

Bank protection is done by different way for example groyne/spur, revetment, bundling works etc. Revetments are usually used in many situations where riverbank is to be protected in its existing position with little work needed to reform or re-shape the bank line or profile (Rahman, 2012). The common way of protecting a river bank e.g revetment has been considered for the research work.

(g) Selection of Protective Material

It is a common engineering practice throughout the world to use stone boulder, loose stones or riprap, C.C blocks etc as protective material and to hold river in place by protecting its bank against erosion (Froehlich, 2009). The behavior of launching apron is different for different materials (RRI, 2010).

Now-a-days geo-bag is being used as an alternative bank protective material as it is less costly than C.C block, easily available, easy to handle and can be prepared quickly. Geo-bags are effective during the emergency protection works when the banks are under the threats of erosion but C.C block cannot be constructed or placing of boulder is not possible (Bhuiyan T. H., 2009). Stone boulder has been used as protective material in this work. Geo-bag has also been used as an alternative protective material to find its behavior as now it is frequently being used in Bangladesh.

(h) Theory for Design of Bank Protection Work

Holding a river in place by protecting its bank against erosion with a continuous covering of loose stones or riprap is a common engineering practice that is used throughout the world. Riveting a bank this way, the armour protection work needs to extend below the lowest bed level expected at the toe of the underwater slope as the streambed scours. The facing can be installed in two general ways: (1) by excavating the bank so that armour material can be placed directly on a prepared slope, or (2) by placing a sufficient quantity of loose stone along the top of the bank so that it will fall

gradually and cover the slope as the bank recedes and undermines the stockpile. The first approach might be preferable, but construction is difficult or costly, especially when underwater excavation is needed. The second method has been used widely to stabilize the banks of both large and small alluvial streams by placing the rock supply on existing ground surfaces or in shallow excavations (Froehlich, 2009).

(i) General Considerations for Falling Apron Design Practices

The fundamental idea behind placing a volume of protective material at the top of an eroding river bank is that it will be launched or deployed by itself without direct human control when the edge of the rock supply is eroded at its base, allowing the material to fall downward along the slope to form a continuous protective cover.

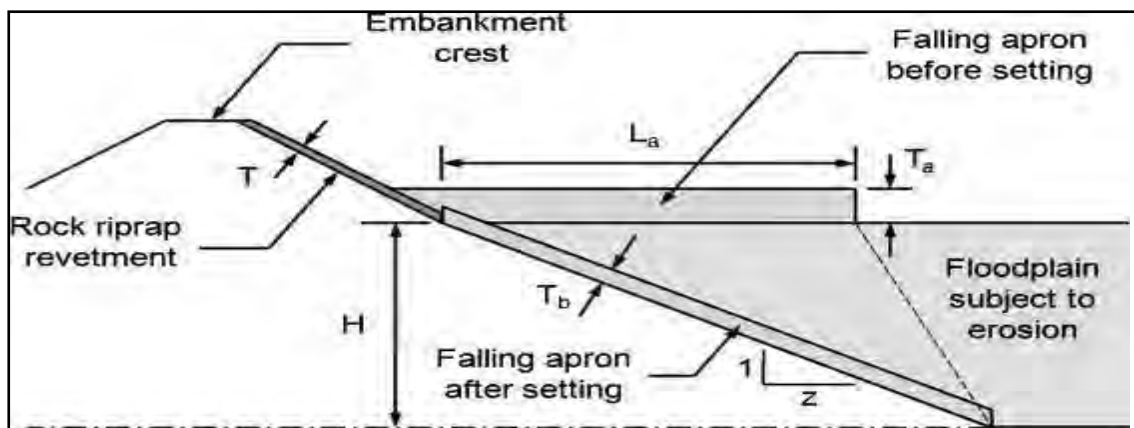


Figure 3.5: General Consideration for Protection Work

(Source: Froehlich C. D., 2009)

(ii) Apron Volume

Falling aprons formed from protective material riprap are often placed horizontally along the toes of embankments that are themselves protected from erosion by a layer of riprap as shown in Figure 3.5. To estimate the material volume needed for the apron, the average thickness of bank coverage T_b is usually assumed to equal some multiple of the thickness T of the loose rock facing placed on the upper embankment. If an upper embankment does not exist, or if the upper revetment is made from a material other than what is used in the falling apron, then for design purposes T equals the thickness of a protective cover that would be constructed on a prepared bank slope

from the apron material. Based on this notion, the volume of material that would be needed per unit length of an apron to cover an eroding bank completely is given by,

$$V_b = T_b H \sqrt{1+z^2}$$

Where, H is the height of the bank that needs to be protected and z is the ratio of the horizontal distance to the vertical distance of the eroded underwater slope covered by the launched material.

(iii) Apron Shape and Thickness

Spring (1903) proposes that the apron thickness at the junction of the apron and the constructed slope be the same as that of the upper slope covering, with the apron thickness increasing towards the riverbed. In such a case the thickness of the river end of apron will be 2.25 times the thickness of the riprap on the slope. This idea is endorsed by Verhagen et al. (2003) who suggest that constructing an apron in the form of a wedge-shaped layer, with more material near the river bank, rather than as a horizontal layer will offer more protection at the beginning of the deployment process.

Bell (1890), Spring (1903), and Gales (1938), all rely on a 2:1 (horizontal:vertical) underwater slope in their designs of falling aprons used to stabilize sand bed rivers in India. Richardson et al. (2001, page 6.31) suggest that when channels are formed in cohesionless soils, falling aprons can be designed for underwater slopes of up to 2:1. Van der Hoeven (2002, page 35) finds that the actual slopes of launched aprons usually range from 1.5:1 to 3:1, but in some cases may even be flatter, with the average about a 2:1 slope.

(iv) Effect of Bank Curvature

Depending on nature of channel a multiplying factor is commonly used for estimating the maximum natural scoured depth as 1.25, 1.5 and 1.75 for straight, moderate bend and severe bend respectively (BWDB, 1993).

(i) Selection of Model Parameters

Based on the requirement and available facilities preliminary parameters of the experimental setups have been calculated for fixing model layout.

(j) Fixation of Model Layout at Field

According to the calculated parameters a detail layout of the model has been developed at field (RRI, Faridpur). Three angles have been selected as 20°, 40° and 60°. Due to lack of time a boundary of 20° to 60° has been taken into considerations.

(k) Experimental Setup according to the Fixed Conditions

Outline for the secondary channel of the model and boundary has been developed before starting of a setup.

(l) Model Run and Collection of Necessary Data

Model run has been carried out according to experimental setups after completion of model construction. Necessary measurements of selected parameter and data collection have been done for each experimental setup before and after each run.

(m) Detail Analysis of Data

The measured data has been subjected to quick checks and a short analysis has been done in order to eliminate any inconsistency or doubt during the running period of the physical model. Again the data obtained from the experimental setup has been analyzed in details which have been presented in chapter 5.

3.9 Summary

Bank erosion and mass failure are common type of erosion. Erosion occur at a channel due to hydro-morphological changes of a channel. This study has been done in order to observe the behaviour of braided river for oblique flow. For understanding the river

nature this study has been carried out considering an undistorted physical model with a scale ratio of 1:50. Common bank protection work as revetment work with stone boulder has been considered in the study. On the other hand launching behaviour of geo bag has been observed as an option for protection material.

Chapter 4 PHYSICAL MODEL SETUP

4.1 General

This research comprises of selection of model parameters and setup of physical model according to parameters, run of the model, collection of data, analysis and discussion.

A preliminary section for main channel and chute channel has been selected from the available facilities of RRI, Faridpur. Total discharge and bed material for the experimental setup has also been identified from the existing facilities. From these predefined independent parameters, other parameters for the physical model have been calculated and the model setup has been completed as per this. Bank protection work has been designed from the model results of T-1 to T-3 and has been incorporated for the experimental setups having protection work.

4.2 Preliminary Calculated Parameters for Physical Model

A general layout of the experimental setup has been taken into considerations for fixing different parameters for the physical model. Figure 4.1 represents the general layout having main channel and chute channel and Figure 4.2 and 4.3 is the cross section of main channel and chute channel respectively at the part of fixed bed.

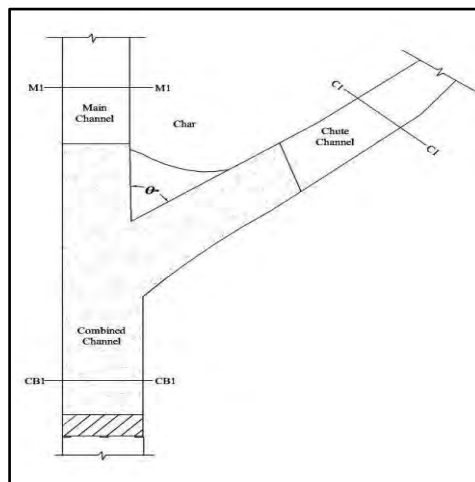


Figure 4.1: General Layout of the Experimental Setup

Figure 4.2 and 4.3 indicates the defined section for main channel and chute channel as section M1-M1 and C1-C1 respectively. The section is at upstream part of the model.

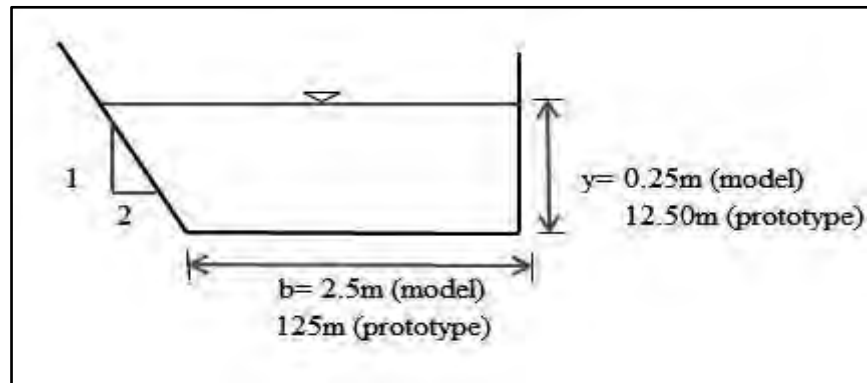


Figure 4.2: Average Section of Main Channel (M1-M1)

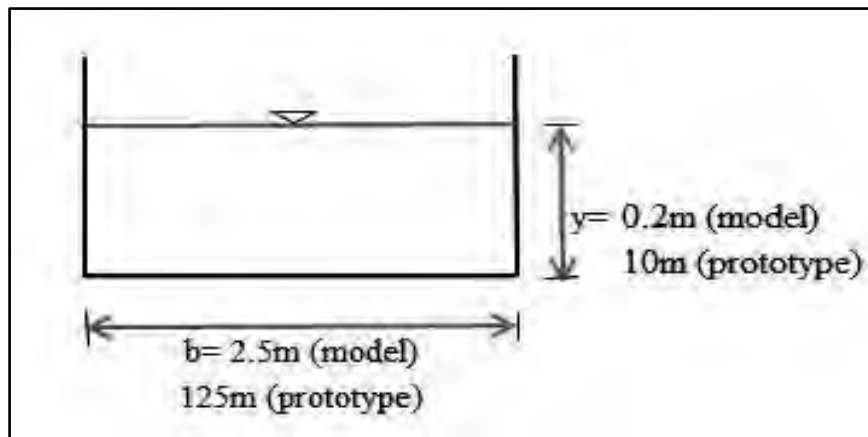


Figure 4.3: Average Section of Chute Channel (C1-C1)

Model scale has been selected as 1:50 as stated earlier. Mean diameter of bed material and bed slope has not been scaled down, as replacement of bed material is not possible in the available facilities. Due to the bed material size velocity enhancement has been done. Preliminary calculation of the major parameters has been presented in Table 4.1. Some of the parameters are variable for initial and final stage of a model. Only initial parameters have been presented here:

Horizontal scale, $L_r = 50$

Vertical scale, $Y_r = 50$

Particle density, $\rho_s = 2650 \text{ kg/m}^3$

Water density, $\rho_w = 1000 \text{ kg/m}^3$

Table 4.1: Preliminary Calculation of Parameter

Parameters Identity	Unit	Prototype		Model		Scale	
		Main Channel	Chute Channel	Main Channel	Chute Channel	Main Channel	Chute Channel
Total length, m	m	3500	3000	70	60	50	50
Length, L	m	1000	400	20	8	50	50
Width, (Top), T	m	150.00	125.00	3.00	2.50	50	50
Width, W (Bottom)	m	125.00	125.00	2.50	2.50	50	50
Water depth, h	m	10.00	10.00	0.20	0.20	50	50
Bed slope, S_f	-	0.00005	0.00007	0.00005	0.00007	1	1
Cross-sectional area, A	m ²	1375.00	1250.00	0.550	0.500	2500	2500
Wetted perimeter, P	m	161.93	145.00	3.239	2.900	50	50
Hydraulic radius, $R=(A/P)$	m	8.4915	8.6207	0.1698	0.1724	50	50
Hydraulic depth, $D=(A/T)$	m	9.1667	10.0000	0.1833	0.2000	50	50
Discharge, Q=	m ³ /s	2651.65	3712.31	0.1500	0.2100	17677.67	17677.67
Average velocity, v	m/s	1.93	2.97	0.273	0.420	7.07	7.07
Shear velocity, $U^*=\sqrt{(g*R*S_f)}$	m/s	0.06454	0.07694	0.00913	0.01088	7.07	7.07
Shields parameter, $\theta =h*i/(\Delta D_{50})$	-	1.54084	2.18998	0.03082	0.04380	50	50
Froude number, $F_r =V/\sqrt{(g*h)}$	-	0.21129	0.32295	0.21129	0.32295	1	1
Critical Shields parameter, $\theta_{cr}=0.14D^{*-0.64}$ (As $4<D^* \leq 10$)	-	0.05567	0.05567	0.05567	0.05567	1	1
Critical shear velocity, $U_{cr}^*=\sqrt{(\Delta*g*D_{50}* \theta_{cr})}$	m/s	0.01227	0.01227	0.01227	0.01227	1	1
Reynolds number, $Re=V*h/k_s$	-	16343.025	25551.040	46.225	72.269	353.55	353.55
Particle Reynolds number, $R_{pe}=U_{cr}^* *D_{50}/\gamma_s$	-	2.04866	2.04866	2.04866	2.04866	1	1
Chezy roughness co-efficient, $C= 18*\log(12*h/K_s)$	m ^{1/2} /s	90.131	90.249	59.550	59.668	1.51	1.51
Critical velocity by shields, $V_{cr}=\sqrt{(\Delta*C^2*D_{50}* \theta_{cr})}$	m/s	0.35	0.35	0.23	0.23	1.51	1.51
Critical velocity by Van Rign, $V_{cr}= 0.19*(D_{50})^{0.1}*\log(12*h/K_s)$	m/s	0.399	0.399	0.263	0.264	1.51	1.51
Fall velocity, $w=(\rho_s-\rho_w)*g*D_{50}^2/(18*K_D)$	m/s	0.02090	0.02090	0.02090	0.02090	1	1

Relative density, $R_D = \rho_s/\rho_w = 2.65$

Relative density of submerged material, $\Delta = (\rho_s - \rho_w)/\rho_w = 1.65$

Kinematic viscosity, $\nu_s = 1.0E-06 = m^2/s$

Dynamic viscosity, $K_D = 1.2E-03 = kg\ s/m^2$

Fineness modulus, $f_m = 1.650$

Gravitational acceleration, $g = 9.81\ m/s^2$

Silt factor, $f = 0.7192$

Bed material mean diameter, $D_{50} = 0.000167\ m$

Average diameter of bed material, $D_{90} = 2 * D_{50} = 0.000334\ m$

Effective bed roughness of a flat bed (m) for sand and gravel material, $k_s = a * D_{90} = 0.001002\ m$ [for $D_{50} \geq 0.1\ m$, $a=3$ for sand and gravel]

Dimensionless particle diameter, $D^* = D_{50} * (\Delta g / \nu_s^2)^{(1/3)}$
 $= 4.224$

* Hydraulic Radius, R has been used in Table 4.1 instead of water depth as the river is braided.

4.3 Physical Model Setup

Approach of the proposed study is to investigate the effect of oblique flow on protected and unprotected bank for straight river bank. Flow angle of chute channel has been formed by selecting the common point of angle in confluence and from that point, centre line for each angle has been obtained. The secondary/chute channel is then constructed for the angles according to the design of model layout. Outer boundary of 20° and 60° has been constructed first and intermediate boundary has been constructed temporally by brick and polythene.

Existing facilities of RRI has been considered for the model layout (Figure 4.4). The investigation has been executed for different flow angle (20° , 40° and 60°) at unprotected condition. Calibration of the physical model has been done in order to fix the water level in gauge point of weir, operation of gate valve, depth of water, tail gate position etc.



Figure 4.4: Physical Model Layout at RRI, Faridpur

Stone boulder has been used as a protective material and revetment work has been completed for the model run. Detail analysis has been carried out to obtain the critical angle from the data obtained at unprotected and protected condition (with stone boulder). Geo-bag has been used as an alternative protective material for the critical angle (obtained from the analysis). The behaviour of the protective work and launching apron, velocity, flow line, scour pattern has been monitored and measured. The model run schedule and different criteria has been followed as per Table 4.2.

4.4 Different Components of Physical Model

The physical model facility has been build at RRI, Faridpur in open air space of about 60.00 m long with 2.75m (average) wide and 80.00 m long with 2.5 m as main channel and chute channel respectively. Width of combined channel was 3.43 m (average). Different component of the physical model, model construction picture and important pictures on experimental setup has been presented in details at appendix-A.

The physical model facility comprises of two types of flume one straight and another bend, storage pools for water supply, weir, stilling basin, a re-circulating canal, measuring device i.e. point gauges, tail gauges, etc. The different components of the model have been described here Figure 4.5 and 4.6.

(a) Straight Flume

The straight flume has been constructed for main channel. The length of flume is about 60 m which leads as main channel. Main channel having a bottom width of 2.5m and top width of 3.00 m and a depth of 0.35 m.

(b) Bend Flume

Bend flume has been used as secondary channel having a length of 80m, 0.3 m high and 2.5 m wide smoothed brick sidewalls. In this case bed length is 4 m with no slope. The bend flume has been considered to use the existing facilities. The two flumes meet and lead as a combined channel. Average top width of combined channel is 3.43 m at the downstream part.

(c) Water Supply System

The water supply is an essential part for the physical model facility. Three types of pump of 5cusec, 7.5 cusec and 10 cusec pump has been used in the setup.

(d) Upstream Reservoir

The upstream reservoir is connected to the re-circulating tank from which water enters the reservoir. Water has been allowed to flow towards gate valve to the storage pool when water level is sufficient for the required discharge.

(e) Downstream Reservoir

The purpose of this reservoir is to store water before delivery to the re-circulating canal.

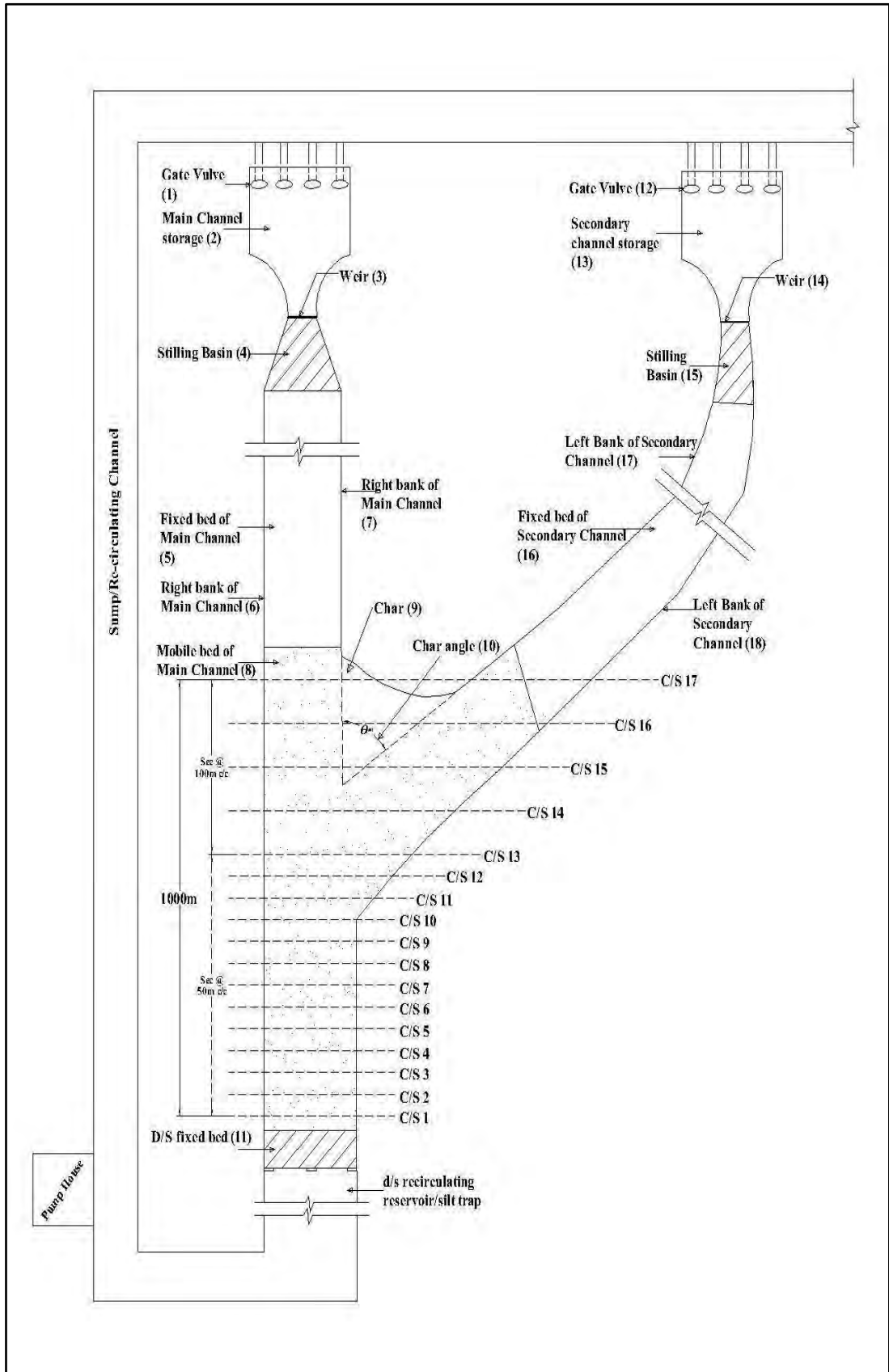


Figure 4.5: Line Diagram of Physical Model Layout

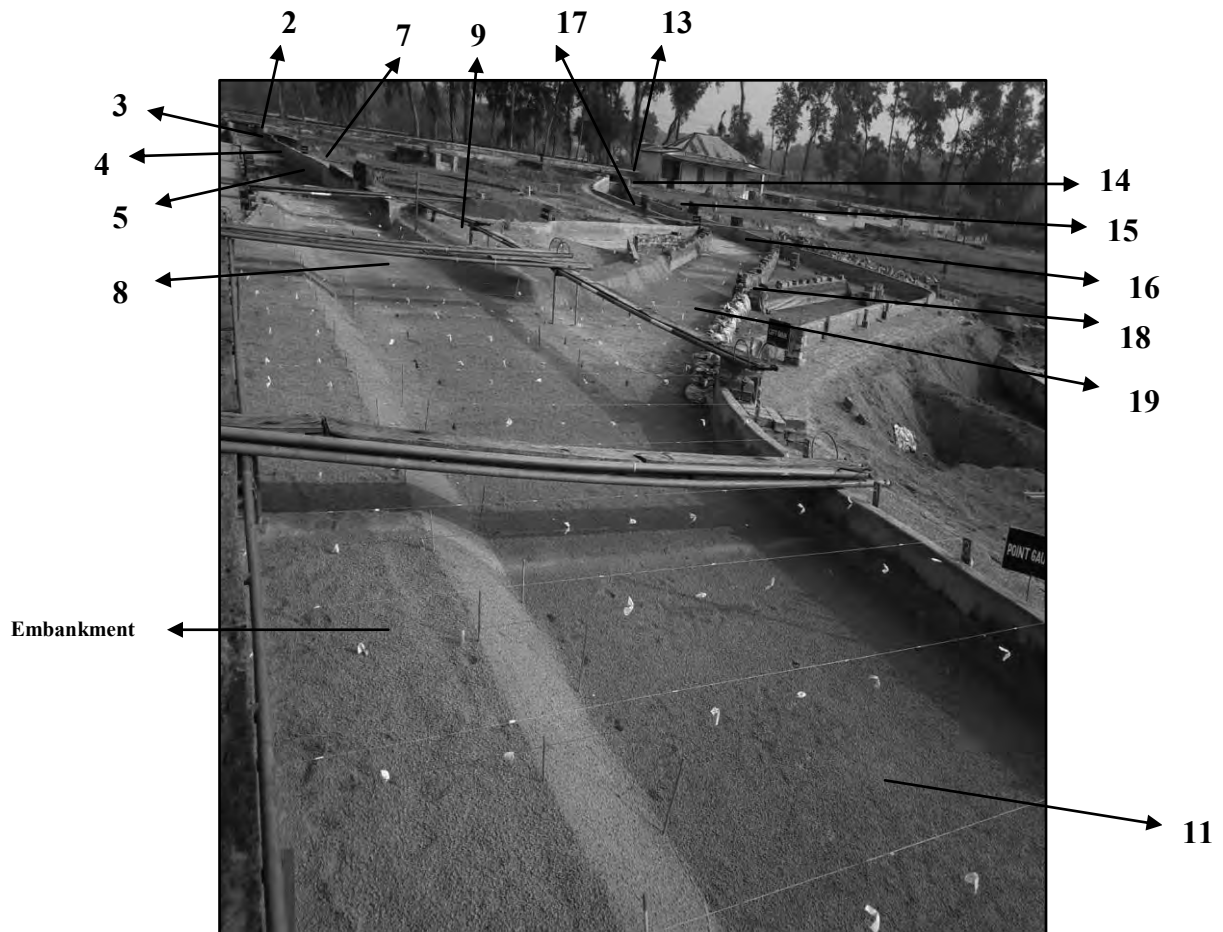


Figure 4.6: Introduction of Physical Model Components

(Numbering for model components have been done according to Figure 4.5)

(f) Weir

At the end of storage pool for both main channel and chute channel a Rehbock weir has been installed for measuring the quantity of water i. e to allow the desired discharge and to observe the state flow (uniform flow). The stilling basin is connected with Rehbock weir (3 and 14 in Figure 4.5 is downstream weir).

(g) Centrifugal Pump

The pump house is located on the western side of storage pool. There are four centrifugal (each of 1.5HP) electric water pump has been connected with the system. The total capacity of the pumps is 400l/s. One larger pump has been used as a loss line

to control supply of water to upstream reservoir and returning excess water to the storage pool.

(h) Re-circulating Canal/ Sump

The re-circulating canal is located on the last part of facility. It connects the downstream reservoir and the upstream reservoir/sump and allows the water to fall back for re-supply. It is 100m long, 2 m wide and 2.0 m deep. It is capable for draining all the water supplied to the system.

There are three drainage plugs connecting the sand bed and re-circulating canal. This plugs are can be used for drying up the bed.

(i) Stilling Basin

When the water comes from weir that time it has much energy and it is to be reduced at a level by stilling basin or wall barrier so that it cannot create any hydraulic jump or wave induced flow in the model (4 and 15 no. component in Figure 4.5).

(j) Point/Discharge Gauge and Reference Plate

There is two discharge gauge one for main channel and another for chute channel. The point gauges is used for water level readings. At the beginning of every measurement first the elevation of accompanying reference plate has been measured then water level has to be adjusted from calculation by adjusting water depth through point gauge.

The point gauges are all manually operated equipment to which an adjustable screw is attached. With the movement of the screw the body of the point gauge slides up or down on a scale. Measurement is taken from the scale reading, corresponding to the zero marked on the point gauge body.

(k) Embankment

The main objective of the research is to find out the effect on river bank, so around 3.5m wide embankment has been developed to observe the most severe effect for designing the protection work at most worst condition.

(l) Strainer

Strainer has been provided at the end of d/s reservoir to free water from any kind of geo-bag or any other type of materials like leaves, paper, insects etc.

(m) Fixed Bed

Fixed bed has been developed from upstream stilling basin to the junction point of mobile bed. A calibration section has been marked at one third of the fixed bed to check discharge, depth of water and velocity of flow. Fixed bed is also essential to control the flow. Fixed bed is also essential to control the flow as a uniform flow to the channel. It has been constructed at both channels to control over flow (5 and 16 no. component in Figure 4.5).

(n) Backwater Flow

A backflow line has been developed below the model bed which is connected to the upstream water drain and an open point has been kept at d/s fixed bed of the model to sock the model bed before direct flow has been operated into the model.

4.5 Equipments Used for the Physical Model

The different equipments used in the experiment are presented below:

(a) Measuring Lines

To indicate the co-ordinate system and the location of different equipment, both sidewalls are equipped with parallel measuring lines indicating the X direction. The

X-distance as measured from a peg to a particular vertical along a cross section. The Y distance is the accumulated distance upstream from the first transect in a study site. Identifying transects by their Y distance is also called stationing. The Z-distance is the elevation of the stream bed at the X, Y-coordinate above the datum.

(b) Velocity Meter

A 2-D velocity meter and Acoustic Doppler Velocimetry has been used for velocity measurements. 2-D velocity meter has featured to measure velocity up to 250cm/s.



Figure 4.7: Photo of 2-D Velocity Meter

ADV meter of probe no. A1054F has been used in the research. The probe head includes one transmitter between two receivers. The remote sampling volume is located 5 cm from the tip of the transmitter. ADV system equipped with N receivers records simultaneously 4N values with each sample that is, for each receiver, a velocity component, signal strength value, a signal-to-noise (SNR) and a correlation value. The signal strength, SNR and correlation values are used primarily to determine the quality and accuracy of the velocity data, although the signal strength (acoustic backscatter intensity). The velocity data is transformed into a Cartesian system of coordinate.

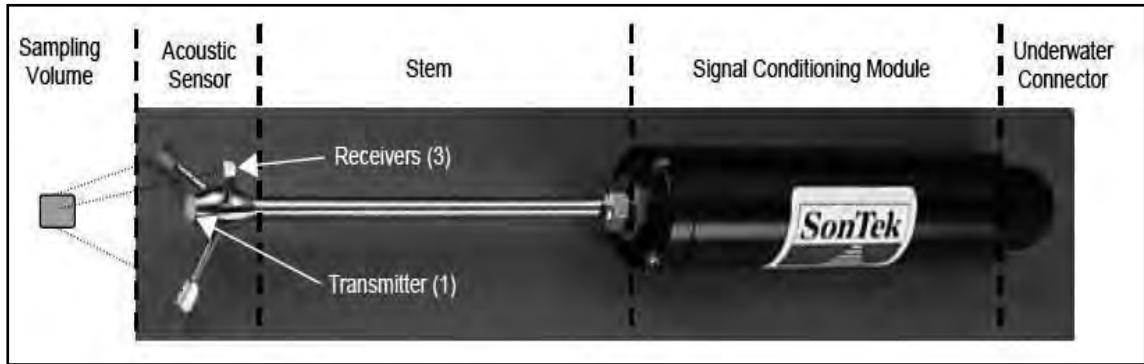


Figure 4.8: Photo of ADV Meter

Main features of the ADV meter are:

- Three-axis velocity measurement
- Sensor mounted on a 25cm stem
- High sampling rates — up to 50 Hz
- Small sampling volume — less than 0.1 cm^3
- High accuracy: 1% of measured range
- Large velocity range: 1 mm/s to 2.5 m/s
- Excellent low-flow performance
- No recalibration needed

Scale, tape etc has been used as some supporting material for the experimental setup.

4.6 Process of Experimental Setup

The Physical Model is consists of twenty one nos experimental setup with upstream and downstream fixed boundary but with variable model conditions. Calibration of model has been done for fixation of model boundary with predefined conditions. Then with this fixed boundary experimental setup with predefined conditions has been done.

(a) Fixation of Reference Level

An arbitrary bench mark of 34.5 m (RL) has been fixed to have the elevation of model bed from wire which has been tied in reference peg at 31 m (RL) for measurement of bathymetry by scale for prototype. The water level and bed level measurement has

been taken with respect to the specific reference level. Staff reading of peg from where section weir has been hanged is considered as 0.97m (RL) for model.

(b) Calibration of the Model

Calibration for Rehbock’s weir’s and sand feeding amount has been done to ease the work for conducting experiments. Calibration test has been done to fix the water level at upstream weir for a fixed discharge, time scale for the dynamic equilibrium condition, u/s and d/s boundary condition.

(c) Calibration of Rehbock Weirs

The discharge equation of a Rehbock weir is (ISO, 1975, after Dekker and van Voorthuizen, 1994) is as follows.

$$Q_R = C_c \sqrt{2g} b h_c^{3/2} \dots\dots\dots (4.1)$$

$$\text{With } h_c = h + h_k = H + 0.0072 \dots\dots\dots (4.2)$$

$$C_c = 0.602 + 0.083 h/p \dots\dots\dots (4.3)$$

Where,

Q_R = Discharge measured over the Rehbock weir.

C_c = Coefficient of discharge.

b = Measured width of the weir.

h_c = The effective piezometric head with respect to the level of the crest.

h = Measured head.

h_k = An experimentally determined quantity which compensate for the influence of surface tension and viscosity.

P = Apex height in meter.

Calibration chart for weir has been completed and for different discharges with the water depth in the storage pool. Discharge gauge has been fixed with zero reading according to the chart and adjusted if needed for each experimental setup.

(d) Calibration of Sand Feeder

Calibration for volume of sand feeding has been done in order to supply the sediment corresponding to a particular discharge so that for the discharge inflow of sediment and outflow of sediment remain same.

(e) Calibration Section

Two calibration sections have been set up at main channel and secondary channel to check the discharge and velocity at the stream.

(f) Discharge Measurement

The individual discharges of main channel and branch channel has been measured with the respective Rehbock weirs. The water level at the crest of the weirs has been measured in stilling basin with point gauges, with an accuracy of 0.05 mm. The zeros of the point gauges are set by filling the two channels with water up to the crest level of the weirs, the point gauges are then being adjusted and the zero is fixed. The water level in the stilling basins has been observed at every 15 minutes.

(g) Preparation of Initial Bed

Fixed bed has been provided before movable bed so that uniform flow can be obtained before it enters at mobile bed zone (As non uniform flow influence the model parameters e.g. sediment transport). Levels along each cross section have been calculated to maintain the bed slope with respect to bench mark. Level pegs have been inserted into the bed and bed was prepared by skilled manual labour for each experimental setup.

4.7 Design of Protective Work

Experimental setup for T-1, T-2 and T-3 has been carried out and data has been analyzed to design the protection work. Revetment work has been considered as a means of bank protection. Bank slope at revetment has not been developed by pitching

of protective material; rather it has been fixed as to observe the severe conditions on bed. Protection work details for stone boulder and geo-bag has been described below:

(a) General Calculations

Design Data for protection work has been taken from Physical model. The detail design has been done according to the standard design procedure (Volume-1, Standard design criteria, BWDB, 1993).

Discharge in model, $Q_m = 0.36 \text{ m}^3/\text{s}$

Discharge in Prototype, $Q_p = Q_m \times (\text{Vertical Scale})^{2.5}$ (from equation 3.4)

$$\begin{aligned} Q_p &= 0.36 \times (50)^{2.5} \\ &= 6363.96 \text{ m}^3/\text{s} \end{aligned}$$

Size of Bed Material, $d_{50} = 0.167 \text{ mm}$

HWL = 14.963 m (RL)

LWL/Bed Level = 4.713 m (RL) (An averaged value from physical model)

Average velocity, $v = 3.88 \text{ m/s}$

(b) Calculation for Scour Depth

Silt factor, $f = 1.76 \times \sqrt{d_{50}}$

$$\begin{aligned} \text{Now } f &= 1.76 \times \sqrt{0.167} \\ &= 0.7192 \end{aligned}$$

As per Lacy's regime scour depth, $R = 0.47 (Q/f)^{1/3}$

$$\begin{aligned} R &= 0.47 \times (6363.96/0.7192)^{1/3} \\ &= 9.721 \text{ m} \end{aligned}$$

(c) Determination of Maximum Scour Depth Below Lowest Bed Level

Considering severe bend Multiplying factor $X = 1.75$

$$\begin{aligned} \text{Depth of scour} &= RX \\ RX &= (1.75 \times 9.721) \text{ m} \\ &= 17.01 \text{ m} \end{aligned}$$

$$\begin{aligned} \text{Maximum anticipated scouring bed level} &= (\text{HFL}-\text{RX}) \\ &= 14.963-17.01 \text{ m (RL)} \\ &= -2.049 \text{ m (RL)} \end{aligned}$$

$$\begin{aligned} \text{Depth of anticipated Scour Depth, } D &= \text{RX}-\text{Y Where, } Y = \text{HFL}-\text{LWL}/\text{Bed Level} \\ &= 17.01-10.25 \text{ (m)} \\ &= 6.762 \text{ m} \end{aligned}$$

Observed maximum scour depth for T3 = 10.600 m (Among T₁, T₂ and T₃)

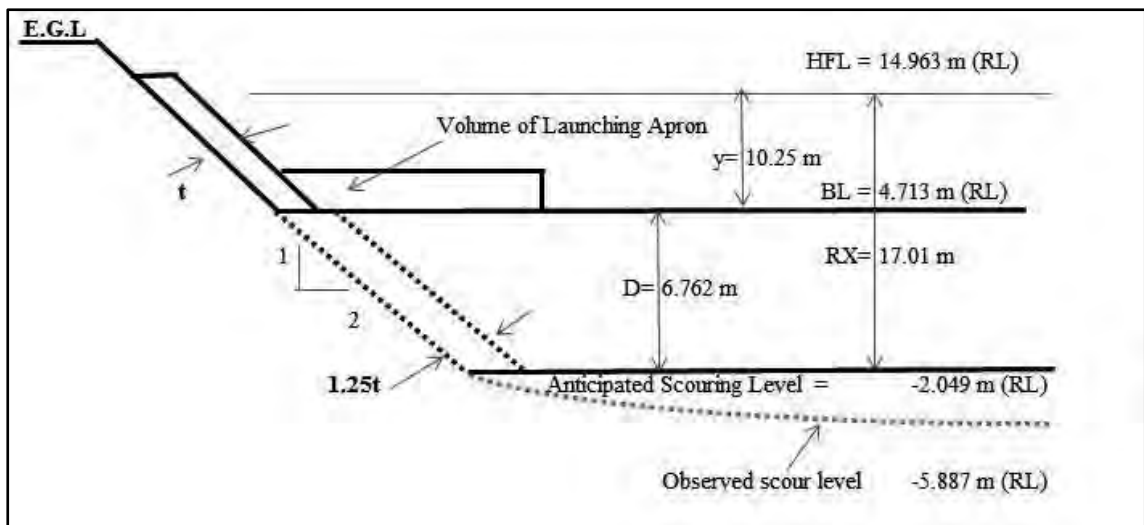


Figure 4.9: Definition Sketch of Design of Bank Protection Work

To avoid slope failure, launching apron has been provided as 1.5 times of maximum observed scour depth to protect the slope.

$$\begin{aligned} \text{So designed scour depth, } D &= 1.5 \times 10.6 \\ D &= 15.900 \text{ m} \\ &\approx 15.000 \text{ m} \end{aligned}$$

(d) Determination of Volume of Launching Apron

Thickness of launching apron is calculated by different ways:

$$\begin{aligned} \text{i) According to English formula, } T &= 0.06 Q^{(1/3)} \\ T &= 0.06 \times 6363.96^{(1/3)} \\ &= 1.1119 \text{ m} \end{aligned}$$

ii) According to Spring for Slope 3 in/mile (5 cm/km) and fine bed materials, $T = 34''$

$$T = 0.864 \text{ m}$$

iii) According to Gales, river discharge of 1.5 million to 2.5 million cusec, $T = 3'-6''+9''$ (Ballest)

$$T = 4'-3'' \\ = 1.290 \text{ m}$$

Among the above three formulas, considering slope thickness of launching apron, $T = 1.112 \text{ m}$

"Considering a launching slope of 1:2 is assumed and the volume of launching apron is calculated following the definition sketch, $V = \sqrt{(2^2+1^2)} \times 1.25 \times t \times D$ "

$$V = 2.79 \text{ tD} \\ = 46.53 \text{ m}^3/\text{m} = 46.00 \text{ m}^3/\text{m}$$

(e) Determination of Thickness and Length of Launching Apron

Launching apron has been designed as a uniform thickness not as a trapezoidal shape. In that case thickness has been considered as average of trapezoidal thickness. On the other hand length of L.A has been determined as per theory.

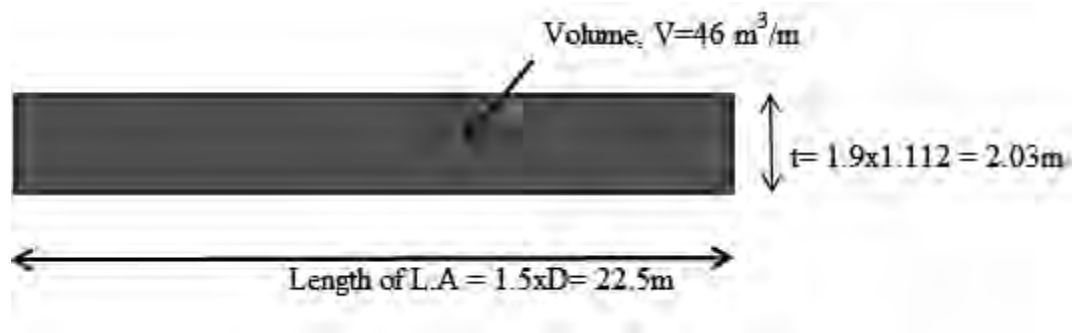


Figure 4.10: Thickness and Length of L.A

(f) Design of Protection Work by Stone Boulder as Protective Material

Grading of riprap:

$$\text{Maximum velocity } v = 3.880 \text{ m/s} \\ = 12.726 \text{ ft/s}$$

From BWDB, Design Manual, volume - I (Page no-208, Table-3, case - II) grading specification has been selected as follows

- a) 100% smaller than 30 inch or 762 mm
- b) At least 20% larger than 24 inch or 609.6 mm
- c) At least 50% larger than 20 inch or 508.0 mm
- d) At least 80% larger than 12 inch or 304.8 mm

(g) Design of Protection Work by Sand Filled Geo-bag as Protective Material

Geo-bag as a protective material has been designed based on model value as the co-efficient of USACE equation cannot be found for prototype. Maximum velocity at unprotected condition has been considered because geo-bag has to be overcome that velocity to have the proper launching behavior. Again at unprotected condition water depth for T1= 12m, T2= 15m, T3= 16.5m. Water depth for T3 has been taken into consideration for the calculation.

(i) Design Data

All values has been taken from physical model and JEMREMP manual

V_i = Velocity for incipient motion, m/s

Depth-averaged velocity at 1/3 bank height, $V = 0.54$ m/s

Depth at 1/3 bank height, $Y = 0.22$ m

Side slope correction, $K_1 = 0.88$

Submerged relative density of Geo-bag, $(s-1) = 1.1$

Shape co-efficient, $C_s = 0.77$

Co-efficient for vertical velocity distribution, $C_v = 1.1$

(ii) Determination of size of Geo-bag

According to USACE equation incipient motion of Geo-bag,

$$V_i = K_1^{0.5} g^{0.5} (s-1)^{0.5} D_{50}^{0.4} Y^{0.1} / (C_s C_v)^{0.4} \text{ (JEMREMP Manual pg no-172)}$$

$$0.54 = 0.88^{0.5} \times 9.81^{0.5} \times 1.1^{0.5} \times D_{50}^{0.4} \times Y^{0.1} / (C_s C_v)^{0.4}$$

By trial and error, $D_{50} = 0.0158$ m

$$= 1.58 \text{ cm}$$

$$\text{Again, } D_{50} = (abc)^{1/3}$$

$$\text{So, } abc = 3.94 \text{ cm}^3$$

So, the weight of sand is = $3.94431 \times 10^{-6} \text{ m}^3$

$$= 0.005916468 \text{ kg (Considering unit weight of sand = } 1500\text{kg/m}^3\text{)}$$
$$= 5.9165 \text{ g}$$

Selecting a square size, we considered the bag size as 2.8cmX2.4cmX0.8cm

Length of influence in model = 5.5 m (5m at revetment zone and 0.5m on straight flow).

(iii) Size Conversion for Prototype

Fill volume at prototype = 0.49304 m³

Weight of bag = 739.56 kg

Size of Bag = 1400mmX1200mmX400mm

(iv) Geo-bag Modification

Literature and Manual represents that 126 kg geo-bag can sustain 4.2m/s velocity (BWDB, 2010). The incipient motion equation for Geo-bag indicates for large size of geobag, so at first available maximum size of 250 kg Geo-bag size has been selected as an option for bank protection material. Again 740 kg geo-bag has been used as protective material to observe its performance.

(v) Calculation for 250 kg Geo-bag

From BWDB Manual, fill volume at Prototype = 0.1664 m³

Bag Size =1200mmX950mm

Length of influence in model = 3.5 m (3m at revetment zone and 0.5m on straight flow to observe its behaviour).

4.8 Measurement for Each Experimental Setup

The following data has been obtained from each experimental setup:

- Bathymetry survey before each run
- Velocity
- Water surface slope
- Flow line
- Scour pattern

- Effect of flow on bank line (for unprotected conditions only)
- Bathymetry survey after each run.

(a) Measurements and Data Analysis

Model has been observed in every half an hour (average) to find the dynamic equilibrium state after starting the model run. Each measurement (according to article 4.7) has been done only after the model reached at dynamic equilibrium condition. The time period for dynamic equilibrium state of model for each individual experimental setup has been presented at appendix-B.

The measured data has been subjected to quick checks and analysis in order to eliminate any inconsistency or doubt during the running period of the physical model and the detail analysis has been carried out in chapter-5.

The physical model setup has been developed in the open air, so sometimes wave at water surface has been generated due to high wind. Water depth and velocity measurement have some inaccuracy in that cases. This limitation has been overcome by carrying out measurements of data for several times or by stopping the measurement until the area has normal wind speed.

Sand feeding has been done by manual labour so there is some human error and deposited materials has been found at the beginning of mobile bed which is not natural for the test (Test result of chapter 5). This limitation could be overcome if mechanical sand feeding can be applied in the experiment.

(b) Conditions for Physical Model and Schedule of Experimental Setup

Different conditions for physical model have been fixed to obtain the research objectives. Experimental setup has been prepared for each condition to run the model. A short description of model conditions and schedule of setup has been presented in Table 4.2.

Table 4.2: Schedule for Experimental Setup and Description of Physical Model Conditions (Shortly)

Model Test No	Date	Model Condition							
		Bank Type	Protective Material type	Provided Protective Work's C/S	Main Criteria	Angle (in degree) (At which chute channel meets main channel)	Dicharge at Main Channel (L/S)	Dicharge at Chute Channel (L/S)	Discharge Ratio
T-0	01.02.2014	Straight	Protected	C/S 14 to C/S 5	Chute channel close	-	350	Close	-
T-1	19.03.2013	Straight	Unprotected	Unprotected	Calibration	20°	150	210	1:1.4
T-2	25.03.2013					40°	150	210	
T-3	30.03.2013					60°	150	210	
T-4	07.04.2013	Straight	Protected (stone boulder)	C/S 14 to C/S 5	Protected	20°	163	197	1:1.2
T-5	08.04.2013						150	210	1:1.4
T-6	09.04.2013						138	222	1:1.6
T-7	11.04.2013	Straight	Protected (stone boulder)	C/S 14 to C/S 5	Protected	40°	163	197	1:1.2
T-8	12.04.2013						150	210	1:1.4
T-9	13.04.2013						138	222	1:1.6
T-10	16.04.2013	Straight	Protected (stone boulder)	C/S 14 to C/S 5	Protected	60°	163	197	1:1.2
T-11	17.04.2013						150	210	1:1.4
T-12	18.04.2013						138	222	1:1.6
T-13	23.04.2013	Straight	Protected (stone boulder)	C/S 14 to C/S 5	Main channel close	Critical Angle (60°)	Close	350	-
T-14	03.05.2013	Straight	Protected (Geo bag type -1 738 kg)	C/S 11 & C/S 12 mid to C/S 6 & C/S 5 mid	Protected	Critical Angle (60°)	163	197	1:1.2
T-15	04.05.2013						150	210	1:1.4
T-16	05.05.2013						138	222	1:1.6
T-17	07.05.2013	Straight	Protected (Geo bag type-1 738 kg)	C/S 13 to C/S 7	Main channel close	Critical Angle (60°)	Close	350	-
T-18	09.05.2013	Straight	Protected (Geo bag type-2 250 kg)	C/S 11 & C/S 10 mid to C/S 8 & C/S 7 mid	Protected	Critical Angle (60°)	163	197	1:1.2
T-19	10.05.2013						150	210	1:1.4
T-20	11.05.2013						138	222	1:1.6

4.9 Summary

Experimental conditions based on the study objective have been finalized and physical model has been constructed accordingly to that at RRI, Faridpur. Model parameters have been also calculated. Finally measurement and observation procedure according to the requirement has been fixed. Bank protection work related with the experimental conditions has also been designed according to standard design manual.

Chapter 5

RESULTS AND DISCUSSIONS

5.1 General

Detail analysis and results have been presented in this chapter. The data associated with bathymetry survey of initial and final bed level, scouring pattern, launching behaviour, comparison of experimental setup etc has been discussed here.

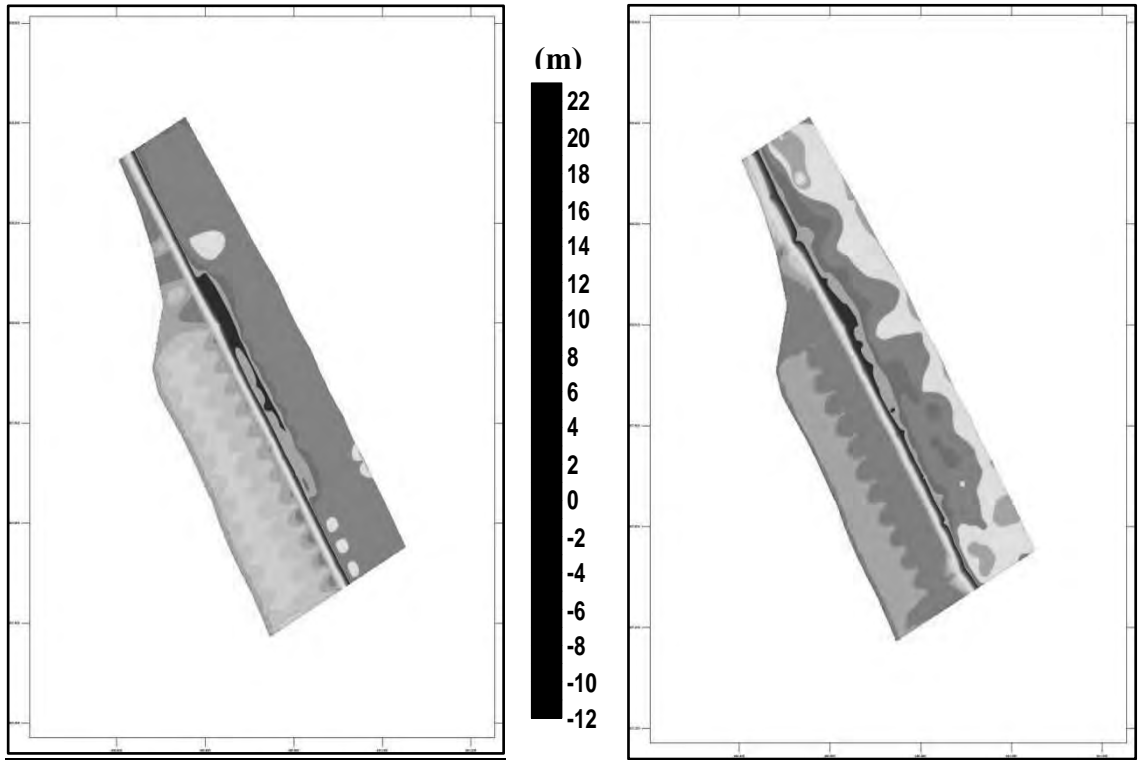
5.2 Experimental Details Before and After Physical Model Run

The total program according to Table 4.2 has been carried out to understand the fluvial process under oblique flow condition. Results of scouring/deposition that means initial and final bed condition for both prototype and model has been presented in Figure 5.1 to 5.31. A short discussion on the model conditions and observations has been made for each experimental setup accordingly with the figures.

5.2.1 Straight Channel without Oblique Flow and Protected Bank:

(a) Results of Physical Model Setup T-0

Experimental condition of the setup is bank is protected by stone boulder from c/s 14 to c/s 5, chute channel is closed. After run there is no significant change in model bed so in launching apron. Maximum scour is 1.5 m to 2.65 m in c/s 6 to 8 and deposition is 2.1 m at left bank side. There is no change in bank line (Figure 5.1). Straight flow in a single channel has no significant effect on bank and bed so bank line remains in the same position. Moreover, deposition occurred on launching apron. There is no secondary flow so sediment deposition occurred. Velocity varies from 2.91m/s to 3.35m/s in the experimental setup. Protective materials remains on the same line and length as no scouring occur to launch material.



(a)

(b)



(c)



(d)

Figure 5.1: Bed and Bank Details for T-0: (a) Before Run for Prototype; (b) After Run for Prototype; (c) Before Run for Model; (d) After Run for Model.

5.2.2 Straight Channel, Unprotected Bank with different Oblique Flow Angle

(a) Results of Physical Model Setup T-1

The main condition of the test is unprotected bank. The flow angle is 20° and discharge ratio is 1:1.4 in the test (Figure 5.2). After run there is deposition in both starting of main channel and chute channel. Maximum deposition occurred in front of char mouth which extended up to the combined channel. Maximum 5.50 m scour occurred at c/s 5 from the end of combined channel towards the downstream. Velocity varies from 1.41 m/s to 4.07 m/s at that cross section for the experimental setup.

The quantity of deposition for MC and CC is same as the flow angle is small and discharge is dominant in main channel, so scouring at bed is more towards right bank due to the push back effect of main channel.

(b) Results of Physical Model Setup T-2

Experimental condition of the test is unprotected bank, oblique flow angle is 40° and discharge ratio is 1:1.4 (Figure 5.3). There is deposition in both starting of main channel and chute channel as like T-1 after run. Deposition in front of char mouth is not much as T-1 rather a small deposited channel has been formed towards main channel bank. Again a deep thalweg has been formed heading from chute channel towards downstream and affecting left bank. Maximum 6.85m scour occurred at c/s 8. Velocity varies from 1.80 m/s to 3.07 m/s at the c/s.

The discharge ratio is fixed in the test as T-1 but flow angle changes so chute channel has been more dominant. Therefore deposition was more at char mouth towards main channel. Again being CC more dominant maximum scoured bed or thalweg is more towards main channel bank. Specially it is clear that due to dominant CC erosion at main channel bank is more than T-1 and scouring is also high near main channel bank. This deep scouring at bed near bank develops slope and mass failure to meet the quantity of washed material from bed.

(c) Results of Physical Model Setup T-3

Bank is unprotected in the setup. The flow angle is 60° and discharge ratio is 1:1.4 in the test (Figure 5.4). Deposition is at only main channel and at a small zone of in front of char mouth. A deep thalweg starts from chute channel passing through combined channel towards downstream. The thalweg directly hit to the main channel right bank i.e it passes more near the main channel bank while it goes towards downstream. Maximum scour is

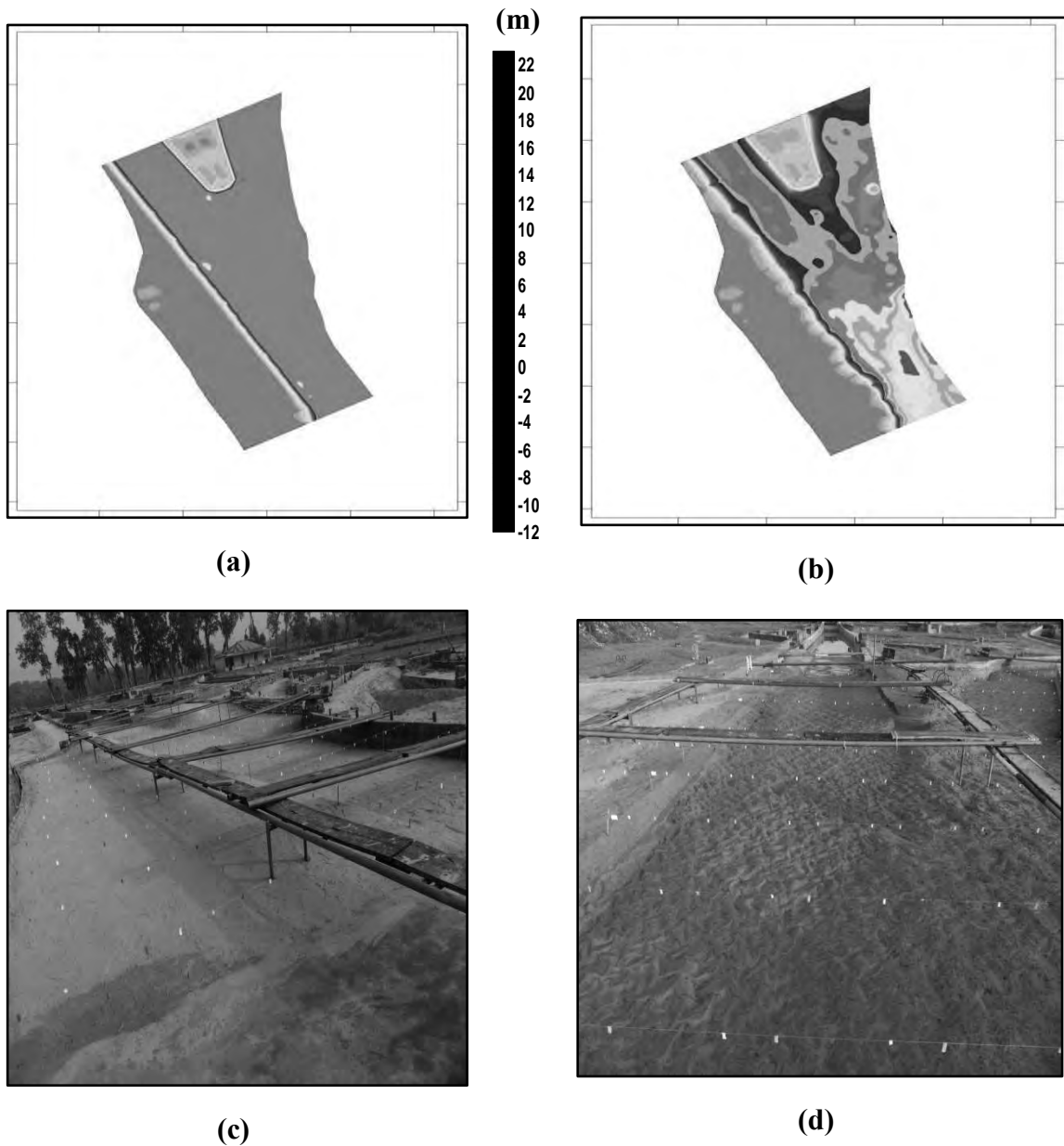


Figure 5.2: Bed and Bank Details for T-1: (a) Before Run for Prototype; (b) After Run for Prototype; (c) Before Run for Model; (d) After Run for Model.

10.60 m at c/s 8 with a varying velocity of 2.22 m/s to 3.32 m/s. 25m bank erosion shifting has been found in the experimental setup.

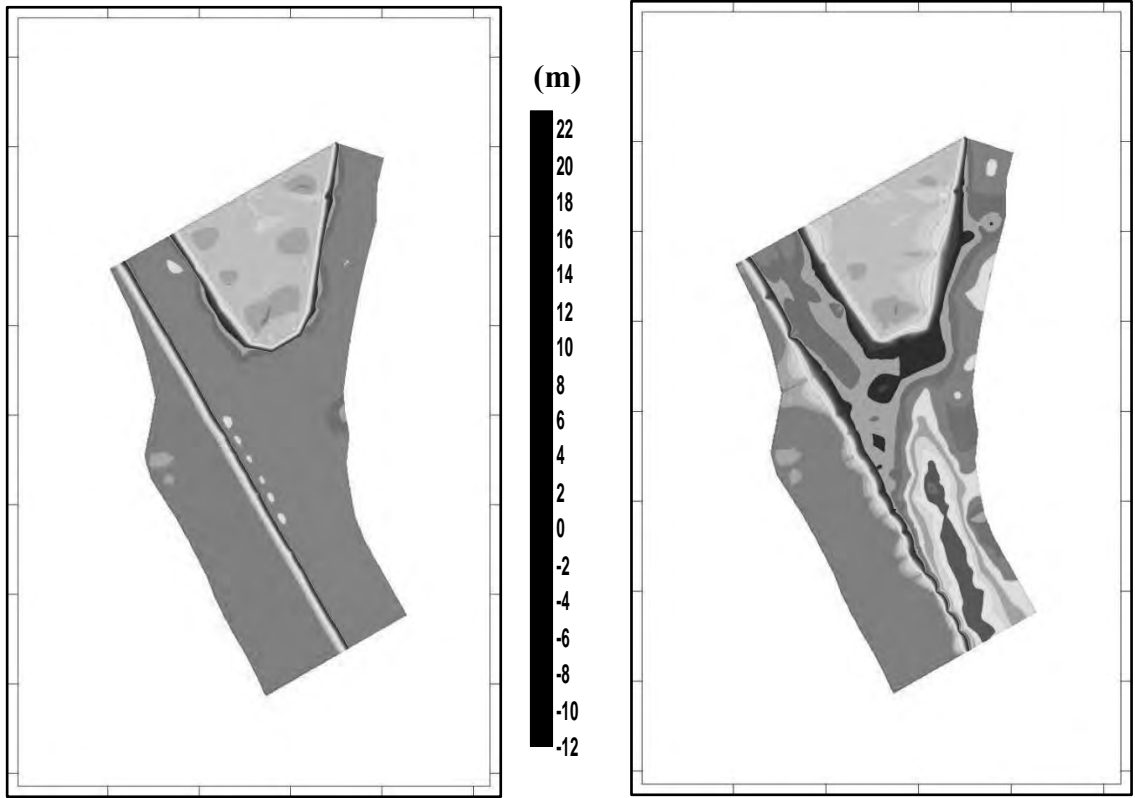
The discharge ratio is fixed in this test as T-1 and T-2 but flow angle changes so chute channel became most dominant with higher angle (among the selected flow angles). Therefore deposition is less at char mouth and higher at main channel. Again being CC more dominant maximum scoured bed or thalweg is more towards main channel bank. In this test due to dominant CC erosion at main channel bank is more than T-1 and T-2 scouring is also high near main channel bank. This deep scouring at bed near bank develops slope and causes mass failure to meet the quantity of washed material from bed.

(d) Provision of Bank Protection Work

The above three experiment it has been observed that scour at river bed accelerates the slope and mass failure from the bank. Velocity varies randomly in those experiments, so erosion is not velocity dependent. It's the secondary flow which accelerates the bank erosion as well as erosion at bed. Bank and bed erosion increases with the increase of chute channel angle.

The above analysis of T-1, T-2, T-3 and also Figure 5.2 to Figure 5.4 reveals that bank protection work is needed at the main channel right bank. Left bank of the setup has been ignored as the research objectives are only to find out the effect of oblique flow on main channel. The most severe part is at combined channel to downstream. A revetment work has been done at right bank which starts from combined channel to the downstream. The bank protection design has been described at 4.7.

According to the research objective to observe the detailed launching apron behaviour revetment slope has been permanently build to the bottom of bed so that slope failure cannot occur. Maximum scour points and thalweg for T-1, T-2 and T-3 is more to the downstream, so a modification has been made in the physical model setup (for T-4 to T-20) at field condition. The channel setup has been shifted to the upward direction keeping all other dimension and parameters same as before.



(a)

(b)

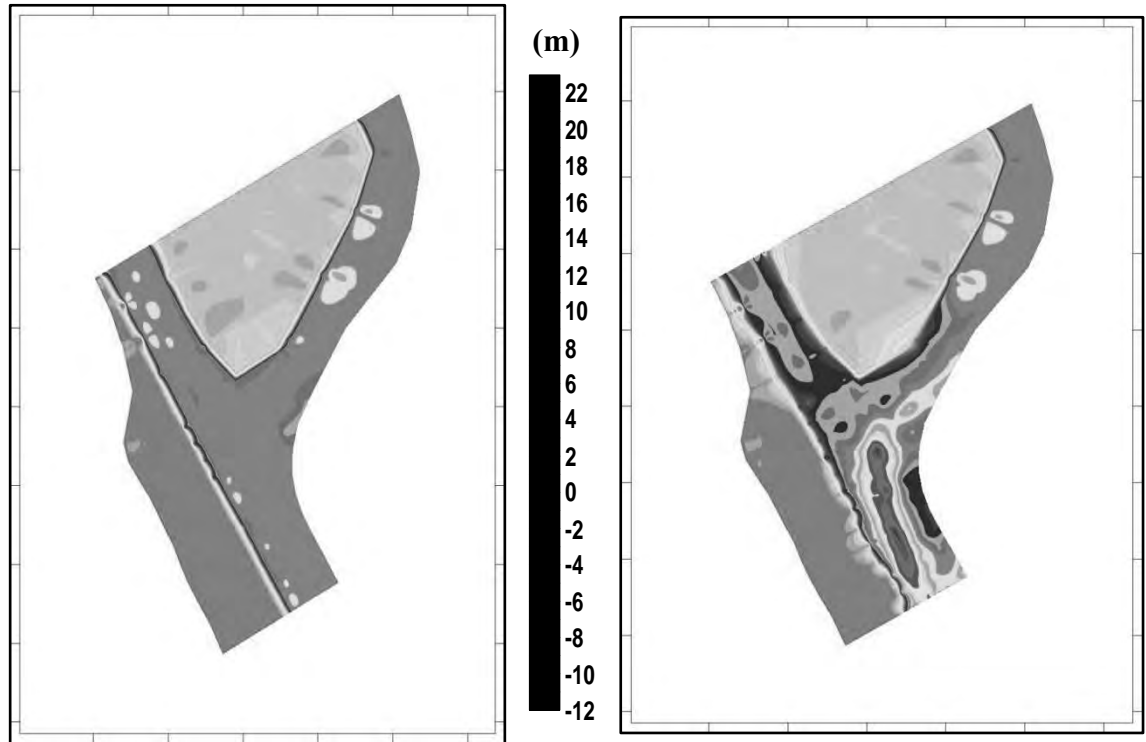


(c)



(d)

Figure 5.3: Bed and Bank Details for T-2: (a) Before Run for Prototype; (b) After Run for Prototype; (c) Before Run for Model; (d) After Run for Model.



(a)

(b)



(c)



(d)

Figure 5.4: Bed and Bank Details for T-3: (a) Before Run for Prototype; (b) After Run for Prototype; (c) Before Run for Model; (d) After Run for Model.

5.2.3 Straight Channel, Protected Bank, 20° Oblique Flow Angle with Different Discharge Ratio

(a) Results of Physical Model Setup T-4

The test has an oblique flow angle of 20° with a discharge ratio of 1:1.2 and protection work has been done by stone boulder (Figure 5.5). There is deposition at both main channel and chute channel, also at char mouth after model run. Erosion at char mouth occurred. Maximum scour is 6.20 m at c/s 11 and velocity varies from 2.33 m/s to 3.11 m/s. Stone boulder launched uniformly with a varying slope of 1:1.33 to 1:2.25 (Table 5.4) and no bare space found throughout the length. The thalweg is near the zone of protective material and it has a sharp slope near protection work. Deposition occurred at right bank. Thalweg channel is not much deeper.

The thalweg is more near the right bank and it did not match with T-1 though two condition of this test is similar to T-1. Actually thalweg channel is more attracted to the protection work. For this thalweg is near the right bank of main channel due to the protection work than T-1. Deposition occurred at upstream of main channel and u/s of launched material due to less dominating character of main channel. There are no bare spaces in the launching apron (Figure 5.6) and stone boulder launched uniformly to cover the bed material.

(b) Results of Physical Model Setup T-5

The test has an oblique flow angle of 20° with a discharge ratio of 1:1.4 and protection work has been done by stone boulder (Figure 5.7). There is deposition at both main channel and chute channel, also at char mouth. Erosion at char mouth occurred. Stone boulder launched at uniform slope of 1:1.33 to 1:2.22 (Table 5.4) and no bare space found throughout the length. The thalweg is near the zone of protective material and it has a sharp slope near protection work. Maximum bed scour is 6.91m at c/s 7 with varying velocity of 2.30m/s to 3.89m/s. Deposition occurred at left bank (Figure 5.8). The thalweg channel is not much deeper.

The reason of this behavior is similar as for T-4. Deposition occurred at upstream of main channel and launched material due to less dominating character of main channel. There is no bare space in the launching apron (Figure 5.8) as stone boulder launched uniformly to cover the bed material. Deeper thalweg channel did not formed as oblique flow angle is small so the effect is small.

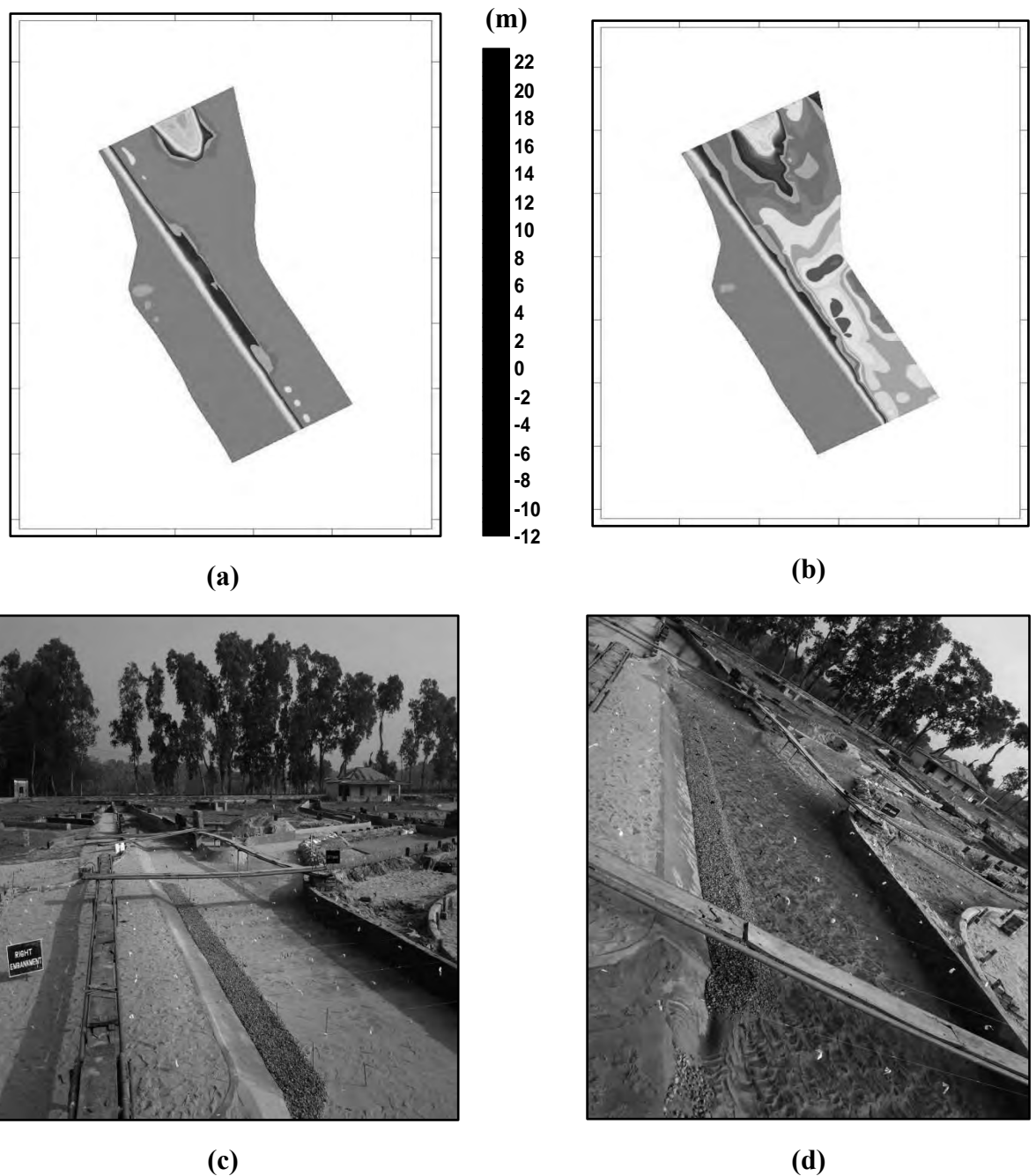


Figure 5.5: Bed and Bank Details for T-4: (a) Before Run for Prototype; (b) After Run for Prototype; (c) Before Run for Model; (d) After Run for Model.

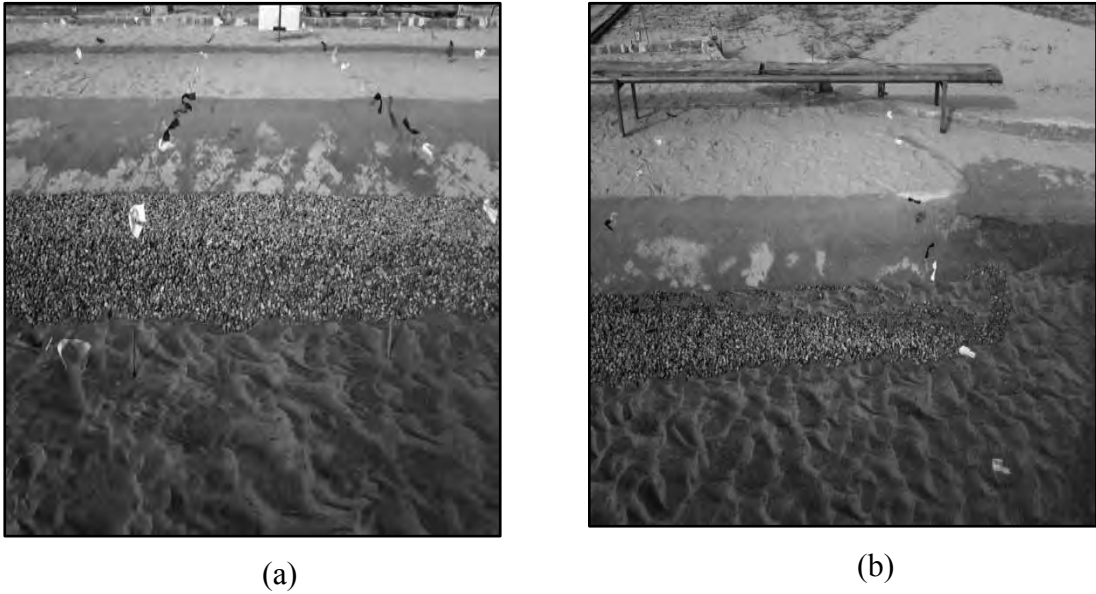
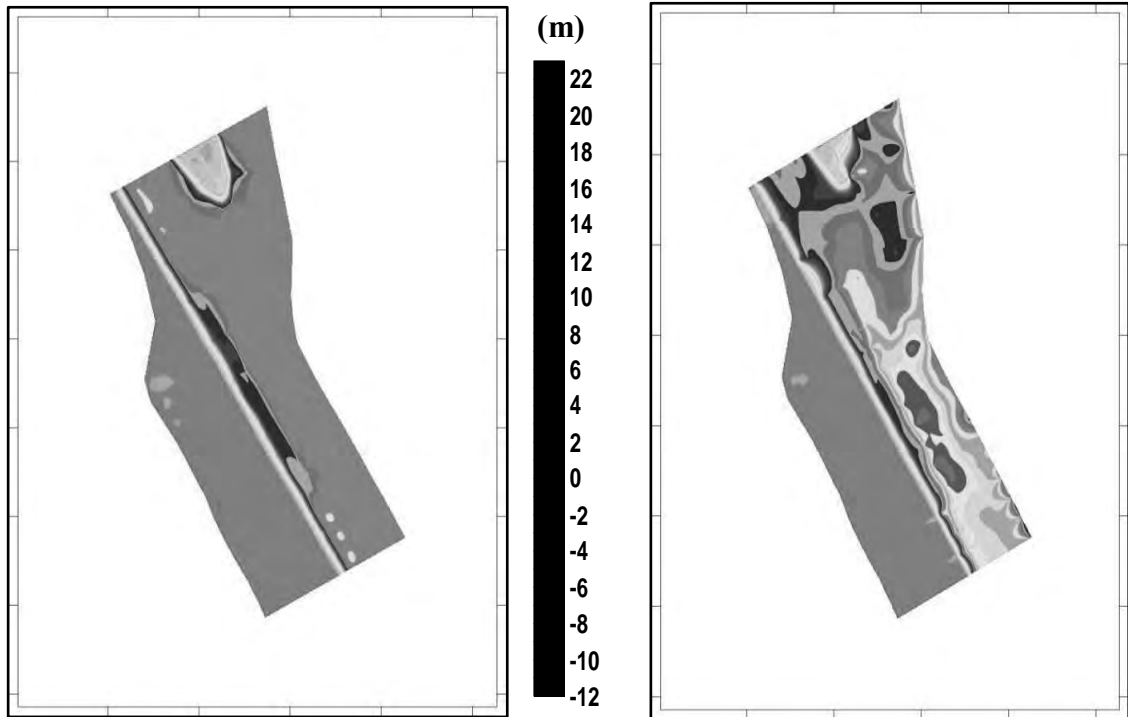


Figure 5.6: Launching Behaviour of Stone Boulder for T-4: (a) At Mid of Revetment; (b) At starting of Revetment

(c) Results of Physical Model Setup T-6

The experimental setup has an oblique flow angle of 20° with a discharge ratio of 1:1.6 and protection work has been done by stone boulder (Figure 5.9). There is deposition at both main channel and chute channel, also at a distance of char mouth. Erosion at char mouth occurred. Stone boulder launched at a uniform slope of 1:1.62 to 1:2.43 (Table 5.4) and no bare space found throughout the length. The thalweg is near the zone of protective material and it is spreaded at maximum zone along the width. Deposition occurred at left bank. The thalweg channel is deeper than T-5. Maximum bed scour is 6.96 m at c/s 8 and having minimum and maximum velocity of 1.98 m/s to 3.71 m/s respectively.

The reason of this behavior is similar as T-4 and T-5. Main channel is less dominating in the test so the total launching apron is affected by its thrust also due to this reason the launching slope variability (1:1.62 to 1: 2.43) is less here. And deeper channel formed near the protective material zone.



(a)

(b)

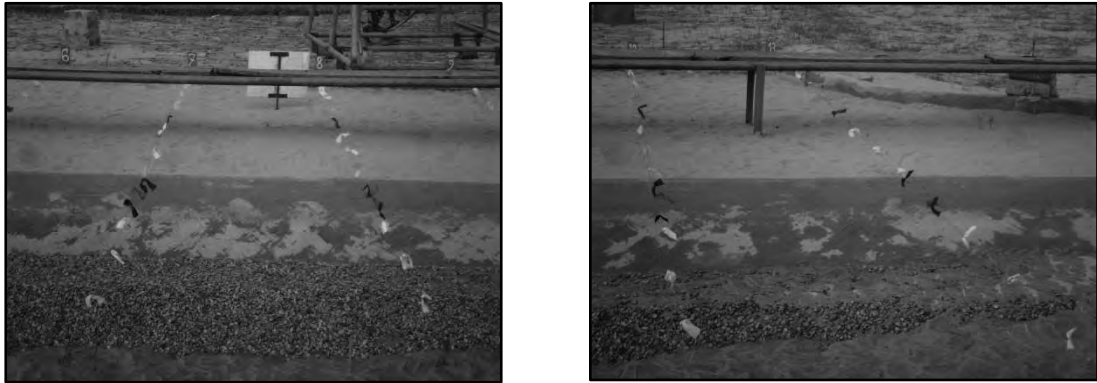


(c)



(d)

Figure 5.7: Bed and Bank Details for T-5: (a) Before Run for Prototype; (b) After Run for Prototype; (c) Before Run for Model; (d) After Run for Model.



(a)

(b)

Figure 5.8: Launching Behaviour of Stone Boulder for T-4: (a) At Mid of Revetment; (b) At starting of Revetment

5.2.4 Straight Channel, Protected Bank, 40° Oblique Flow Angle with Different Discharge Ratio

(a) Results of Physical Model Setup T-7

The test has an oblique flow angle of 40° with a discharge ratio of 1:1.2 and protection work has been done by stone boulder (Figure 5.10). Rate of deposited material at main channel is less but deposition occurred at left bank. Maximum erosion is 8.70 m at c/s 9. Velocity varies from 2.72 m/s to 3.50 m/s at the c/s. Thalweg channel is more attracted to the main channel bank. No bare space found throughout the launching slope. Stone boulder launched at a uniform slope of 1:1.31 to 1:2.41 (Table 5.4). Chute channel is more dominating than T-4 as the angle is higher so the thrust of oblique flow directly hit to the main channel bank develop a deep thalweg. Due to push back effect deposition occurred at left bank.

(b) Results of Physical Model Setup T-8

The test has an oblique flow angle of 40° with a discharge ratio of 1:1.4 and protection work has been done by stone boulder (Figure 5.11). Maximum bed scour is 10.41 m at c/s 9 with velocity ranges between 2.47 m/s to 3.92 m/s. Rate of deposited material at main channel is less but deposition occurred at left bank. Thalweg channel is more

attracted to the main channel bank. No bare space found throughout the launching slope. Stone boulder launched at a uniform slope of 1:1.26 to 1:2.30 (Table 5.4). Chute channel is more dominating than T-5 as the angle is higher so the thrust of oblique flow directly hit to the main channel bank develop a deep thalweg. Due to push back effect and dominating chute channel more deposition than T-7 occurred at left bank. Thalweg channel is uniform along the protective work for changing in oblique flow angle.

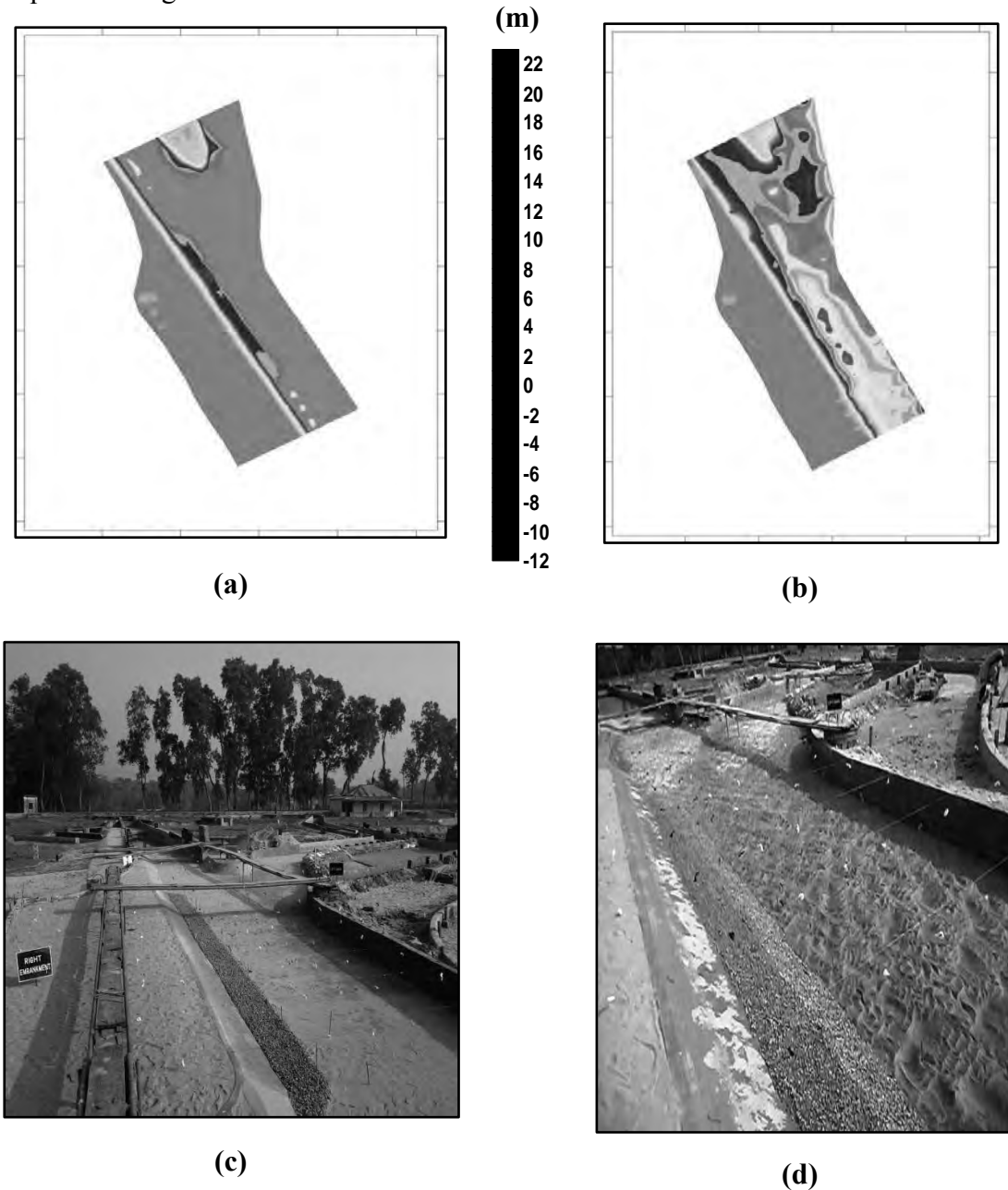
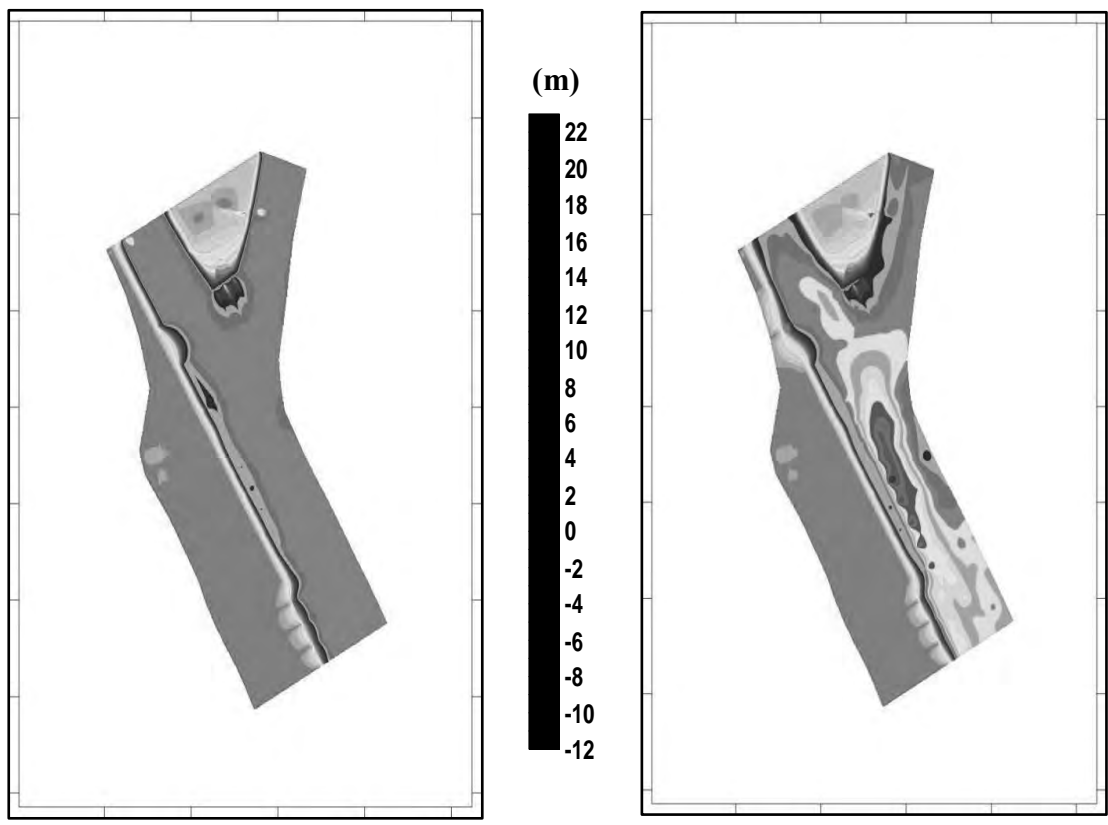


Figure 5.9: Bed and Bank Details for T-6: (a) Before Run for Prototype; (b) After Run for Prototype; (c) Before Run for Model; (d) After Run for Model.



(a)

(b)

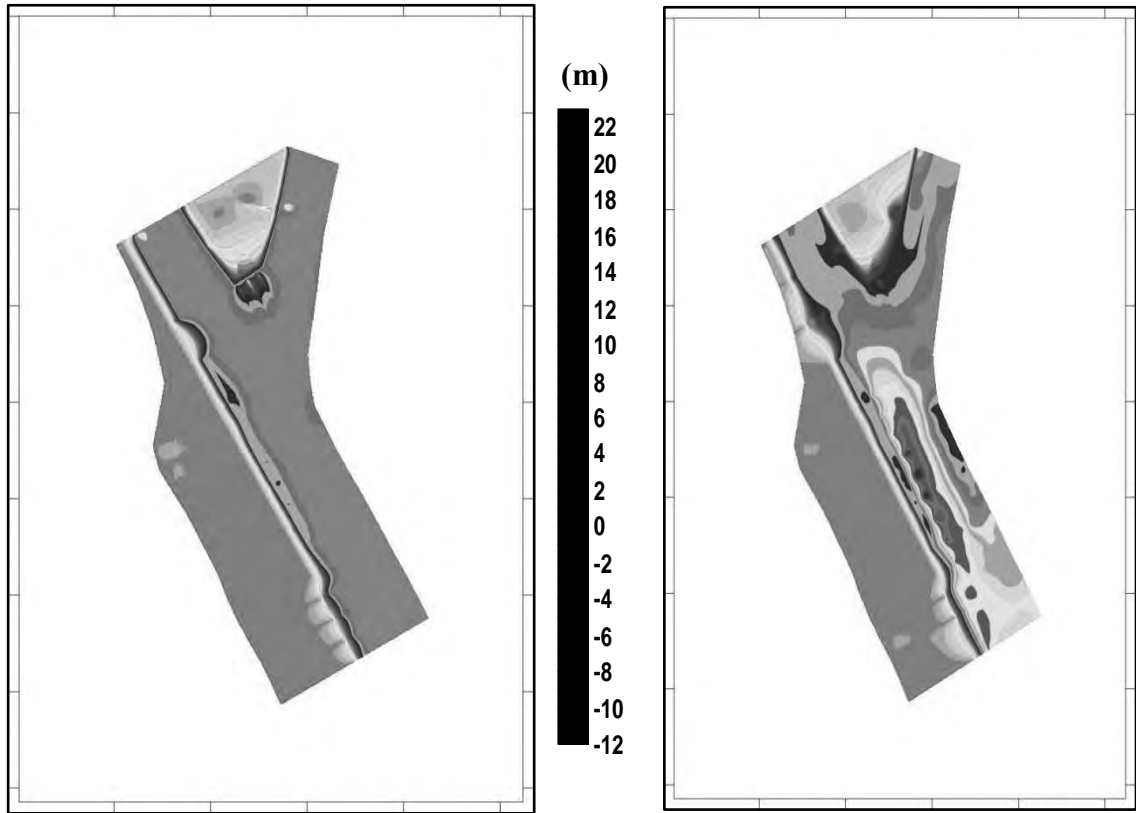


(c)



(d)

Figure 5.10: Bed and Bank Details for T-7: (a) Before Run for Prototype; (b) After Run for Prototype; (c) Before Run for Model; (d) After Run for Model.



(a)

(b)



(c)



(d)

Figure 5.11: Bed and Bank Details for T-8: (a) Before Run for Prototype; (b) After Run for Prototype; (c) Before Run for Model; (d) After Run for Model.

(c) Results of Physical Model Setup T-9

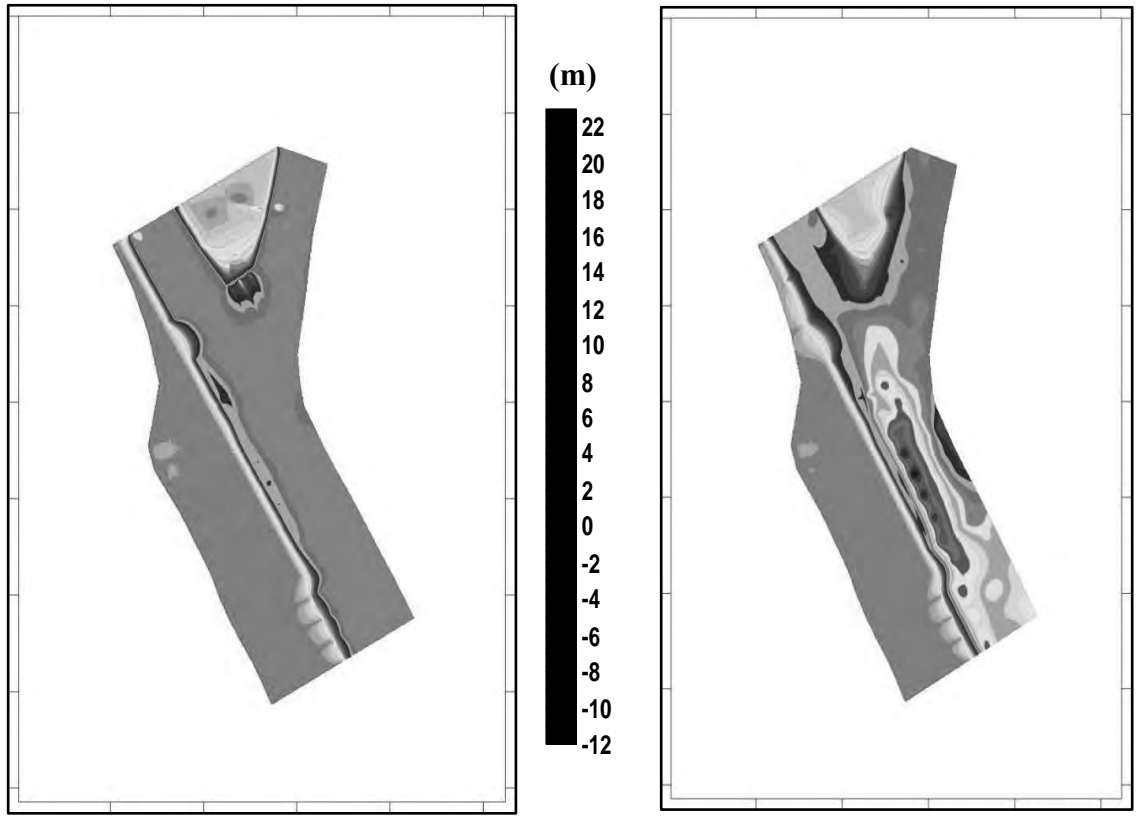
The test has an oblique flow angle of 40° with a discharge ratio of 1:1.6 and protection work has been done by stone boulder (Figure 5.12). Thalweg channel is more attracted to the main channel bank and deeper than T-7 and T-8. Maximum bed scour is 11.16 m at c/s 9 and velocity varies from 2.54 m/s to 3.99 m/s. No bare space found throughout the launching slope. Stone boulder launched at a slope of 1:0.78 to 1:1.98 (Table 5.4). Deposition occurred at left bank. Erosion at char mouth occurred but that material deposited along the main channel.

This test has a more dominating chute channel so thalweg is deeper along the protection work and as well as deposition at left bank. The flow characteristic in chute channel is higher so eroded material from char mouth deposited along main channel. No bare spaces in the launched slope indicate uniform behavior of protection material which protect the bed with the bank well. Sedimentation occurred at starting of protection work (Figure 5.13) due to less dominating main channel. Uniform launching occurred at the sections where oblique flow starts affecting on the protection work. At the sedimentation zone it has a flat slope.

5.2.5 Straight Channel, Protected Bank, 60° Oblique Flow Angle with Different Discharge Ratio

(a) Results of Physical Model Setup T-10

The test has an oblique flow angle of 60° with a discharge ratio of 1:1.2 and protection work has been done by stone boulder (Figure 5.14). Thalweg channel and launching behavior is same as T-4 and T-7 but the effect is more than those. Maximum 11.26 m bed scour found at c/s 9 in the experimental setup with velocity varies from 2.41 m/s to 4.30 m/s. The characteristics are same as previous tests. The variation of behavior is in launched slope. Stone boulder launched at a slope of 1:1.53 to 1:2.18 (Table 5.4). This occurred as the oblique flow effect is more than the other tests so the flow from the chute channel is more effective at main channel bank thus developing the slope.



(a)

(b)



(c)



(d)

Figure 5.12: Bed and Bank Details for T-9: (a) Before Run for Prototype; (b) After Run for Prototype; (c) Before Run for Model; (d) After Run for Model.

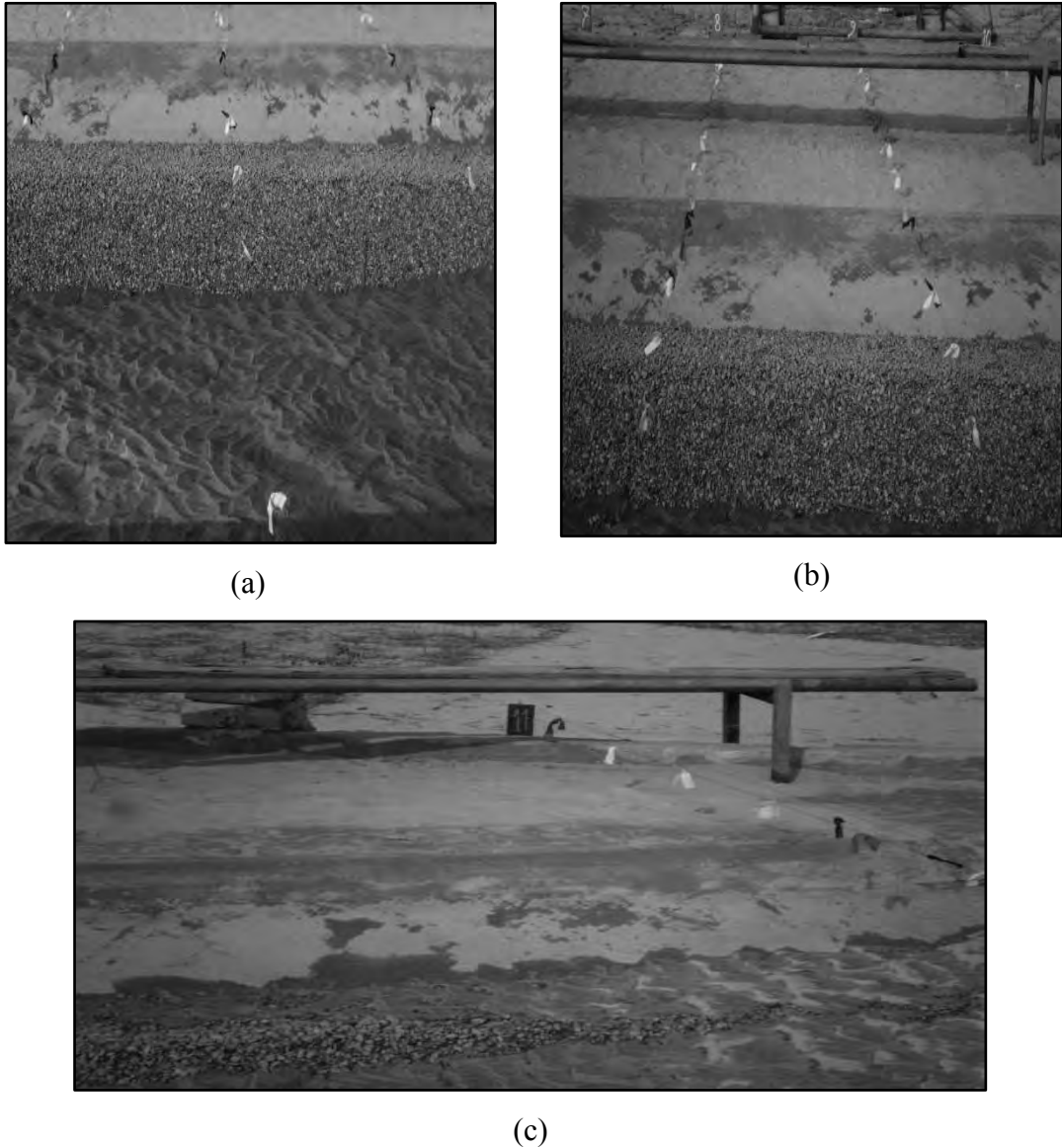


Figure 5.13: Launching Behaviour at Setup for T-9 (a) at Starting of Revetment (b) at Mid part of Revetment (c) Sedimentation at Starting of Launching Apron

(b) Results of Physical Model Setup T-11

The test has an oblique flow angle of 60° with a discharge ratio of 1:1.4 and protection work has been done by stone boulder (Figure 5.15). Thalweg channel and launching behavior is same as T-5 and T-7 but the effect is more than those. Maximum bed scour is 14.86 m at c/s 10 and velocity varies between 2.47 m/s to 3.80 m/s. The characteristics are same as previous tests T-5 and T-7. The variation of behavior is in launched slope. Stone boulder launched at a slope of 1:1.55 to 1:2.42 (Table 5.4)

without bare spaces. This occurred as the oblique flow effect is more than the other tests so the flow from the chute channel is more effective at main channel bank thus developing the slope.

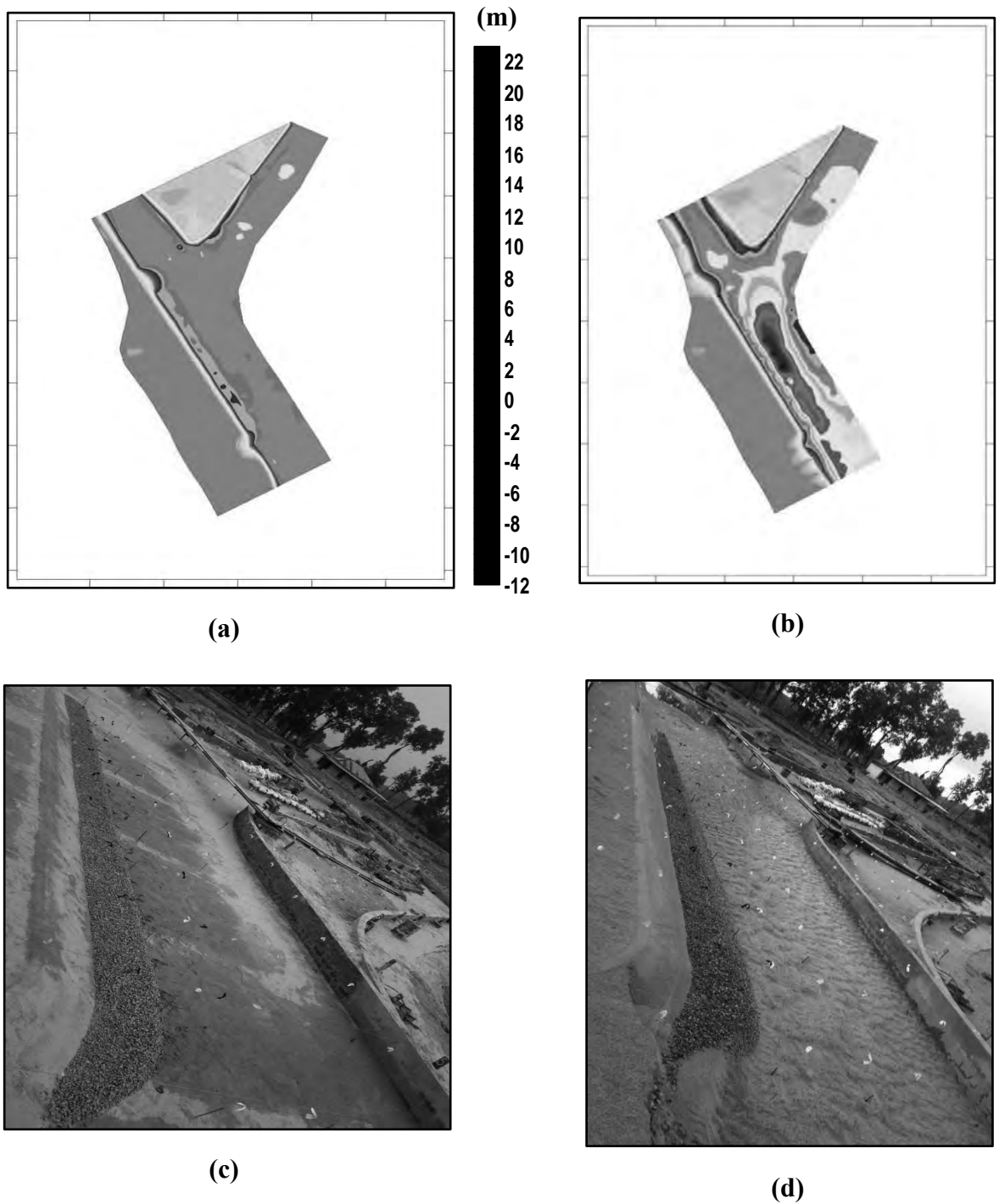
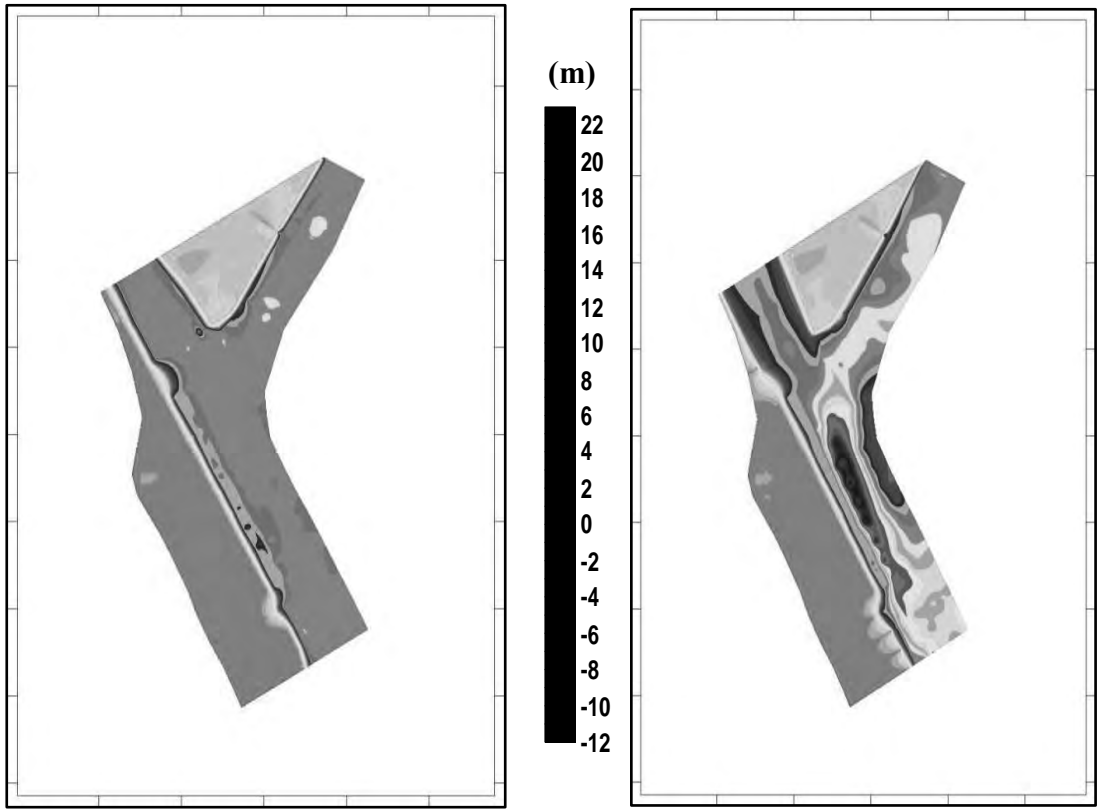


Figure 5.14: Bed and Bank Details for T-10: (a) Before Run for Prototype; (b) After Run for Prototype; (c) Before Run for Model; (d) After Run for Model.



(a)

(b)



(c)



(d)

Figure 5.15: Bed and Bank Details for T-11: (a) Before Run for Prototype; (b) After Run for Prototype; (c) Before Run for Model; (d) After Run for Model.

(c) Results of Physical Model Setup T-12

Experimental condition has been fixed as protected bank by stone boulder, oblique flow angle is 60° and discharge ratio is 1:1.6 (Figure 5.16). Maximum 15.91 m bed scour found at c/s 10 with varying velocity between 2.68 m/s to 4.02 m/s after model run. Thalweg channel and launching behavior is same as T-6 and T-9 but the effect is most severe than the all tests described before. There has more sedimentation zone at the u/s of protection work (Figure 5.17).

Stone boulder launched at a slope of 1:1.53 to 1:2.24 (Table 5.4). No bare spaces in the launched material indicate uniform launching of protective material. The setup has the extreme oblique flow angle and the discharge ratio is the highest. In that test chute channel is most dominating and affect the protection work most. So sedimentation zone at upstream part of the model is most extended than the other tests.

(d) Selection of critical angle

The rest experimental setups from T-13 to T-20 have been decided to run at the most critical oblique flow angle. The analyses of test results represent maximum bed scour and launching of protective material occurred at 60° angle. Thus 60° angle has been selected as critical.

5.2.6 Straight Channel, Protected Bank by Stone Boulder and Main Channel Close:

(a) Results of Physical Model Setup T-13

The test has an oblique flow angle of 60° with a discharge ratio of 1:1.6 and protection work has been done by stone boulder (Figure 5.18). Deep thalweg channel developed near launching apron. Stone boulder launched uniformly at a slope of 1:2.06 to 1:3.20 (Table 5.4) without bare spaces. Excessive deposition occurred at left bank. There is also excessive deposition at chute channel. Maximum bed scour is 12.21 m at c/s 10 and velocity varies between 1.34 m/s to 4.91 m/s.

Excessive deposition at chute channel occurred due to excess sand feeding because this work has been done manually and rate of sand feeding cannot be controlled. Protection material launched at uniform slope. Though the slope is quite flatter but thalweg channel have deepest point just at the end of protective material. This setup has been done for most severe conditions. It has the extreme oblique flow angle and the discharge ratio is the highest so a wide range for velocity has been found. In that test chute channel is only dominating and affect the protection work most. There is stagnant water at main channel so sedimentation zone is most extended at upstream than the other tests.

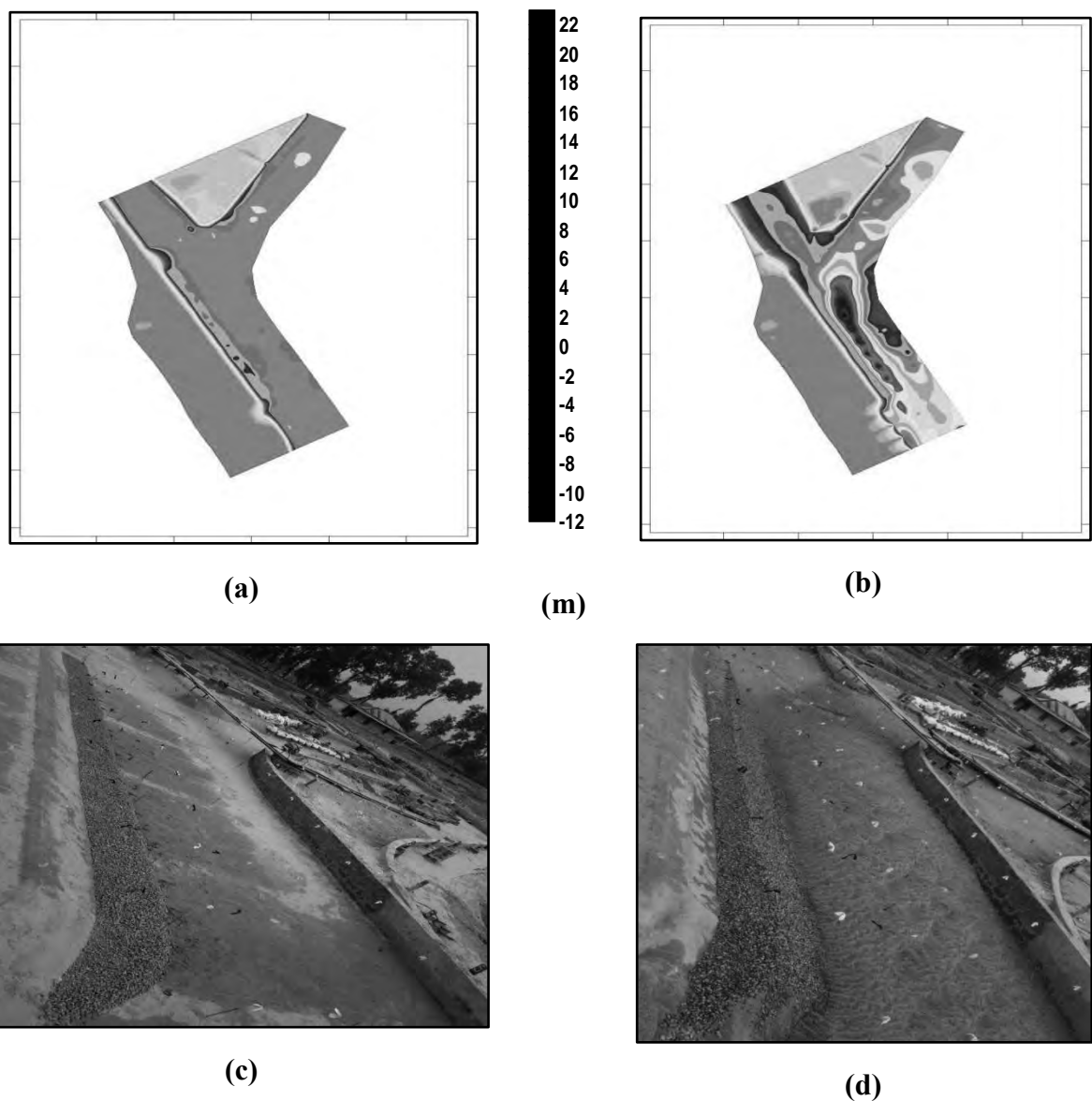


Figure 5.16: Bed and Bank Details for T-12: (a) Before Run for Prototype; (b) After Run for Prototype; (c) Before Run for Model; (d) After Run for Model.

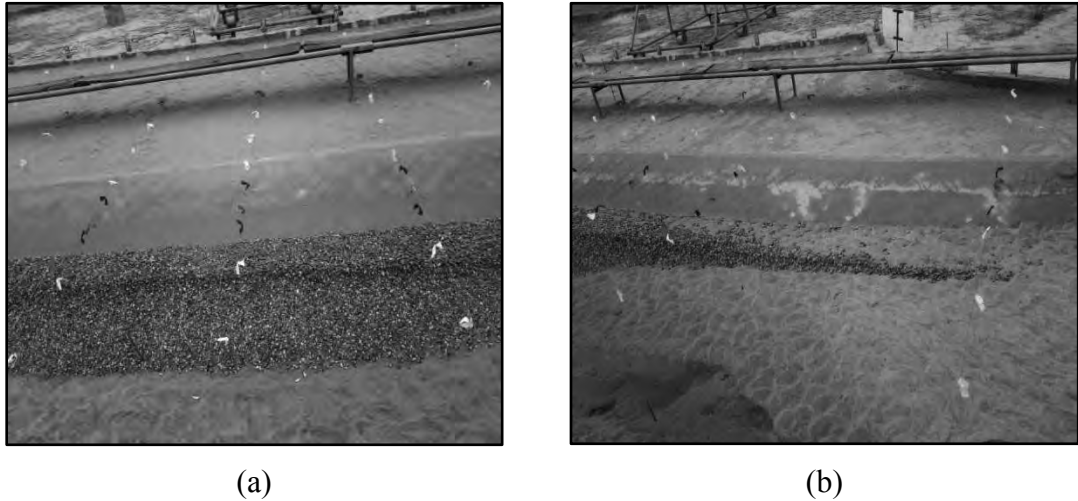


Figure 5.17: Launching Behaviour at T-12: (a) at Revetment Part (b) Sedimentation on Launching Apron

5.2.7 Straight Channel, Protected Bank by Geo-bag Type-1, 60° Oblique Flow Angle with Different Discharge Ratio

(a) Results of Physical Model Setup T-14

Experimental condition for the setup has been fixed by protection work with geo-bag type-1, oblique flow angle is 60° and discharge ratio is 1:1.2 (Figure 5.19). Maximum bed scour is 12.25 m at c/s 11 and velocity at that cross section is 1.08 m/s to 3.79 m/s. Deposition also occurred but area of deposition is less. Thalweg channel developed from the combined channel and goes to the d/s of the channel and shape of thalweg has a bowl shape. Launching slope is more flat at a slope of 1:1.28 to 1:1.66 (Table 5.4). Bare spaces are frequently present in the launching apron (Figure 5. 20).

The higher angularity of protective material develop more spreaded thalweg channel. Geo-bag spreaded not only in the slope but also in the bed. The slope is quite flat and protective material scattered along the bed due to its non uniformed launching behavior. Due to oblique flow a secondary flow generates that tries to suck the material and drop it at some distance from it until it loses energy to carry the material. Due to non uniform launching behavoiur this area remains uncovered (Figure 5. 20).

(b) Results of Physical Model Setup T-15

Bank is protected by geo-bag type-1, oblique flow angle is 60° and discharge ratio is 1:1.4 in this setup (Figure 5.21). Thalweg channel developed from the combined part and goes to the d/s of the channel. The deep part of the thalweg channel has a scour of 14.96 m at c/s 11 with varying velocity of 1.33 m/s to 3.33 m/s. Launching slope is more flat having slope of 1:1.78 to 1:1.99 (Table 5.4) and shape of thalweg has a bowl shape. Deposition also occurred but area of deposition is less. Bare spaces are frequently present in the launching apron (Figure 5.22). Most of all the behaviour is same as T-14 but intensity is more than it.

(c) Results of Physical Model Setup T-16

Experimental condition for the setup has been fixed as protected bank by geo-bag type-1, oblique flow angle is 60° and discharge ratio is 1:1.6 (Figure 5.23). All the behaviour is same as T-14 and T-15 but intensity is more than these. Maximum scour depth is 15.21 m at c/s 11. Velocity at that section is 1.20 m/s to 3.69 m/s. Protective material (geo-bag type-1) launched at a slope of 1:1.95 to 1:2.17 (Table 5.4) with frequent bare spaces. Protective materials hang at top of launched slope and work as a group in spite of covering the launched area.

The protective material is not effective as a quick response material to meet the erosion, so there are bare spaces (Figure 5.24). These case causes possibility of slope failure. High current removes materials from below the launching apron and thus causes slope failure.

5.2.8 Straight Channel, Protected Bank by Geo-bag type -1 and Main Channel Close:

(a) Results of Physical Model Setup T-17

The test has an oblique flow angle of 60° where main channel is closed and protection work has been done by geo-bag type-1 (Figure 5.25). Deep thalweg channel developed where launching apron ends and maximum 12.00 m bed scour found at c/s

10. Excessive deposition occurred at left bank. There is also excessive deposition at main channel upstream.

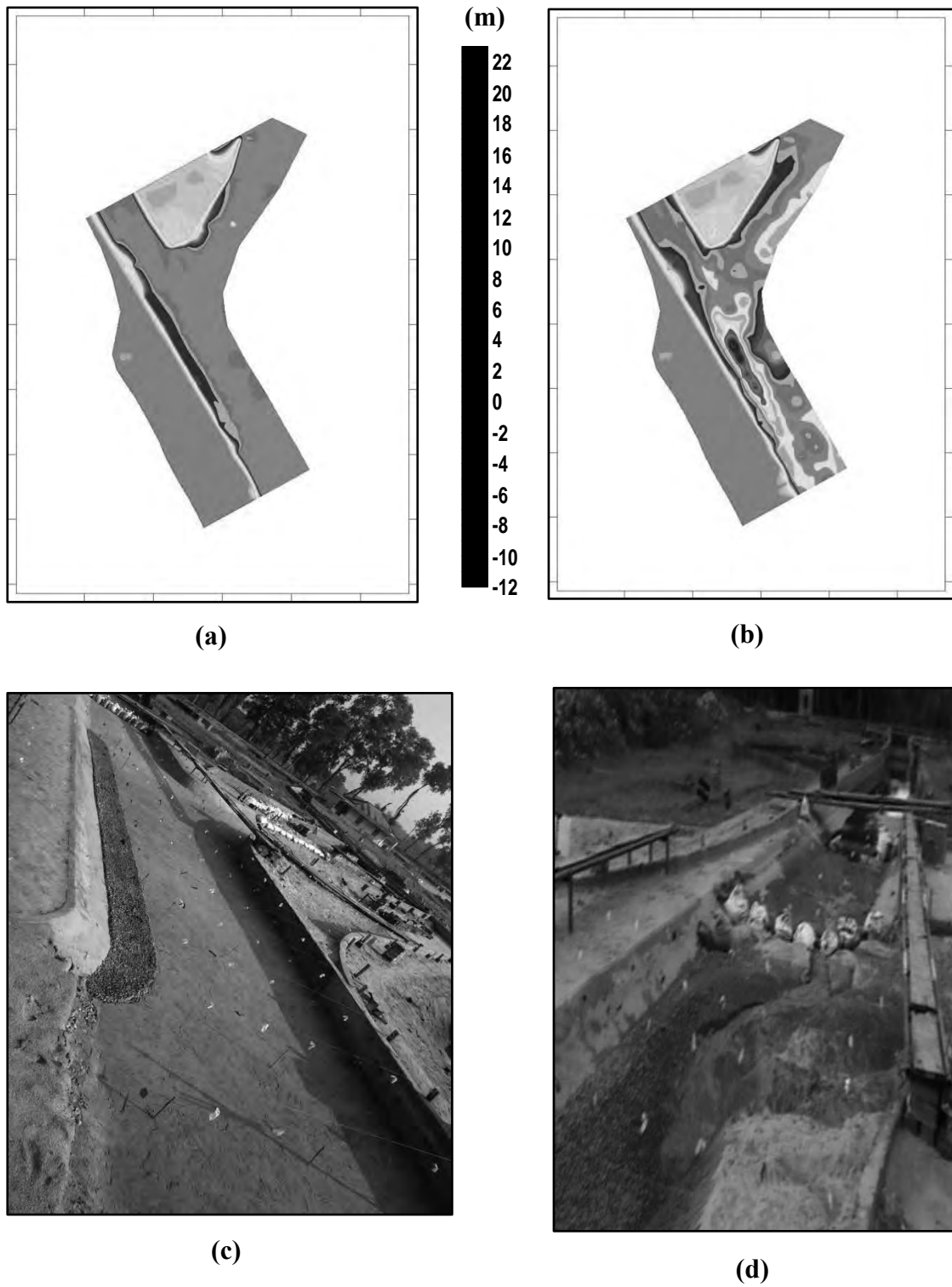
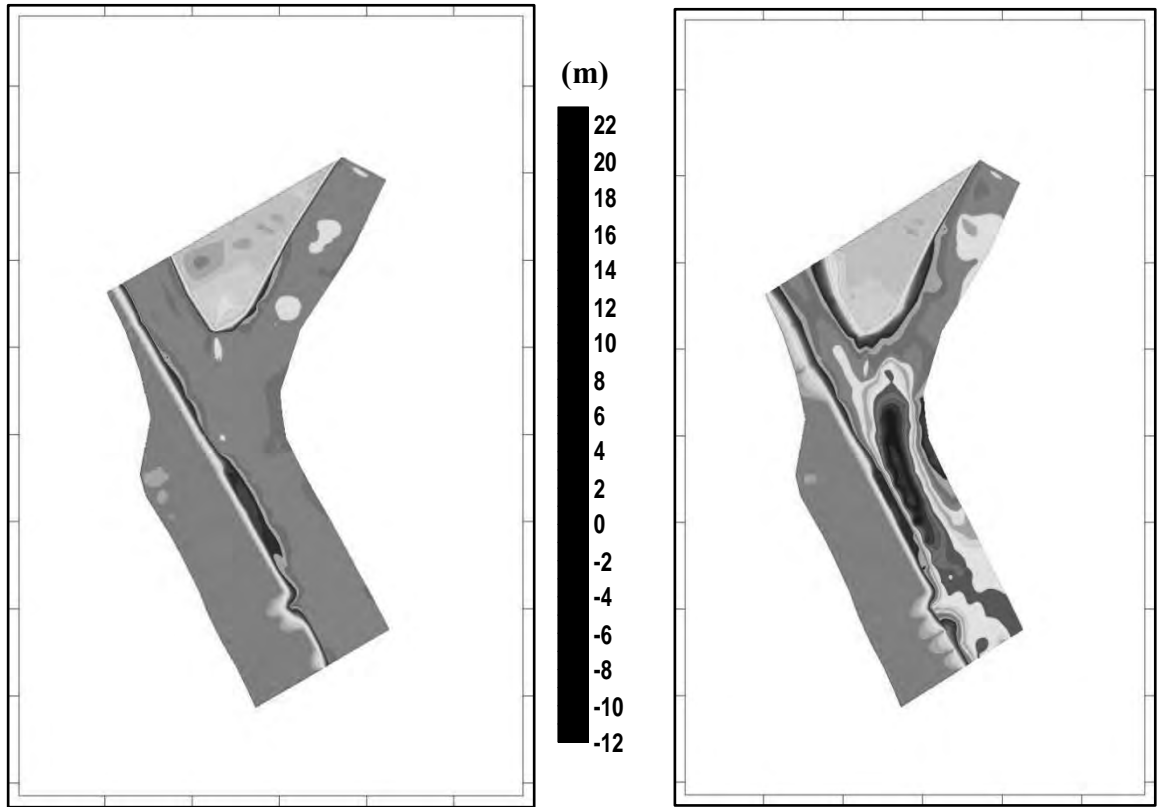


Figure 5.18: Bed and Bank Details for T-13: (a) Before Run for Prototype; (b) After Run for Prototype; (c) Before Run for Model; (d) After Run for Model.



(a)

(b)



(c)



(d)

Figure 5.19: Bed and Bank Details for T-14: (a) Before Run for Prototype; (b) After Run for Prototype; (c) Before Run for Model; (d) After Run for Model.

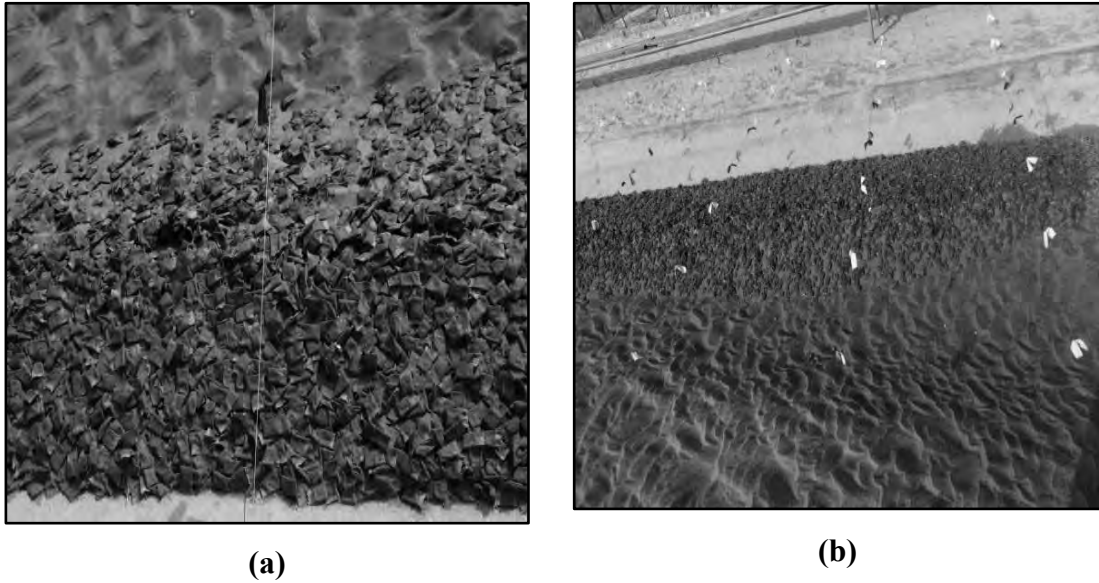


Figure 5.20: Launching Behaviour of Geo-bag Type-1 in T-14: (a) Bare Spaces in Launching Apron; (b) Top view of Revetment

Protective material (geo-bag type-1) launched at a slope of 1:1.55 to 1:2.35 (Table 5.4) and bare spaces found in launched slope. Sediment has been carried over launched slope (Figure 5.26). Velocity varies between 2.33 m/s to 4.45 m/s at that c/s. Chute channel is dominating in the setup so it causes excessive deposition at right bank and a more deep (than T-14 to T-16) and less flat thalweg channel. The other behavior is same and has been describes at 5.2.7.

5.2.9 Straight Channel, Protected Bank by Geo-bag Type-2, 60° Oblique Flow Angle with Different Discharge Ratio

(a) Results of Physical Model Setup T-18

Bank has been protected by geo-bag type-2, oblique flow angle is 60° and discharge ratio is 1:1.2 (Figure 5.27). Maximum bed scour of 9.5 m at c/s 10 with varying velocity of 0.70 m/s to 3.78 m/s has been found in the experimental setup. Protective material (geo-bag type-2) launched at a slope of 1:1.14 to 1:1.56 (Table 5.4) with bare spaces and protective materials hang at tope of launched slope and work as a group in spite of covering the launched area and the percentage is more than T-14 to T-16.

Launching slope has not been measured accurately as the launching apron takes a spreaded thalweg form. An approximate length for launching material after run has been taken in the setup. The protective material is not effective as a quick response material to meet the erosion, so there remains the possibility of slope failure (Figure 5.28).

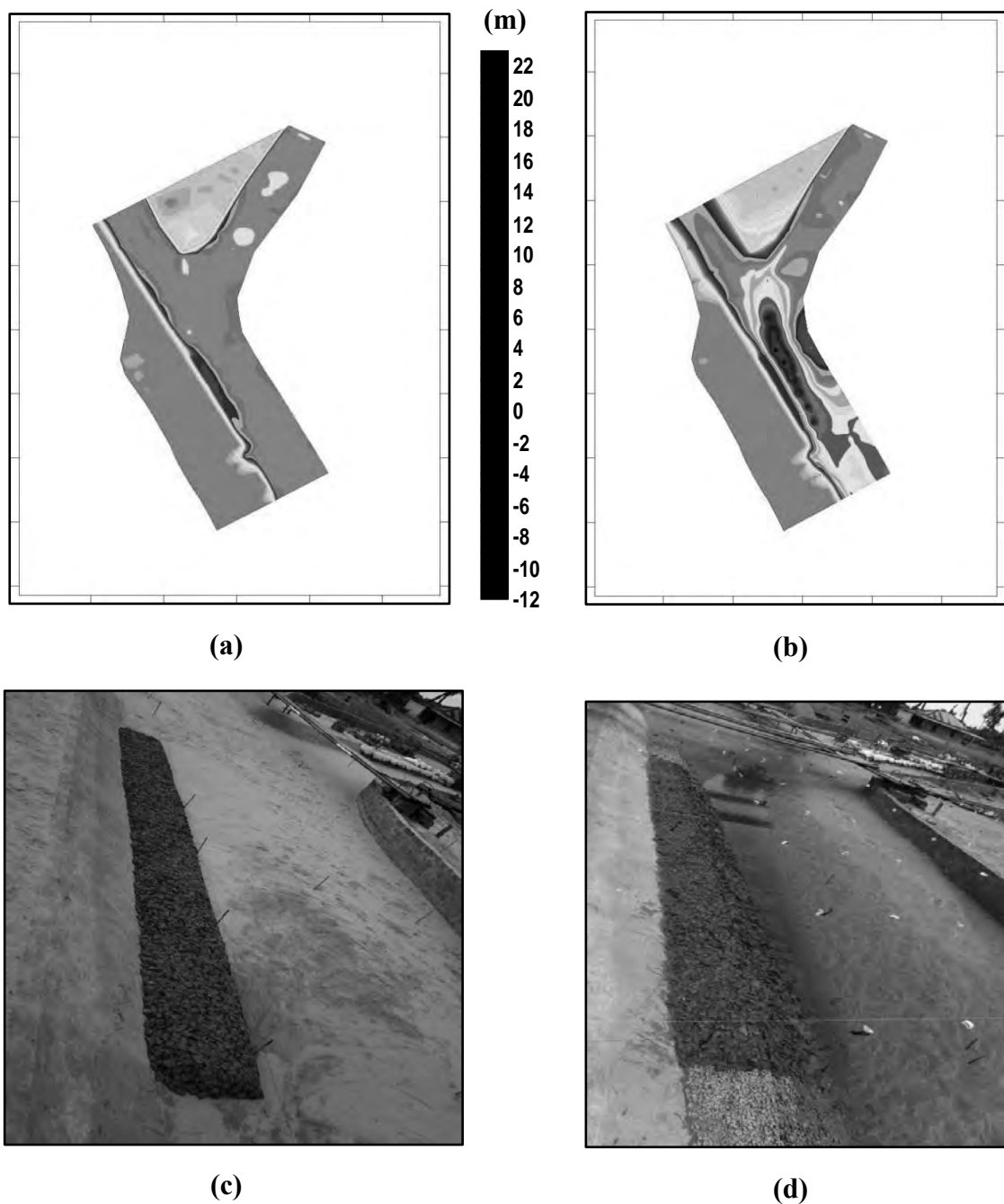


Figure 5.21: Bed and Bank Details for T-15: (a) Before Run for Prototype; (b) After Run for Prototype; (c) Before Run for Model; (d) After Run for Model.

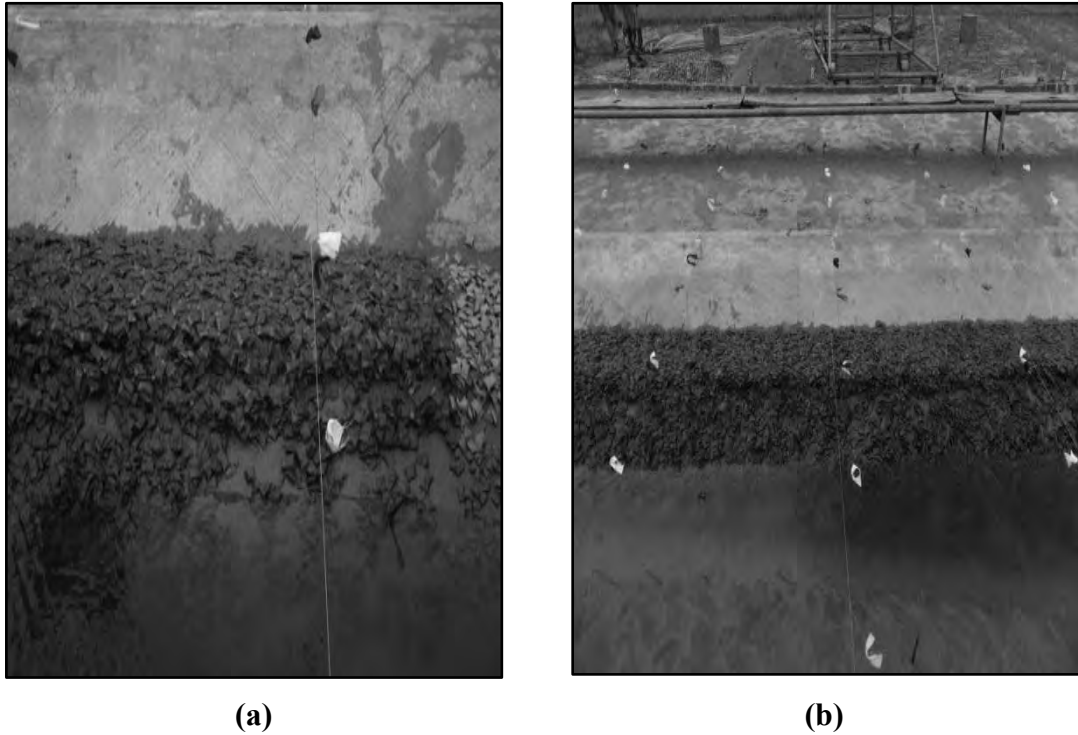


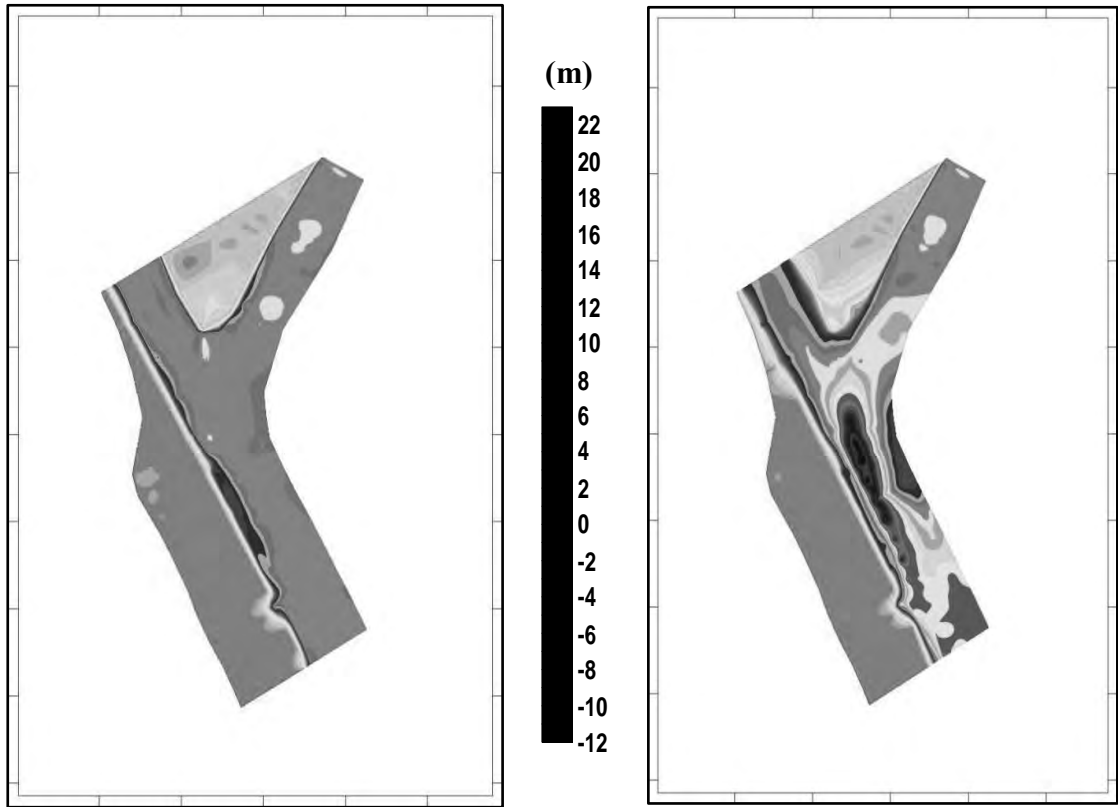
Figure 5.22: Launching Behaviour on T-15: (a) Bare Spaces at Starting Point; (b) at Mid of Revetment

(b) Results of Physical Model Setup T-19

Bank has been protected by geo-bag type-2, oblique flow angle is 60° and discharge ratio is 1:1.4 (Figure 5.29). Protective material (geo-bag type-2) launched at a slope of 1:0.91 to 1:2.26 (Table 5.4). Maximum 13.71 m scour occurred at c/s 7 with velocity of 3.32 m/s to 3.81 m/s. In spite of that all the behaviour is same as T-18.

(c) Results of Physical Model Setup T-20

In this setup bank has been protected by geo-bag type-2, oblique flow angle is 60° and discharge ratio is 1:1.6 (Figure 5.30). Protective material (geo-bag type-2) launched at a slope of 1:1.30 to 1:2.24 (Table 5.4). Percentage of bare spaces is more than T-18 and T-19. Maximum 12.75 m bed scour found at c/s 11 with a velocity between 2.26 m/s to 3.35 m/s. Displacement of launching materials are more in the setup (Figure 5.31).



(a)

(b)



(c)

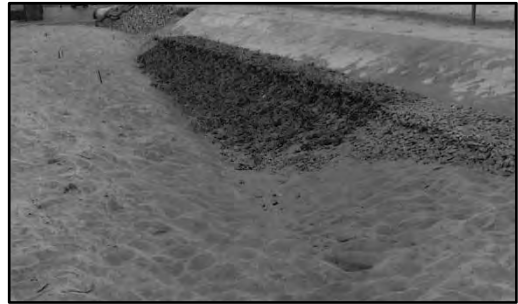


(d)

Figure 5.23: Bed and Bank Details for T-16: (a) Before Run for Prototype; (b) After Run for Prototype; (c) Before Run for Model; (d) After Run for Model.

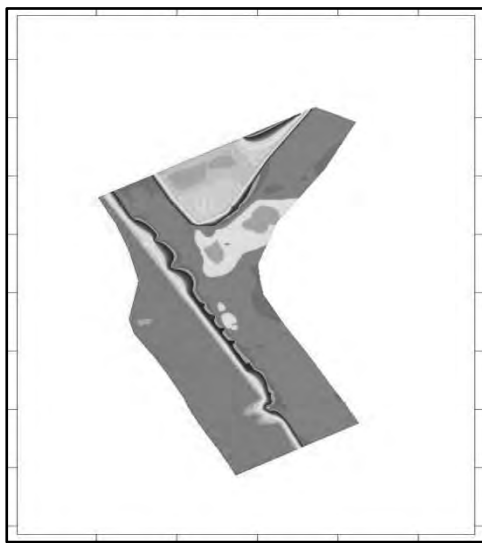


(a)

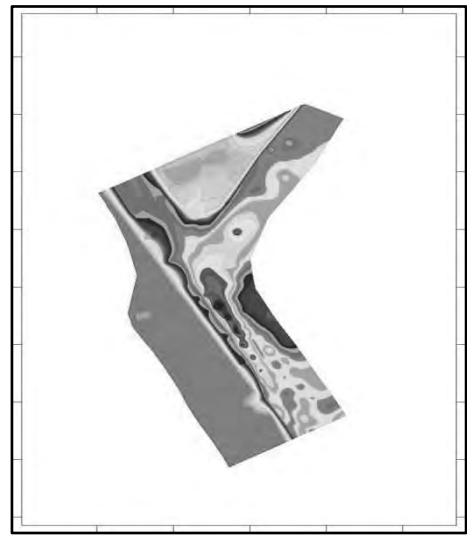


(b)

Figure 5.24: Launching Behaviour on T-16: (a) Bare spaces; (b) Spreaded Protective Material



(a)



(b)



(c)

(m)



(d)

Figure 5.25: Bed and Bank Details for T-17: (a) Before Run for Prototype; (b) After Run for Prototype; (c) Before Run for Model; (d) After Run for Model.

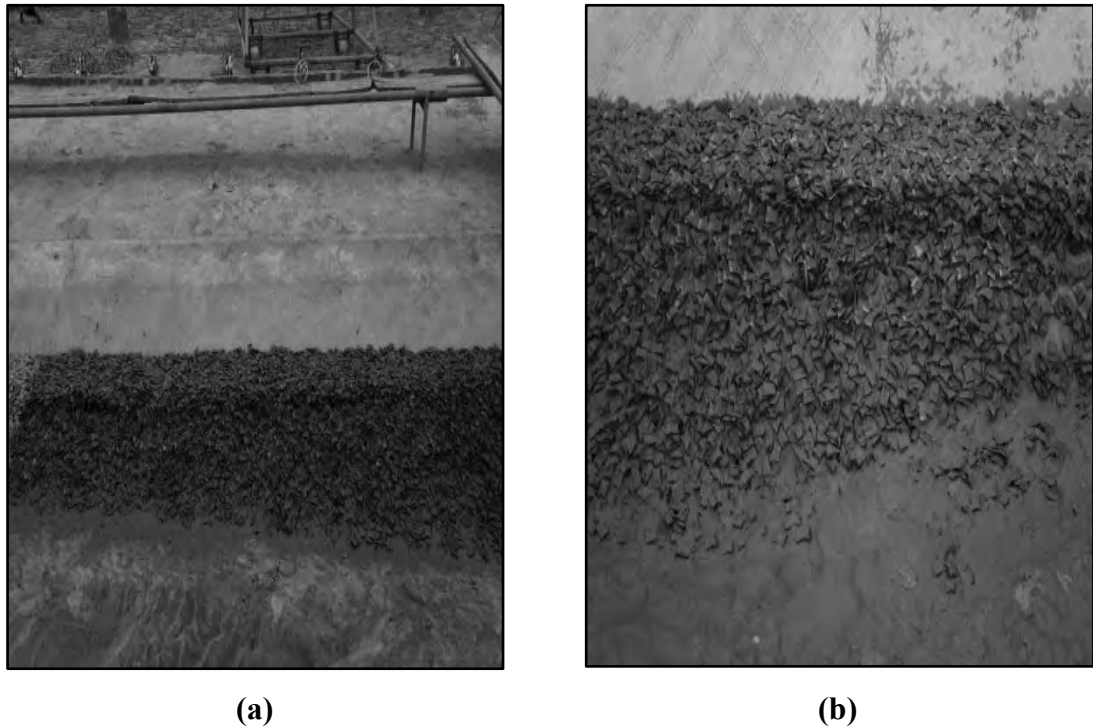
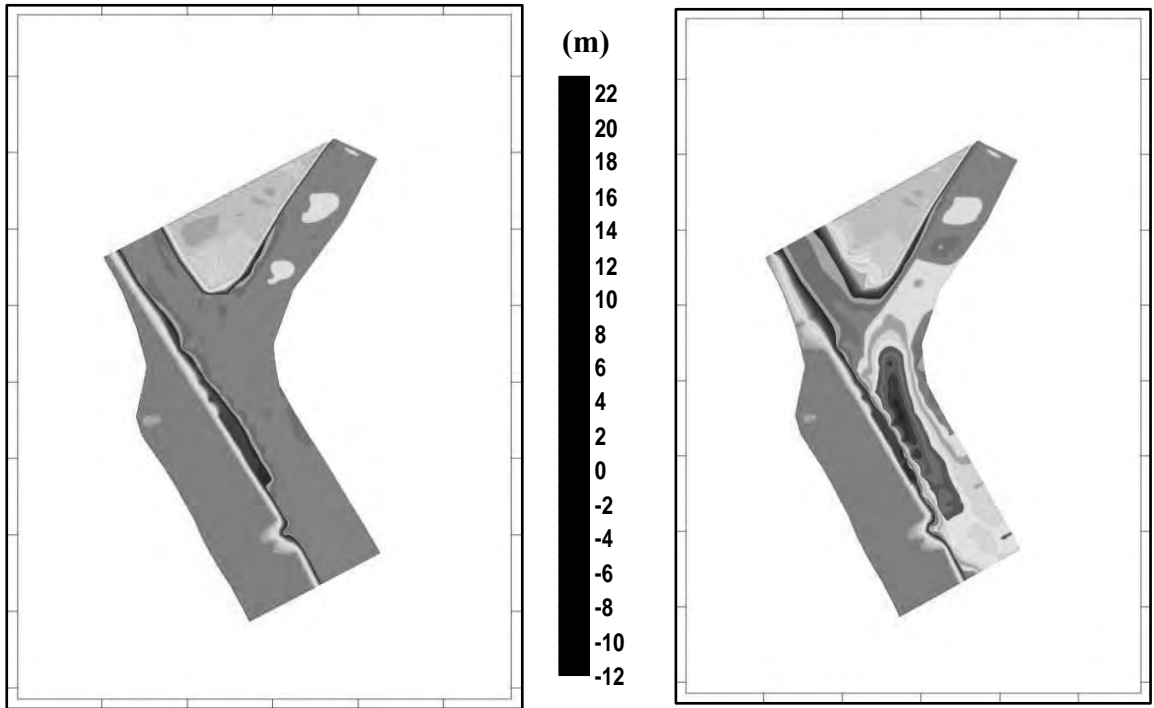


Figure 5.26: Launching Behaviour on T-17: (a) Spreded Protective Material; (b) Bare spaces.

Finally a drawback has been found at field condition in measuring launching slope for test T-14 to T-17. According to Table 5.2 more flat slope has been found in calculation but according to the figure there is less steep slope for these setups. The slope length has been measured by taking a single measurement within 1m zone. The protective materials (Geo-bag) is scattered so length has been measured on an average at field condition. The real value has not been found in that measurement. Again when oblique flow is more dominating it acts as main flow on revetment and bed. In this kind of flow environment, secondary flows generate causes the change in roughness between revetment surface and bed. Thus the secondary flow accelerates the protective material to launch in order to meet the erosion.



(a)

(b)

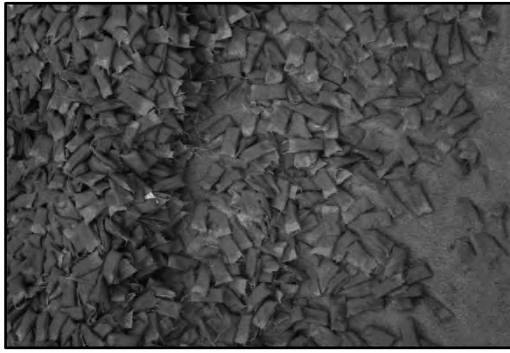


(c)

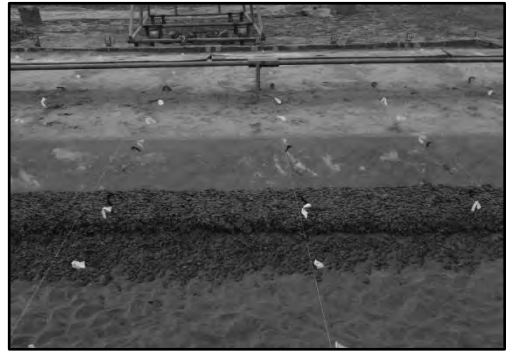


(d)

Figure 5.27: Bed and Bank Details for T-18: (a) Before Run for Prototype; (b) After Run for Prototype; (c) Before Run for Model; (d) After Run for Model.



(a)

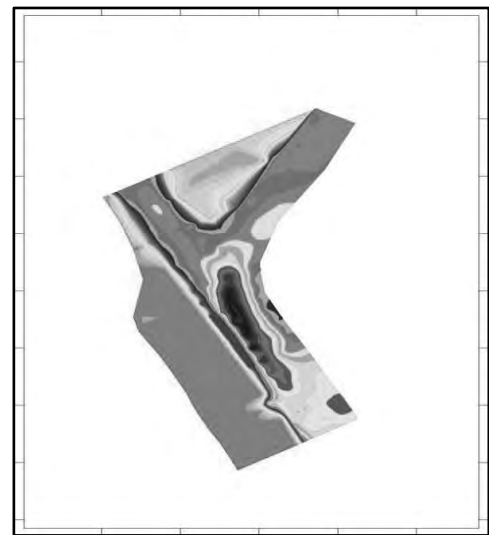


(b)

Figure 5.28: Launching Behaviour on T-18: (a) Spreded Protective Material; (b) Bare spaces.



(a)



(b)

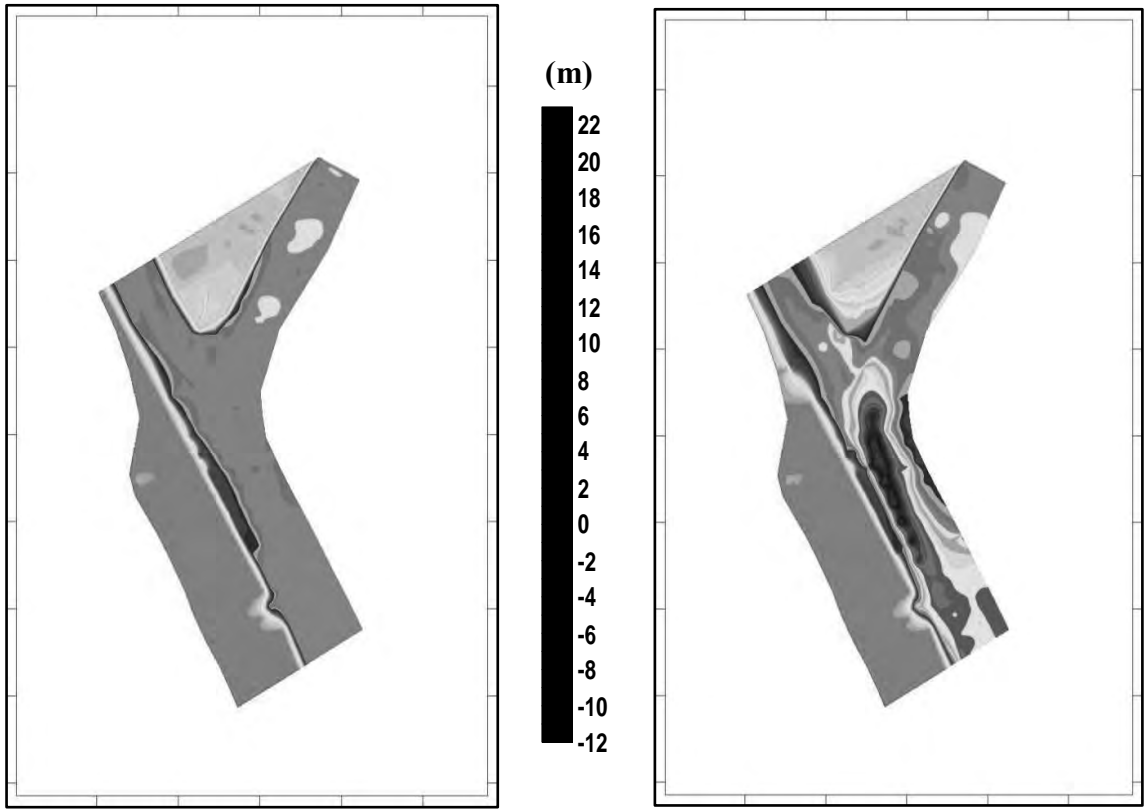


(c)



(d)

Figure 5.29: Bed and Bank Details for T-19: (a) Before Run for Prototype; (b) After Run for Prototype; (c) Before Run for Model; (d) After Run for Model.



(a)

(b)



(c)



(d)

Figure 5.30: Bed and Bank Details for T-20: (a) Before Run for Prototype; (b) After Run for Prototype; (c) Before Run for Model; (d) After Run for Model.

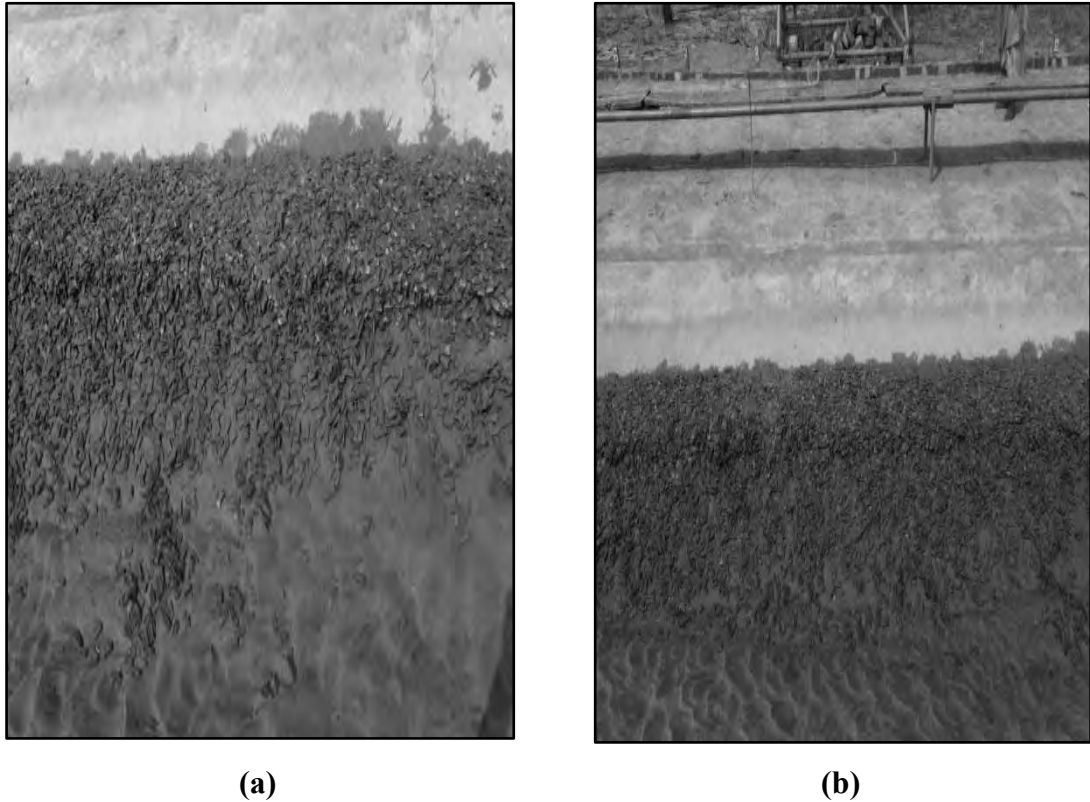


Figure 5.31: Launching Behaviour on T-20: (a) Spreaded Protective Material; (b) Bare Spaces and Sedimentation on Protective Material.

5.3 Comparison of Channel Cross Sections for Maximum Scour

A detail comparison of channel cross sections at maximum scour sections (according to Table-5.1 and Table-5.2) for different experimental setup has been presented by figure 5.32 to 5.82. The analysis has been done to compare the experimental setup having mostly similar nature/condition. The comparison has been done by analyzing governing cross sections having maximum scour. For each experimental setup three cross sections (maximum scoured c/s and two sections before and after of the section) have been taken into considerations. For example T-1, T-2 and T-3 having maximum scoured section is 5, 8 and 8 respectively, so c/s 4, 5, 6, 7, 8 and 9 has been considered for group-1. The analysis for all experimental setup has been done in the same way.

Table 5.1: Group Description for Comparison of Maximum Scour Sections (Grouping based on same oblique flow angle)

Group ID	Combination of Tests	Discharge Ratio	C/S Taken	Group Condition	Protection Material
G-1	T-1, T-2 and T-3	1:4	C/S 4 to C/S 9	Discharge ratio 1:1.4	Unprotected bank
G-2	T-4, T-5 and T-6	1:2, 1:4 and 1:6	C/S 6 to C/S 12	Oblique flow angle 20°	Stone boulder
G-3	T-7, T-8 and T-9	1:2, 1:4 and 1:6	C/S 8 to C/S 10	Oblique flow angle 40°	Stone boulder
G-4	T-10, T-11 and T-12	1:2, 1:4 and 1:6	C/S 8 to C/S 11	Oblique flow angle 60°	Stone boulder
G-5	T-14, T-15 and T-16	1:2, 1:4 and 1:6	C/S 10 to C/S 12	Oblique flow angle 60°	Geobag type -1 (738 kg)

5.3.1 Comparison of Channel Cross Section for Group-1

Group-1 is the combination of T-1, T-2 and T-3 and observed maximum scour section for the tests is 5, 8 and 8 for respectively (Figure 5.32 to 5.37).

The superimposed graphs of group-1 shows that at C/S-4 there is around 12.5 m bank erosion for T-3 (maximum 25 m observed), at C/S-6 it is around 12.5 m for both T-2 and T-3. There is also more or less 5 m to 10 m erosion in other sections. The deep scour or thalweg has been developed towards more to the right bank due to the push back effect of main channel. T-3 has a more dominant chute channel, so thalweg is towards right bank.

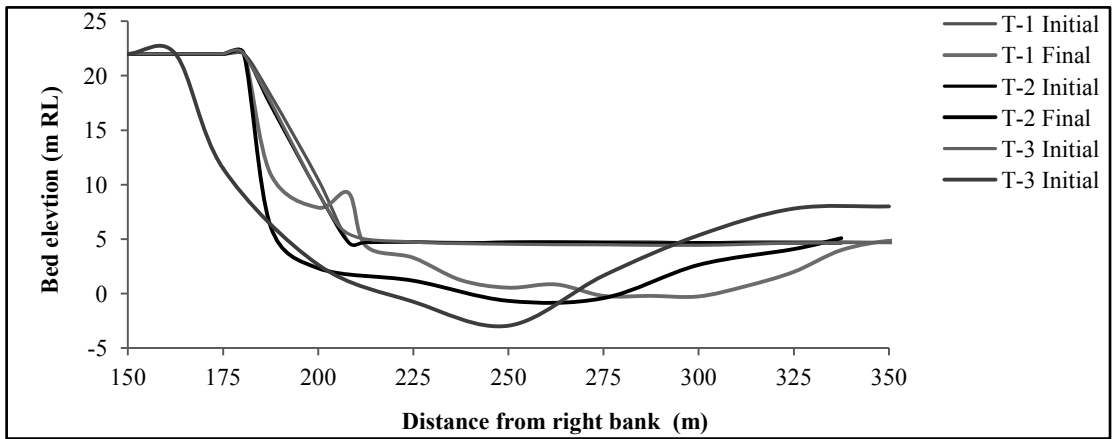


Figure 5.32: Scour for Group-1 at Cross Section 4

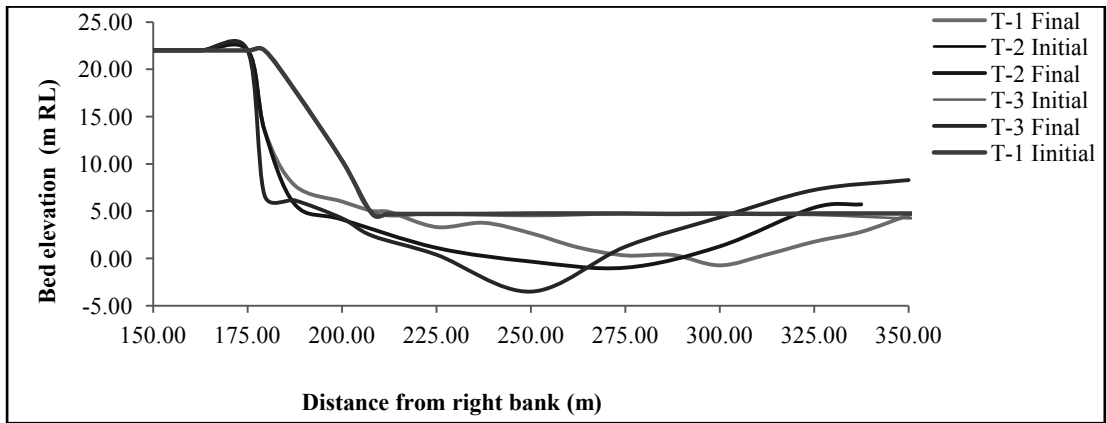


Figure 5.33: Scour for Group-1 at Cross Section 5

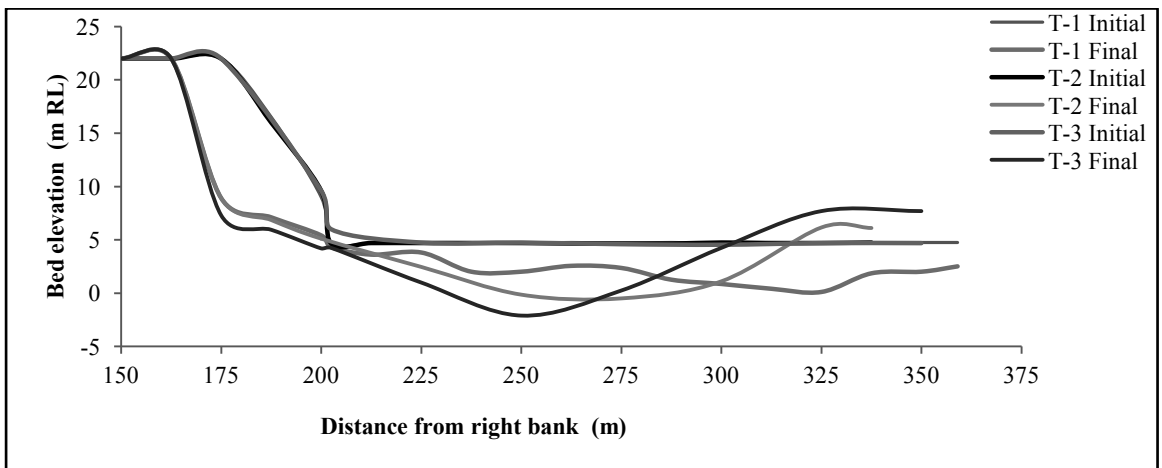


Figure 5.34: Scour for Group-1 at Cross Section 6

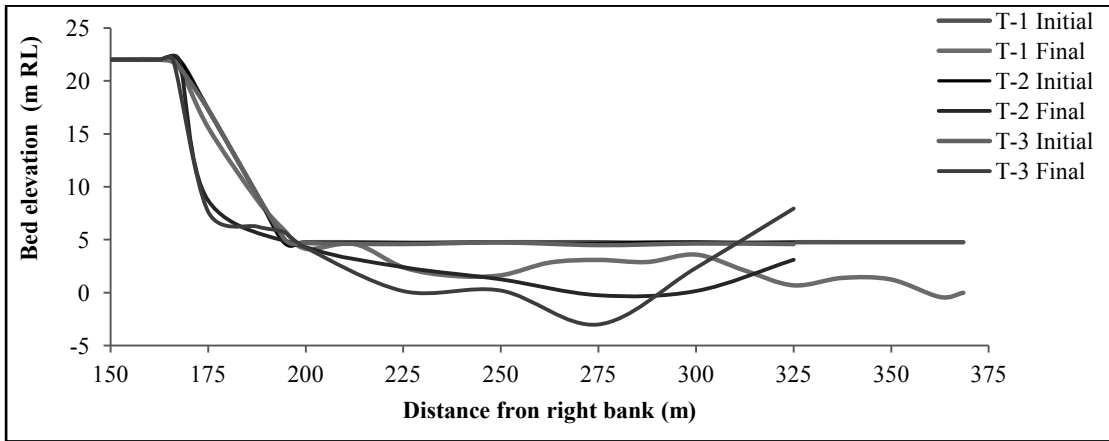


Figure 5.35: Scour for Group-1 at Cross Section 7

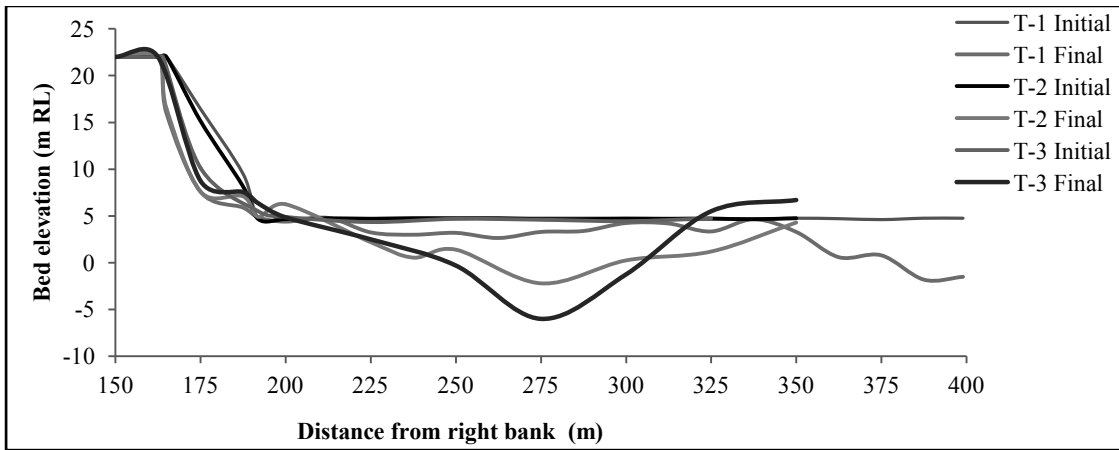


Figure 5.36: Scour for Group-1 at Cross Section 8

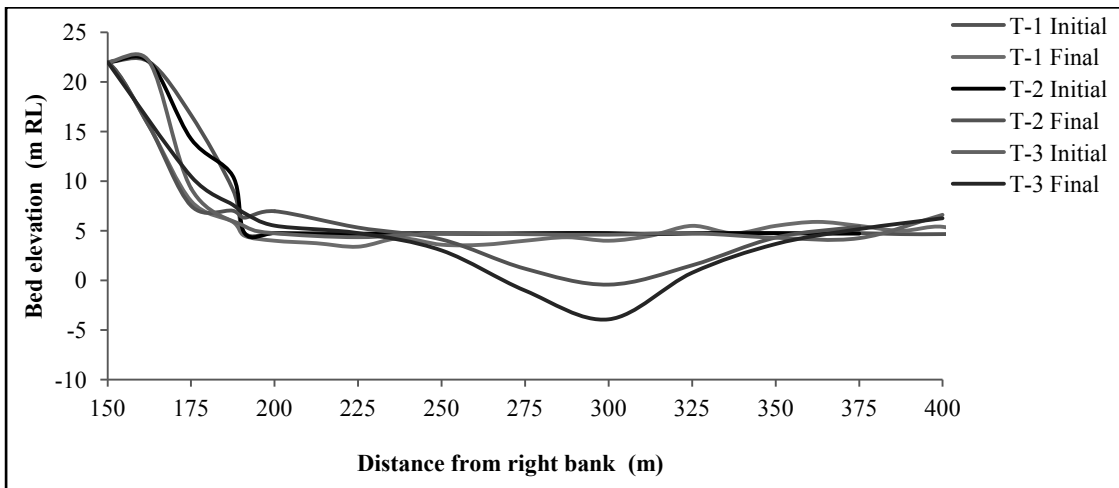


Figure 5.37: Scour for Group-1 at Cross Section 9

5.3.2 Comparison of Channel Cross Section for Group -2

Group-2 is the combination of T-4, T-5 and T-6 and observed maximum scour section for the tests is 11, 7 and 8 for respectively (Figure 5.38 to 5.44).

The superimposed graph of group-2 is a combination when flow angle is fixed (20°) but discharge ratio is variable. The cross sections from 6 to 9 is mostly affected and developed thalweg channel in the sections has a sharp edge where launching apron ends. This situation occurs as stone boulder had less angularity. The thalweg channel is flat type beyond cross section 9 as the effect of oblique flow starts effective from combined channel and it starts creating the channel which is more effective after section 12 to D/S. The more the discharge ratio the more is scour depth but the zone/cross section is different for different tests. When chute channel become more dominant then flow from CC directly hit the protective work and make MC less active resulting sedimentation at upstream of protective work.

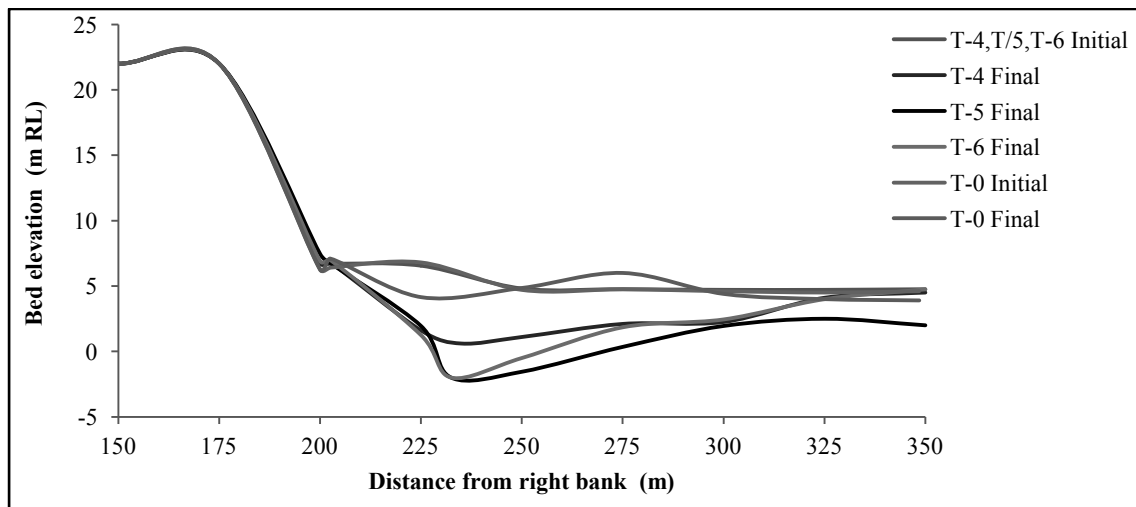


Figure 5.38: Scour for Group-2 at Cross Section 6

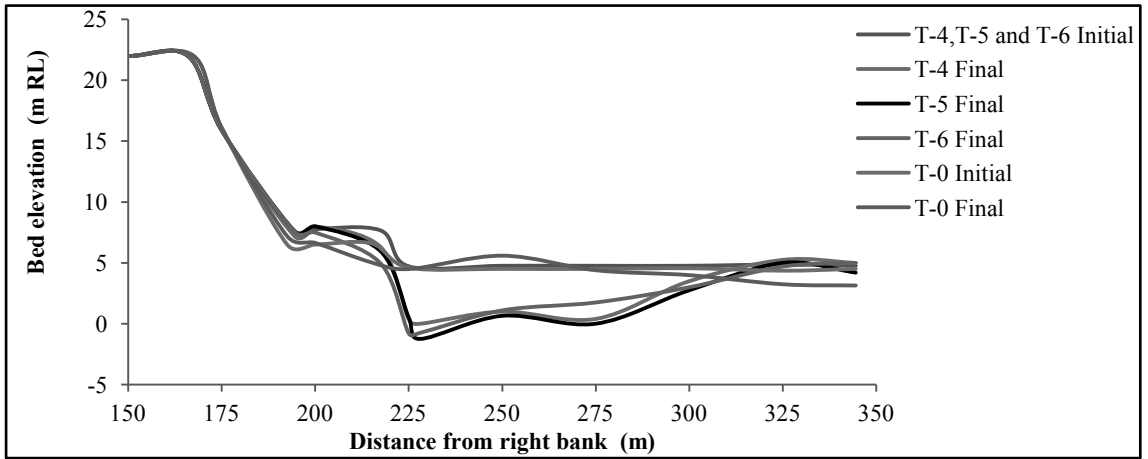


Figure 5.39: Scour for Group-2 at Cross Section 7

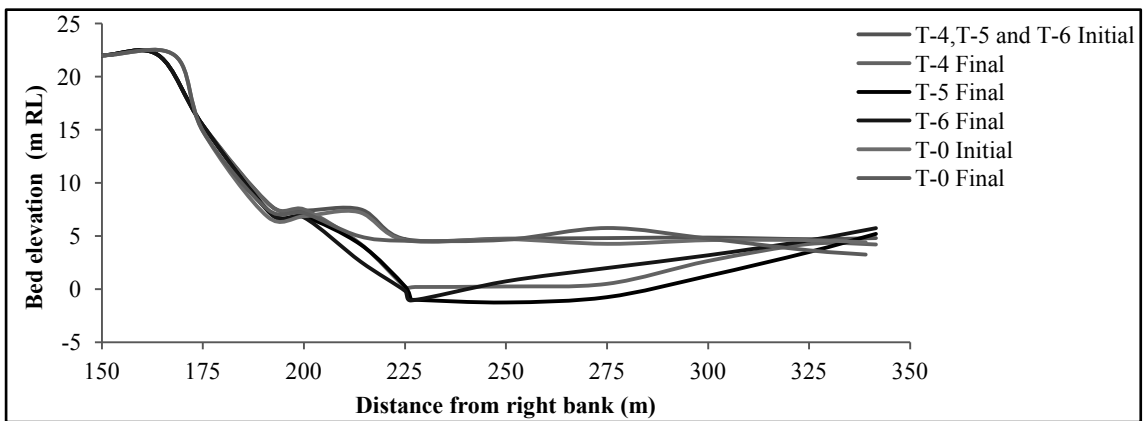


Figure 5.40: Scour for Group-2 at Cross Section 8

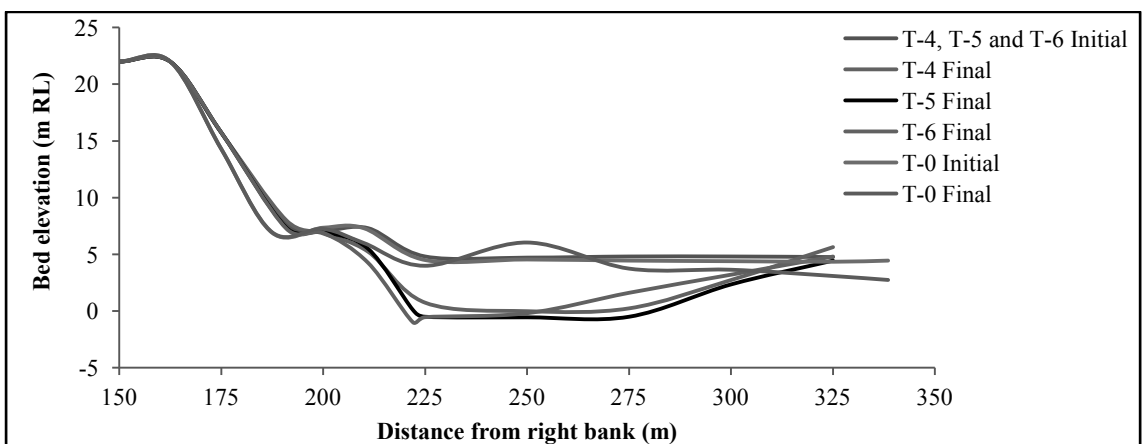


Figure 5.41: Scour for Group-2 at Cross Section 9

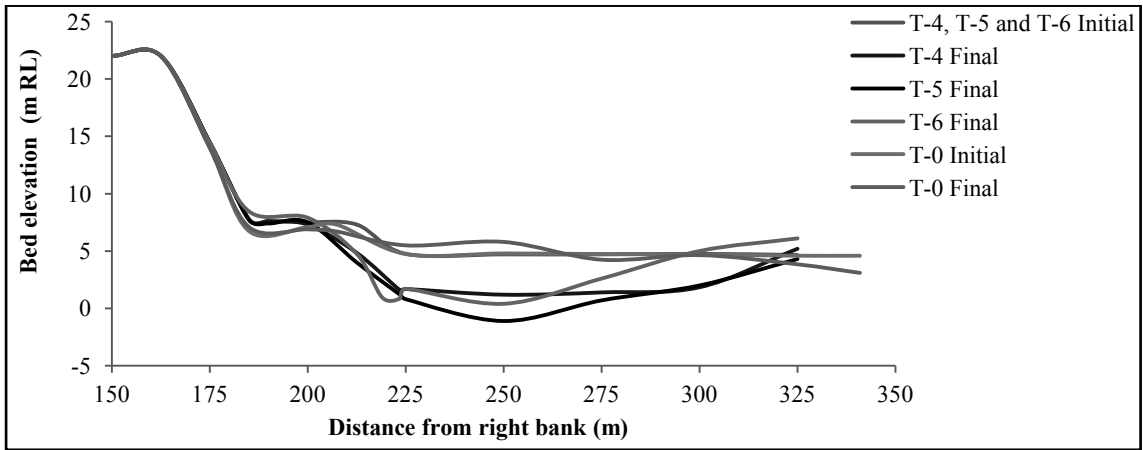


Figure 5.42: Scour for Group-2 at Cross Section 10

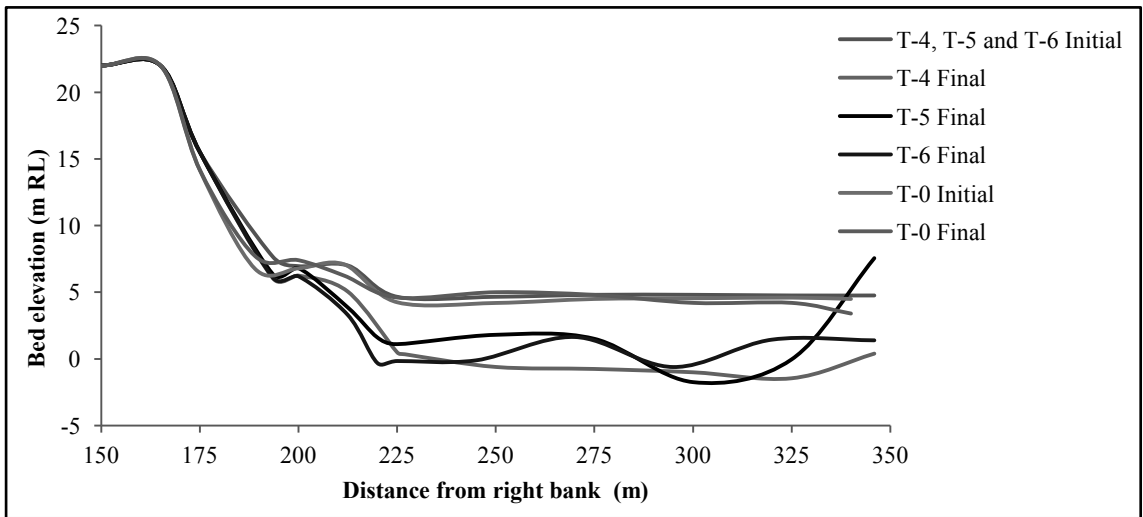


Figure 5.43: Scour for Group-2 at Cross Section 11

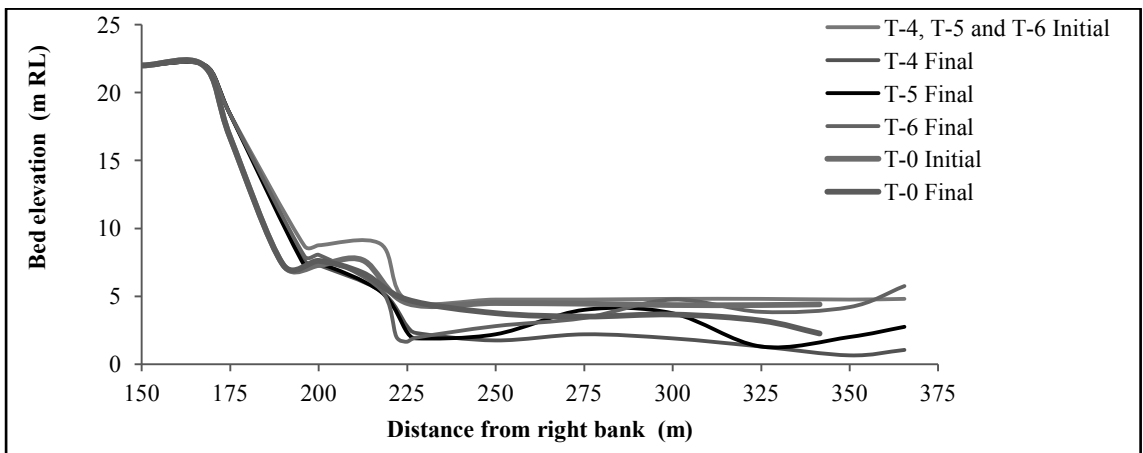


Figure 5.44: Scour for Group-2 at Cross Section 12

5.3.3 Comparison of Channel Cross Section for Group -3

Group-3 is the combination of T-7, T-8 and T-9 and observed maximum scour section for the tests is 9 (Figure 5.45 to 5.47).

The superimposed graph of group-3 is a combination when flow angle is fixed (40°) but discharge ratio is variable. Here flow angle being more dominant than G-2, this combination has a different behavior. The more the discharge ratio the more is scour depth but the zone/cross section is different for different tests. G-3 has a similar behavior for the tests of it. The thalweg channel pattern is same for the tests of the combination only the depth of channel is more for large discharge ratio.

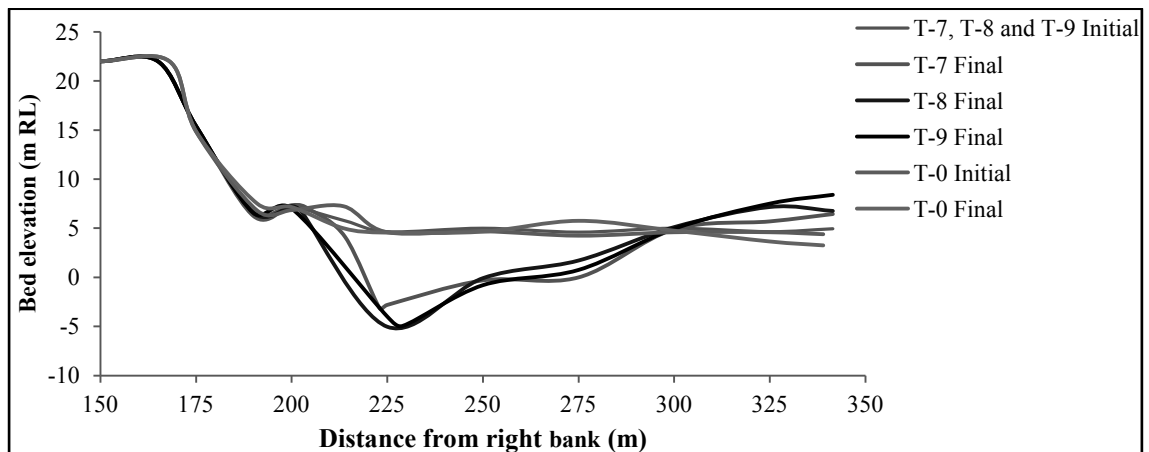


Figure 5.45: Scour for Group-3 at Cross Section 8

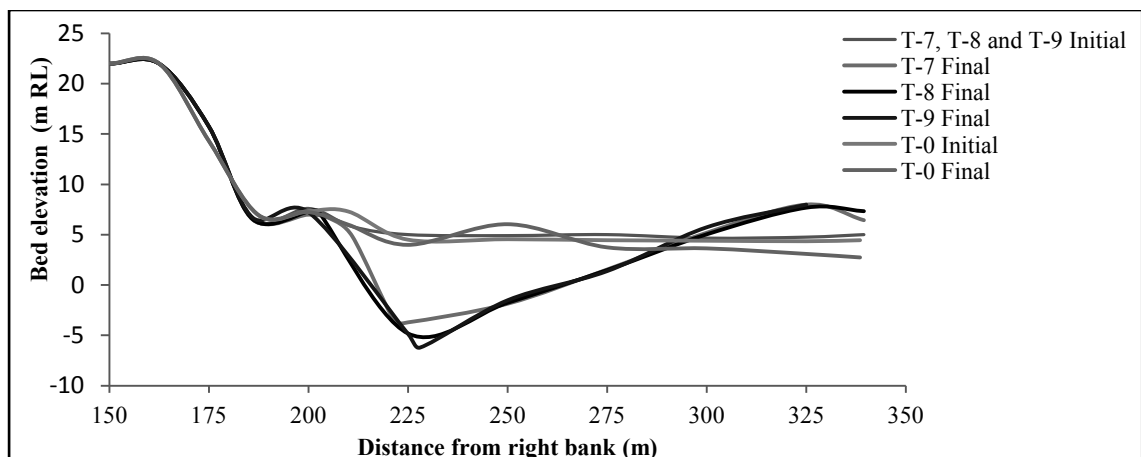


Figure 5.46: Scour for Group-3 at Cross Section 9

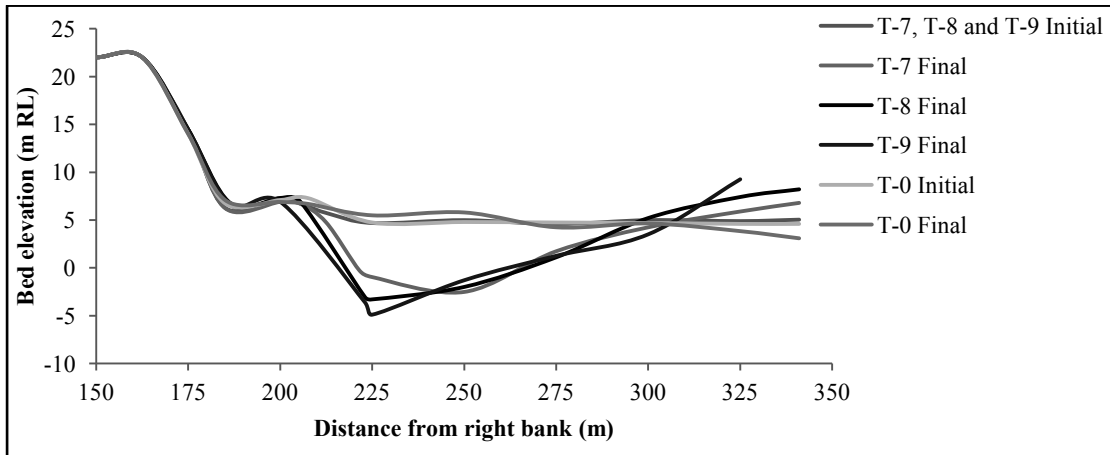


Figure 5.47: Scour for Group-3 at Cross Section 10

5.3.4 Comparison of Channel Cross Section for Group -4

Group-4 is the combination of T-10, T-11 and T-12 and observed maximum scour section for the tests is 9, 10 and 10 for respectively (Figure 5.48 to 5.51). The superimposed graph of group-4 is a combination when flow angle is fixed (60°) but discharge ratio is variable. Here flow angle being more dominant than group-2 and group-3. This combination presents a totally different behavior. Without the sedimentation zone the thalweg channel is same in shape for the three test, but dominant chute channel shift the flow thrust to the main channel bank thus creating a more deep channel and makes sedimentation in right bank. There is also sedimentation towards the main channel as chute channel is more dominant than group-2 and group-3.

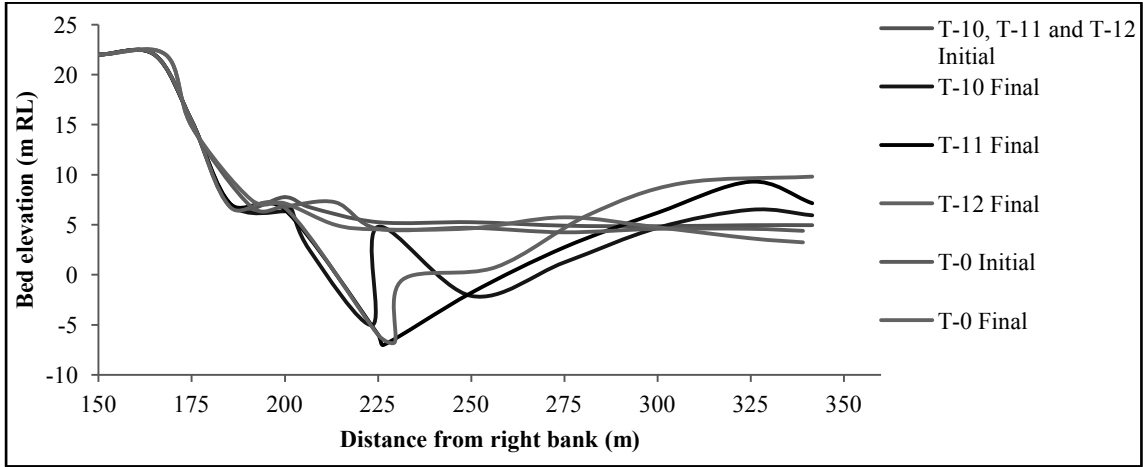


Figure 5.48: Scour for Group -4 at Cross Section 8

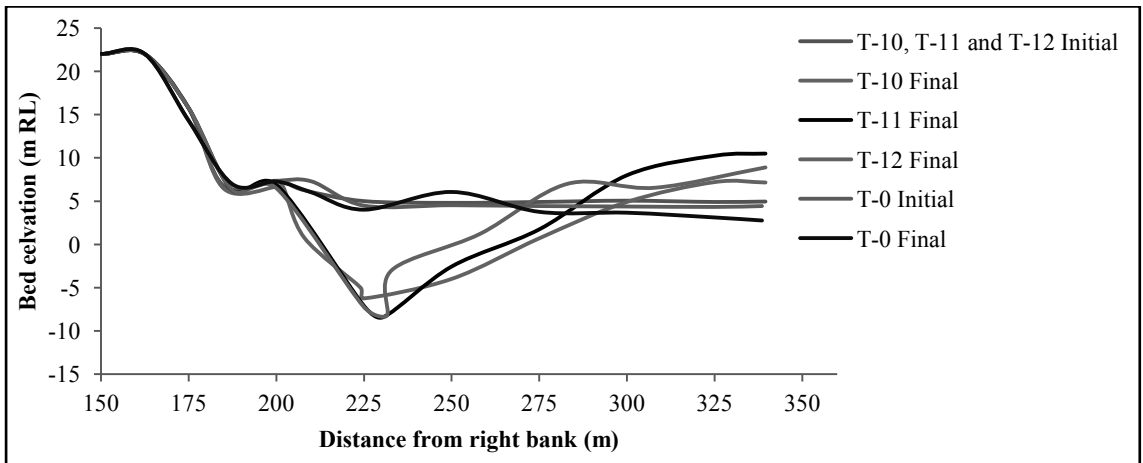


Figure 5.49: Scour for Group -4 at Cross Section 9

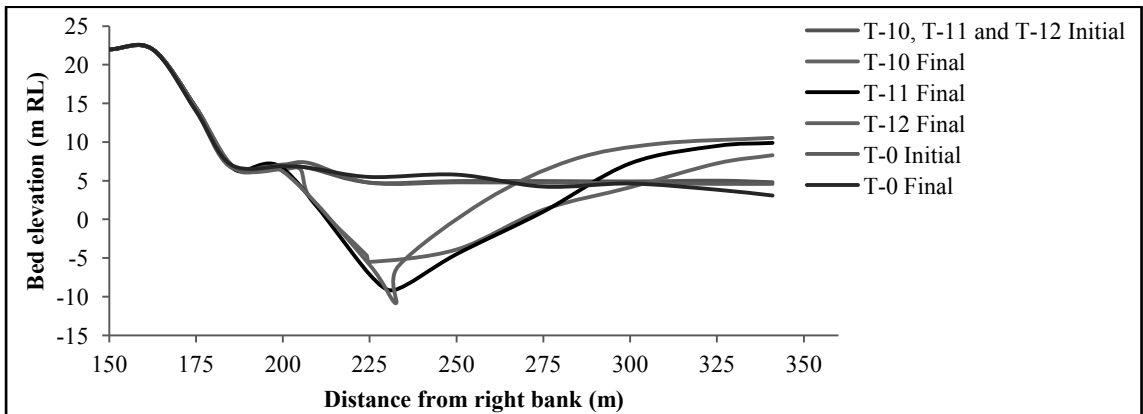


Figure 5.50: Scour for Group -4 at Cross Section 10

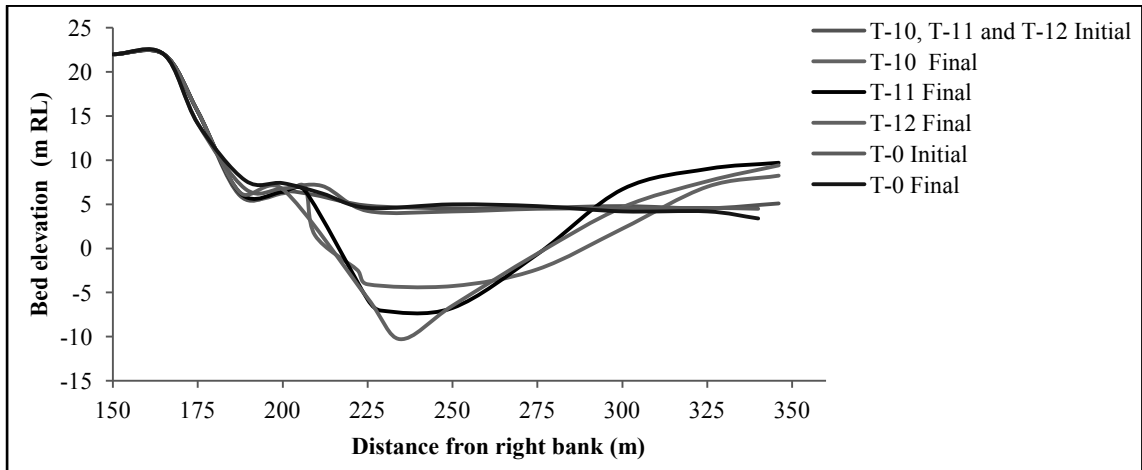


Figure 5.51: Scour for Group -4 at Cross Section 11

5.3.5 Comparison of Channel Cross Section for Group -5

Group-5 is the combination of T-14, T-15 and T-16 and observed maximum scour section for the tests is 11 (Figure 5.52 to 5.54).

The superimposed graph of group-5 is a combination when flow angle is fixed (60°) but discharge ratio is variable and bank has been protected by Geo-bag type-1. This combination have a similar behavior as group-4 but thalweg channel have a uniform shape throughout the width of section due to higher angularity of protective material volume of launching material is less. The thalweg channel then takes a uniform shape though the dominant chute channel shift the flow thrust to the main channel bank but amount of deposition in the left bank is less due to the effect.

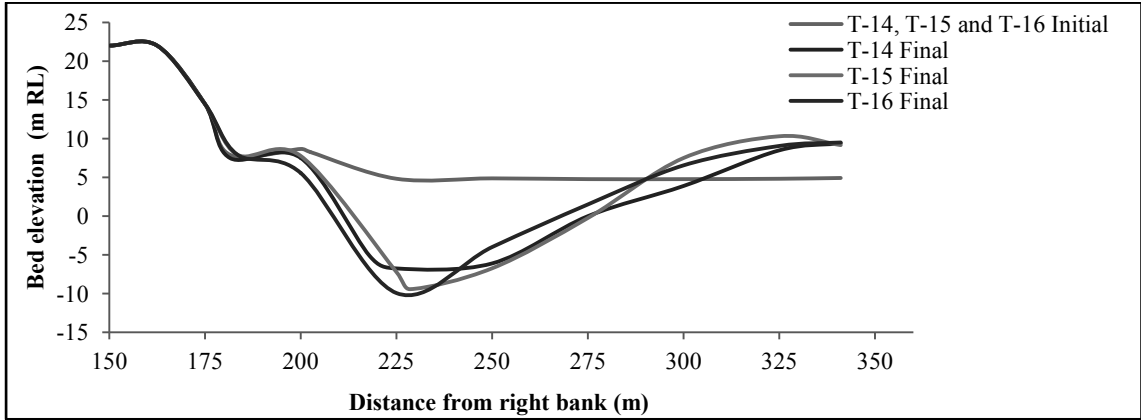


Figure 5.52: Scour for Group-5 at Cross Section 10

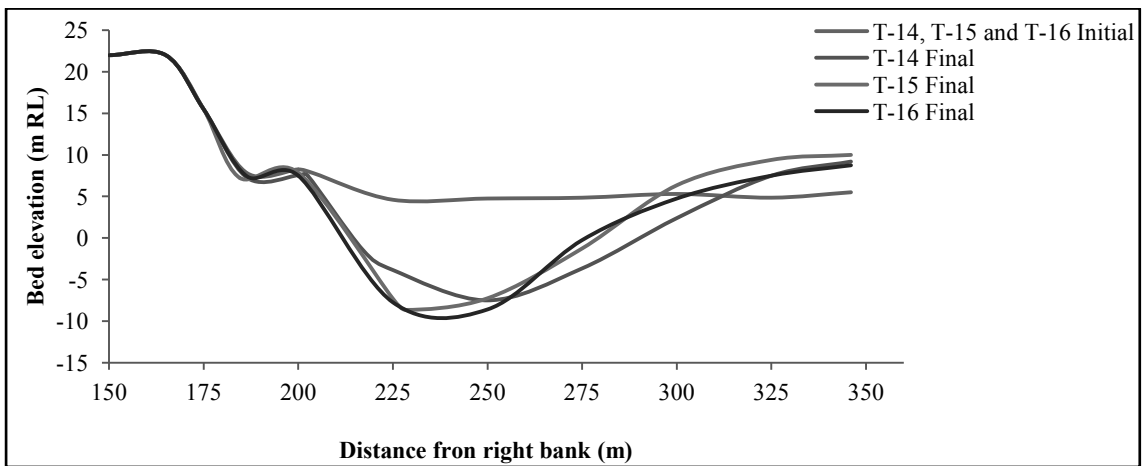


Figure 5.53: Scour for Group-5 at Cross Section 11

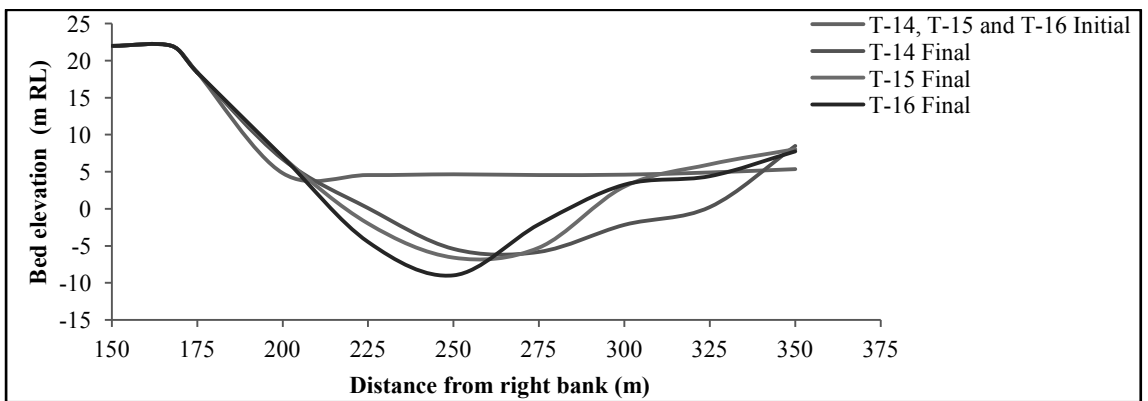


Figure 5.54: Scour Sections Group-5 at Cross Section 12

5.3.6 Comparison of Channel Cross Section for Group -6

Group-6 is the combination of T-18, T-19 and T-20 and observed maximum scour section for the tests is 10, 7 and 11 for respectively (Figure 5.55 to 5.61).

The superimposed graph of group-6 is a combination when flow angle is fixed (60°) but discharge ratio is variable and bank has been protected by Geo-bag type-2. The behavior of thalweg channel is more similar to group-4 than group-5 as the angularity of protective material is less than geo-bag type-1. Without that the total sectional behavior is same as group -5.

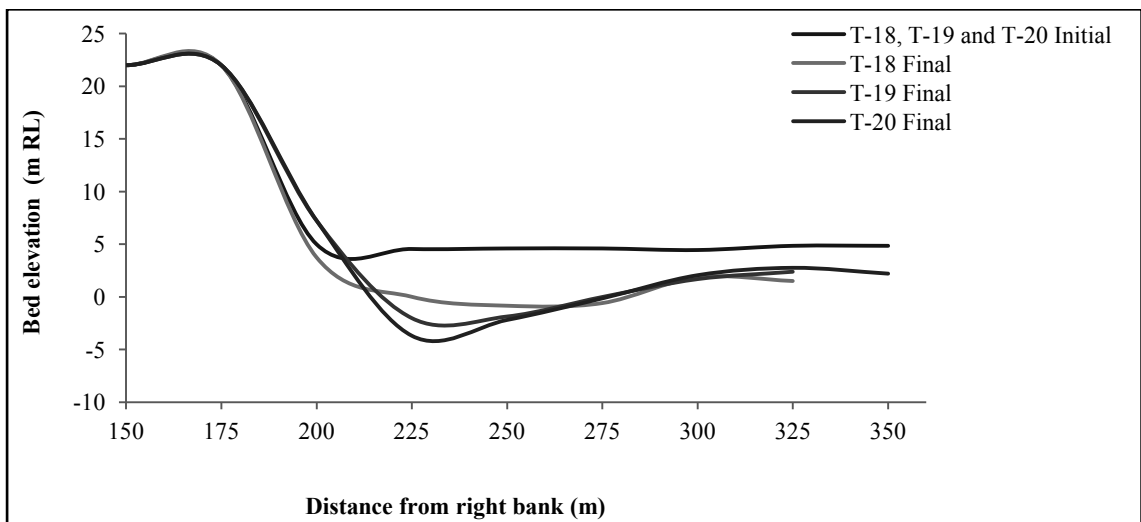


Figure 5.55: Scour for Group-6 at Cross Section 6

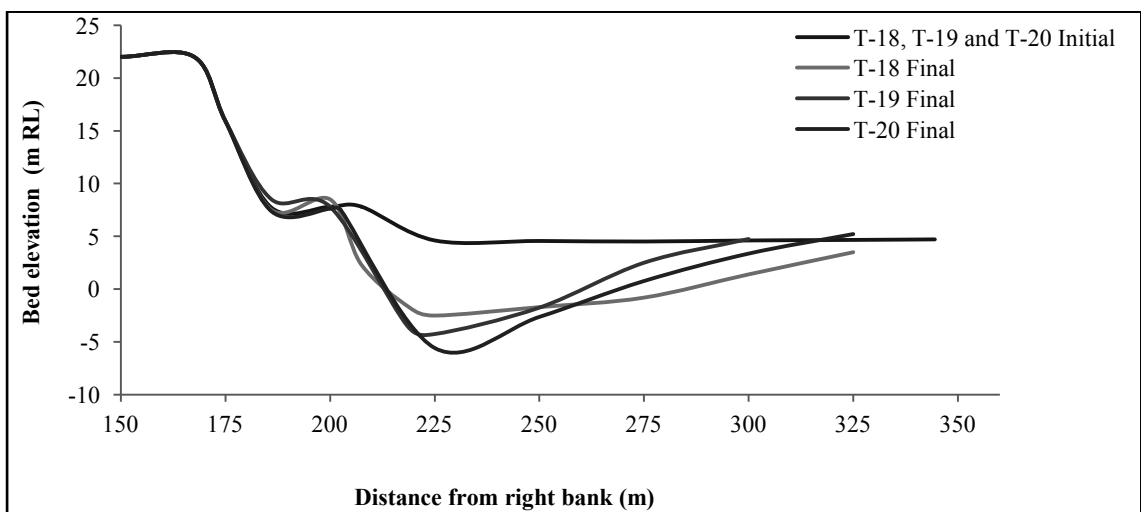


Figure 5.56: Scour for Group-6 at Cross Section 7

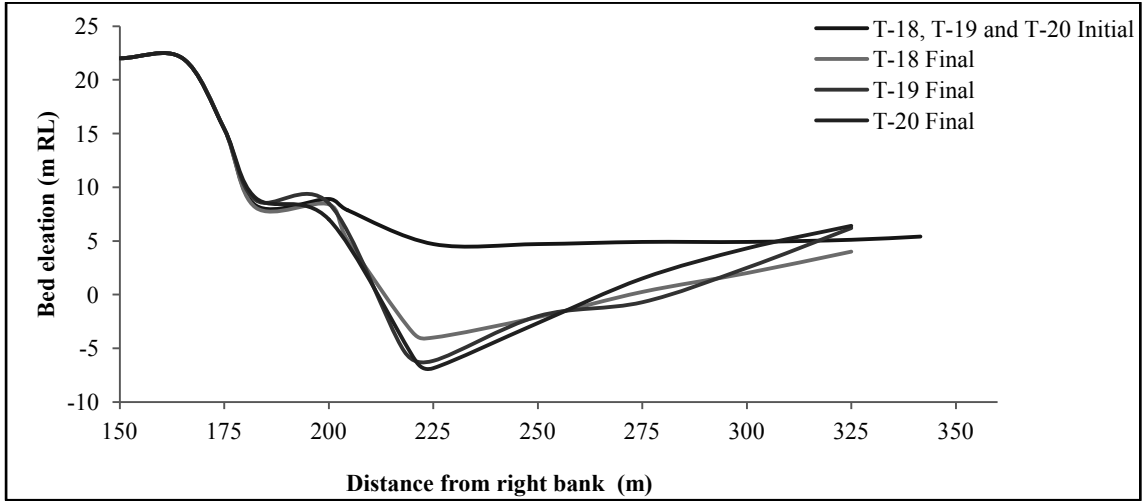


Figure 5.57: Scour for Group-6 at Cross Section 8

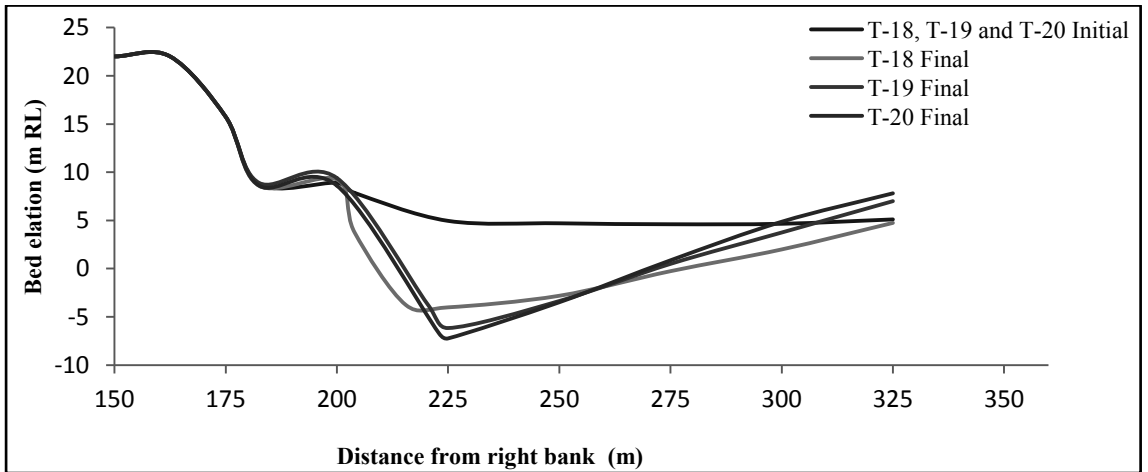


Figure 5.58: Scour for Group-6 at Cross Section 9

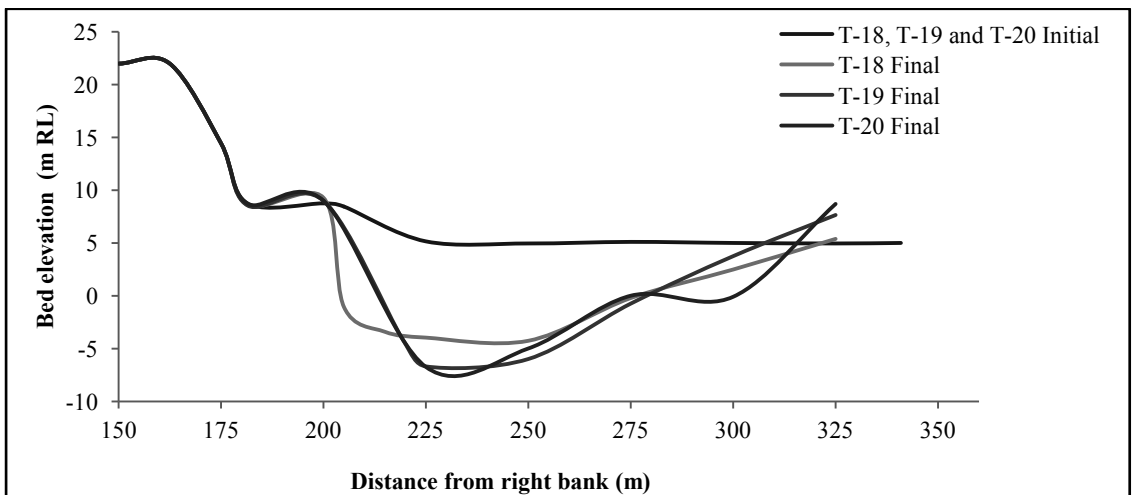


Figure 5.59: Scour for Group-6 at Cross Section 10

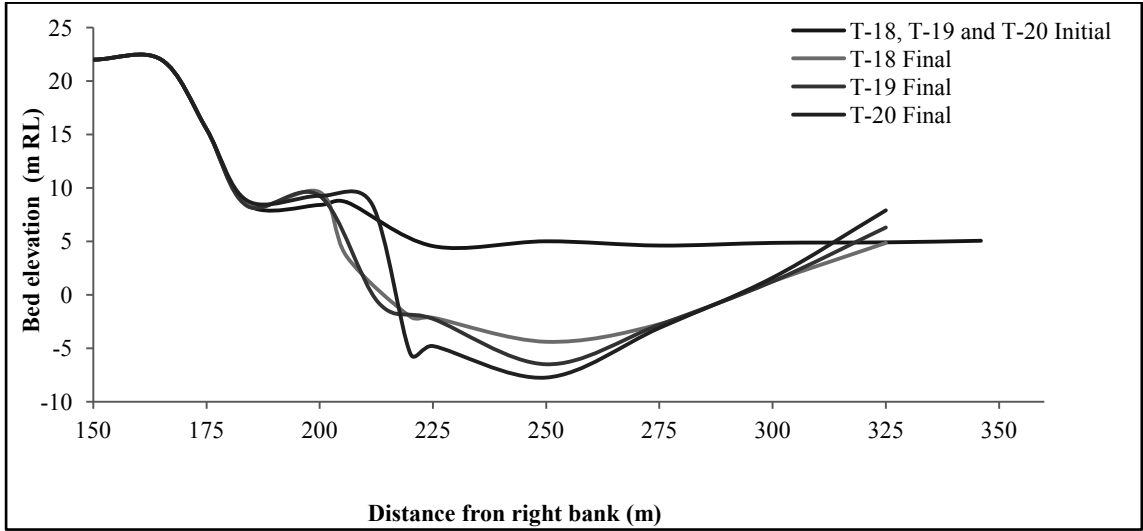


Figure 5.60: Scour for Group-6 at Cross Section 11

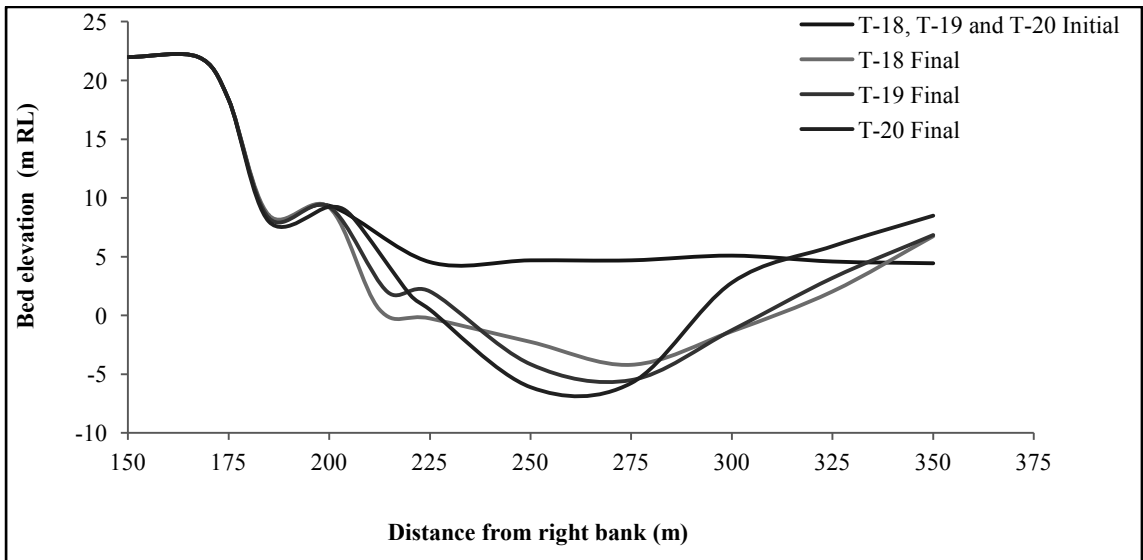


Figure 5.61: Scour for Group-6 at Cross Section 12

Table 5.2: Group Description for Comparison of Maximum Scour Sections (Grouping based on fixed discharge ratio)

Group ID	Combination of Tests	Discharge Ratio	C/S Taken	Group Condition	Protection Material
G-7	T-13 and T-17	-	C/S 9 to C/S 11	Main channel is closed	Stone boulder and Geo-bag type-1
G-8	T-4, T-7, T-10, T-14 and T-18	1:2	C/S 8 to C/S 12	Discharge ratio is fixed	Stone boulder, Geo-bag type-1 and Geo-bag type-2
G-9	T-5, T-8, T-11, T-15 and T-19	1:4	C/S 6 to C/S 12	Discharge ratio is fixed	Stone boulder, Geo-bag type-1 and Geo-bag type-2
G-10	T-6, T-9, T-12, T-16 and T-20	1:6	C/S 7 to C/S 12	Discharge ratio is fixed	Stone boulder, Geo-bag type-1 and Geo-bag type-2

5.3.7 Comparison of Channel Cross Section for Group-7

Group-7 is the combination of T-13 and T-17 and observed maximum scour section for the tests is 10 (Figure 5.62 to 5.64).

The superimposed graphs of group-7 are a combination when main channel is closed to observe the effect of only oblique flow on bank protection work. The combination has been done for protection work with stone boulder and geo-bag type-1. Here due to angularity effect deeper and sharp thalweg has been developed for stone boulder (T-13). The flow from chute channel directly hit the main channel (as it has the maximum angle) and there is no flow from main channel upstream so deep channel formed near the right bank and maximum deposition in the left bank.

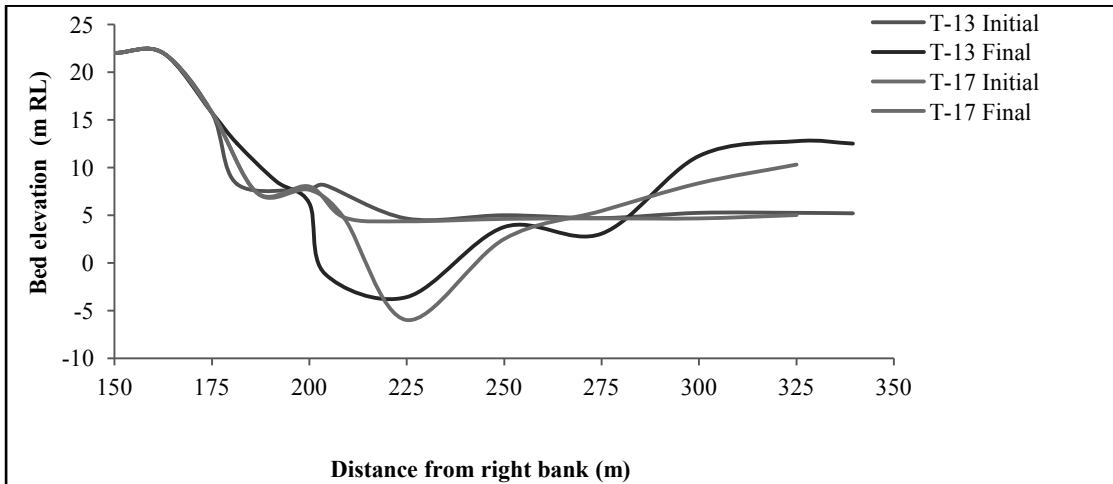


Figure 5.62: Scour for Group-7 at Cross Section 9

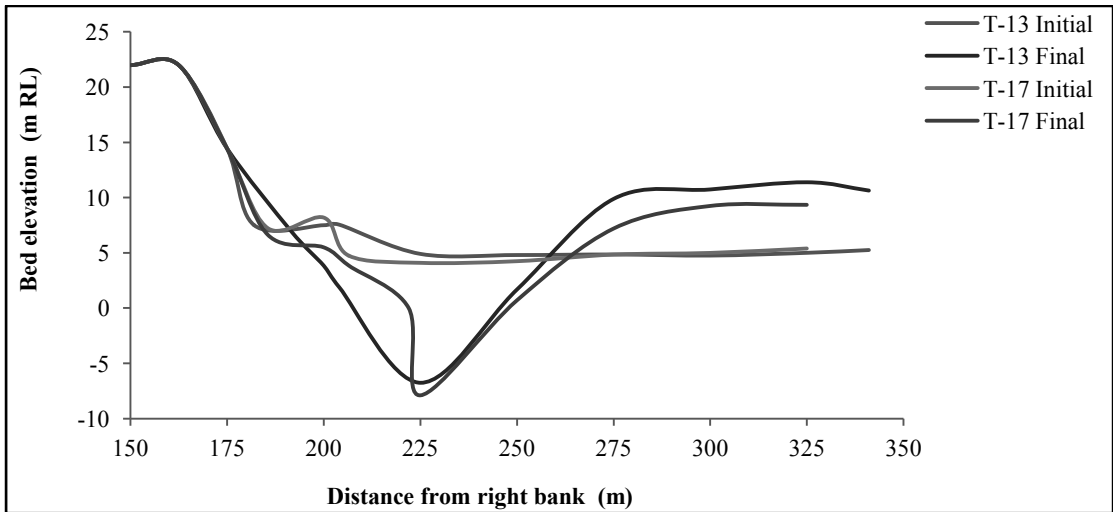


Figure 5.63: Scour for Group-7 at Cross Section 10

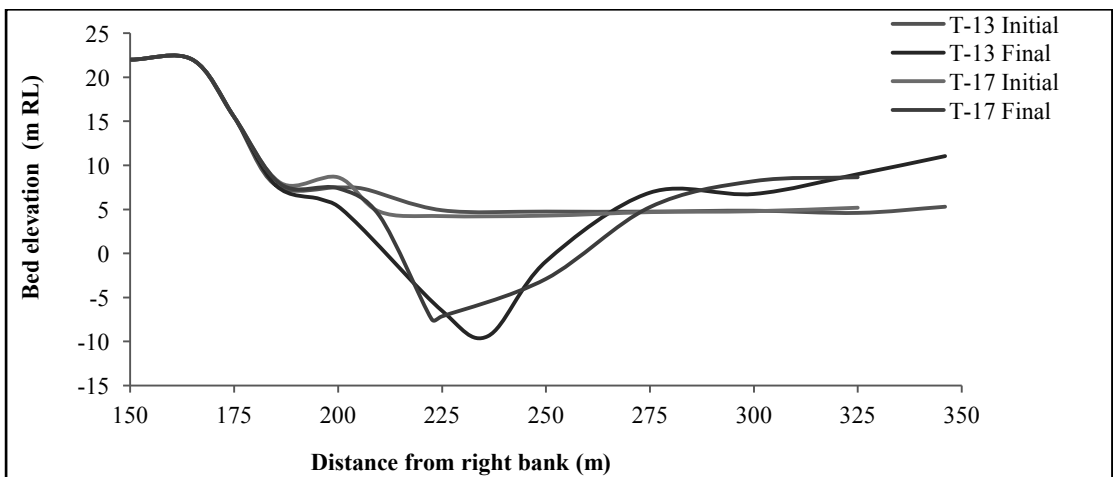


Figure 5.64: Scour for Group-7 at Cross Section 11

5.3.8 Comparison of Channel Cross Section for Group-8

Group-8 is the combination of T-4, T-7, T-10, T-14 and T-18 and observed maximum scour section for the tests is 11, 9, 9, 11 and 10 respectively (Figure 5.65 to 5.69).

The superimposed graph of group-8 is a combination when only discharge ratio (1:1.2) is fixed but oblique flow angle is different for each test. Scour increases with the increase of oblique flow angle i.e also for the char movement and affect the main channel bank with protective work. The dominating sections for the tests in the combination is different (the behaviour of the thalweg and reason has been described as before).

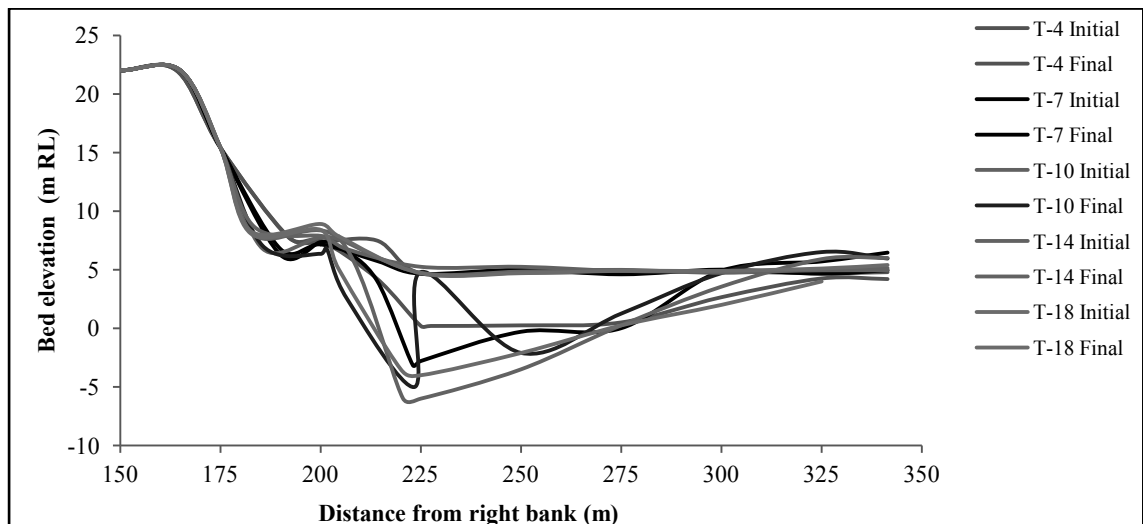


Figure 5.65: Scour for Group-8 at Cross Section 8

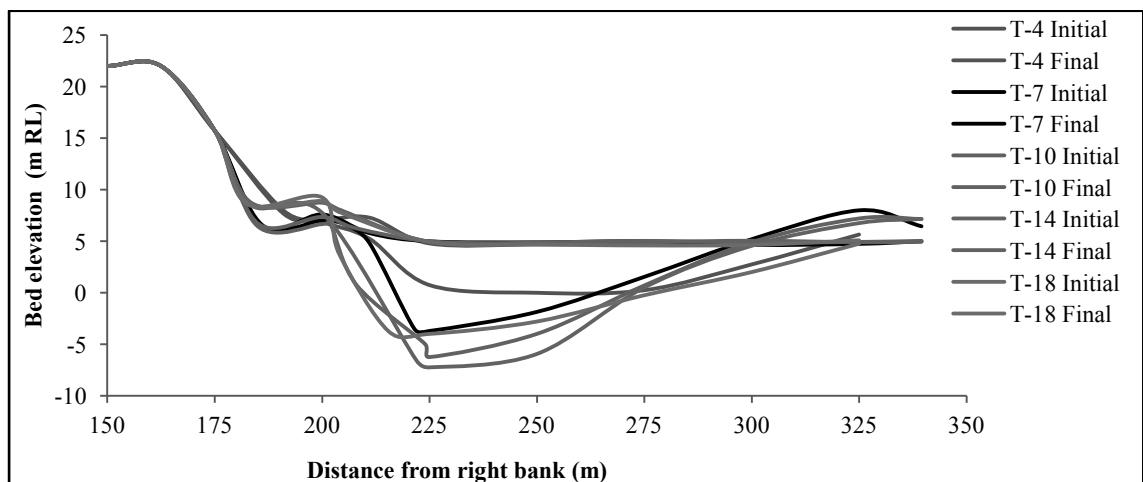


Figure 5.66: Scour for Group-8 at Cross Section 9

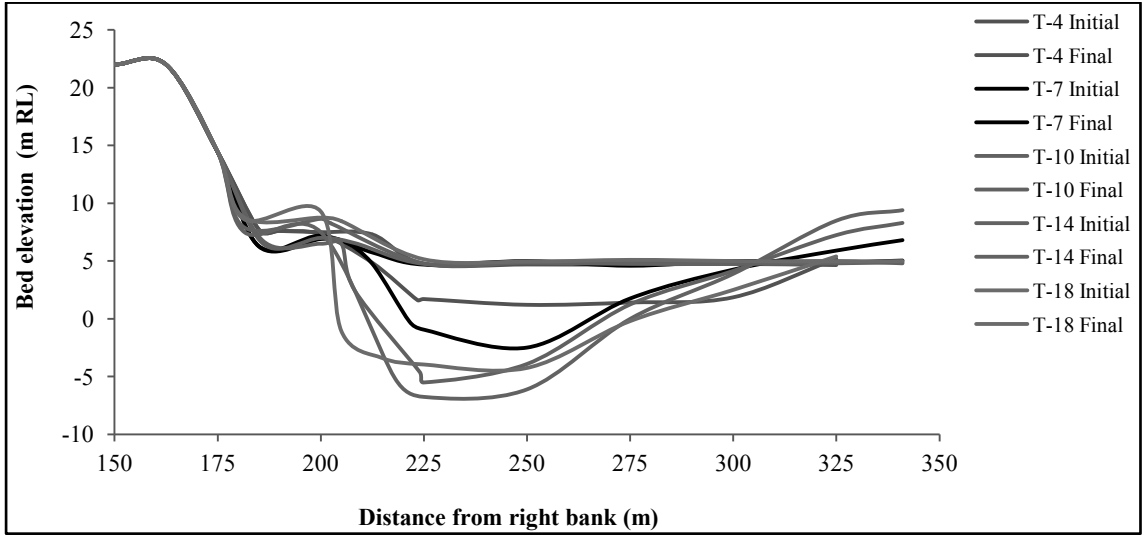


Figure 5.67: Scour for Group-8 at Cross Section 10

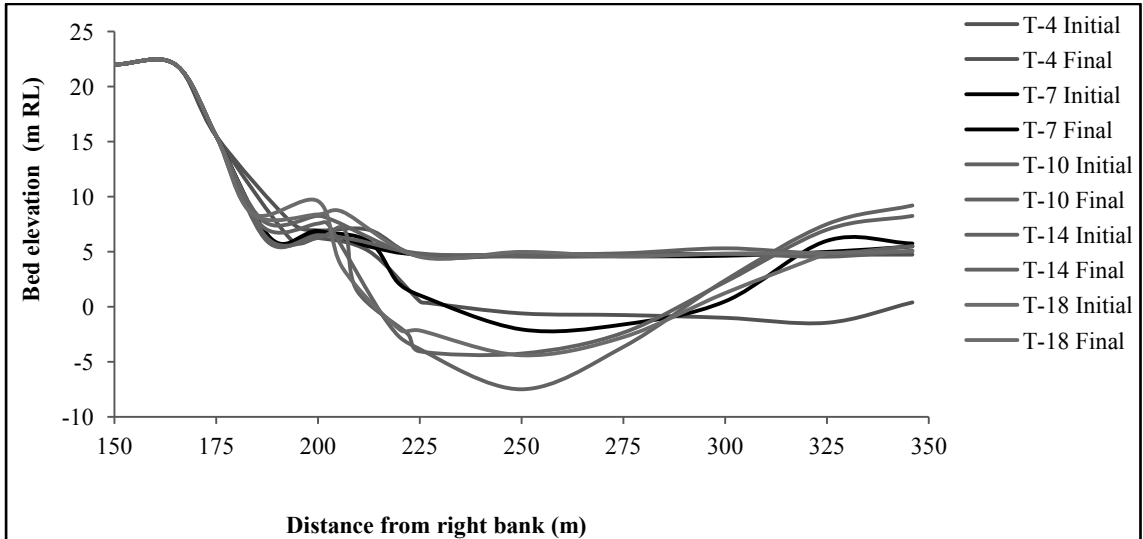


Figure 5.68: Scour for Group-8 at Cross Section 11

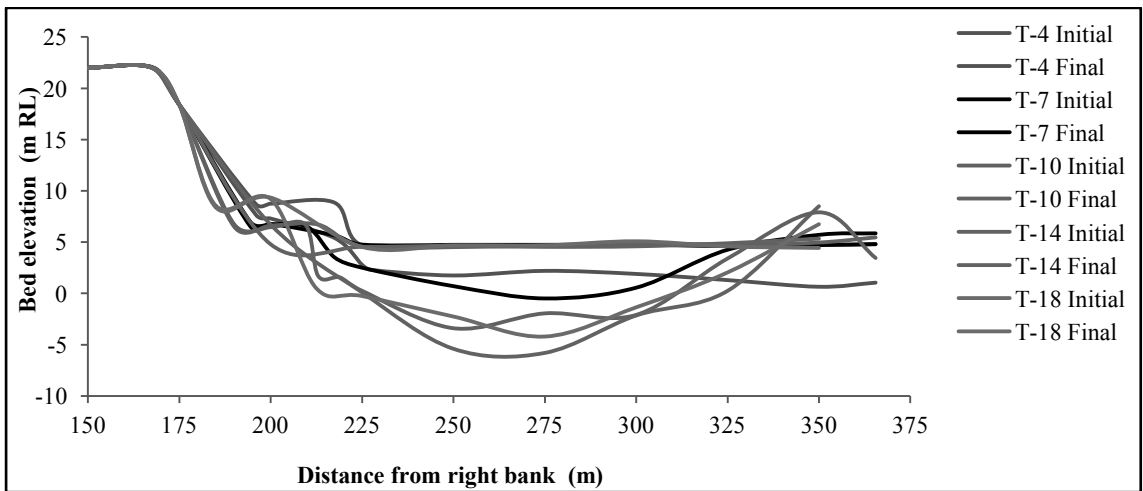


Figure 5.69: Scour for Group-8 at Cross Section 12

5.3.9 Comparison of Channel Cross Section for Group-9

Group-9 is the combination of T-5, T-8, T-11, T-15 and T-19 and observed maximum scour section for the tests is 7, 9, 10, 11 and 7 respectively (Figure 5.70 to 5.76).

The superimposed graphs of group-9 are a combination when only discharge ratio (1:1.4) is fixed but oblique flow angle is different for each test. Here more dominated chute channel develops with flow angle variation and then it follows the same depositional and scouring behavior as described before.

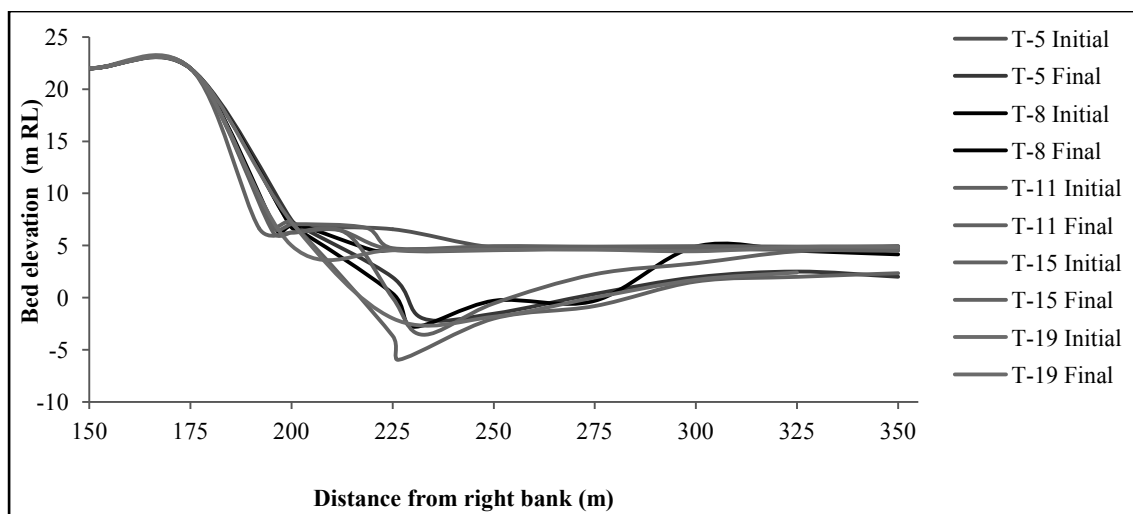


Figure 5.70: Scour for Group-9 at Cross Section 6

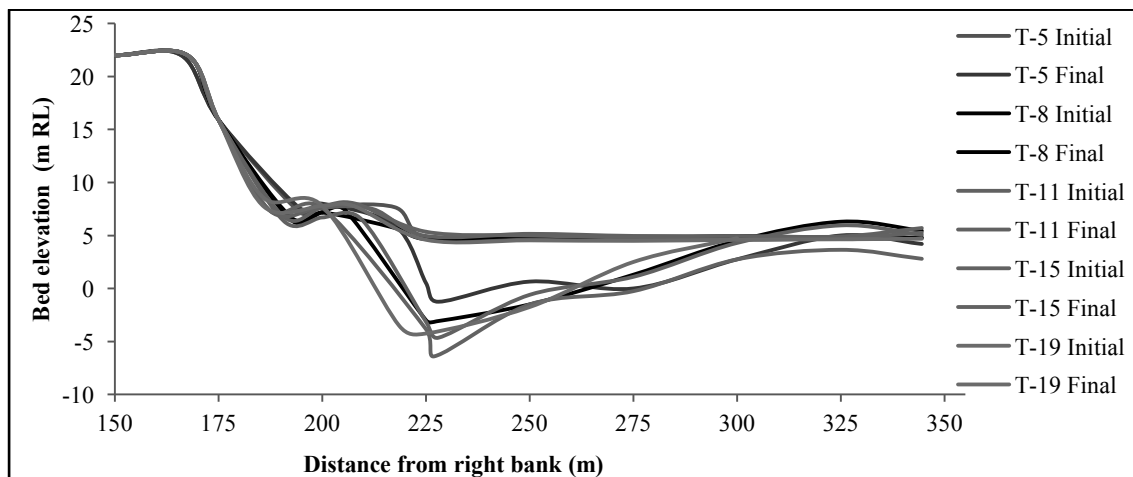


Figure 5.71: Scour for Group-9 at Cross Section 7

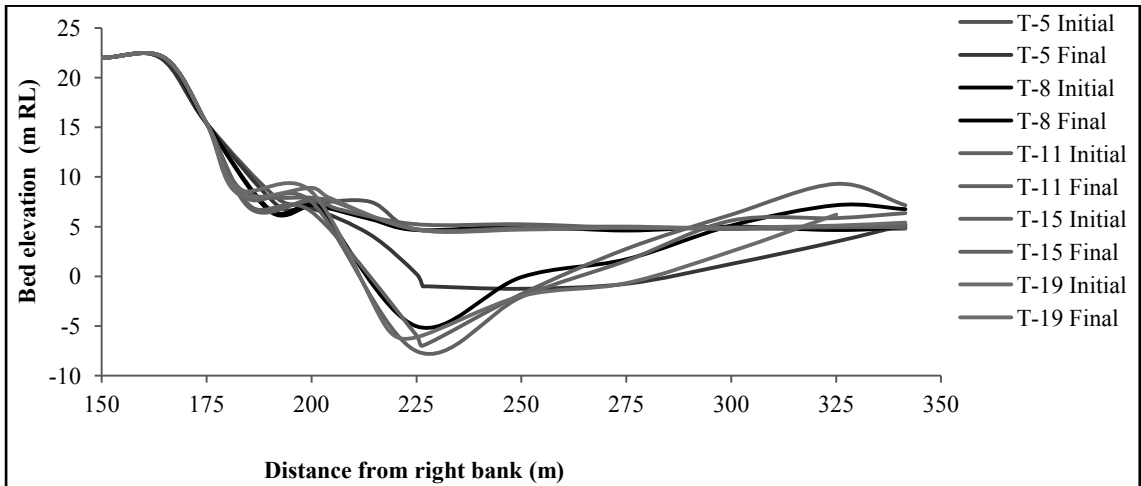


Figure 5.72: Scour for Group-9 at Cross Section 8

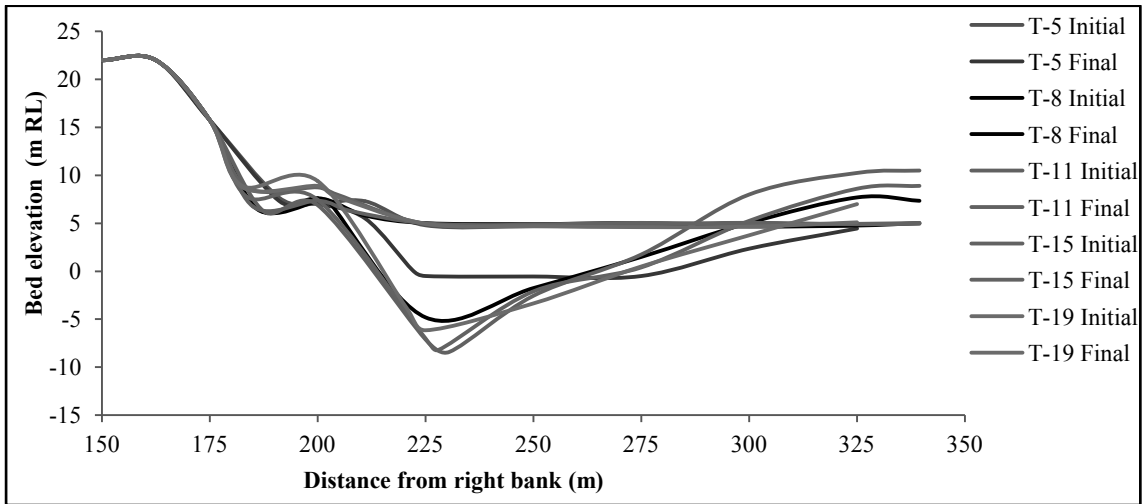


Figure 5.73: Scour for Group-9 at Cross Section 9

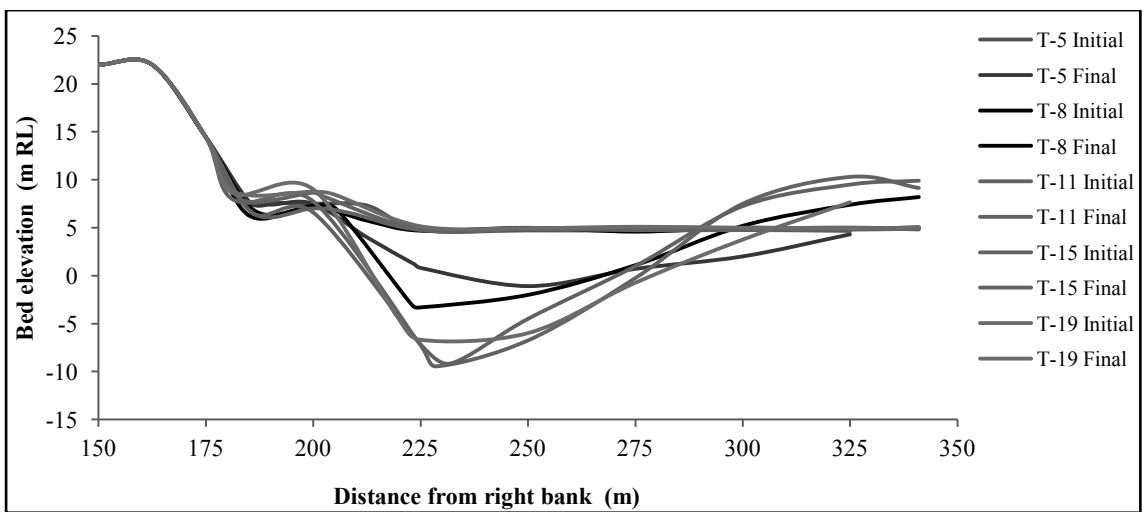


Figure 5.74: Scour for Group-9 at Cross Section 10

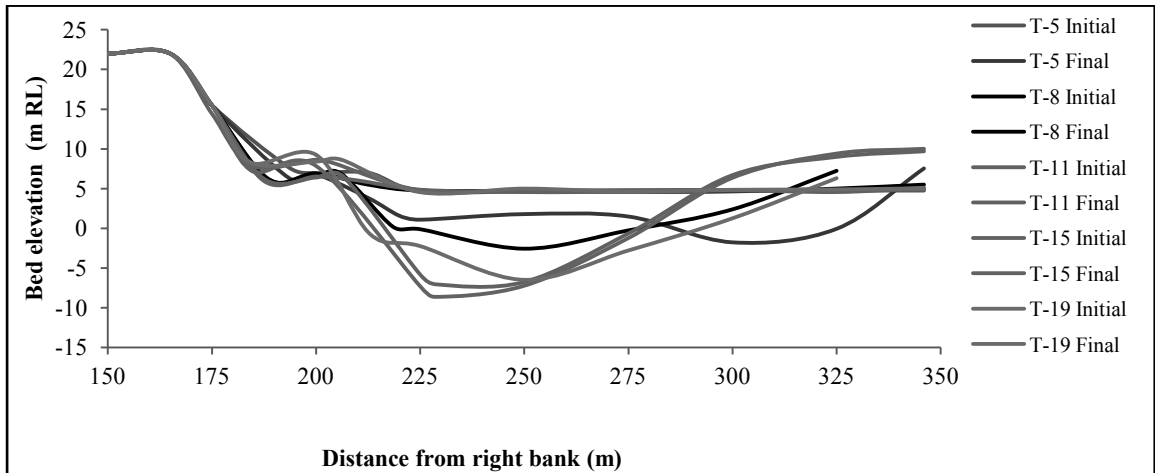


Figure 5.75: Scour for Group-9 at Cross Section 11

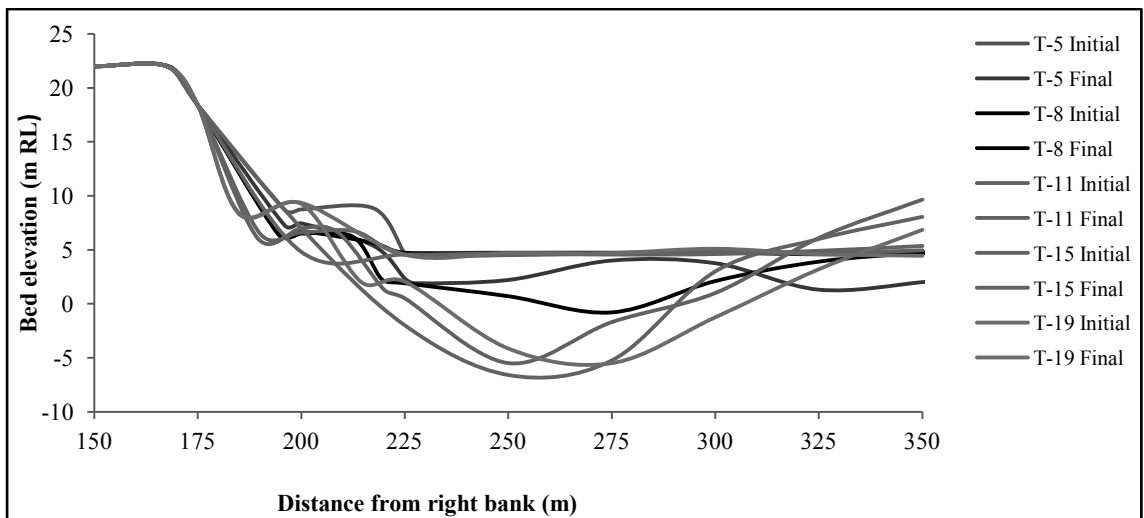


Figure 5.76: Scour for Group-9 at Cross Section 12

5.3.10 Comparison of Channel Cross Section for Group-10

Group-10 is the combination of T-6, T-9, T-12, T-16 and T-20 and observed maximum scour section for the tests is 8, 9, 10, 11 and 11 respectively (Figure 5.77 to 5.82).

The superimposed graphs of group-10 are the last combination when discharge ratio (1:1.6) is fixed but oblique flow angle is different for each test. Here more dominated chute channel develops with flow angle variation, and then it follows the same

depositional and scouring behavior as described before. This combination carries the maximum conditions from all the tests.

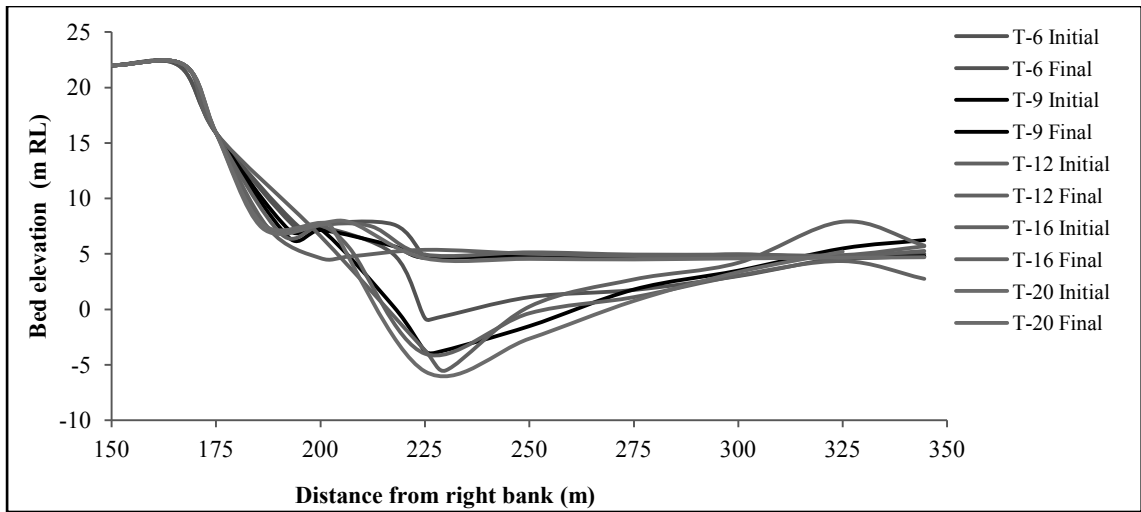


Figure 5.77: Scour for Group-10 at Cross Section 7

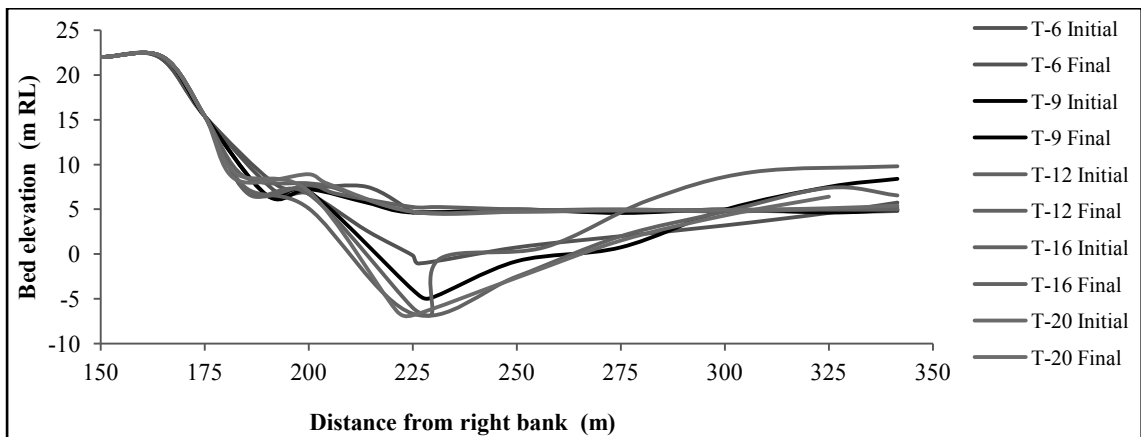


Figure 5.78: Scour for Group-10 at Cross Section 8

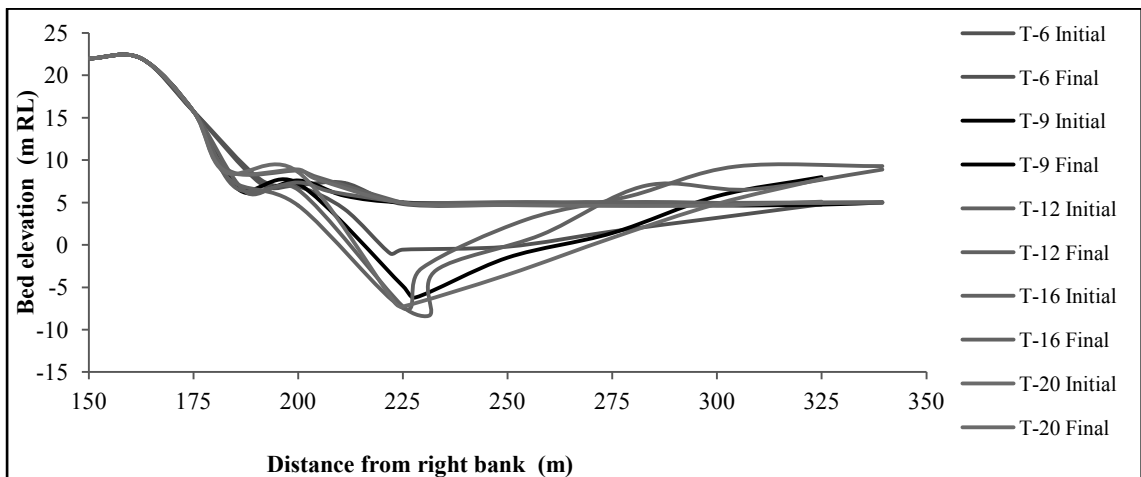


Figure 5.79: Maximum Scour Sections for Group-10 at Cross Section 9

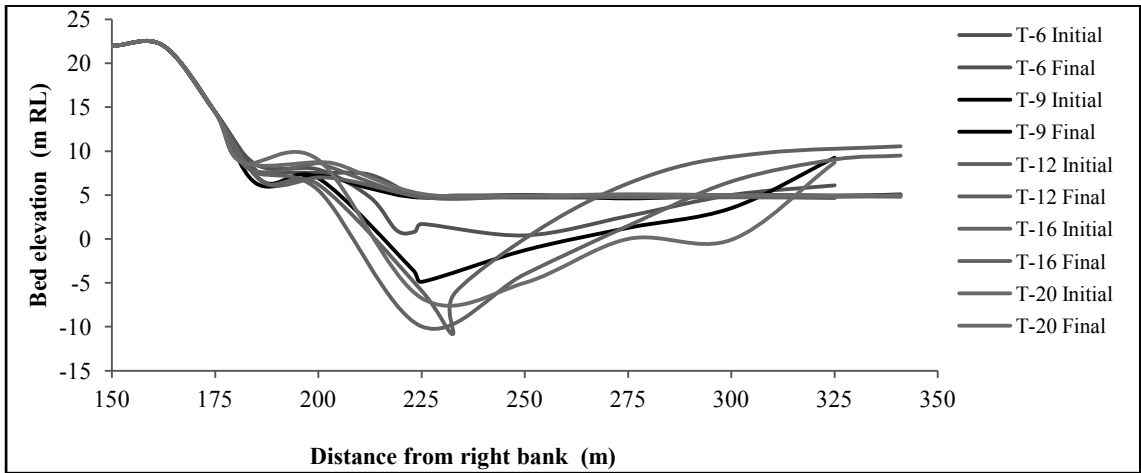


Figure 5.80: Scour for Group-10 at Cross Section 10

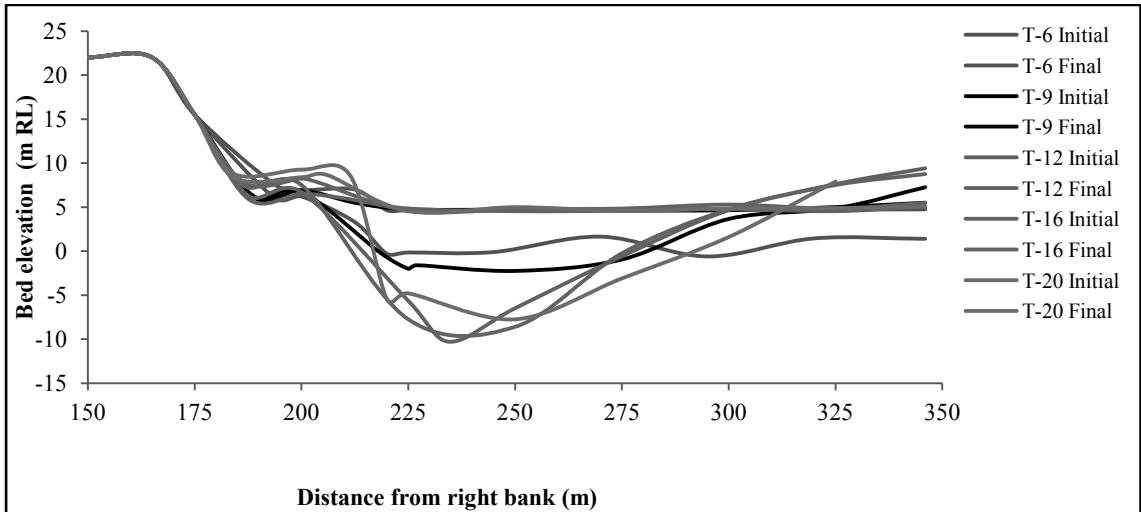


Figure 5.81: Scour for Group-10 at Cross Section 11

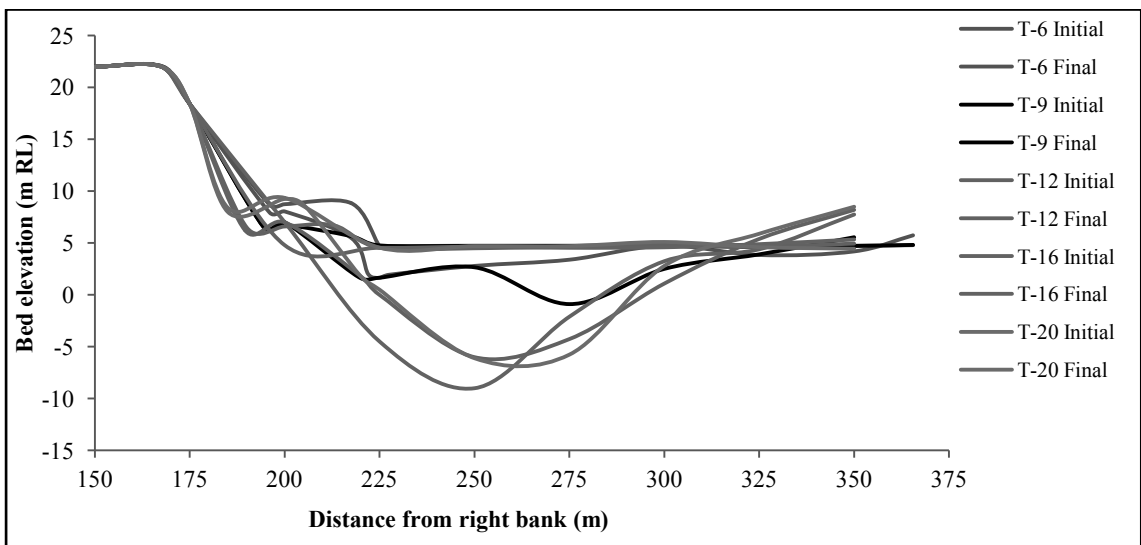


Figure 5.82: Scour for Group-10 at Cross Section 12

5.4 Comparison of Estimated and Measured Scour Depth

Generally scour depth depends on bed material and discharge of channel. This phenomenon has different characteristics when oblique flow meets with a straight flow. Scour depth becomes independent of bed material, discharge, velocity and water depth. A dominating chute channel accelerates the scouring process. Due to that calculated and measured scour for the experimental setup varies randomly. This comparative variation has been presented in Table 5.3. The table represents larger secondary flow angle accelerates the bed scour i.e deep thalweg. Comparison for the scour has been made from the observed scour and calculated scour from formula. Measured scour varied from 2.65m to 15.91m depending on experimental conditions.

Table 5.3: Comparison between Estimated and Measured Scour

Test no	Average Water depth, m	Average velocity at dominating c/s, m/s	Measured scour depth for prototype, m	Maximum scour occurred c/s no	Estimated Scour, m		
					X= 1.25	X= 1.5	X= 1.75
T-0	11.21	3.23	2.65	6	1.90	4.33	6.76
T-1	9.20	2.88	5.50	5			
T-2	10.08	2.60	6.85	8			
T-3	10.91	2.83	10.60	8			
T-4	11.38	2.89	6.20	11			
T-5	11.23	3.30	6.91	7			
T-6	11.65	3.01	6.96	8			
T-7	11.60	3.14	8.70	9			
T-8	13.17	3.28	10.41	9			
T-9	12.88	3.22	11.16	9			
T-10	12.76	3.41	11.26	9			
T-11	11.54	3.05	14.86	10			
T-12	13.61	3.24	15.91	10			
T-13	8.96	3.29	12.21	10			
T-14	13.08	2.66	12.25	11			
T-15	14.17	2.48	14.96	11			
T-16	14.06	2.71	15.21	11			
T-17	11.57	3.66	12.00	10			
T-18	11.70	3.04	9.50	10			
T-19	16.10	3.54	13.71	7			
T-20	13.30	2.84	12.75	11			

5.5 Assessment of Flow Behaviour for Oblique Flow

As measured and calculated scour depth varies due to oblique flow so an assessment has been done in Table 5.3 to suggest a suitable extra multiplication factor for oblique flow depending on its angle. The calculation reveals that generally used multiplication factors are to be increased in some extent to make a revetment work sustainable and durable. This assessment has been done to find a best suited extra multiplication factor that is to be multiplied with general multiplication factor that is available in Lacy's equation to obtain actual scour depth for a channel having oblique channel which is common in a braided river.

As straight bank has been taken into consideration so the extra multiplication factor has been calculated with respect to factor for straight channel i.e 1.25. From the table it has been found that when oblique flow hits on a straight bank at an angle of 20 to 60 degree, multiplication factor for designing the protective work becomes higher than 1.25. It varies from 1.30 to 2.15 and the value has been calculated from the available data of the experimental setups.

Table 5.4: Assessment of Flow Behaviour for Oblique Flow

Test ID	Oblique flow angle	Bank protection type	Scour depth measured for prototype, m	Assessment of multiplication factor, X	Extra multiplication factor for oblique flow, X_{OF}
T-0	No oblique flow	Stone Boulder	2.65	1.25*	-
T-1	20°	Unprotected	5.50	1.62	1.30
T-2	40°	Unprotected	6.85	1.76	1.41
T-3	60°	Unprotected	10.60	2.15	1.72
T-4	20°	Stone	6.20	1.69	1.35
T-5	20°	Stone	6.91	1.77	1.41
T-6	20°	Stone Boulder	6.96	1.77	1.42
T-7	40°	Stone Boulder	8.70	1.95	1.56
T-8	40°	Stone Boulder	10.41	2.13	1.70
T-9	40°	Stone Boulder	11.16	2.20	1.76
T-10	60°	Stone Boulder	11.26	2.21	1.77
T-11	60°	Stone Boulder	14.86	2.58	2.07
T-12	60°	Stone Boulder	15.91	2.69	2.15
T-13	60°	Stone Boulder	12.21	2.31	1.85
T-14	60°	Geo-bag type-1	12.25	2.31	1.85
T-15	60°	Geo-bag type-1	14.96	2.59	2.07
T-16	60°	Geo-bag type-1	15.21	2.62	2.10
T-17	60°	Geo-bag type-1	12.00	2.29	1.83
T-18	60°	Geo-bag type-2	9.50	2.03	1.63
T-19	60°	Geo-bag type-2	13.71	2.47	1.97
T-20	60°	Geo-bag type-2	12.75	2.37	1.89

* As it is recommended of using $X=1.25$ for straight channel. (Ref. BWDB, Manual-I)

5.6 Launching Behavior of Protection Work due to Oblique Flow

Initially 22.50m launching apron has been provided on 4.713m (RL) bed level for protection work. Protective material launches and develops a slope after run. Length of launching apron and slope after each model run has been calculated in Table 5.5.

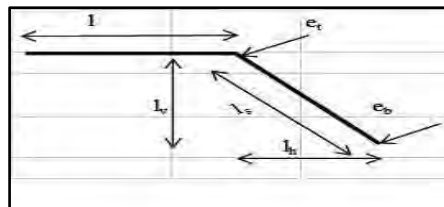


Figure 5.83: Sketch for Measurement of Launching Behaviour of Protection Work

Table 5.5: Analysis of Launching Behaviour for Different Protective Materials and Oblique Flow

Test ID	C/S no	Length of Launching apron after run, l (m)	Horizontal length of Launched slope, l _h (m)	Vertical height of launching l _v (m)	Launched slope	Launched angle, (degree)	Total scour (m)
T-0	14 to 5	22.50	0.00	-	-	-	-
T-4	14	22.50	4.00	3.00	1:1.33	36.86	1.41
	13	20.00	5.00	3.60	1:1.39	35.75	2.36
	12	19.50	7.50	5.05	1:1.49	33.95	3.11
	11	19.00	8.00	4.75	1:1.68	30.69	2.91
	10	18.50	9.50	5.75	1:1.65	31.18	4.16
	9	17.50	11.50	6.10	1:1.89	27.94	4.66
	8	16.50	16.00	7.10	1:2.25	23.92	5.36
	7	17.00	15.50	7.80	1:1.99	26.71	5.41
	6	17.50	15.00	6.45	1:2.33	23.26	4.91
	5	14.50	8.00	5.35	1:1.50	33.77	3.96
T-5	14	22.50	4.00	3.00	1:1.33	36.86	1.41
	13	19.50	6.50	4.30	1:1.51	33.48	2.66
	12	19.25	9.00	5.35	1:1.68	30.73	3.36
	11	19.00	10.00	4.50	1:2.22	24.22	2.76
	10	18.00	12.00	7.00	1:1.71	30.26	5.01
	9	16.00	13.00	7.45	1:1.74	29.82	5.96
	8	15.75	17.00	8.35	1:2.04	26.15	6.41
	7	15.50	16.50	8.80	1:1.88	28.07	6.91
	6	17.00	14.00	7.65	1:1.83	28.65	6.26
	5	19.00	7.50	4.95	1:1.52	33.42	3.46

Test ID	C/S no	Length of Launching apron after run, l (m)	Horizontal length of Launched slope, l_h (m)	Vertical height of launching $l_v = (e_t - e_b)$ (m)	Launched slope	Launched angle, (degree)	Total scour (m)
T-6	14	Sedimentation					
	13	20.00	5.50	3.40	1:1.62	31.72	1.31
	12	19.50	9.50	6.05	1:1.57	32.49	3.96
	11	19.00	10.00	6.20	1:1.61	31.79	4.11
	10	17.50	11.50	6.80	1:1.69	30.59	5.26
	9	16.00	13.00	7.80	1:1.67	30.96	6.06
	8	15.50	17.50	8.95	1:1.96	27.08	6.96
	7	17.00	13.50	8.00	1:1.69	30.65	6.06
	6	17.50	15.50	8.30	1:1.87	28.16	6.81
	5	14.00	13.50	5.55	1:2.43	22.34	4.46
T-7	14	21.00	4.00	1.85	1:2.16	24.82	0.11
	13	20.50	4.50	2.95	1:1.53	33.24	0.81
	12	19.25	4.00	3.05	1:1.31	37.32	1.36
	11	18.75	10.00	4.15	1:2.41	22.53	2.86
	10	18.25	12.75	7.00	1:1.82	28.76	5.81
	9	17.25	17.00	9.55	1:1.78	29.32	7.91
	8	17.00	16.00	9.85	1:1.62	31.62	8.16
	7	16.50	18.00	9.65	1:1.87	28.19	7.66
	6	16.75	15.25	8.10	1:1.88	27.97	6.46
5	16.25	14.75	7.10	1:2.08	25.70	5.36	
T-8	14	21.50	4.50	2.30	1:1.96	27.03	0.46
	13	21.00	6.00	3.05	1:1.97	26.91	1.41
	12	20.00	7.00	4.15	1:1.69	30.61	2.51
	11	19.00	12.00	6.45	1:1.86	28.26	4.66
	10	20.00	12.50	9.95	1:1.26	38.43	8.31
	9	19.50	22.50	12.40	1:1.81	28.92	10.41
	8	19.00	21.00	11.75	1:1.79	29.19	10.16
	7	17.50	20.00	10.65	1:1.88	28.01	8.71
	6	15.50	17.00	8.85	1:1.92	27.51	7.61
	5	15.00	15.50	6.75	1:2.30	23.49	5.16
T-9	14	22.50					
	13	19.50	7.00	3.75	1:1.87	28.13	1.86
	12	17.00	4.00	5.15	1:0.78	52.04	3.61
	11	16.00	16.00	8.30	1:1.93	27.39	6.61
	10	15.00	20.00	11.75	1:1.70	30.46	10.21
	9	14.00	25.00	12.95	1:1.93	27.39	11.16
	8	13.00	24.00	12.15	1:1.98	26.79	10.31
	7	14.00	20.00	11.00	1:1.82	28.78	8.91
	6	15.00	16.00	9.80	1:1.63	31.52	8.16
	5	15.00	14.00	7.15	1:1.96	27.03	5.46

Test ID	C/S no	Length of Launching apron after run, l (m)	Horizontal length of Launched slope, l _h (m)	Vertical height of launching l _v = (e _t -e _b) (m)	Launched slope	Launched angle, (degree)	Total scour (m)
T-10	14	22.50					
	13	16.50	6.50	3.00	1:2.17	24.74	1.96
	12	16.00	9.50	6.20	1:1.53	33.16	4.36
	11	15.50	15.50	9.50	1:1.63	31.53	7.91
	10	15.00	21.00	12.25	1:1.71	30.31	10.66
	9	14.50	22.50	12.75	1:1.76	29.60	11.26
	8	13.50	25.50	11.70	1:2.18	24.64	9.91
	7	16.50	21.00	10.30	1:2.04	26.11	8.31
	6	15.50	17.00	8.95	1:1.90	27.75	6.66
	5	16.50	16.00	7.55	1:2.12	25.25	5.71
T-11	14	22.50					
	13	17.50	8.00	3.30	1:2.42	22.45	1.41
	12	18.25	10.50	6.40	1:1.64	31.37	4.31
	11	17.00	22.00	14.20	1:1.55	32.82	12.21
	10	15.25	29.00	16.40	1:1.77	29.46	14.86
	9	13.00	29.50	15.45	1:1.91	27.63	13.76
	8	14.25	28.00	13.60	1:2.06	25.89	12.11
	7	14.50	24.50	11.85	1:2.07	25.78	9.76
	6	15.25	21.00	10.00	1:2.10	25.46	8.66
	5	15.50	17.50	8.85	1:1.98	26.79	6.81
T-12	14	Sedimentation					
	13	Sedimentation					
	12	15.50	14.50				
	11	13.50	26.50	17.35	1:1.53	33.17	15.26
	10	14.50	29.25	17.60	1:1.66	31.06	15.91
	9	13.50	29.00	15.10	1:1.92	27.51	13.31
	8	12.75	29.00	13.65	1:2.12	25.25	11.66
	7	13.00	25.50	12.65	1:2.02	26.33	10.56
	6	15.25	24.25	10.85	1:2.24	24.06	9.46
	5	15.50	20.50	9.70	1:2.11	25.35	7.71
T-13	14	Sedimentation					4.71
	13	10.50	18.00	8.75	1:2.06	25.89	6.46
	12	11.50	29.00	11.60	1:2.50	21.80	9.01
	11	11.50	31.00	14.50	1:2.14	25.04	12.16
	10	10.50	34.50	14.50	1:2.38	22.79	12.21
	9	10.50	35.00	10.95	1:3.20	17.35	8.96
	8	11.50	31.75	10.35	1:3.07	18.04	8.56

Test ID	C/S no	Length of Launching apron after run, l (m)	Horizontal length of Launched slope, l _h (m)	Vertical height of launching l _v = (e _t -e _b) (m)	Launched slope	Launched angle, (degree)	Total scour (m)
T-13							
	7	12.75	22.50	8.50	1:2.65	20.67	6.46
	6	13.00	20.00	7.45	1:2.68	20.46	5.41
	5	13.50	11.50	5.00	1:2.30	23.49	3.01
T-14	11	19.50	12.00	9.40	1:1.28	37.99	6.36
	10	19.00	22.00	13.40	1:1.64	31.37	10.66
	9	19.00	22.60	14.30	1:1.58	32.33	11.91
	8	20.25	20.50	13.25	1:1.55	32.83	10.81
	7	19.50	19.25	11.60	1:1.66	31.06	9.01
	6	19.00	16.50	10.25	1:1.61	31.84	7.21
T-15	11	20.50	31.00	17.45	1:1.78	29.33	14.96
	10	24.00	33.50	16.85	1:1.99	26.68	13.81
	9	20.50	28.00	14.85	1:1.89	27.88	12.61
	8	19.50	26.50	14.40	1:1.84	28.52	11.71
	7	19.50	25.50	14.20	1:1.80	29.05	11.71
	6	15.50	20.00	11.05	1:1.81	28.92	8.81
T-16	11	18.50	37.00	17.70	1:2.09	25.56	15.21
	10	18.75	38.00	17.50	1:2.17	24.74	14.46
	9	20.00	33.25	15.40	1:2.16	24.84	13.21
	8	18.70	28.00	14.20	1:1.97	26.91	11.46
	7	18.50	26.75	12.90	1:2.07	25.78	10.41
	6	16.00	20.75	10.65	1:1.95	27.15	8.41
T-17	13	18.00	10.50	4.60	1:2.28	23.68	1.71
	12	15.00	17.50	11.30	1:1.55	32.83	8.41
	11	14.50	27.50	13.80	1:1.99	26.68	11.41
	10	13.50	33.00	14.05	1:2.35	23.05	11.81
	9	15.50	28.50	12.95	1:2.20	24.44	10.41
	8	21.50	26.50	11.75	1:2.26	23.86	9.36
	7	16.50	22.50	11.55	1:1.95	27.14	8.81
	6	19.00	19.00	10.00	1:1.90	27.76	7.56
T-18	12	19.50	13.00	8.35	1:1.56	32.66	4.06
	11	20.50	14.50	9.65	1:1.50	33.69	5.61
	10	21.50	14.00	10.50	1:1.33	36.94	6.81
	9	20.00	13.50	11.85	1:1.14	41.25	8.21
	8	20.00	13.50	11.40	1:1.18	40.25	7.86
	7	17.00	12.00	9.55	1:1.26	38.43	6.41

Test ID	C/S no	Length of Launching apron after run, l (m)	Horizontal length of Launched slope, l_h (m)	Vertical height of launching $l_v = (e_t - e_b)$ (m)	Launched slope	Launched angle, (degree)	Total scour (m)
T-19							
	12	16.50	13.00	5.75	1:2.26	23.86	1.76
	11	22.00	9.00	9.40	1:0.96	46.16	5.31
	10	21.50	18.50	14.55	1:1.27	38.21	10.81
	9	22.00	16.00	14.10	1:1.13	41.50	10.56
	8	20.00	20.50	14.70	1:1.39	35.73	10.76
	7	21.00	16.00	17.50	1:0.91	47.69	13.71
T-20	12	18.00	16.00	7.60	1:2.11	25.35	3.46
	11	22.00	17.00	12.95	1:1.31	37.35	9.46
	10	20.50	21.00	15.50	1:1.35	36.52	11.81
	9	21.00	19.75	15.25	1:1.30	37.56	12.06
	8	18.50	20.50	15.40	1:1.33	36.94	11.96
	7	14.00	23.50	10.50	1:2.24	24.05	8.71

5.7 Some Observations on Development and Execution of Physical Model

(a) Discharge:

Total discharge in the Physical modelling has been considered as $6363\text{m}^3/\text{s}$. It is well known that most of the braided river has more discharge than this value. Discharge is an important factor for calculating anticipated scour depth. This value of discharge has been selected because providing higher discharge in the existing facilities of RRI was not possible. This is a research project so discharge has been considered as per available facility.

(b) Bed Material

Mean diameter of bed material for the physical model has been selected as $D_{50}=0.167\text{mm}$. If the bed material is converted to model scale then the bed material type turns to clay. Internationally synthetic material is used as bed material. Use of this synthetic material is very costly and not affordable and changing the bed material size of the existing facilities of RRI is not possible. Moreover mean diameter of braided river is nearly 0.167mm in Bangladesh (BWDB, 2010). Instead of using

synthetic material locally available sand has been used. So velocity has been enhanced in the physical model.

As per literature, generally velocity is enhanced depending on the Reynold's curve or critical shear equation from Van Rign. As the gradation of bed material is not uniform so the values don't fall under the Reynold's curve. So, Van Rign equation has been used to calculate critical velocity. According to the theory if velocity is enhanced upto 2 to 5 times then model condition becomes independent of bed material. But a higher value gives irregular model bed configurations and model becomes uncontrolled. Thus velocity has been enhanced at a value of 2 times so that the model can be well controlled.

Velocity enhancement doesn't affect the model condition, rather it indicates a deviation from Froudian condition. More factorization indicates more deviation from the Froudian condition and an uncontrolled model configuration.

(c) Vertical Left Bank

When oblique flow hits a main channel then its effect on other bank can be ignored. In this study oblique flow hits to the right bank. Left bank of the model has been developed by brick wall. The study objective is to observe the effect of oblique flow on the directly affected channel bank so the condition of another bank has been ignored. Moreover oblique flow has a total effect on right bank of the channel. So the effect of confined left bank is very less for a part of a braided river.

(d) Non-perpendicular cross section mark in Chute Channel

A continuous section mark has been done starting from right bank of main channel to the left bank of the secondary channel outline. Thus section marks at chute channel part become non perpendicular to the direction of flow. Bathymetry of model bed has been measured as per this section mark and this section has been marked to identify the point from which perpendicular section has been identified to measure velocity.

(e) Consideration of velocity resultant and angle

Generally return current is 60% of main current. So velocity of X-axis has been used in bank protection design. Generally material doesn't move for the resultant of two perpendicular forces rather one of the force act on it in static condition. After movement material moves any of the two directions. When oblique flow comes then it act as a force to lift up the material and only then main flow move the material, thus launching of material occur. It is clear that in T-0 for only straight flow no material has displaced or launched. But when oblique flow comes it changes the behaviour.

The drag force can be obtained by measuring 3-D current. But due to non availability of scope this parameter has not been taken only velocity at 3 directions has been recorded.

5.8 Effect of Discharge Ratio on Scour

Relation between scour depth and discharge ratio of main channel to chute channel has been analyzed and shown in Figure 5.84. The graph only consist the experimental setups having protection work done by stone boulder.

The graph represents that scour depth is less susceptible to discharge ratio (between straight and oblique channel). Variation in scour depth for different discharge ratio is small for small secondary channel angle. It increases with the increase of oblique flow angle. Scour depth varies at a short range (6.20 m o 6.96m) for a small angle 20°. Scour depth varies from 8.70m to 11.16m for 40° oblique flow, whereas for 60° the range becomes 11.26m to 15.91m. Though maximum scour depth has been found at discharge ratio of 1:1.6, it has an optimum range of 1:1.4 because before that line scour depth increases firstly and after that discharge ratio scour depth varies slowly.

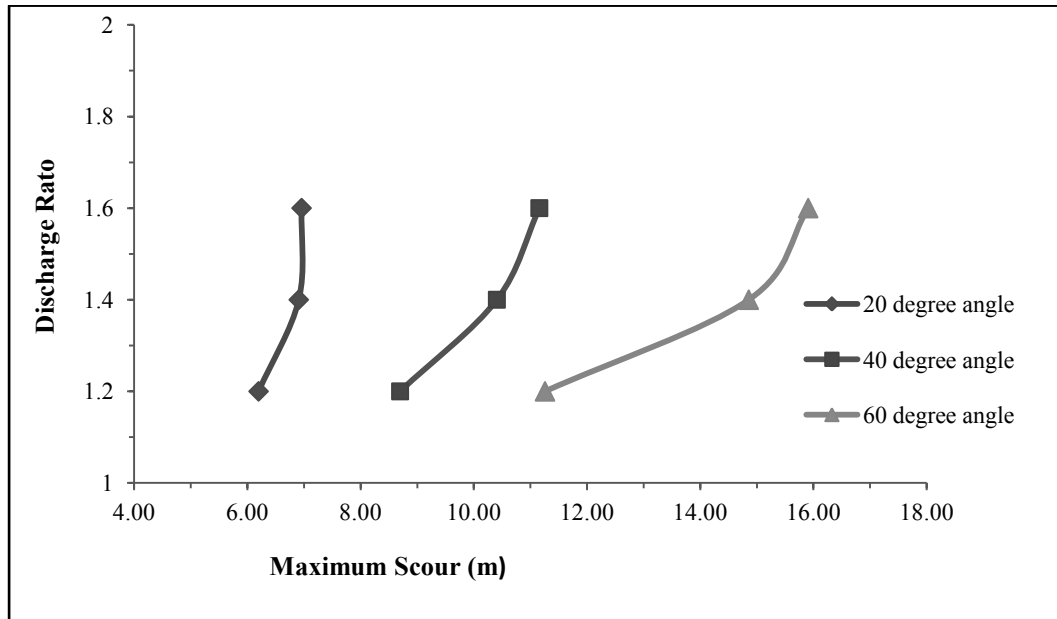


Figure 5.84: Relation of Scour Depth with Discharge Ratio for Oblique Flow (Protected by stone boulder)

5.9 Effect of Oblique Flow Angle on Scour

Figure 5.85 represents the relation between scour depth and flow angle. The relation has been developed with the experimental setup those have protection work by stone boulder. Scour depth increases appreciably with angle of secondary channel for the same discharge ratio. For a discharge ratio of 1:1.2 scour depth varies from 6.20m to 11.26 m for a secondary flow angle range between 20° to 60°, for 1:1.4 it has a range of 6.91 m to 14.86 m and for 1:1.6 ratio it becomes 6.96m to 15.91m.

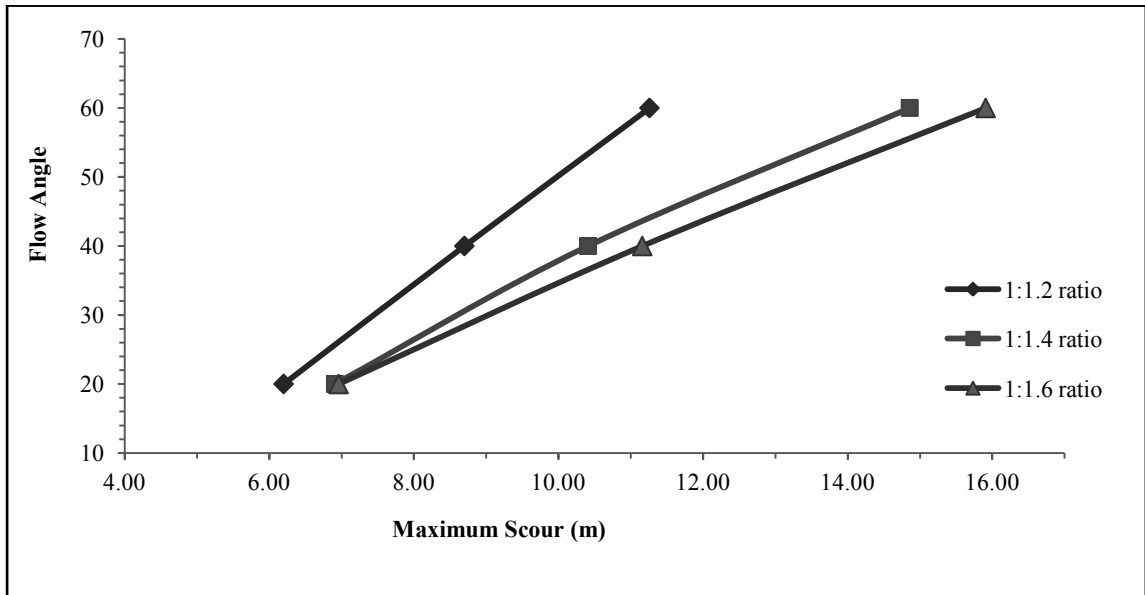


Figure 5.85: Relation of Scour Depth with Oblique Flow Angle (Protected by stone boulder)

In both Figure 5.84 and 5.85 it has been found that the discharge ratio of 1:1.4 is an optimum level after which increment of bed scour is less (than a less discharge value), if discharge ratio is increased.

5.10 Bare Space in Launching Slope

Bare spaces in launching slope of stone boulder have not been found. But there are frequent bare spaces for both type of geo-bag as stated in article 5.2. Percentage of bare space in that case has been presented in Table 5.6. No of geo-bag has been counted in a 1m strip. Average width of launched slope has been taken into consideration for calculating launched area. For 738 kg geo-bag percentage of bare space is 26% to 30%, whereas in case of 250 kg this value turns in 37% to 57%.

Table 5.6: Calculation of Bare Spaces in Launching Slope

Test no	Number of bag on slope	Width of launched area (m)	Total launched area, m²	Geo-bag, kg	Area of single bag, m²	Total area covered by bag, m²	% of area uncovered
T-14	600	0.55	0.55	738	0.000672	0.4032	26.69
T-16	766	0.74	0.74	738	0.000672	0.5148	30.44
T-18	300	0.32	0.32	250	0.000456	0.1368	57.25
T-20	650	0.475	0.475	250	0.000456	0.2964	37.60

5.11 Summary

Rivers have unique nature for oblique flow. Bed and bank erosion pattern changes for the flow angle at secondary channel. Relation between different controlling parameters as discharge ration of main channel to chute channel, oblique flow angle, scour depth has been established in the study. Moreover, launching behaviour of different protection materials (stone boulder and geo-bag) for this condition has been discussed. The reason of variable behaviour of protection materials has also been discussed in the study.

Chapter 6

CONCLUSION AND RECOMMENDATIONS

6.1 General

The study focused on the erosion pattern in a braided river and effect of oblique flow on its straight bank. It reveals the behaviour of protective material. Finally it can be said that when a straight channel is in regime condition it do not bring any significant changes in channel fluvial process for protected and unprotected condition. Though some scouring and deposition has been found in the single channel (T-0) as roughness of channel reduces than natural condition for channel lining and weathering effect. Defining the variation due to roughness cannot be found in small scale of 1:50.

Secondary channel causes unstable flow pattern. That unstable flow pattern changes the channel fluvial process causes excess erosion than for a single channel. Factor for regime scour depth in design of bank protection work changes with the change of oblique flow. The study reveals that the factor increases with the increase of angle of oblique flow. So the factor needs to be reassessed for a channel having oblique flow because bed scour becomes independent of discharge and velocity in such situation. The total fluvial process of a braided river can be only defined or predicted by means of physical or mathematical modeling.

6.2 Conclusion of the Study

The overall analysis of the experimental setups can be summarized as below:

1. Scour parent and most affected zone due to oblique flow in the main channel changes with the characteristics of chute channel.
2. Scour depth increases with the increase of discharge ratio but the variation in scour depth is high for higher secondary channel angle.
3. Erosion rate in main channel increases with a dominant oblique flow i. e with the increase of oblique flow angle.
4. Thalweg channel pattern changes with protective material type.

5. Launching behavior changes with the change of material type. Launching behaviour of stone boulder and geo-bag is different. Stone boulder launches at a maximum slope of 1:2.42 without any bare spaces and the slope varies from mild to steep slope with the changes of discharge ratio and oblique flow angle. On the other hand there is no uniformity of slopes of geo-bag and frequent bare spaces found while it launch to meet the scour.
6. Launching slope of 738 kg geo-bag has been recorded at a range of 23.68° to 37.99° at 60° oblique flow, for 250 kg geo-bag the range is between 23.86° to 47.69°. Whereas for stone boulder the range is between 23.24° to 52.04°.
7. Stone boulder has a better launching property than geo-bag. It maintains a well defined areal coverage.
8. Geo-bag has less areal coverage as a protective material. Sometimes it works as a bundle. Due to non responsive behaviour there always remains the probability of slope failure.
9. The percentage of bare spaces for Geo-bags increases with the increase of discharge ratio and as well as flow angle. For 738 kg geo-bag percentage of bare space is 26% to 30%, whereas in case of 250 kg this value turns in 37% to 57%.
10. Movement of geo-bags from launching area in some extent has been found.

6.3 Recommendations of the Study

The research has been done to observe only a few parameters of braided river. Further study on the following topics is expected to be a complete guidance for defining the nature of braided river for oblique flow.

1. Research on a total braided river section containing several chars to define a complete behaviour of braided river.
2. Modeling work with true prototype condition i.e. unconfined right bank.
3. Protection work completed by only slope pitching and launching apron without extending the slope up to the bottom of model bed would be helpful in identifying mode of slope failure in a braided river and launching behavior due to oblique flow.

REFERENCES

1. ASCE, 1998, "River Width Adjustment. II: Modeling", *Journal of Hydraulic Engineering*, Vol. 124, No. 9, pp 903-917.
2. Ashmore P.E, Ashworth P.J., Ferguson R.I, Paola C., Powell D.M. and Presegaard K.L., 1993, "Measurement in a Braided River Chute and Lobe, Flow pattern, sediment transport and channel change", *Water resources Reserarch Volume*. 28, No. 7, pp 1877-1886.
3. BWDB, 2013, "Prediction of River Bank Erosion along the Jamuna, the Ganges and the Padma rivers in 2013" prepared by CEGIS.
4. BWDB, 2012, "Bangladesher Nod-Nodi", published by Hydrology, BWDB, Dhaka.
5. BWDB, 2011, "Annual Report", published by Bangladesh Water Development Board.
6. BWDB, 2010, "Guidelines for Bank Protection", Jamuna-Meghna River Erosion Mitigation Project (JMREMP), funded by ADB.
7. Bhuiyan A.M.T.H, 2009, "A Study on the performance of Geo-bags as an alternative approach to river bank and bed protection", M. Engineering Project, Department of Water Resources Engineering, BUET, Dhaka.
8. BWDB, 2006, "Feasibility Study for River bank Protection of Left Bank of Jamuna River at Horindhara and Ulia of Kulkandi and Noapara in Upazilla Islampur under Jamalpur District", prepared by IWM.
9. Benda L. and Andras K., 2004, "Confluence effects in rivers: Interactions of basin scale, network geometry, and disturbance Regimes", *Water Resources Research*, Vol. 40, W05402.
10. Best J. L. and Ashworth P. J, 1997, "Scour in large braided rivers and the recognition of sequence stratigraphic boundaries", *Department of Earth Sciences, Nature*, Vol. 387, Issue. 6630, Accession No. 9705276122, pp 275-277.

11. BWDB, 1993, "Guide to Planning and Design of River Training and Bank Protection Works", Design Manual.
12. Bhuiyan R. R., 1991, "An Experimental study of Confluence Flow," M.Sc Engineering Thesis, Department of Water Resources Engineering, BUET, Dhaka.
13. BWDB, 1983, "Guide to Planning and Design of River Training and Bank Protection Works", Design Circle-2, BWDB, Dhaka.
14. Chen H. Y., Fiuzat A. A. and Roberts R. B., 1985, "Salt River Channelization Project: Model Study", Journal of Hydraulic Engineering, Vol. 111, pp 0002-0267, Paper No.19500.
15. Duan G. J., 2001, "Numerical Analysis of River Channel Processes With Bank Erosion", Journal of Hydraulic Engineering, Vol. 126, No. 4, pp 702-703.
16. DHV Consultants BV, 2000, "River Erosion Prevention and Morphology Study", the Netherlands.
17. EU and Bangladesh, 1993, "Morphological Behaviour of the Major Rivers in Bangladesh," Proceedings of the international workshop at Dhaka.
18. Froehlich C. D., 2009, "River Bank Stabilization Using Rock Riprap Falling Aprons", River Research and Application 25: 1036–1050.
19. Gray D. and Harding J. S., 2007, "A literature review of physical habitats and aquatic invertebrate communities", published by Science & Technical Publishing, ISBN 978-0-478-14341-6.
20. Garde R.J., 2006, "River Morphology", published by New Age International (P) Ltd., Publishers, ISBN (13): 978-81-224-2841-4.
21. Georgiou, E. F. and Sapozhnikov, V., 2000, "Scale Invariances in the Morphology and Evolution of Braided Rivers", Mathematical Geology, Vol. 33, No. 3, pp 0273-0400.
22. Griffiths A. G., 1993, "Sediment Translation Waves in Braided Gravel Bed Rivers", Journal of Hydraulic Engineering, Vol. 119, No. 8, pp 0008-0924, Paper no. 4779.

23. Hossain B.M., Sakai T. and Hossain Z. M., 2010, “River Embankment and Bank Failure in Bangladesh: A Study on Geotechnical Characteristics and Stability Analysis”, Proc. of International Conference on Environmental Aspects of Bangladesh (ICEAB10), Japan.
24. Halcrow Group Limited, 2002, “Jamuna-Meghna River Erosion Mitigation Project”, UK, prepared for BWDB.
25. Halder S. K., 1990, “Study on changes in River-Section characteristics of Brahmaputra-Jamuna at selected station”, M.Sc Engineering Thesis, Department of Water Resources Engineering, BUET, Dhaka.
26. Holly M. F. and Karim F. M., 1986, “Simulation of Missouri River Bed Degradation”, Journal of Hydraulic Engineering, Vol. 112, No. 6, pp 0006-0497, Paper no. 20687.
27. Lane E. W., 1957, “A study of the shape of channels formed by natural streams flowing in erodible material”, Missouri River Division Sediment Series No. 9, U.S. Army Engineering Division Missouri River, Corps of Engineers, Omaha, Nebraska.
28. Leopold L.B and Wolman M.G., 1957, “River channels Patterns: Braided, Meandering and Straight”, USGS Professional Paper, Volume. 282-B, pp 39-103.
29. Michael M.M., 2012, “Micro-scale Physical Modelling as a tool to investigate Braided River Evolution”, Nile Basin Water Science & Engineering Journal, Vol.5.
30. MoWR, Bangladesh, 2009, “Five Year Strategic Plan of BWDB, Roadmap for realizing Organizational Goals”.
31. Mosselman E., 2006 “Bank protection and river training along the braided Brahmaputra-Jamuna River, Bangladesh,” Delft University of Technology & WL/Delft Hydraulics, The Netherlands.
32. Mukherjee P., 1995, “A Study on Morphological behaviour of Brahmaputra-Jamuna River,” M.Sc Engineering Thesis, Department of Water Resources Engineering, BUET, Dhaka.

33. Millar G.R. and Quick C.M., 1993, “Effect of Bank Stability on Geometry of Gravel Rivers”, *Journal of Hydraulic Engineering*, Vol. 119, No.12, pp 0012-1343, Paper no. 4792.
34. Nykanen D. Sapozhnikov V. and Georgiou E., 1998, “Study of Spatial Scaling in Braided river patterns using synthetic aperture radar imagery”, *Water Resources Research*, Vol. 34, No. 7, pp 1795-1807.
35. Queensland Government 2006, “Natural Resources and Water, Managing Queensland’s natural resources- for today and tomorrow”, www.nrw.qld.gov.au, on 11/02/2013.
36. Rahman M.M., Mahmud F. and Uddin N. M, 2012, “Effect of Sand Bars on failure of bank protection work along large sand bed Braided River”, ICSE6-064, Paris .
37. Rahman M. R., 2012, “Effectiveness of River Training Structures in Bangladesh”, ICSE6 Paris - August 27-31.
38. Reza I. 2011, “Term Paper on Tracking the morphological change of a river extent of Bangladesh using satellite images in ArcGIS”, Introduction to GIS, CRP 514 – (101) City & Regional Planning Department.
39. Rahman M. R., 2010, “Impact of Riverbank erosion hazard in the Jamuna floodplain areas in Bangladesh”, *J. Sci. Foundation*, 8(1&2), pp 55-65, ISSN 1728-7855.
40. RRI, 2010, “Additional tests to carry out investigation regarding performance of falling aprons drop tests for dumping of Geo-bags and outflanking problems by physical modelling to address the bank erosion problem in Bangladesh”, final report of RRI, prepared for BWDB.
41. Richardson W. R. and Thorne C. R., 1998, “Secondary currents around braid bar in brahmaputra river, Bangladesh”, *Journal of Hydraulic Engineering*, Vol.124, No. 3, pp 0325-0328.
42. Sumer B. M., 2013, “Physical Modeling and its Relation to Mathematical Modeling in River Engineering Design”, report prepared for Danish Hydraulic Institute (DHI).

43. Sarker, M.H., Hugue, I., Alam, M. and Koudstaul, R., 2003, "Rivers, Chars and Char Dwellers of Bangladesh", *International Journal of River Basin Management*, Vol. 1, No.1, pp 61-80.
44. Sapozhnikov V. and Georgiou E., 1996, "Self-affinity in Braided Rivers", *Water Resources Research*, Vol. 32, No. 5, pp 1429-1439.
45. Schumm S. A. and Khan H. R., 1972, "Experimental Study of Channel Patterns", Department of Geology and Engineering Research Center, Colorado State University, *Geological Society of America Bulletin*, Vol. 83, pp 1755-1770.
46. Tockner K., Paetzold A., Karaus U. and Claret C., 2003, "Ecology of Braided Rivers", IAS Special Publication.
47. The World Bank, 1995, "Bangladesh River Bank Protection Project", Report No. 15090-BD.
48. Uddin A.F.M. A. and Basak J.K. 2012, "Effects of Riverbank Erosion on Livelihood", Unnayan Onneshan.
49. U.S. Department of the Interior Bureau of Reclamation, 2011, "Calibration of Numerical Models for the Simulation of Sediment Transport, River Migration, and Vegetation Growth on the Sacramento River, California," Technical Report No. SRH-2009-27.
50. Wang G., Xia J. and Wu B., 2008, "Numerical Simulation of Longitudinal and Lateral Channel Deformations in the Braided Reach of the Lower Yellow River", *Journal of Hydraulic Engineering*, Vol. 134, No. 8, pp 1064–1078.
51. Wheelock S., 2002, "New Perspectives on Braided Rivers", Indiana University Bloomington, Indiana, Terrigenous Clastic Deposition, Final Paper.
52. Wang K.H., Cleveland T.G., Fitzgerald S. and Ren X., 1996, "Hydrodynamic Flow Modelling at Confluence of Two Streams", *Journal of Hydrology*, Vol. 122, No. 10, pp 0994-1002.
53. Young W.J. and Warburton J., 1996, "Principals and practice of hydraulic modeling of braided gravel-bed rivers", *Journal of Hydrology*, Vol. 35, No. 2, pp 175-198.

54. Zhang H. W., Wieprecht S. and Borthwick A. G. L, 2004, “Modeling of Hyper-concentrated Sediment-Laden Floods in Lower Yellow River”, *Journal of Hydraulic Engineering*, Vol. 130, No. 10, pp 1025–1032.

APPENDICES

Appendix-A

Pictures for Physical Model Setup and Model Run

Picture has been taken during layout fixation, model construction and test run. Some of these representative pictures have been presented by Figure A.1 to A.50.

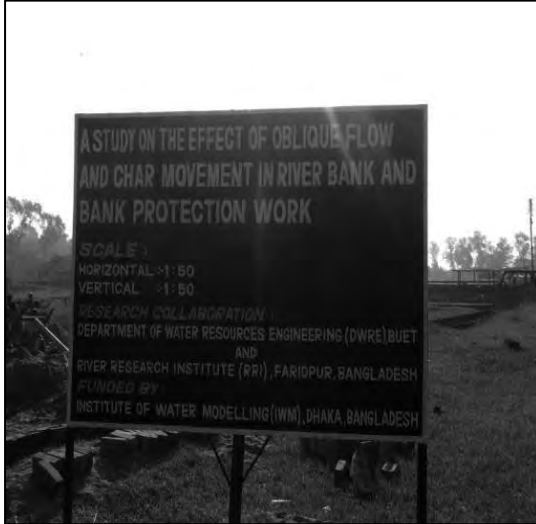


Figure A.1: Signboard



Figure A.2: Sand Sieving



Figure A.3: Placing of Sand at Model Bed



Figure A.4: Layout Fixation for Model Boundary



Figure A.5: Construction of Model Boundary

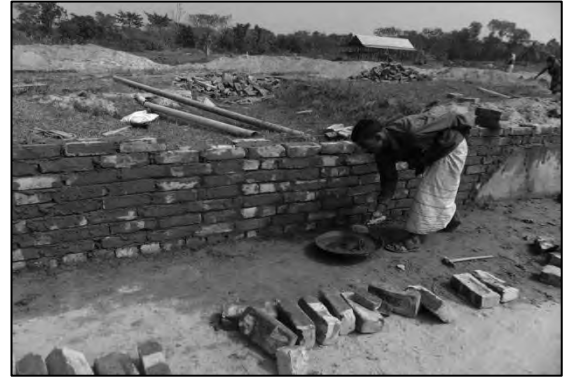


Figure A.6: Model Boundary of CC under Construction



Figure A.7: Carrying of Bricks for Construction



Figure A.8: Construction of MC Boundary



Figure A.9: Construction of Brick Wall



Figure A.10: Plastering Work at Boundary



Figure A.11: Rapping of Drainage Pipe with Coconut Fiber



Figure A.12: Carrying the Drainage Pipe to the Position



Figure A.13: Placing of Drainage Pipe



Figure A.14: Connecting the Backflow Pipe



Figure A.15: Construction of Fixed Bed



Figure A.16: Brick Flat Soling



Figure A.17: Socking of Sand for Model Bed



Figure A.18: Gate Volute at Weir



Figure A.19: Construction of D/S Tailgate



Figure A.20: Completion of a Boundary for Total Model (T-0 to T-20)



Figure A.21: Preparation of Model Bed



Figure A.22: Bench Mark Fixation



Figure A.23: Survey Work-1



Figure A.24: Survey Work-2



Figure A.25: Fixed Bed of Main Channel



Figure A.26: Stilling Basin



Figure A.27: Downstream Storage Pool



Figure A.28: Storage Pool



Figure A.29: Discharge gauge



Figure A.30: Downstream weir



Figure A.31: Re-circulating Reservoir



Figure A.32: D/S Weir with Backflow Point



Figure A.33: D/S Pump for Withdrawing Water



Figure A.34: Pump for Delivering Water to the Sump



Figure A.35: Preparation of Geo-bag-2



Figure A.36: Preparation of Geo-bag-1



Figure A.37.a: Sweing of Geo-bag



Figure A.38: Bank Erosion at Unprotected Condition



Figure A.39: Sliding of Bank

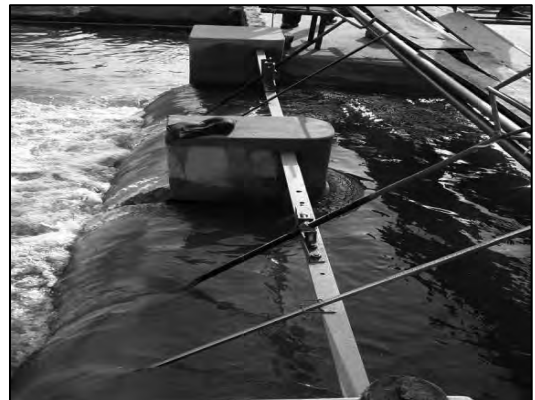


Figure A.40: Tail Gate during Run



Figure A.41: Bank Erosion at D/S



Figure A.42: Sand Feeding (manual)



Figure A.43: A Top View of Model during Run

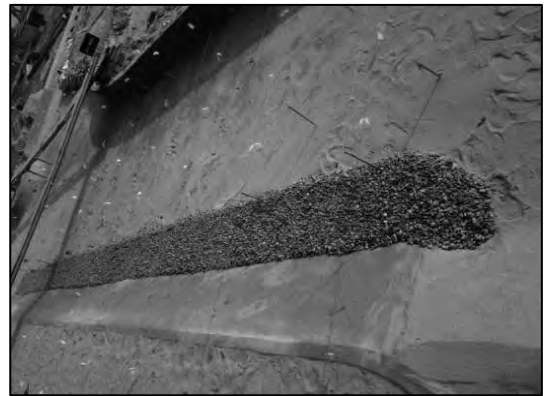


Figure A.44: Launching Apron at Initial Stage (Stone boulder)



Figure A.45: Launching Behaviour of Stone Boulder



Figure A.46: Launching Apron at Initial Stage (Geo-bag of 738 kg)



Figure A.47: Launching Behaviour of Geo-bag (738 kg)

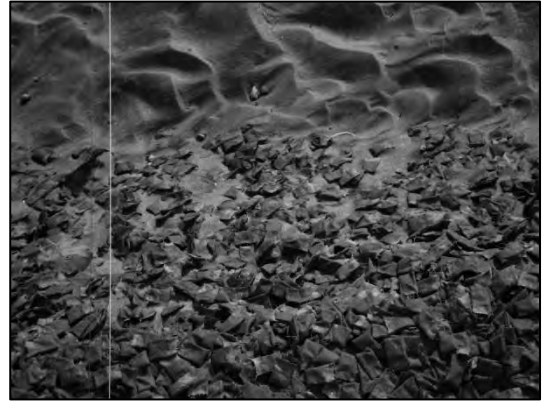


Figure A.48: Bare Spaces at Launched Slope (Geo-bag 738 kg)



Figure A.49: Launching Apron at Initial Stage (Geo-bag of 250 kg)

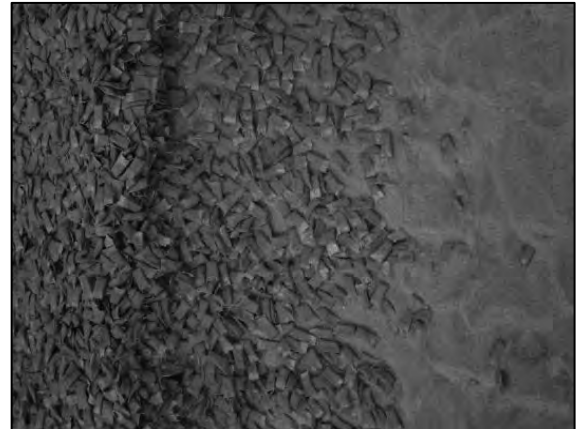


Figure A.50: Bare Spaces at Launched Slope (Geo-bag 250 kg)

Appendix-B

Dynamic Equilibrium State of Physical Model

Dynamic equilibrium state of the Physical Model has been identified by observing bed erosion. Three or four cross section has been selected and rate for depth of erosion/deposition has been plotted as per figure B-1 to B-21. Dynamic equilibrium is the state when depth of scour/erosion has a same horizontal path to the x-axis. Model parameters have been measured when model reaches a dynamic equilibrium state (All distance has been measured from left bank of the model). Figure B.0 has been provided as representative figure to indicate the distances or points where dynamic equilibrium has been observed with respect to time for each cross section. Time of starting model has been presented as per global clock.

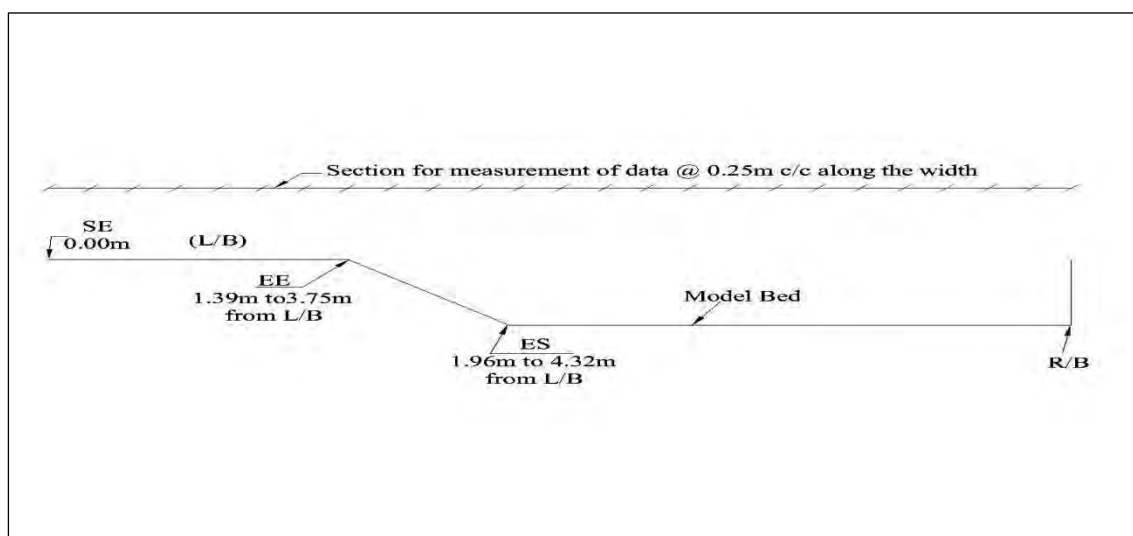


Figure B.0: Representative Picture for Points of Observations in Dynamic Equilibrium

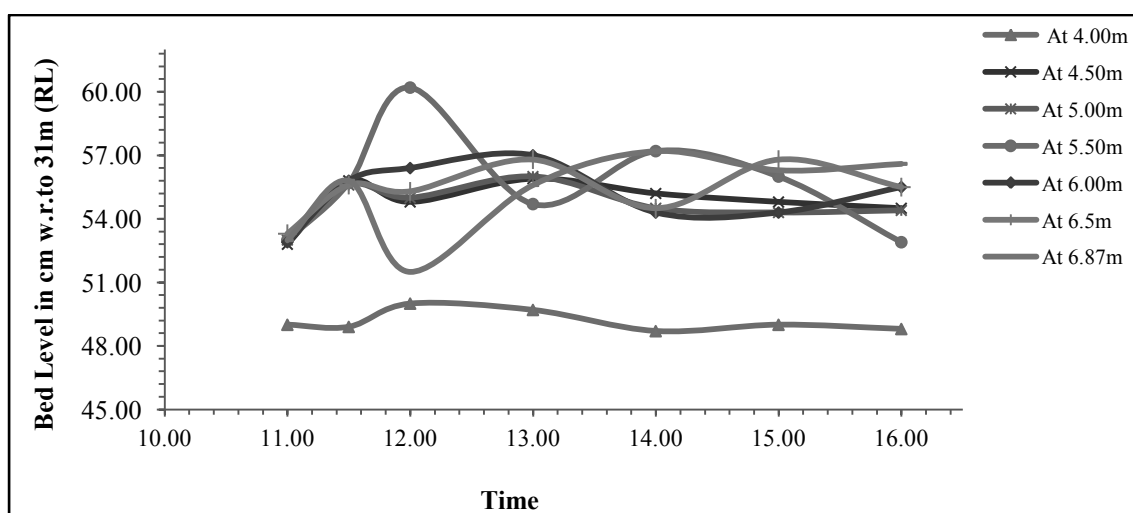


Figure B.1: Dynamic Equilibrium for T-0 (C/S-12)

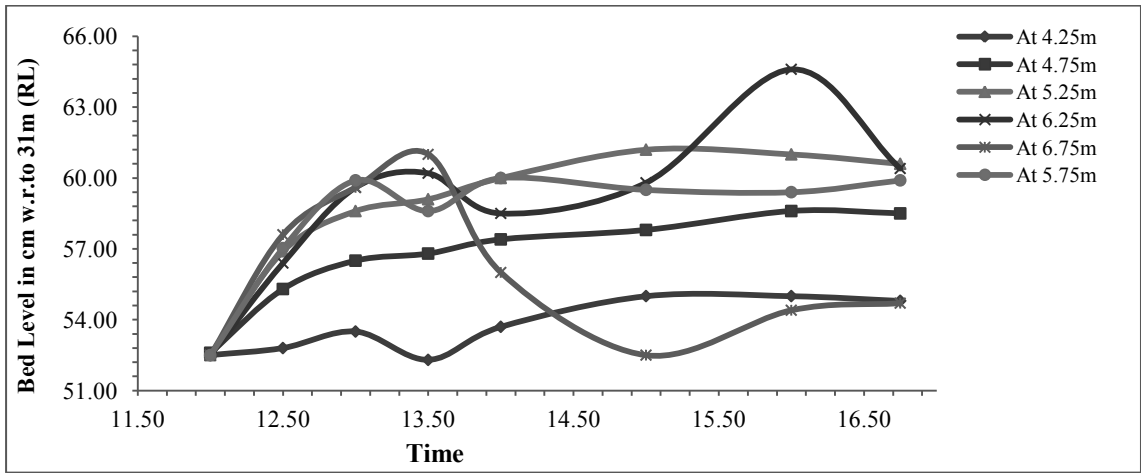


Figure B.2: Dynamic Equilibrium for T-1 (C/S-4)

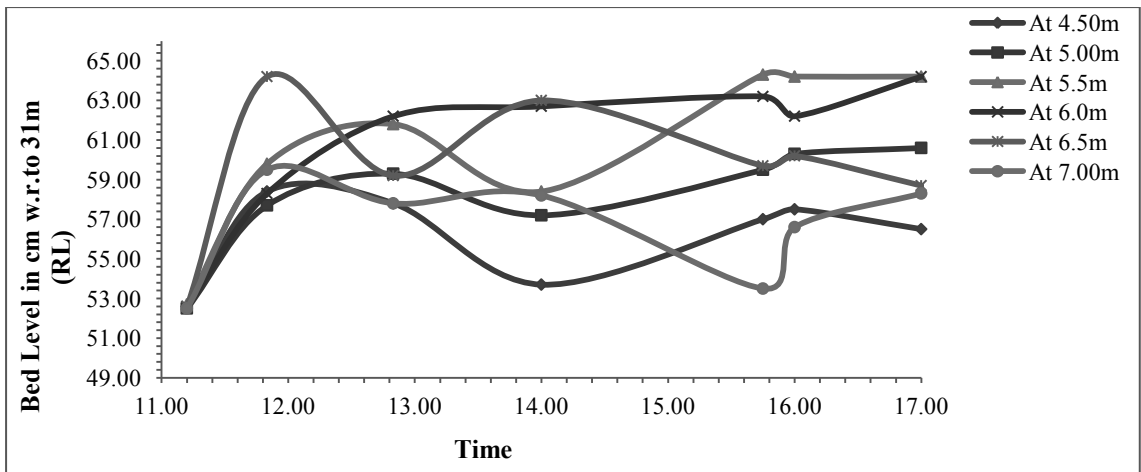


Figure B.3: Dynamic Equilibrium for T-2 (C/S-8)

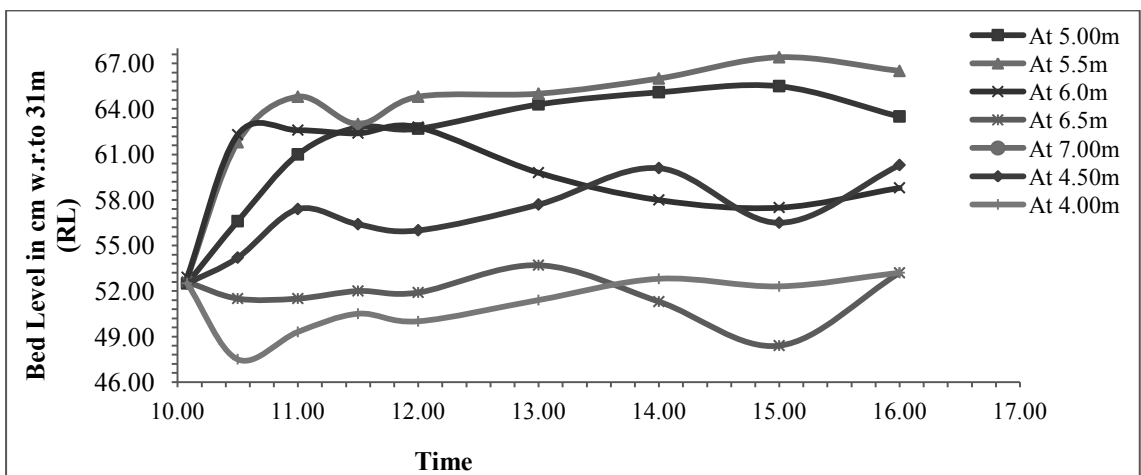


Figure B.4: Dynamic Equilibrium for T-3 (C/S-6)

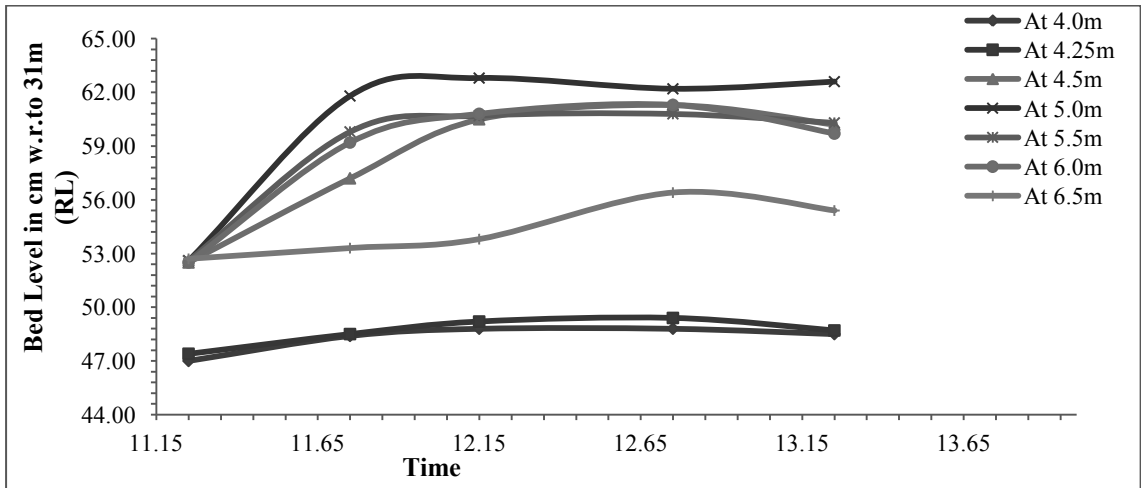


Figure B.5: Dynamic Equilibrium for T-4 (C/S-10)

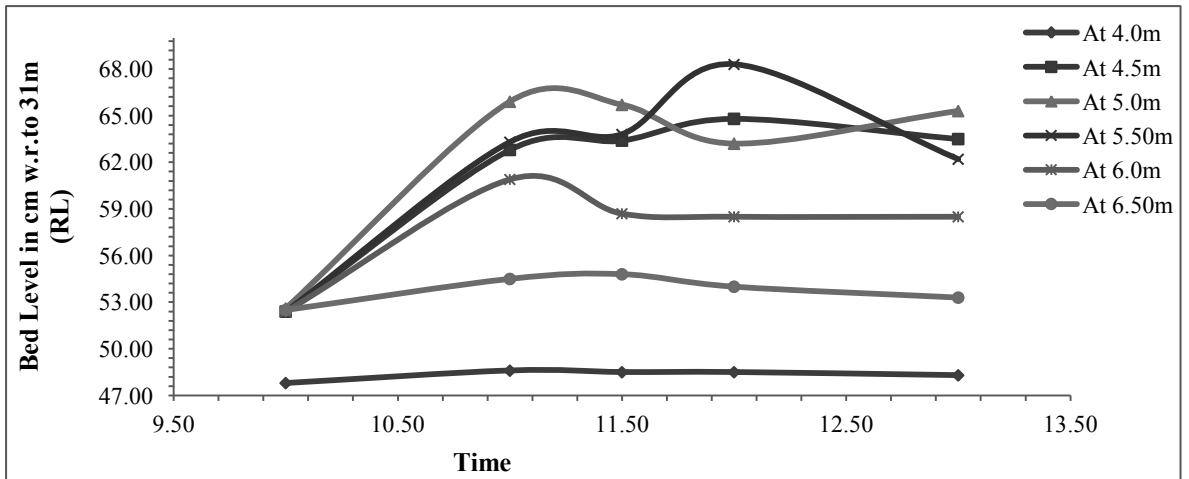


Figure B.6: Dynamic Equilibrium for T-5 (C/S-9)

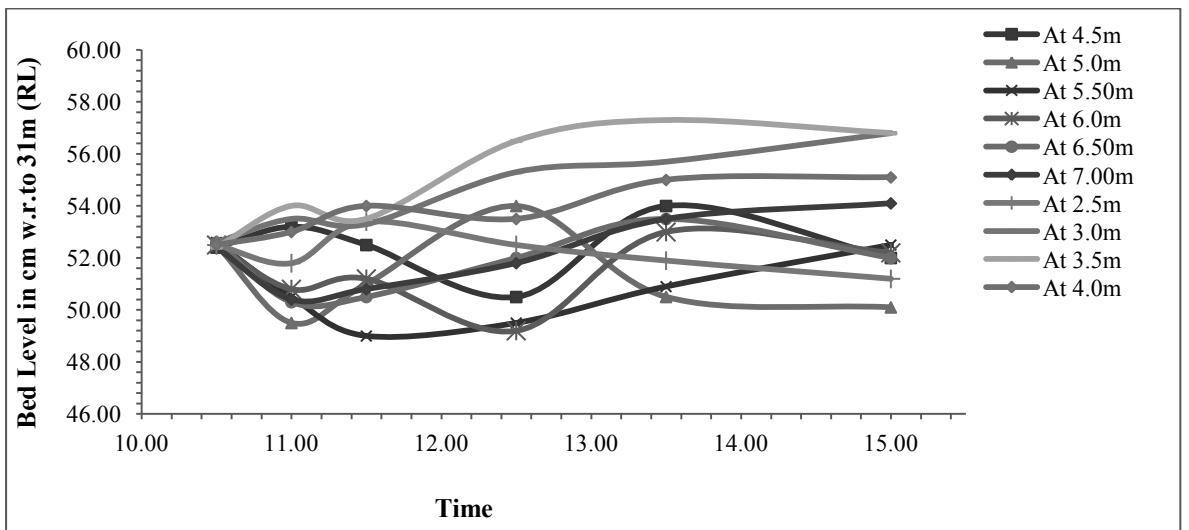


Figure B.7: Dynamic Equilibrium for T-6 (C/S-14)

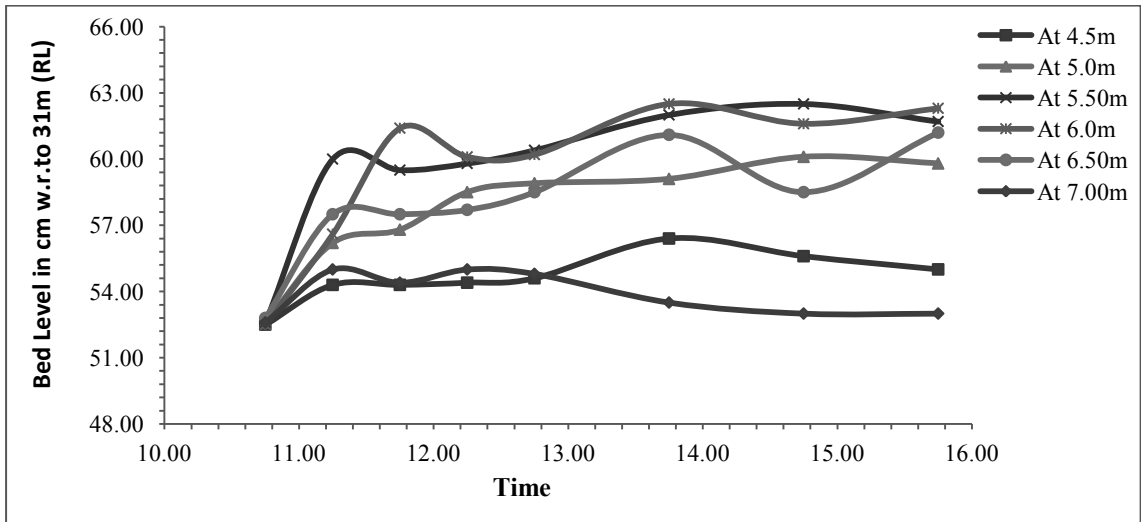


Figure B.8: Dynamic Equilibrium for T-7 (C/S-12)

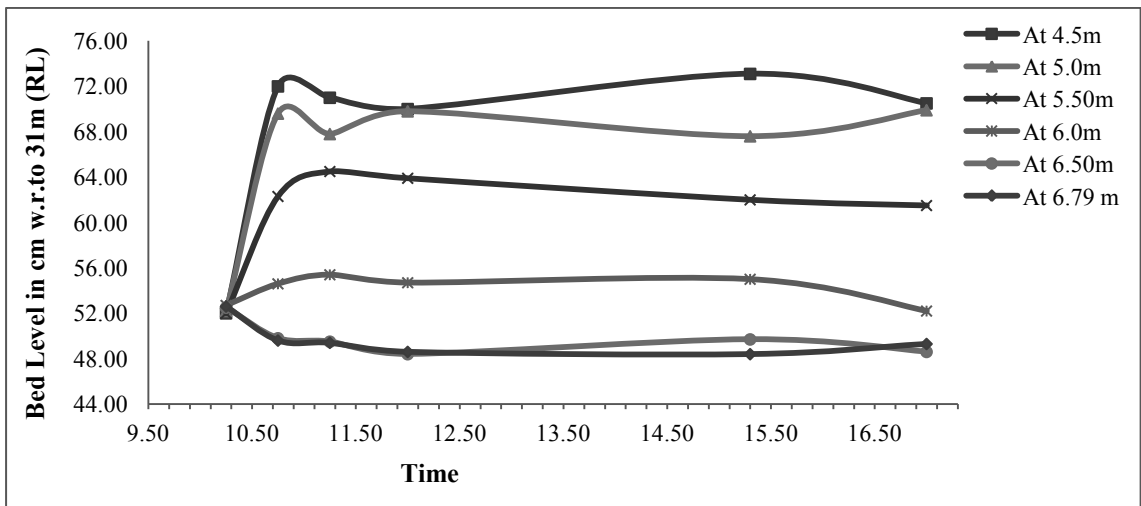


Figure B.9: Dynamic Equilibrium for T-8 (C/S-9)

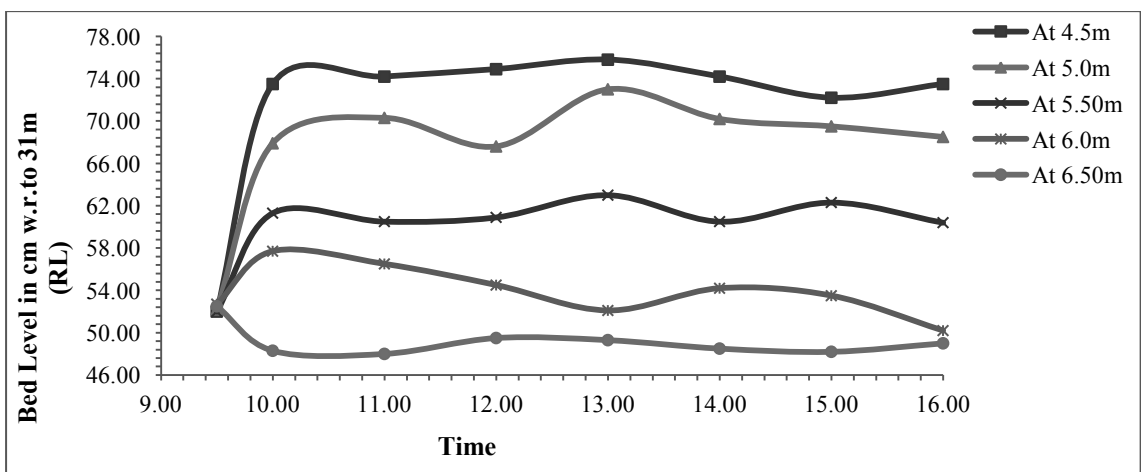


Figure B.10: Dynamic Equilibrium for T-9 (C/S-9)

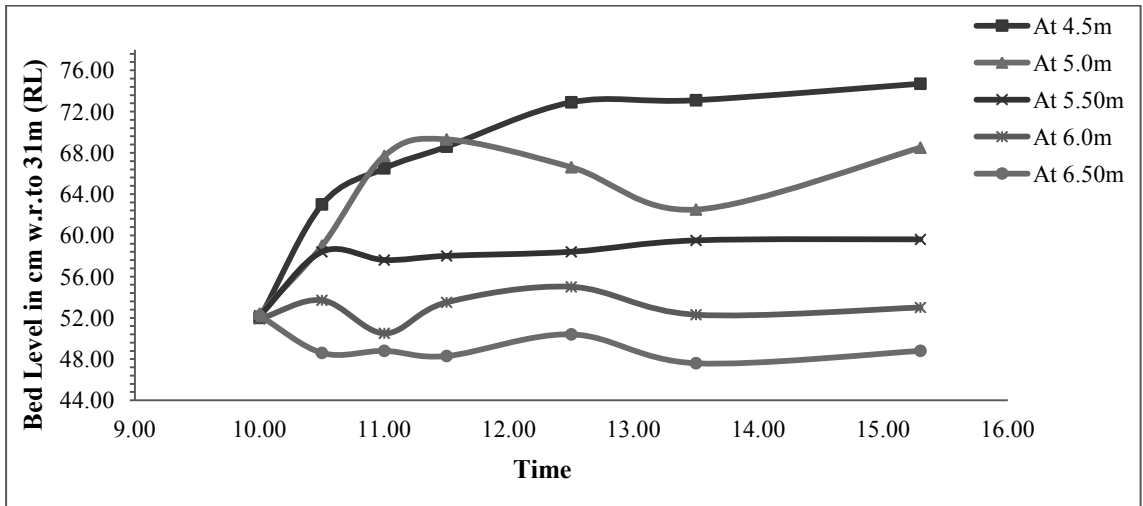


Figure B.11: Dynamic Equilibrium for T-10 (C/S-9)

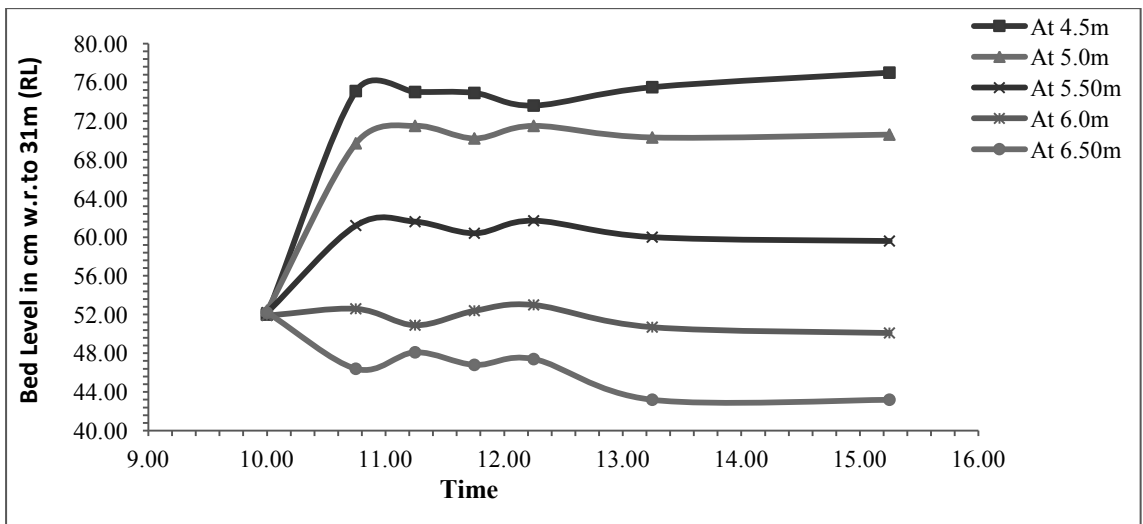


Figure B.12: Dynamic Equilibrium for T-11 (C/S-9)

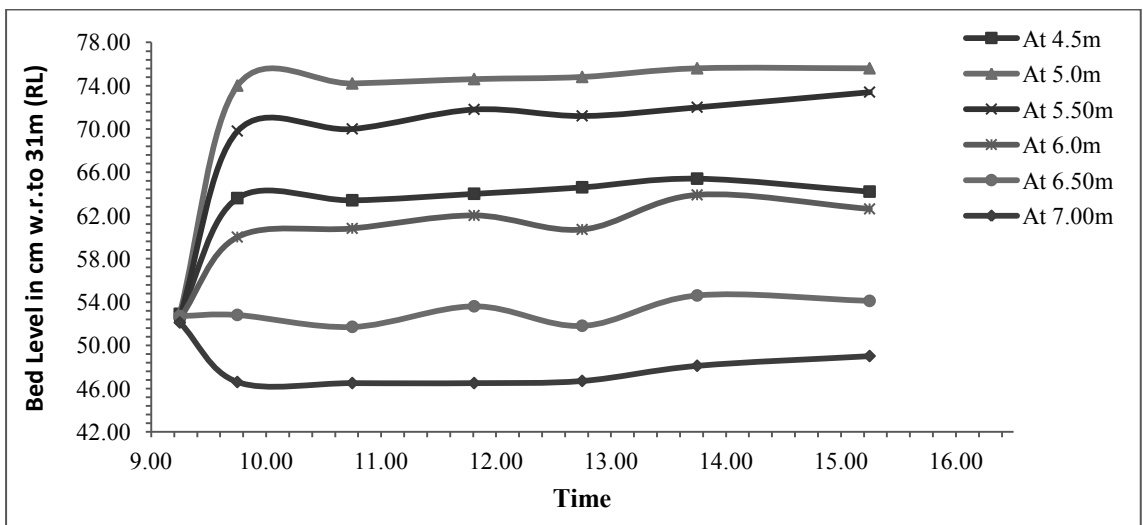


Figure B.13: Dynamic Equilibrium for T-12 (C/S-12)

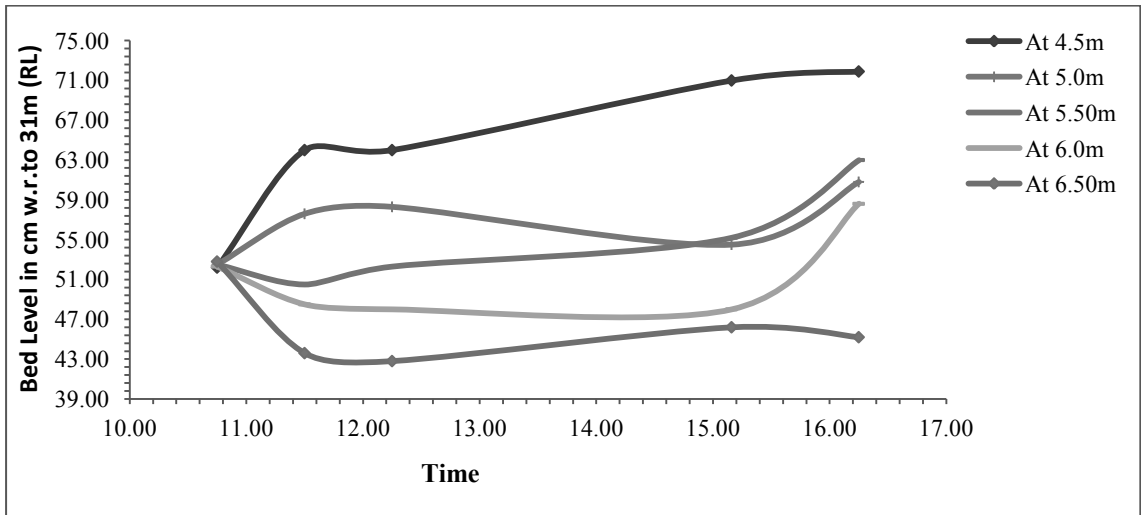


Figure B.14: Dynamic Equilibrium for T-13 (C/S-11)

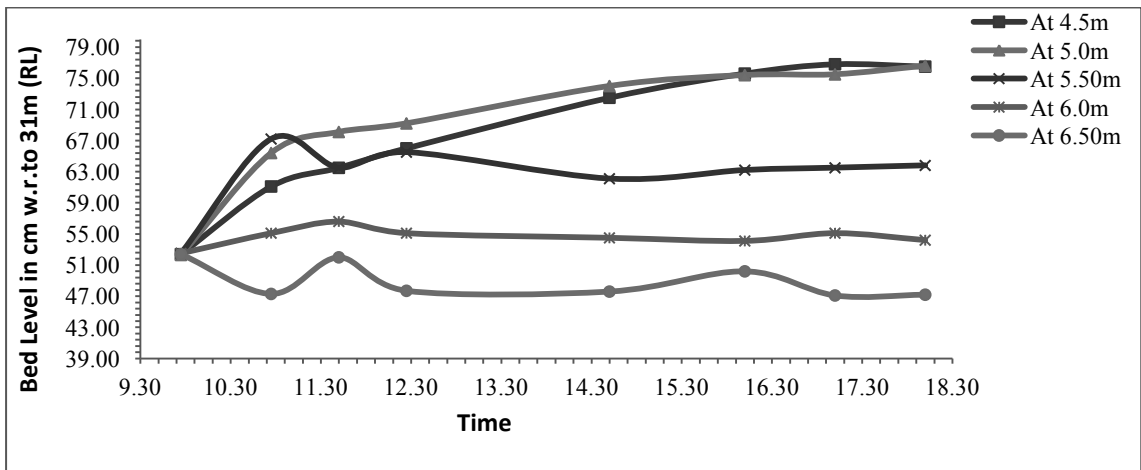


Figure B.15: Dynamic Equilibrium for T-14 (C/S-10)

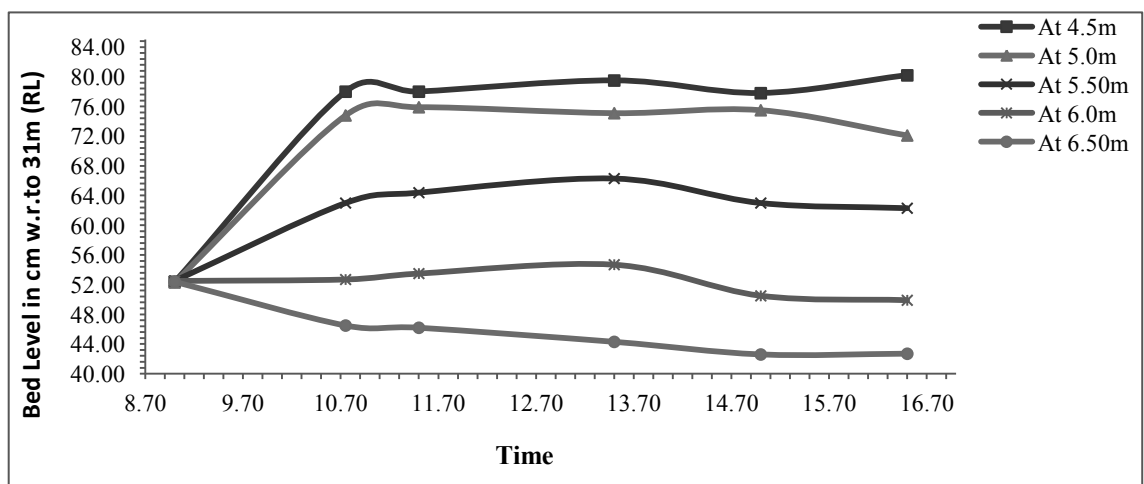


Figure B.16: Dynamic Equilibrium for T-15 (C/S-10)

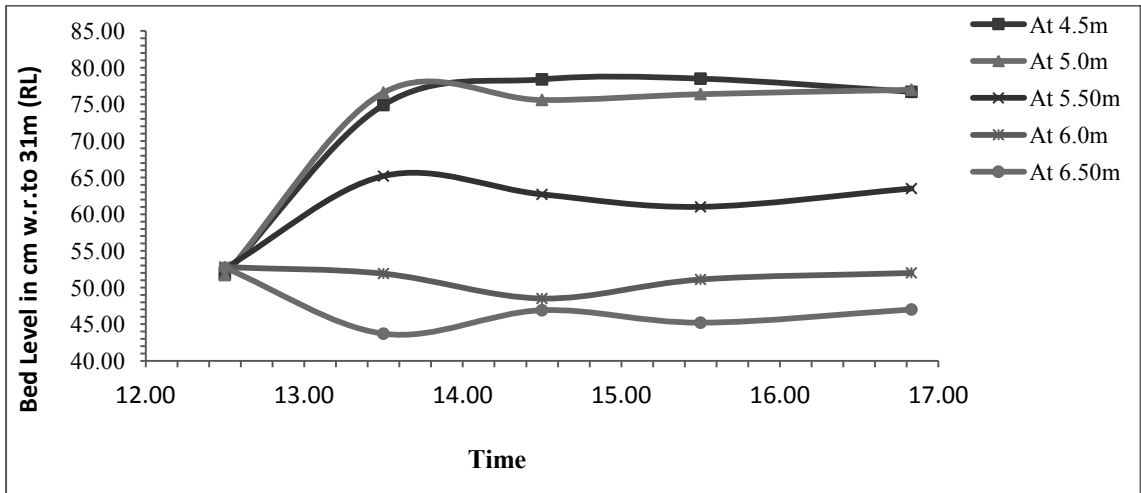


Figure B.17: Dynamic Equilibrium for T-16 (C/S-11)

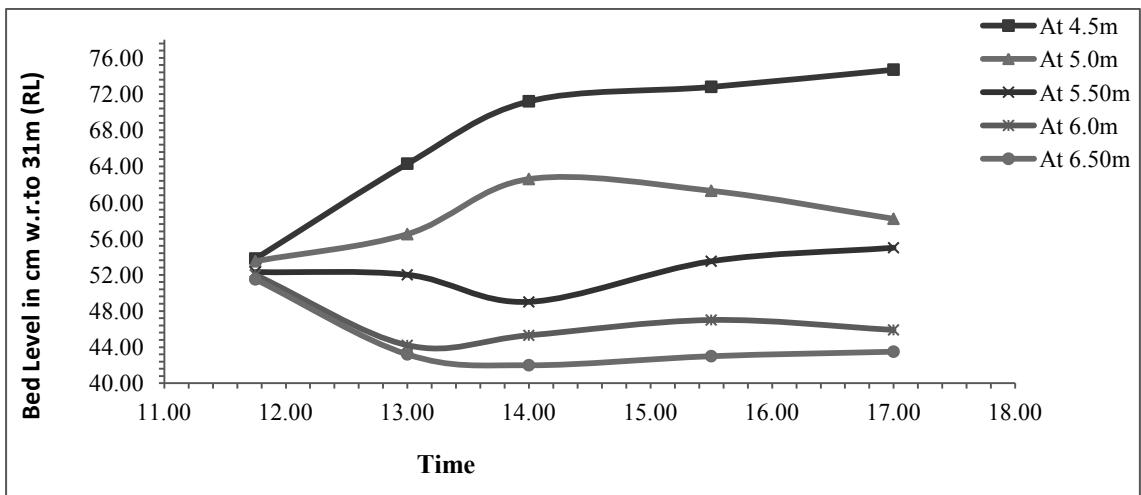


Figure B.18: Dynamic Equilibrium for T-17 (C/S-10)

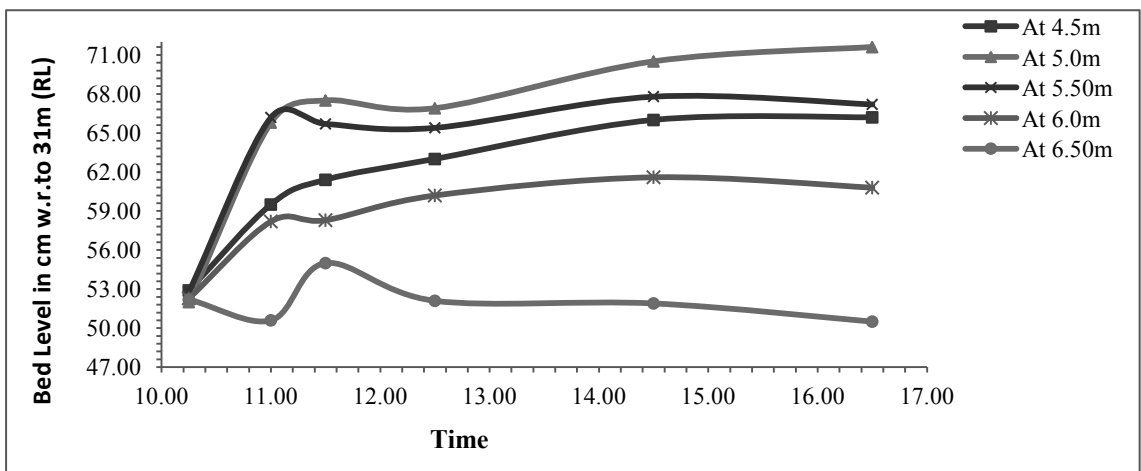


Figure B.19: Dynamic Equilibrium for T-18 (C/S-11)

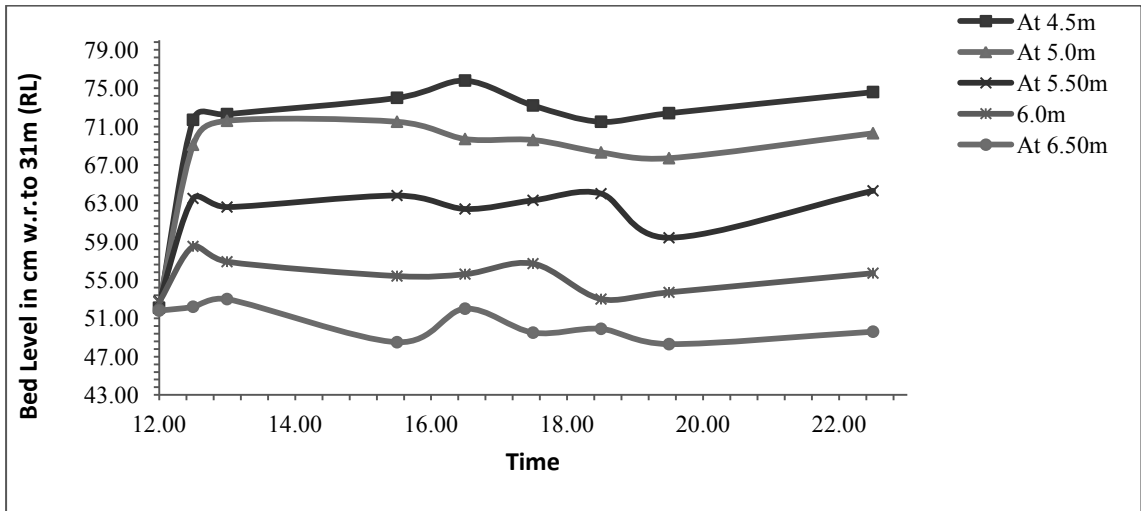


Figure B.20: Dynamic Equilibrium for T-19 (C/S-9)

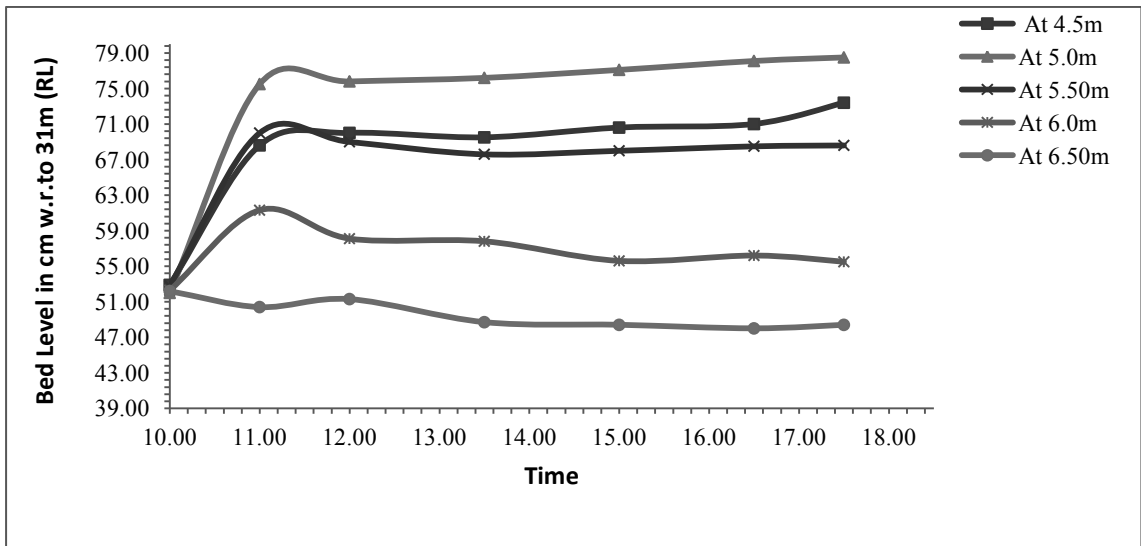


Figure B.21: Dynamic Equilibrium for T-20 (C/S-11)

Appendix-C

Flow Line Diagram Drawn by Float Position

Float at a continuous rate has been dropped in the flowing water from the calibration sections to identify the flow line/path (Figure C.1 to C.21). The schematic diagram has been presented below according to the test identity (Flow line diagram has been drawn by float position). A representative layout for float position and identity has been presented by Figure C.0 by a uniform color code for same position of each float for every setup. Total time required for a single float to pass from both main channel calibration section to c/s 1 and secondary channel calibration section to c/s 1 has been presented in table C.1. This data has been recorded for some of the tests.

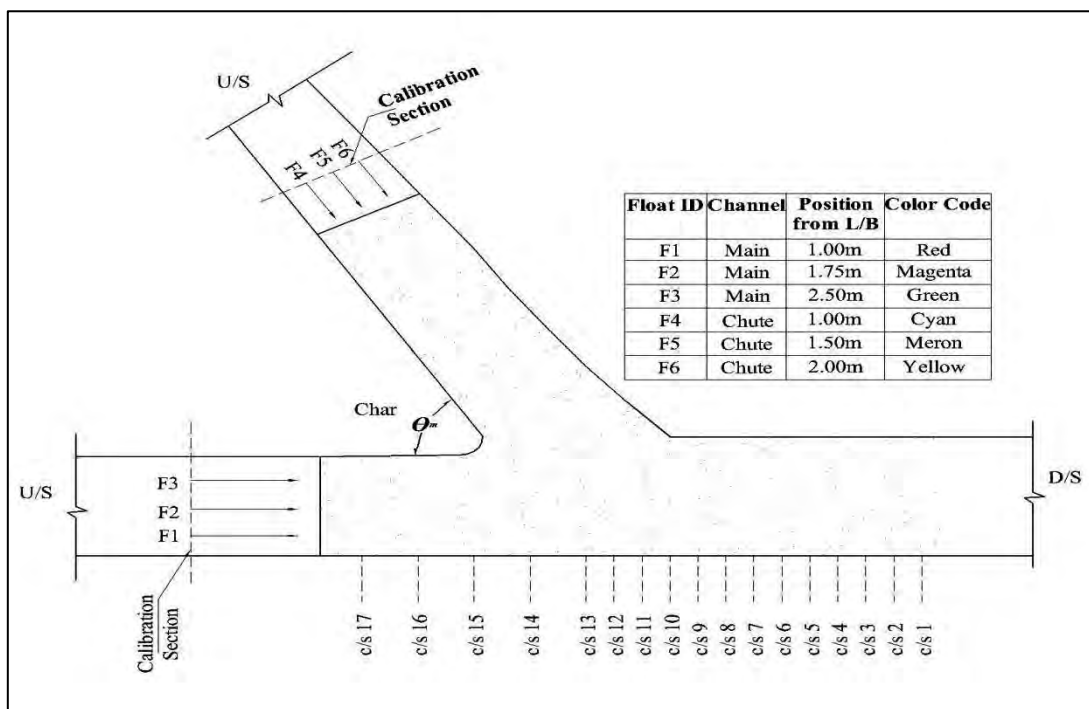


Figure C.0: Representative Model Layout for Float Position and ID

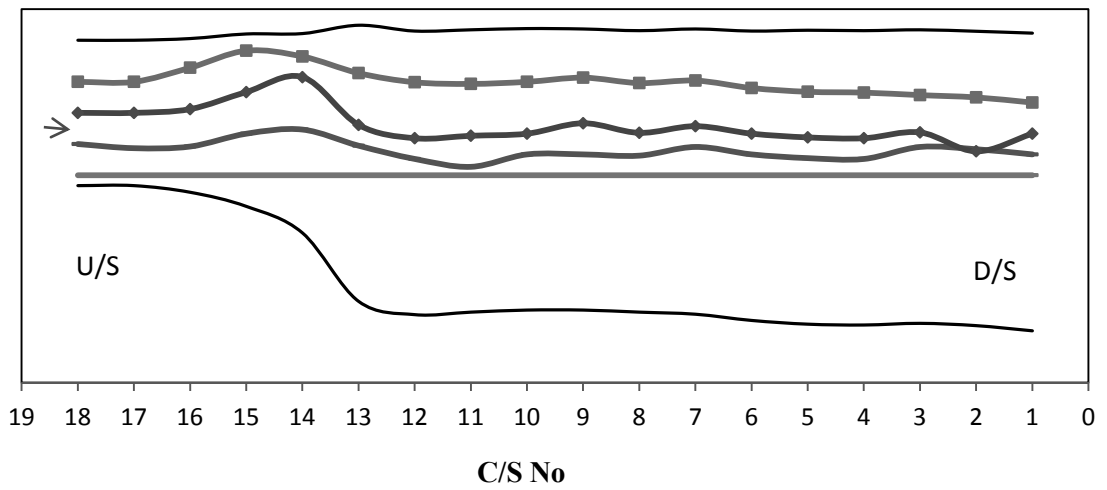


Figure C.1: Flow Line Diagram for T-0

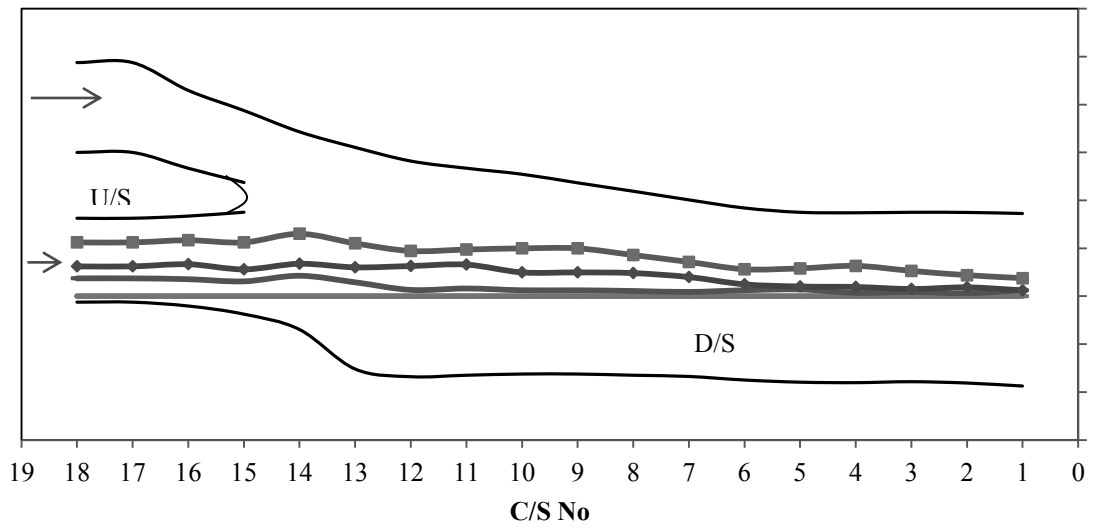


Figure C.2: Flow Line Diagram for T-1

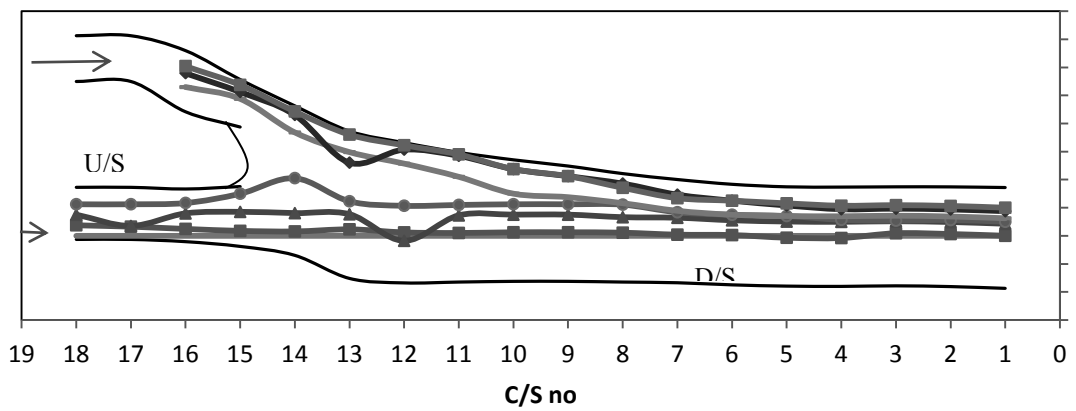


Figure C.3: Flow Line Diagram for T-2

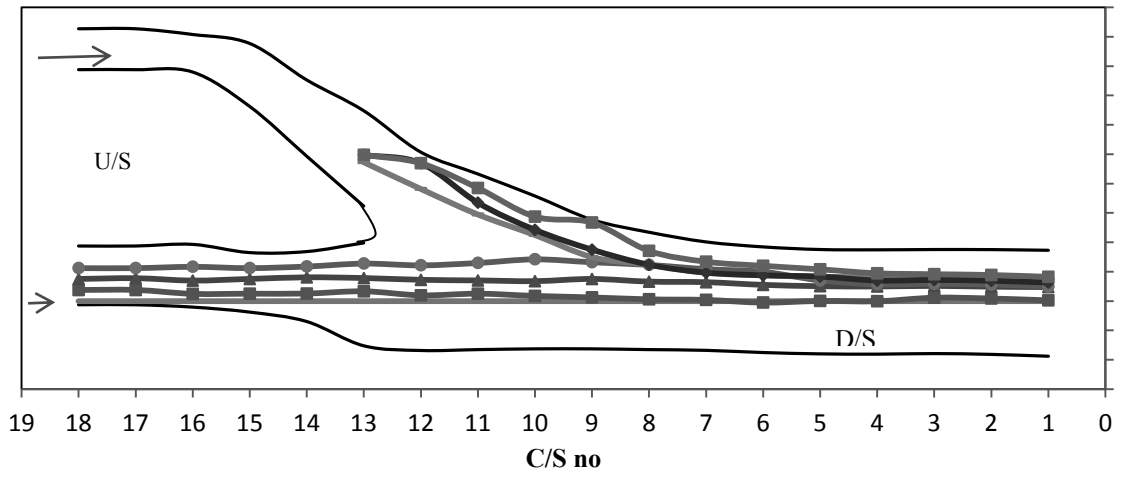


Figure C.4: Flow Line Diagram for T-3

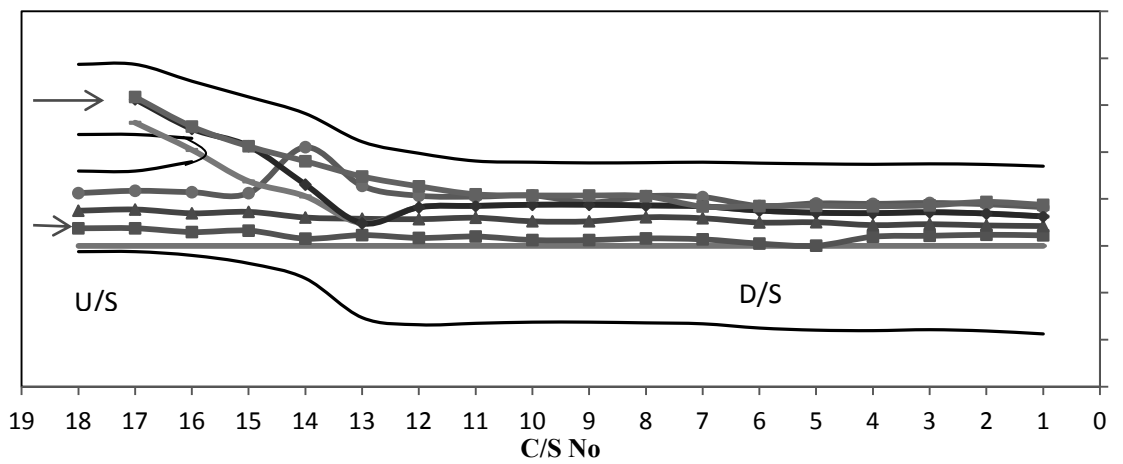


Figure C.5: Flow Line Diagram for T-4

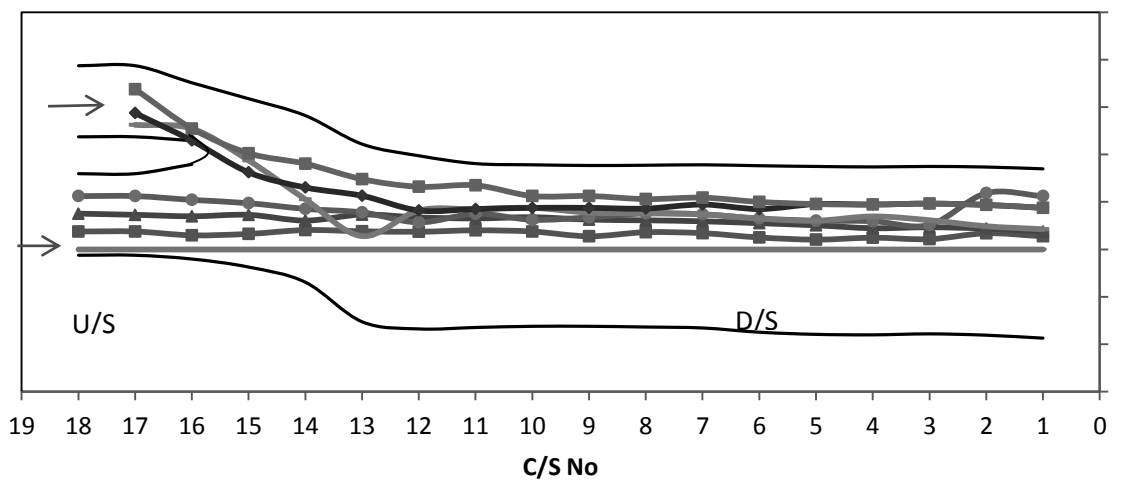


Figure C.6: Flow Line Diagram for T-5

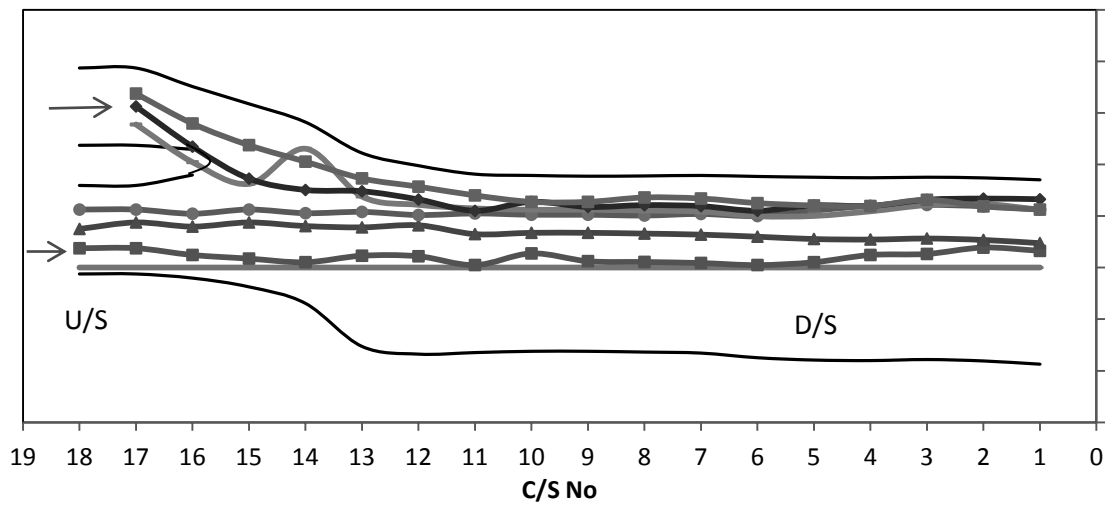


Figure C.7: Flow Line Diagram for T-6

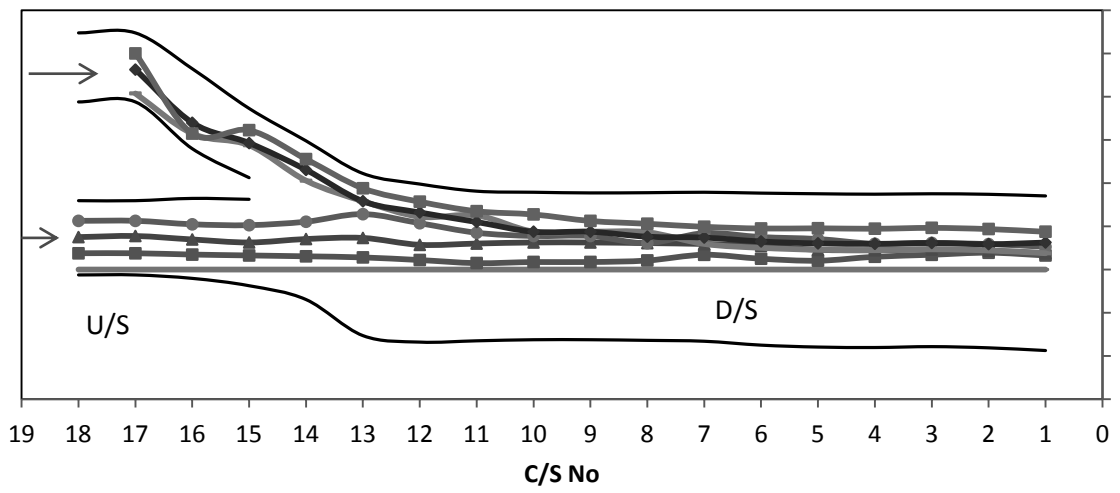


Figure C.8: Flow Line Diagram for T-7

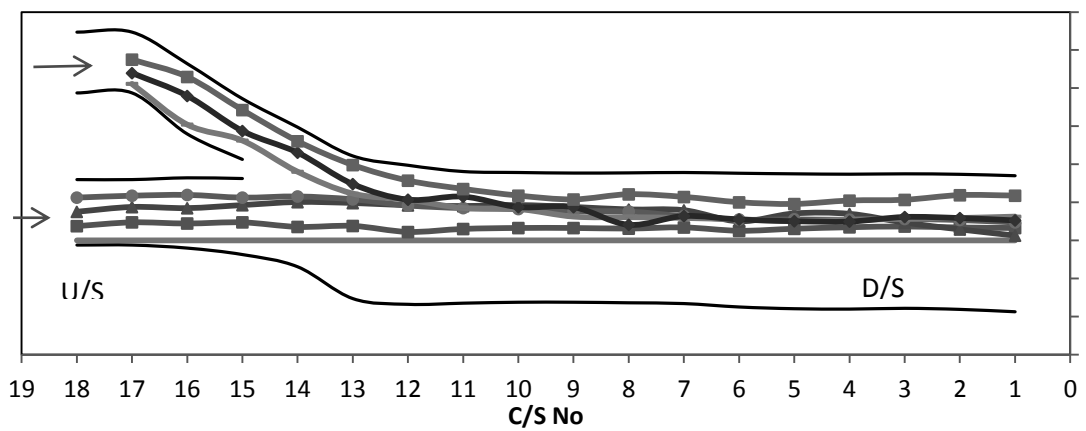


Figure C.9: Flow Line Diagram for T-8

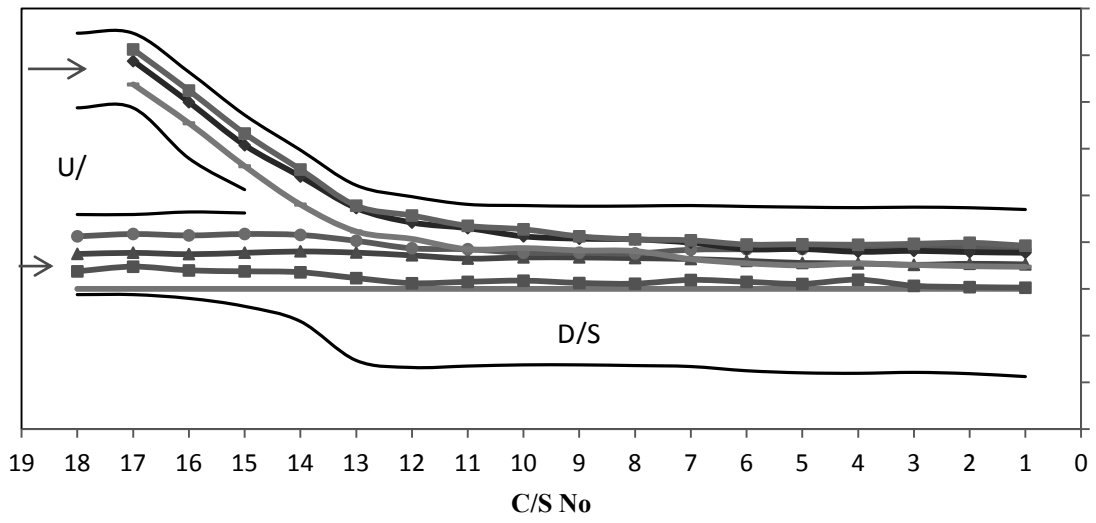


Figure C.10: Flow Line Diagram for T-9

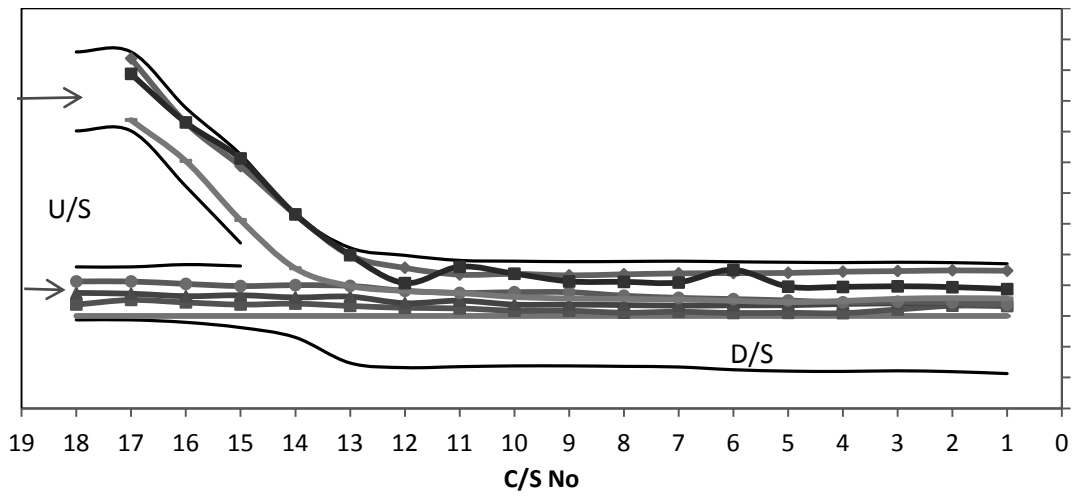


Figure C.11: Flow Line Diagram for T-10

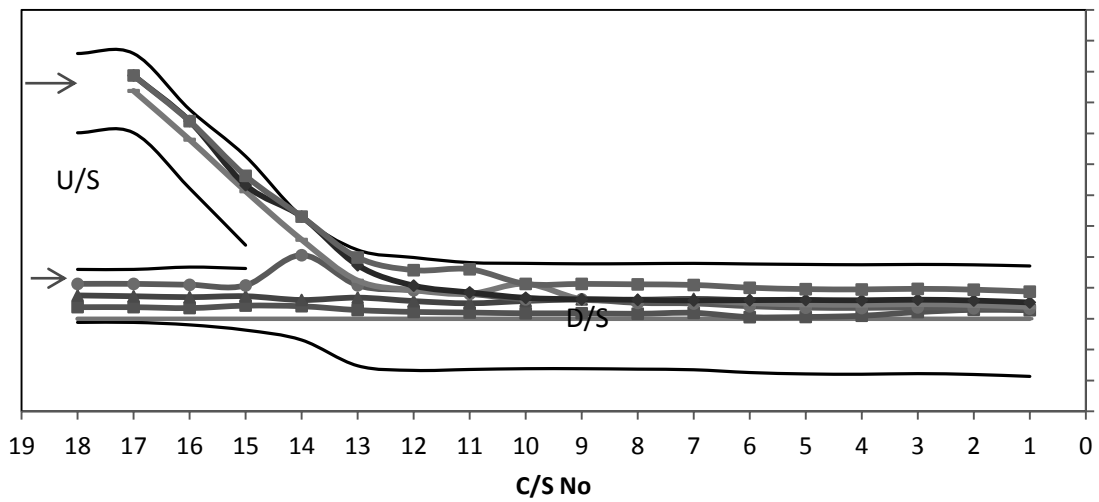


Figure C.12: Flow Line Diagram for T-11

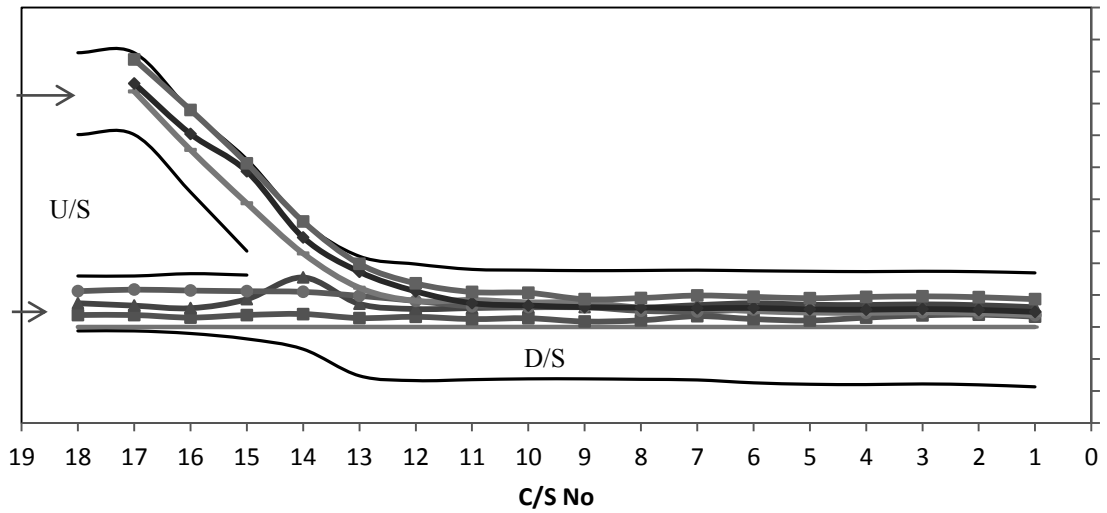


Figure C.13: Flow Line Diagram for T-12

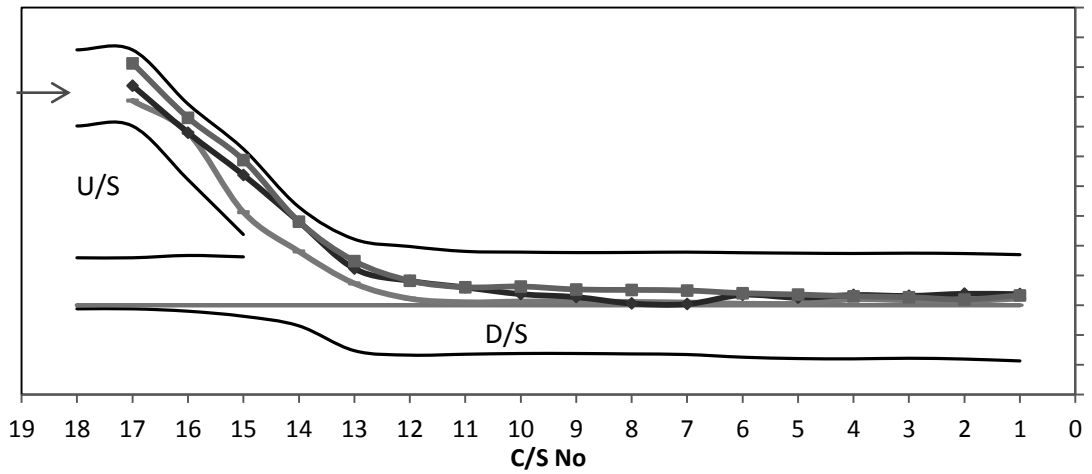


Figure C.14: Flow Line Diagram for T-13

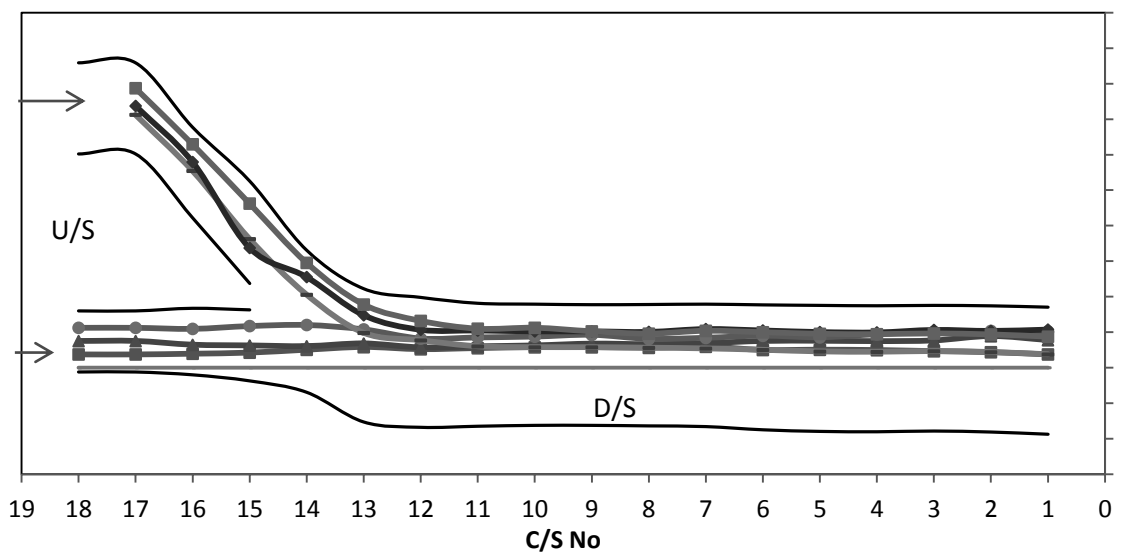


Figure C.15: Flow Line Diagram for T-14

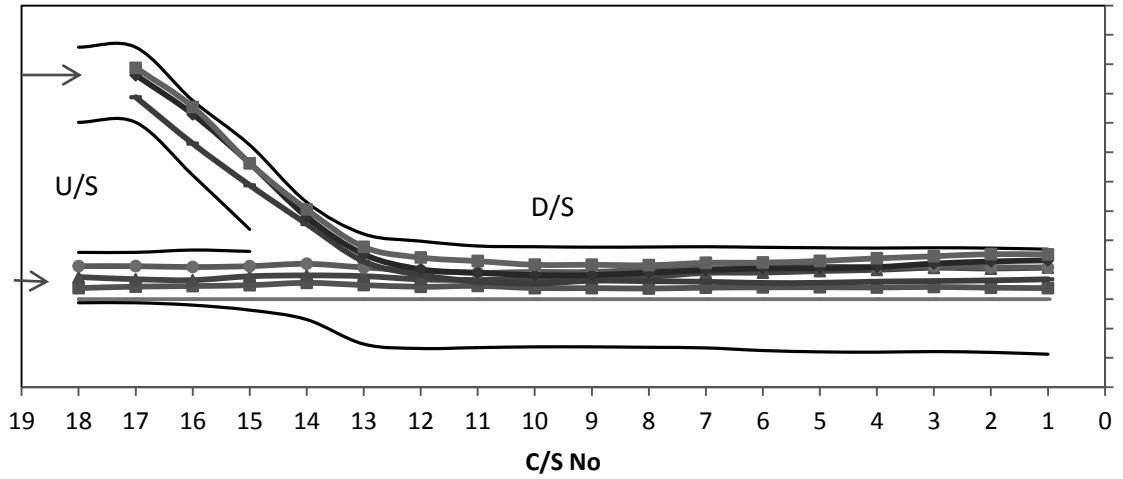


Figure C.16: Flow Line Diagram for T-15

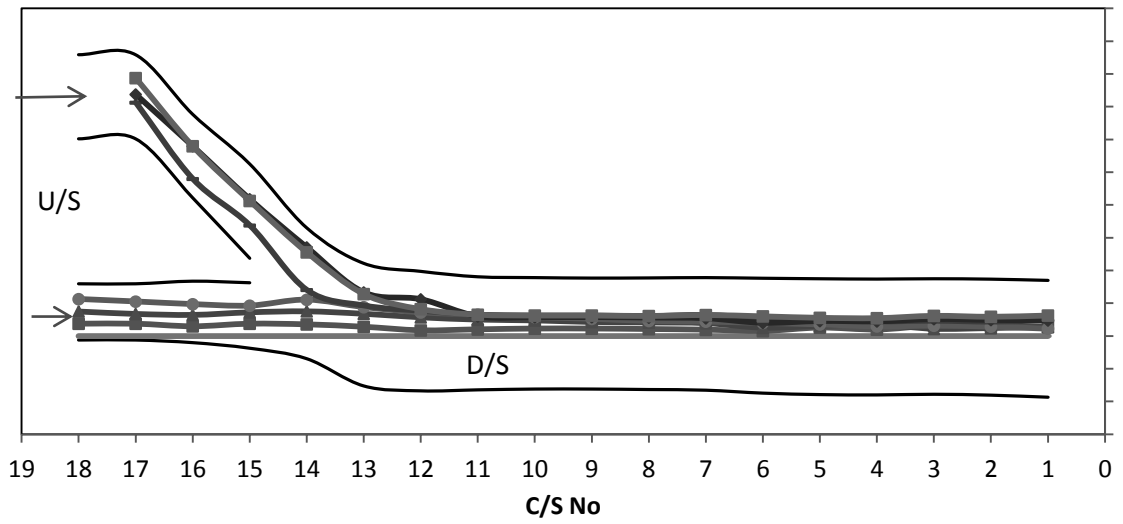


Figure C.17: Flow Line Diagram for T-16

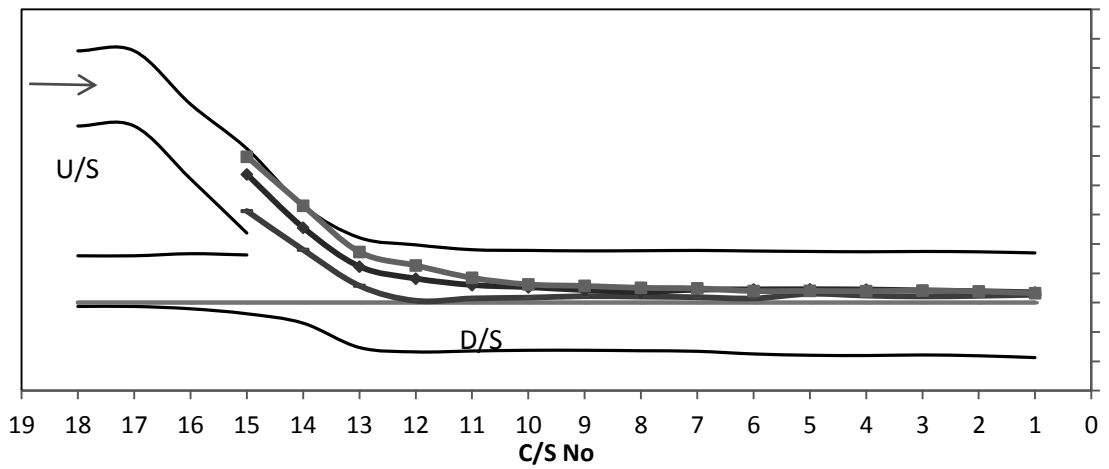


Figure C.18: Flow Line Diagram for T-17

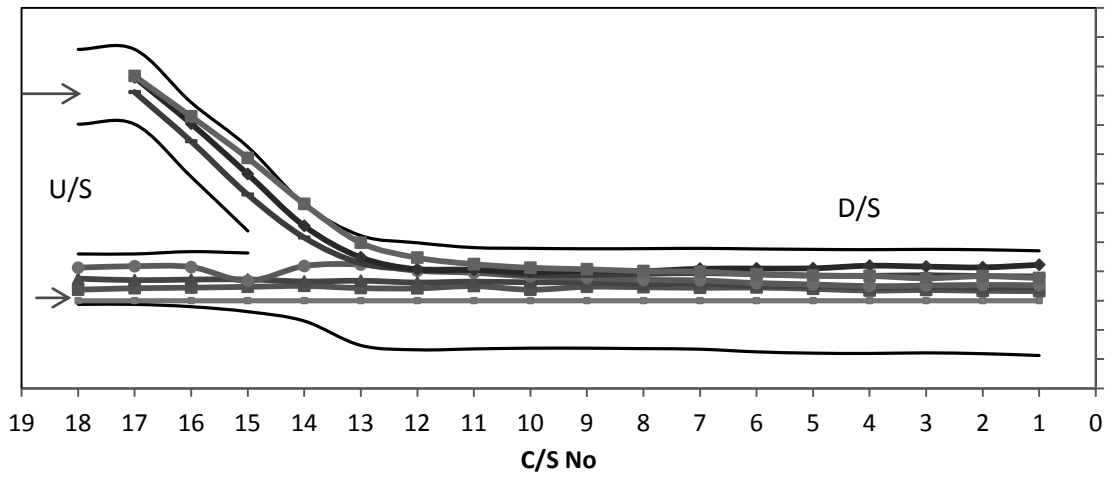


Figure C.19: Flow Line Diagram for T-18

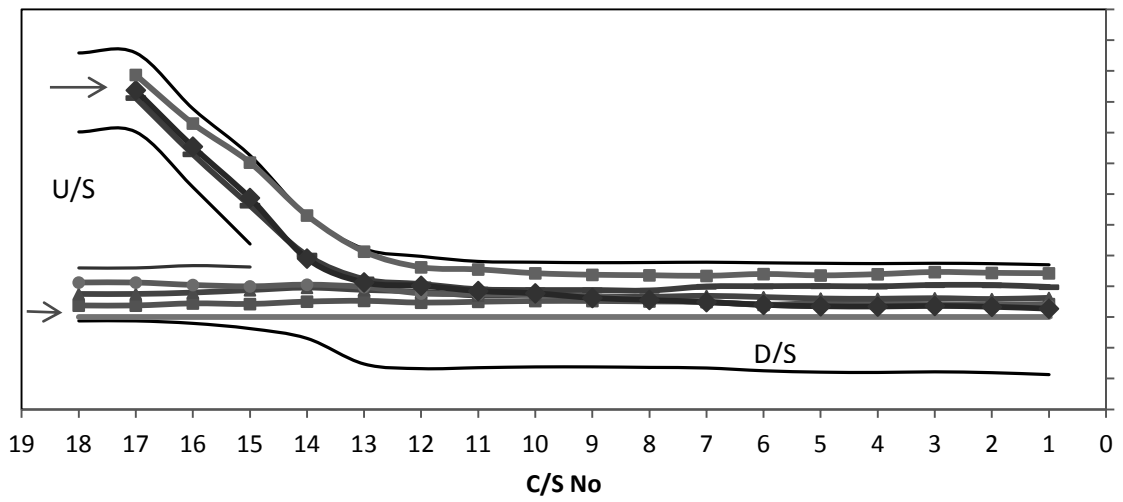


Figure C.20: Flow Line Diagram for T-19

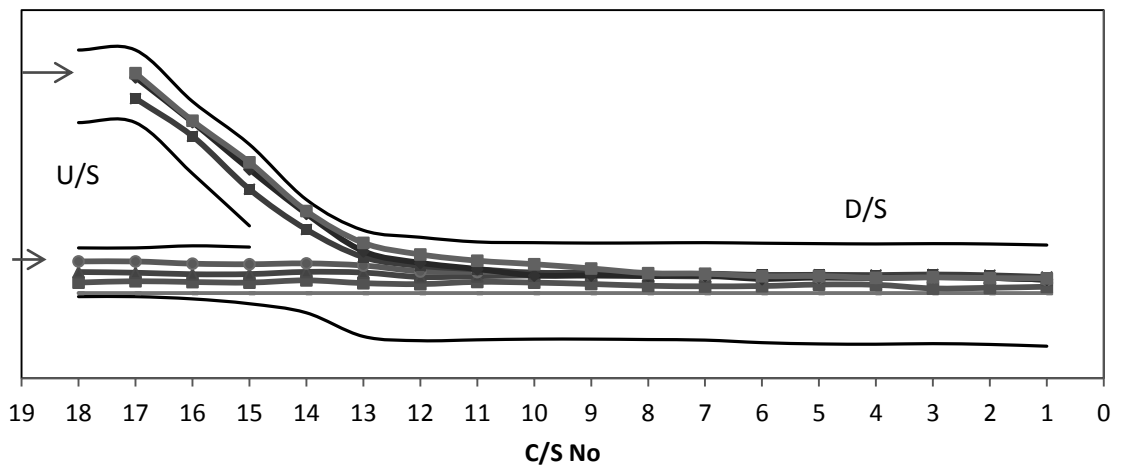


Figure C.21: Flow Line Diagram for T-20

Table- C.1: Time for Single Float to Pass through the Model

Test ID	Time in second for a Float to pass the model from calibration section to D/S	
	MC (Traveled length = 22.5m)	CC (Traveled length = 25m)
T-10	43.73	40.23
T-11	45.25	46.01
T-12	45.42	44.28
T-13	-	31.95
T-14	44.75	45.62
T-15	47.41	43.37
T-16	49.79	41.78
T-17	-	34.02
T-18	42.36	41.17
T-20	49.67	39.64

Appendix-D

Calibration of Weir for Discharge

Discharge quantity has been controlled by internal gate valve at weir-1 (for MC) and weir-2 (for CC). The controlling height of water for a particular discharge has been calculated by Rebokh's formula. Details of weir for both main channel and chute channel have been presented below:

a. Features of Main Channel:

Weir height = 0.416667m

Weir length = 1.80 m

Initial head = 0.01m

Initial Q= 0.01 m³/s

Rate of height variation for calculating discharge = 0.001

Table D.1: Calibration of Main Channel Weir

Effective Head, H_e (m)	Coefficient of Discharge, K	Velocity of Approach (m/s)	Discharge with Velocity Approach, m³/s	Discharge without Velocity Approach, m³/s
0.114	1.849	0.134	0.130	0.128
0.115	1.850	0.135	0.131	0.130
0.116	1.850	0.137	0.133	0.132
0.117	1.851	0.139	0.135	0.133
0.118	1.852	0.140	0.137	0.135
0.119	1.852	0.142	0.139	0.137
0.120	1.853	0.143	0.140	0.139
0.121	1.853	0.145	0.142	0.140
0.122	1.854	0.147	0.144	0.142
0.123	1.854	0.148	0.146	0.144
0.124	1.855	0.150	0.148	0.146
0.125	1.855	0.151	0.150	0.148
0.126	1.856	0.153	0.151	0.149
0.127	1.857	0.155	0.153	0.151
0.128	1.857	0.156	0.155	0.153
0.129	1.858	0.158	0.157	0.155
0.130	1.858	0.160	0.159	0.157
0.131	1.859	0.161	0.161	0.159
0.132	1.859	0.163	0.163	0.161
0.133	1.860	0.165	0.165	0.162

Effective Head, H_e (m)	Coefficient of Discharge, K	Velocity of Approach (m/s)	Discharge with Velocity Approach, m^3/s	Discharge without Velocity Approach, m^3/s
0.134	1.861	0.166	0.167	0.164
0.135	1.861	0.168	0.169	0.166
0.136	1.862	0.170	0.171	0.168
0.137	1.862	0.171	0.173	0.170
0.138	1.863	0.173	0.175	0.172
0.139	1.863	0.175	0.177	0.174
0.140	1.864	0.176	0.179	0.176
0.141	1.865	0.178	0.181	0.178
0.142	1.865	0.180	0.183	0.180
0.143	1.866	0.181	0.185	0.182
0.144	1.866	0.183	0.187	0.184
0.145	1.867	0.185	0.189	0.186
0.146	1.867	0.186	0.191	0.188
0.147	1.868	0.188	0.193	0.189
0.148	1.868	0.190	0.195	0.191
0.149	1.869	0.191	0.197	0.193
0.150	1.870	0.193	0.199	0.196
0.151	1.870	0.195	0.201	0.198
0.152	1.871	0.196	0.203	0.200
0.153	1.871	0.198	0.205	0.202
0.154	1.872	0.200	0.207	0.204
0.155	1.872	0.202	0.209	0.206
0.156	1.873	0.203	0.212	0.208
0.157	1.874	0.205	0.214	0.210
0.158	1.874	0.207	0.216	0.212
0.159	1.875	0.208	0.218	0.214
0.160	1.875	0.210	0.220	0.216
0.161	1.876	0.212	0.222	0.218
0.162	1.876	0.214	0.225	0.220
0.163	1.877	0.215	0.227	0.222
0.164	1.877	0.217	0.229	0.224
0.165	1.878	0.219	0.231	0.227
0.166	1.879	0.220	0.233	0.229
0.167	1.879	0.222	0.236	0.231
0.168	1.880	0.224	0.238	0.233
0.169	1.880	0.226	0.240	0.235
0.170	1.881	0.227	0.242	0.237

Effective Head, H_e (m)	Coefficient of Discharge, K	Velocity of Approach (m/s)	Discharge with Velocity Approach, m^3/s	Discharge without Velocity Approach, m^3/s
0.171	1.881	0.229	0.245	0.239
0.172	1.882	0.231	0.247	0.242
0.173	1.883	0.233	0.249	0.244
0.174	1.883	0.234	0.251	0.246
0.175	1.884	0.236	0.254	0.248
0.176	1.884	0.238	0.256	0.250
0.177	1.885	0.240	0.258	0.253
0.178	1.885	0.241	0.261	0.255
0.179	1.886	0.243	0.263	0.257
0.180	1.886	0.245	0.265	0.259
0.181	1.887	0.247	0.268	0.262
0.182	1.888	0.248	0.270	0.264
0.183	1.888	0.250	0.272	0.266
0.184	1.889	0.252	0.275	0.268
0.185	1.889	0.254	0.277	0.271
0.186	1.890	0.256	0.280	0.273
0.187	1.890	0.257	0.282	0.275
0.188	1.891	0.259	0.284	0.277
0.189	1.892	0.261	0.287	0.280
0.190	1.892	0.263	0.289	0.282
0.191	1.893	0.264	0.292	0.284
0.192	1.893	0.266	0.294	0.287
0.193	1.894	0.268	0.297	0.289
0.194	1.894	0.270	0.299	0.291
0.195	1.895	0.272	0.301	0.294
0.196	1.895	0.273	0.304	0.296
0.197	1.896	0.275	0.306	0.298
0.198	1.897	0.277	0.309	0.301
0.199	1.897	0.279	0.311	0.303
0.200	1.898	0.281	0.314	0.306
0.201	1.898	0.282	0.316	0.308
0.202	1.899	0.284	0.319	0.310
0.203	1.899	0.286	0.321	0.313
0.204	1.900	0.288	0.324	0.315
0.205	1.901	0.290	0.327	0.318
0.206	1.901	0.291	0.329	0.320
0.207	1.902	0.293	0.332	0.322

Effective Head, H_e (m)	Coefficient of Discharge, K	Velocity of Approach (m/s)	Discharge with Velocity Approach, m^3/s	Discharge without Velocity Approach, m^3/s
0.208	1.902	0.295	0.334	0.325
0.209	1.903	0.297	0.337	0.327
0.210	1.903	0.299	0.339	0.330
0.211	1.904	0.300	0.342	0.332
0.212	1.905	0.302	0.345	0.335
0.213	1.905	0.304	0.347	0.337
0.214	1.906	0.306	0.350	0.340
0.215	1.906	0.308	0.352	0.342
0.216	1.907	0.310	0.355	0.345
0.217	1.907	0.311	0.358	0.347
0.218	1.908	0.313	0.360	0.350
0.219	1.908	0.315	0.363	0.352
0.220	1.909	0.317	0.366	0.355
0.221	1.910	0.319	0.368	0.357
0.222	1.910	0.320	0.371	0.360
0.223	1.911	0.322	0.374	0.362
0.224	1.911	0.324	0.377	0.365
0.225	1.912	0.326	0.379	0.367
0.226	1.912	0.328	0.382	0.370
0.227	1.913	0.330	0.385	0.372
0.228	1.914	0.332	0.387	0.375
0.229	1.914	0.333	0.390	0.378
0.230	1.915	0.335	0.393	0.380
0.231	1.915	0.337	0.396	0.383
0.232	1.916	0.339	0.398	0.385
0.233	1.916	0.341	0.401	0.388

b. Features of Chute Channel:

Weir height = 0.511m

Weir length = 1.52 m

Initial head = 0.01m

Initial Q= 0.01 m³/s

Rate of height variation for calculating discharge= 0.001

Table D.2: Calibration of Chute Channel Weir

Effective Head, H _e (m)	Coefficient of Discharge, K	Velocity of Approach (m/s)	Discharge with Velocity Approach, m ³ /s	Discharge without Velocity Approach, m ³ /s
0.128	1.844	0.132	0.130	0.128
0.129	1.844	0.133	0.131	0.130
0.130	1.845	0.134	0.133	0.131
0.131	1.845	0.136	0.134	0.133
0.132	1.846	0.137	0.136	0.135
0.133	1.846	0.139	0.138	0.136
0.134	1.847	0.140	0.139	0.138
0.135	1.847	0.142	0.141	0.139
0.136	1.847	0.143	0.142	0.141
0.137	1.848	0.144	0.144	0.142
0.138	1.848	0.146	0.146	0.144
0.139	1.849	0.147	0.147	0.146
0.140	1.849	0.149	0.149	0.147
0.141	1.850	0.150	0.151	0.149
0.142	1.850	0.152	0.152	0.150
0.143	1.851	0.153	0.154	0.152
0.144	1.851	0.154	0.156	0.154
0.145	1.852	0.156	0.157	0.155
0.146	1.852	0.157	0.159	0.157
0.147	1.853	0.159	0.161	0.159
0.148	1.853	0.160	0.162	0.160
0.149	1.853	0.162	0.164	0.162
0.150	1.854	0.163	0.166	0.164
0.151	1.854	0.165	0.168	0.165
0.152	1.855	0.166	0.169	0.167
0.153	1.855	0.168	0.171	0.169
0.154	1.856	0.169	0.173	0.170
0.155	1.856	0.170	0.174	0.172

Effective Head, H_e (m)	Coefficient of Discharge, K	Velocity of Approach (m/s)	Discharge with Velocity Approach, m^3/s	Discharge without Velocity Approach, m^3/s
0.156	1.857	0.172	0.176	0.174
0.157	1.857	0.173	0.178	0.176
0.158	1.858	0.175	0.180	0.177
0.159	1.858	0.176	0.182	0.179
0.160	1.858	0.178	0.183	0.181
0.161	1.859	0.179	0.185	0.183
0.162	1.859	0.181	0.187	0.184
0.163	1.860	0.182	0.189	0.186
0.164	1.860	0.184	0.191	0.188
0.165	1.861	0.185	0.192	0.190
0.166	1.861	0.187	0.194	0.191
0.167	1.862	0.188	0.196	0.193
0.168	1.862	0.190	0.198	0.195
0.169	1.863	0.191	0.200	0.197
0.170	1.863	0.193	0.202	0.198
0.171	1.864	0.194	0.203	0.200
0.172	1.864	0.196	0.205	0.202
0.173	1.864	0.197	0.207	0.204
0.174	1.865	0.199	0.209	0.206
0.175	1.865	0.200	0.211	0.208
0.176	1.866	0.202	0.213	0.209
0.177	1.866	0.203	0.215	0.211
0.178	1.867	0.205	0.217	0.213
0.179	1.867	0.206	0.219	0.215
0.180	1.868	0.208	0.220	0.217
0.181	1.868	0.209	0.222	0.219
0.182	1.869	0.211	0.224	0.221
0.183	1.869	0.212	0.226	0.222
0.184	1.869	0.214	0.228	0.224
0.185	1.870	0.216	0.230	0.226
0.186	1.870	0.217	0.232	0.228
0.187	1.871	0.219	0.234	0.230
0.188	1.871	0.220	0.236	0.232
0.189	1.872	0.222	0.238	0.234
0.190	1.872	0.223	0.240	0.236
0.191	1.873	0.225	0.242	0.238
0.192	1.873	0.226	0.244	0.240

Effective Head, H_e (m)	Coefficient of Discharge, K	Velocity of Approach (m/s)	Discharge with Velocity Approach, m^3/s	Discharge without Velocity Approach, m^3/s
0.193	1.874	0.228	0.246	0.241
0.194	1.874	0.229	0.248	0.243
0.195	1.875	0.231	0.250	0.245
0.196	1.875	0.233	0.252	0.247
0.197	1.875	0.234	0.254	0.249
0.198	1.876	0.236	0.256	0.251
0.199	1.876	0.237	0.258	0.253
0.200	1.877	0.239	0.260	0.255
0.201	1.877	0.240	0.262	0.257
0.202	1.878	0.242	0.264	0.259
0.203	1.878	0.243	0.266	0.261
0.204	1.879	0.245	0.269	0.263
0.205	1.879	0.247	0.271	0.265
0.206	1.880	0.248	0.273	0.267
0.207	1.880	0.250	0.275	0.269
0.208	1.881	0.251	0.277	0.271
0.209	1.881	0.253	0.279	0.273
0.210	1.881	0.254	0.281	0.275
0.211	1.882	0.256	0.283	0.277
0.212	1.882	0.258	0.285	0.279
0.213	1.883	0.259	0.288	0.281
0.214	1.883	0.261	0.290	0.283
0.215	1.884	0.262	0.292	0.285
0.216	1.884	0.264	0.294	0.288
0.217	1.885	0.265	0.296	0.290
0.218	1.885	0.267	0.298	0.292
0.219	1.886	0.269	0.301	0.294
0.220	1.886	0.270	0.303	0.296
0.221	1.886	0.272	0.305	0.298
0.222	1.887	0.273	0.307	0.300
0.223	1.887	0.275	0.309	0.302
0.224	1.888	0.277	0.311	0.304
0.225	1.888	0.278	0.314	0.306
0.226	1.889	0.280	0.316	0.308
0.227	1.889	0.281	0.318	0.311
0.228	1.890	0.283	0.320	0.313
0.229	1.890	0.285	0.323	0.315

Effective Head, H_e (m)	Coefficient of Discharge, K	Velocity of Approach (m/s)	Discharge with Velocity Approach, m^3/s	Discharge without Velocity Approach, m^3/s
0.230	1.891	0.286	0.325	0.317
0.231	1.891	0.288	0.327	0.319
0.232	1.892	0.289	0.329	0.321
0.233	1.892	0.291	0.332	0.323
0.234	1.892	0.293	0.334	0.326
0.235	1.893	0.294	0.336	0.328
0.236	1.893	0.296	0.338	0.330
0.237	1.894	0.297	0.341	0.332
0.238	1.894	0.299	0.343	0.334
0.239	1.895	0.301	0.345	0.337
0.240	1.895	0.302	0.348	0.339
0.241	1.896	0.304	0.350	0.341
0.242	1.896	0.306	0.352	0.343
0.243	1.897	0.307	0.355	0.345
0.244	1.897	0.309	0.357	0.348
0.245	1.897	0.310	0.359	0.350
0.246	1.898	0.312	0.362	0.352
0.247	1.898	0.314	0.364	0.354
0.248	1.899	0.315	0.366	0.356
0.249	1.899	0.317	0.369	0.359
0.250	1.900	0.319	0.371	0.361
0.251	1.900	0.320	0.374	0.363
0.252	1.901	0.322	0.376	0.365
0.253	1.901	0.323	0.378	0.368
0.254	1.902	0.325	0.381	0.370
0.255	1.902	0.327	0.383	0.372
0.256	1.903	0.328	0.386	0.375
0.257	1.903	0.330	0.388	0.377
0.258	1.903	0.332	0.390	0.379
0.259	1.904	0.333	0.393	0.381
0.260	1.904	0.335	0.395	0.384
0.261	1.905	0.337	0.398	0.386
0.262	1.905	0.338	0.400	0.388

Extra notations that has been used in the study is as follow:

CC	Chute Channel
c/s	Cross Section
d/s	Down stream
EE	End of Embankment
ELA	End of Launching Apron
ER	End of Revetment
ES	End of Slope
HWL	Highest Water Level
LA	Launching Apron
LB	Left Bank
LWL	Lowest Water Level
MC	Main Channel
R/B	Right Bank
SLA	Start of Launching Apron
SR	Start of Revetment
SE	Start of Embankment
u/s	Upstream